

Dispersion approach to quark-binding effects in weak decays of heavy mesons

Dmitri Melikhov

*Institut für Theoretische Physik der Universität Heidelberg,
Philosophenweg 16, D-69120, Heidelberg, Germany**

The dispersion approach based on the constituent quark picture and its applications to weak decays of heavy mesons are reviewed. Meson interaction amplitudes are represented within this approach as relativistic spectral integrals over the mass variables in terms of the meson wave functions and spectral densities of the corresponding Feynman diagrams. Various applications of this approach are discussed:

Relativistic spectral representations for meson elastic and transition form factors at spacelike momentum transfers are constructed. Form factors at $q^2 > 0$ are obtained by the analytical continuation. As a result of this procedure, form factors are given in the full q^2 range of the weak decay in terms of the wave functions of the participating mesons.

The $1/m_Q$ expansion of the obtained spectral representations for the form factors for the particular limits of the heavy-to-heavy and heavy-to-light transitions are analysed. Their full consistency with the constraints provided by QCD for these limits is demonstrated.

Predictions for form factors for $B_{(s)}$ and $D_{(s)}$ decays to light mesons are given.

The $B \rightarrow \gamma \ell \nu$ decay and the weak annihilation in rare radiative decays are considered. Nonfactorizable corrections to the $B^0 - \bar{B}^0$ mixing are calculated.

Inclusive weak B decays are analysed and the differential distributions are obtained in terms of the B meson wave function.

PACS numbers: 13.20.He, 12.39.Ki, 12.39.Hg, 13.40.Hq

*On leave from: *Nuclear Physics Institute, Moscow State University, Moscow, Russia*

Contents

I	Introduction	4
II	Spectral representation for bound state transition form factors	8
A	Bound state description within dispersion relations	8
B	Quark structure of pseudoscalar mesons	11
1	Leptonic decay constant	12
2	Two-photon decay of a neutral pseudoscalar meson	14
3	Elastic electromagnetic form factor	15
4	Dispersion approach in terms of the light-cone variable	16
C	Form factors of meson transitions	18
1	The pseudoscalar meson transition form factor at $q^2 < 0$	18
2	Transition form factors at $q^2 > 0$	21
D	A simple model for pseudoscalar mesons	24
E	Discussion	30
III	Heavy quark expansion and universal form factors in the dispersion approach	32
A	Meson transition amplitudes and heavy-quark expansion in QCD	33
B	Transition form factors in the dispersion approach	37
C	Heavy-quark expansion in the dispersion approach for heavy-to-heavy transitions	39
D	Heavy-to-light meson transitions	48
E	Numerical estimates for the universal form factors	50
F	Discussion	53
IV	Calculation of the weak form factors	55
A	Parameters of the model	55
1	The form factors F_+ , F_T , V , T_1 , and A_0	57
2	The form factors F_0 , A_1 , A_2 , T_2 and T_3	58
B	Charmed meson decays	60
1	$D \rightarrow K, K^*$	60
2	$D \rightarrow \pi, \rho$	61
C	Beauty meson decays	62
1	$B \rightarrow D, D^*$	62
2	$B \rightarrow K, K^*$	63
3	$B \rightarrow \pi, \rho$	64
D	Decays of the strange mesons D_s and B_s	67
1	$D_s \rightarrow K, K^*$	67
2	$D_s \rightarrow \eta, \eta', \phi$	68
3	$B_s \rightarrow K, K^*$	70
4	$B_s \rightarrow \eta, \eta', \phi$	71
E	Discussion	72
V	Weak annihilation in the rare radiative $B \rightarrow \rho\gamma$ decay and the $B \rightarrow \gamma\ell\nu$ form factors	73
A	The effective Hamiltonian, the amplitude and the decay rate	74
1	The penguin amplitude	75
2	The weak annihilation amplitude	75
B	Form factors for the $B \rightarrow \gamma\ell\nu$ transition	79
1	The form factor F_A	79
2	The form factor F_V	81
C	The form factor G_V	83
D	Numerical estimates	84
E	Discussion	85

VI	Nonfactorizable effects in the $B^0 - \bar{B}^0$ mixing	86
A	Effective Hamiltonian and the structure of the amplitude	87
B	ΔB in terms of the local gluon condensate	88
C	Form factors in the dispersion approach	89
D	Numerical results.	91
E	Discussion.	92
VII	Quark-binding effects in inclusive decays of heavy mesons	93
A	Free quark decay and OPE	97
B	Inclusive meson decay in the dispersion approach	99
	1 The spacelike region	100
	2 The timelike region and the anomalous contribution	102
C	The $1/m_Q$ expansion of the semileptonic decay rate and $d\Gamma/dq^2$	104
D	$d\Gamma/dM_X$	108
E	The electron energy spectrum	109
F	Discussion	111
VIII	Conclusion	112

I. INTRODUCTION

Weak decays of hadrons provide an important source of information on the parameters of the standard model, the structure of weak currents, and internal structure of hadrons. Therefore for many years weak decays have been in the focus of experimental and theoretical investigations.

In the last decade, the main emphasis has been laid on weak B decays which allow to measure the unknown parameters of the Cabibbo-Kobayashi-Maskawa (CKM) matrix describing the mixing of heavy c , b and t quarks, and the CP-violation: semileptonic and nonleptonic B decays induced by the charged-current quark transition $b \rightarrow u, c$ provide a direct access to the CKM matrix elements V_{ub} and V_{cb} and the weak CP-violating phase.

Rare semileptonic B decays induced by the flavour-changing neutral current transitions $b \rightarrow s$ and $b \rightarrow d$ measure V_{ts} and represent an important test of the standard model and of the physics beyond it. Rare decays are forbidden at the tree level in the standard model and occur through loop diagrams. Thus they provide the possibility to probe at the relatively low energies of B decays the structure of the electroweak sector at large mass scales from contributions of virtual particles in the loop diagrams. Interesting information about the structure of the theory is contained in the Wilson coefficients in the effective Hamiltonian which describes the $b \rightarrow s, d$ transition at low energies. These Wilson coefficients take different values in different theories with testable consequences in rare B decays.

However, along with the interesting parameters of the standard model, the decay rates and differential distributions measurable in the decay process contain also quantities related to the presence of hadrons in the decay process. Therefore the extraction of the interesting standard model parameters from the decay experiments requires reliable information on hadron structure and hadronic amplitudes of the weak quark currents.

Theoretical description of hadronic amplitudes of the quark currents is one of the key problems of particle physics as such amplitudes provide a bridge between QCD formulated in the language of quarks and gluons and observable phenomena which deal with hadrons. The difficulty in such calculations lie in the fact that hadron formation occurs at large distances where perturbative QCD methods are not applicable and therefore a nonperturbative consideration is necessary.

The presence of heavy quarks with the masses much bigger than the confinement scale of QCD provide important constraints upon the long distance effects due to a new spin-flavour symmetry which emerges in this limit [1,2]. This symmetry leads to a heavy quark effective theory (HQET) [3] for QCD with heavy quarks. HQET restricts the structure of the expansion of the hadronic transition amplitudes in inverse powers of the heavy quark mass.

In inclusive B decays the combination of the heavy-quark and the operator product expansions allow one to connect the decay rate of the quark bound in a heavy hadron to the decay rate of the free quark. An important consequence of the operator product expansion is the appearance of the corrections to the free quark decay rate only at the second power of the $1/m_Q$ [4,5]. Therefore, these corrections are numerically small. Providing quite reliable predictions for the integrated rates, the theoretical approach based on the OPE turns out to be less efficient for the description of the differential distributions. In this case a more precise information on the details of the b quark motion inside the B meson is necessary.

For the exclusive $b \rightarrow c$ decays, HQET provides constraints on the structure of the expansion of the meson transition form factors in the inverse powers of the b and c quark masses and leads to the appearance of universal process-independent form factors at each order of the $1/m_Q$ expansion [6,7]. Moreover, heavy quark symmetry provides the absolute value of the leading order universal form factor - the Isgur-Wise function at zero recoil (maximum momentum transfer) thus allowing for a reliable description of the $b \rightarrow c$ decay in this kinematical region. HQET however cannot calculate the universal form factors as functions of the momentum transfer. Moreover, the $1/m_c$ corrections for the $b \rightarrow c$ transition form factors turn out to be not small because the c quark is not sufficiently heavy.

For the exclusive $b \rightarrow u, s$ transitions, when the final quark is light, relations between the form factors describing meson transition induced by different currents emerge in the region near zero recoil [8]. In the opposite region of large recoils, where the final quark is fast, one can construct another effective theory, so called large energy effective theory (LEET) which allows the double expansion of the transition form factors in inverse powers of m_b and the energy E of the light quark produced in the weak decay [9]. LEET predicts the appearance of several universal form factors at the leading order of the $1/E$ and $1/m_b$ expansion, but does not calculate these form factors, and also does not constrain the structure of higher order corrections.

Thus, heavy-quark symmetry provides important constraints for the form factors but does not allow to calculate them in full detail. This task requires a detailed treatment of the nonperturbative effects.

Theoretical approaches for calculating transition form factors are quark models [10–27], QCD sum rules [28–39], and lattice QCD [40–48]. Approaches combining different methods are also extensively used [49–56].

In spite of the considerable progress made in the recent years theoretical uncertainties are still uncomfortably large, around 10-15%. The main difficulty in obtaining the full picture of the form factors for various decays and for all q^2 lies in the fact that methods more directly related to QCD, such as lattice QCD and QCD sum rules have only a

limited range of applicability, whereas the results from quark models are sensitive to the details of the model and the parameters used.

QCD sum rules are suitable for describing the low q^2 region of the form factors. Sum rule calculations require various inputs such as the condensates or the distribution amplitudes of the light mesons produced in the heavy meson decay. The higher q^2 region is hard to get and higher order calculations are not likely to give real progress because of the appearance of many new parameters. The accuracy of the method cannot be arbitrarily improved because of the necessity to isolate the contribution of the states of interest from others.

Lattice QCD gives good results for the high q^2 region. But because of the many numerical extrapolations involved this method does not provide for a full picture of the form factors and for the relations between the various decay channels.

Quark models do provide such relations connecting different processes through the meson soft wave functions, and give the form factors in the full q^2 range. However, quark models are not closely related to the QCD Lagrangian (or at least this relationship is not well understood yet) and therefore have input parameters which are not directly measurable and may not be of fundamental significance.

Since quark models are not directly deduced from QCD it is important to match the results for the transition form factors obtained within quark models to rigorous QCD predictions for these form factors in the specific limit of heavy quark masses.

The application of various versions of the constituent quark picture to decay processes has a long history. First models were based on a relativistic [10] or nonrelativistic [11,12] considerations. They could not fully incorporate the quark dynamics and spin structure and therefore could not satisfy rigorous relations for the transition form factors based of the spin-flavour symmetry in the heavy quark limit of QCD.

A self-consistent relativistic treatment of the quark spins can be performed within the light-front quark model [57,58]. The model allows for a calculation of the reference-frame dependent partonic contribution to the form factor. However, the non-partonic contribution cannot in general be calculated. At spacelike momentum transfers the nonpartonic part can be killed by an appropriate choice of the reference frame. Therefore, the partonic contribution calculated in this specific reference frame gives the full form factor. At timelike momentum transfers the nonpartonic contribution does not vanish for any accessible choice of the reference frame, and the knowledge of the frame-dependent partonic contribution is not sufficient to determine the form factor.

A relativistic dispersion approach to the decay processes based on the constituent quark picture overcomes the above difficulties. It has been formulated in [24–27] and applied to the study of the long-distance effects in many pocesses involving the B meson: such as exclusive semileptonic [24–27,59–61] and rare [62,63] B decays, the $B \rightarrow \gamma l \nu$ form factor and the weak annihilation in the rare radiative $B \rightarrow \rho \gamma$ decay [64,65], nonfactorizable corrections for the $B^0 - \bar{B}^0$ mixing [66], calculation of the differential distributions in inclusive $B \rightarrow X_c l \nu$ decays [67].

The approach is based on a consistent treatment of the two-particle singularities of the Feynman diagrams describing meson interactions. Amplitudes of these processes are given by the relativistic spectral representations over the mass variables in terms of the wave functions of the participating mesons and spectral densities of the corresponding Feynman diagrams. In particular, meson transition form factors both at spacelike and timelike momentum transfers are given by the double spectral representations.

We discuss in this paper applications of the dispersion approach to various processes involving heavy mesons, laying the main emphasis on the calculation of the form factors for heavy meson decays.

Let us highlight the main features of our dispersion formulation of the constituent quark model:

1. The physical picture

The constituent quark picture is based on the following phenomena expected from QCD:

- the chiral symmetry breaking in the low-energy region which provides for the masses of the constituent quarks;
- a strong peaking of the nonperturbative meson wave functions in terms of the quark momenta with a width of the order of the confinement scale;
- a $q\bar{q}$ composition of mesons in terms of constituent quarks.

As is well known, the $q\bar{q}$ component of the meson wave function in terms of current quarks dominates the exclusive form factors in the deep inelastic region, i.e. for large spacelike momentum transfers. A successesfull description of the mass spectrum of mesons as $q\bar{q}$ states in terms of the constituent quarks obtained in [68] shows that the $q\bar{q}$ approximation works well also in the soft region, where one however has to take into account the transition of the current quarks to constituent quarks. The $q\bar{q}$ meson component in terms of the constituent quarks leads to a good description of the elastic form factors at small and intermediate momentum transfers [69,70]. Therefore, one can

expect the two-particle approximation to be quite reliable for the description of the range of momentum transfers relevant for heavy meson decays.

An important shortcoming of previous quark model predictions was a strong dependence of the results on the special form of the quark model and on the parameter values. We demonstrate that once

- (a) a proper relativistic formalism is used for the description of the transition form factors and
- (b) the numerical parameters of the model are chosen properly (we discuss criteria for such a proper choice below),

the quark model yields results in full agreement with the existing experimental data and in accord with the predictions of more fundamental theoretical approaches. In addition, our approach allows to predict many other form factors which have not yet been measured.

2. The formalism

For the description of the transition form factors in their full q^2 -range and for various initial and final mesons, a fully relativistic treatment is necessary. The dispersion formulation of the quark model provides for such a relativistic treatment and guarantees the correct spectral and analytical properties of the obtained form factors.

The form factors are given by the double spectral representations over the variables s_1 and s_2 , the squares of the invariant masses of the initial and final $Q\bar{q}$ pairs, respectively. The integrations in s_1 and s_2 run along the two-particle cuts in the complex s_1 and s_2 planes. The spectral functions of these spectral representations involve the wave functions of the participating mesons and the double discontinuities of the corresponding triangle Feynman diagrams.

We start our analysis of the transition form factors from the spacelike region $q^2 < 0$, where the double discontinuities can be calculated by means of the Landau-Cutkosky rules.

The form factors in the decay region $q^2 > 0$ are obtained by the analytical continuation in q^2 . A specific feature of the timelike decay region of q^2 , is the appearance of the anomalous cuts in the complex s_1 and s_2 planes and, respectively, of the anomalous contributions to the form factors. Let us point out that the anomalous contribution as well as the normal one is completely determined by the wave functions of the participating mesons in the physical region. The anomalous contribution is small for small positive q^2 but becomes increasingly important as q^2 rises.

The form factors obtained by this procedure obey all rigorous constraints from QCD on the structure of the long-distance corrections in the heavy quark limit: they develop the correct heavy-quark expansion at leading and next-to-leading orders in $1/m_Q$ in accordance with QCD in the case when both quarks participating in the weak transition are heavy, i.e. have masses much larger than the confinement scale of QCD.

For the heavy-to-light transition, i. e. when only the initial quark is treated as heavy, the transition form factors of the dispersion approach satisfy the relations between the form factors of vector, axial-vector, and tensor currents valid at small recoil. In the limit of the heavy-to-light transitions at small q^2 the form factors obey the lowest order $1/m_Q$ and $1/E$ relations of the Large Energy Effective Theory.

We want to emphasise once more that form factors for meson decays in the physical decay region $q^2 > 0$ are directly calculated through the meson wave functions.

3. Parameters of the model

In previous applications of quark models the transition form factors turned out to be sensitive to the numerical parameters, such as the quark masses and the slopes of the meson soft wave functions.

A possible way to control quark masses and the meson soft wave functions is to use the lattice results for the $B \rightarrow \rho$ form factors at large q^2 as 'experimental' inputs. The b and u constituent quark masses and slope parameters of the B , π , and ρ wave functions assuming for them a simple Gaussian form are obtained through this procedure [59]. The Gaussian wave functions of the charm and strange mesons and the effective masses m_c and m_s are fixed by fitting the measured rates for the decays $D \rightarrow (K, K^*)l\nu$ [61].

With these few inputs, numerous predictions for the form factors for the $D_{(s)}$ and $B_{(s)}$ decays into light mesons are obtained [61] which nicely agree with the experimental results at places where data are available. The calculated transition form factors are also found to be in good agreement with the results from lattice QCD and from sum rules in their regions of validity.

Thus, in spite of the rather different masses and properties of mesons involved in weak transitions, all existing data on the form factors can be understood in the quark picture, i.e. all form factors can be described by the few degrees of freedom of constituent quarks. Details of the soft wave functions are not crucial; only the spatial extension of these

wave functions of order of the confinement scale is important. In other words, only the meson radii are essential for the decay processes.

The paper is organised as follows:

In Chapter II we present details of the composite system description using spectral representations over mass variables. We start with the amplitude of the constituent interaction in the low-energy region and its analytical properties. We then consider the interaction of the bound state with the external electromagnetic field and construct the gauge and relativistic invariant amplitude of the bound state interaction. The elastic electromagnetic form factor is discussed and the relativistic wave function is introduced. The normalization condition for the wave function is obtained which corresponds to the electric charge conservation.

Properties of pseudoscalar mesons are studied. A single spectral representation for the weak leptonic decay constant and double spectral representations for the elastic electromagnetic and the weak transition form factors in terms of the wave function are obtained at $q^2 < 0$. For comparison with the light-cone quark model results we rewrite our explicitly invariant spectral representations in terms of the light-cone variables and demonstrate the equivalence of the form factors obtained within our dispersion approach and the light-cone quark model for $q^2 < 0$.

The weak transition form factor at $q^2 > 0$ is obtained by the analytical continuation which is discussed in full detail.

We then consider the case when one of the quarks in the pseudoscalar meson is heavy, $m_Q \rightarrow \infty$ and analyse the size of the $1/m_Q$ effects in the form factors for quark masses in the range of the b and c quarks.

Chapter III contains a detailed discussion of the weak transitions of the pseudoscalar mesons to pseudoscalar and vector mesons. The double spectral representation for both cases are constructed starting from $q^2 < 0$ and going to $q^2 > 0$ by the analytical continuation. A procedure of fixing the subtraction prescription in the double spectral representations is discussed.

We then perform the $1/m_Q$ expansion of the dispersion form factors for the heavy-to-heavy transition to next-to-leading order accuracy in $1/m_Q$. For the heavy-to-light transition the expansion within the leading order in $1/m_Q$ is developed. Full consistency with the structure of the heavy-quark expansion in QCD for both of these cases to the orders considered is verified.

Spectral representation for the Isgur-Wise function and subleading universal form factors is obtained in terms of the wave function of an infinitely heavy meson. Numerical estimates for the universal form factors are given.

In Chapter IV the choice of the numerical parameters of the model is discussed and form factors for many $D(D_s)$ and $B(B_s)$ to light mesons are calculated. Convenient parametrizations for the calculated form factors are given. Strong coupling constants of heavy mesons are estimated by analysing the residues of the form factors in the poles located beyond the physical region of meson decay. The strong coupling constant obtained by this procedure are found in agreement with the results of the direct calculation within our dispersion approach.

A detailed comparison with the experimental data and results from other approaches is presented. In all cases a good agreement with the available experimental data on form factors and strong coupling constants is observed.

In Chapter V the $B \rightarrow \gamma l \nu$ form factors and the weak annihilation in rare $B \rightarrow \rho \gamma$ decay is analysed within the factorization approximation. A detailed analysis of the contact terms in the weak annihilation amplitude is presented. A new contribution missed in the previous analyses of the weak annihilation is reported. Parameter-free numerical estimates of the relevant form factors are given.

Chapter VI contains the analysis of the nonfactorizable effects in the $B^0 - \bar{B}^0$ mixing due to soft gluon exchanges. Assuming the dominance of the local gluon condensate, the correction to factorization can be expressed in terms of the specific B meson transition form factors at zero momentum transfers. It is shown that the correction is strictly negative independent of the values of the form factors. The form factors are calculated within the dispersion approach and numerical estimates for them are obtained.

In Chapter VII the application of the dispersion approach to inclusive $B \rightarrow X_c l \nu$ decays is presented. Spectral representation for the integrated semileptonic rate in terms of the B meson wave function is constructed. The subtraction prescription is discussed and the absence of the $1/m_Q$ correction in the ratio of the bound to free quark decay rates is verified. Differential distributions are calculated in terms of the B meson wave function.

Conclusion summarises the main results.

II. SPECTRAL REPRESENTATION FOR BOUND STATE TRANSITION FORM FACTORS

This Chapter presents a formalism for the relativistic description of hadron form factors within the constituent quark picture [24,69–75].

Our approach is based on representing the amplitudes of hadron interactions in the form of the dispersion integrals over the hadron mass in terms of the hadron soft wave function. This procedure corresponds to a consistent relativistic treatment of the leading two-particle singularities of the scattering amplitude and the bound state form factors at spacelike momentum transfer q . The form factors at the timelike momentum transfers corresponding to the decay process $M_{ini} \rightarrow M_{final}$ are obtained by performing the analytical continuation in the variable q^2 from its negative to positive values. As a result, the weak decay form factors in the kinematical region $q^2 \leq (M_{ini} - M_{final})^2$ can be expressed through the bound state wave function.

The application of spectral representations to the description of composite systems has a long history [76–80]. Usually, spectral representations in q^2 are considered, q being the momentum transfer. In this case anomalous singularities in q^2 appear in the explicit form as separate contributions to spectral representations.

We present here an approach to the bound state description based on spectral representations in mass variables. Within this approach anomalous contributions turn out to be included in the usual dispersion integrals for the form factors at spacelike momentum transfers, relevant for the scattering problems. Form factors at timelike momentum transfers, corresponding to the decay processes, are obtained by performing the analytic continuation from the spacelike region. In this case, anomalous cuts give separate contributions to spectral representations for the form factors.

An important advantage of spectral representations in mass variables is the possibility to introduce in a consistent way a relativistic-invariant function which describes the motion of the constituents inside the bound state and which can be interpreted as the bound state wave function. We show how this function emerges when keeping in a relativistic and gauge-invariant way only two-particle singularities of the Feynman graphs.

In Section II A we give some details of describing relativistic bound state using spectral representations.

In Section II B we present all technical details of the description of a pseudoscalar meson within the dispersion approach (leptonic weak decay, two-photon decay, elastic electromagnetic form factor) and demonstrate the equivalence of the dispersion approach and the light-cone constituent quark model [57].

In Section II C we study form factors describing weak transitions between pseudoscalar mesons starting with the region of spacelike momentum transfers. As the next step, we perform the analytic continuation to the region $q^2 > 0$ and show how the anomalous contribution to the form factor in this region emerges. The origin of this anomalous contribution is connected with the non-Landau-type singularities of the Feynman triangle diagrams.

In Section II D we analyse electroweak properties of pseudoscalar mesons using a simplified parameterization of the meson wave function based on the heavy quark symmetry. This allows us to study the dependence of the axial-vector decay constant f_P and the heavy-meson elastic form factor on the heavy quark mass m_Q . In particular, we study the transition to the heavy quark limit $m_Q \rightarrow \infty$ and discuss the size of the subleading $1/m_Q$ -corrections for the heavy quark mass in the region of b and c quark masses. We calculate weak decay form factors at timelike momentum transfers and compare our results with other theoretical analyses and the experimental data.

A. Bound state description within dispersion relations

In this section we present some aspects of the dispersion approach to the relativistic description of the bound states. For the sake of argument we consider the case of two spinless constituents with the masses m_1 and m_2 interacting via exchanges of a meson with the mass μ . We start with the scattering amplitude of the real constituents

$$A(s, t) = \langle k'_1, k'_2 | S | k_1, k_2 \rangle, \quad s = (k_1 + k_2)^2, \quad t = (k_1 - k'_1)^2, \\ k_1^2 = k'^2_1 = m_1^2, \quad k_2^2 = k'^2_2 = m_2^2. \quad (2.1)$$

The amplitude as a function of s has the threshold singularities in the complex s -plane connected with elastic rescatterings of the constituents and production of new mesons at

$$s = (m_1 + m_2)^2, (m_1 + m_2 + \mu)^2, (m_1 + m_2 + 2\mu)^2 \dots \quad (2.2)$$

We assume that an S -wave bound state with the mass $M < m_1 + m_2$ exists, then the partial wave amplitude $A_0(s)$ has a pole at $s = M^2$. The amplitude $A(s, t)$ has also t -channel singularities with thresholds at $t = (n\mu)^2$; $n = 1, 2, 3 \dots$ connected with meson exchanges. If one needs to construct the amplitude in the low-energy region $s \geq (m_1 + m_2)^2$ the dispersion N/D representation turns out to be convenient. Consider the S -wave partial amplitude

$$A_0(s) = \int_{-1}^1 dz A(s, t(s, z)), \quad (2.3)$$

where $t(z) = -(1-z)\lambda(s, m_1^2, m_2^2)/2s$, $z = \cos\theta$ in the c.m.s. The $A_0(s)$ as a function of complex s has the right-hand singularities related to s -channel singularities of $A(s, t)$. In addition, it has left-hand singularities located at $s = (m_1 + m_2)^2 - (n\mu)^2$; $n = 1, 2, 3, \dots$. They come from t -channel singularities of $A(s, t)$. The unitarity condition in the region $s \approx (m_1 + m_2)^2$ reads

$$\text{Im } A_0(s) = \rho(s) |A_0(s)|^2, \quad \rho(s) = \frac{\lambda(s, m_1^2, m_2^2)}{16\pi s} \quad (2.4)$$

with $\rho(s)$ the two-particle phase space. The N/D method represents the partial amplitude as $A_0(s) = N(s)/D(s)$, where the function N has only left-hand singularities and D has only right-hand ones. The unitarity condition yields

$$\begin{aligned} D(s) &= 1 - \int_{(m_1+m_2)^2}^{\infty} \frac{d\tilde{s}}{\pi} \frac{\rho(\tilde{s})N(\tilde{s})}{\tilde{s} - s} \\ &\equiv 1 - B(s). \end{aligned} \quad (2.5)$$

Assuming the function N to be positive we introduce $G(s) = \sqrt{N(s)}$.

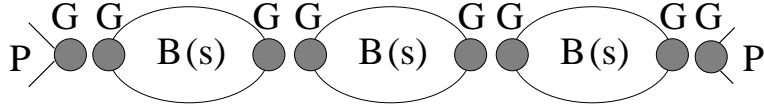


Fig. 1. One of the terms in the expansion of $A_0(s)$

Then the partial amplitude takes the form

$$\begin{aligned} A_0(s) &= G(s) [1 + B(s) + B^2(s) + B^3(s) + \dots] G(s) \\ &= \frac{G(s)G(s)}{1 - B(s)}. \end{aligned} \quad (2.6)$$

This expression can be interpreted as a series of loop diagrams of Fig.1 with the basic loop diagram

$$B(s) = \int_{(m_1+m_2)^2}^{\infty} \frac{d\tilde{s}}{\pi} \frac{\rho(\tilde{s}) G^2(\tilde{s})}{\tilde{s} - s}. \quad (2.7)$$

The bound state with the mass M corresponds to a pole both in the total and partial amplitudes at $s = M^2$ so $B(M^2) = 1$. Near the pole one has for the total amplitude

$$\begin{aligned} A &= \langle k'_1, k'_2 | p \rangle \frac{1}{M^2 - p^2} \langle p | k_1, k_2 \rangle + \text{regular terms} \\ &\equiv \chi_p^*(k'_1, k'_2) \frac{1}{M^2 - s} \chi_p(k_1, k_2) + \dots \end{aligned} \quad (2.8)$$

where $\chi_p(k_1, k_2)$ is the amputated Bethe-Salpeter amplitude of the bound state. The dispersion amplitude near the pole reads

$$\begin{aligned} A &= N/D + \text{regular terms related to other partial waves} \\ &= \frac{G^2(M^2)}{(M^2 - s)B'(M^2)} + \dots \\ &\equiv \frac{G_v^2(M^2)}{M^2 - s} + \dots \end{aligned} \quad (2.9)$$

where G_v is a vertex of the bound state transition to the constituents and

$$B'(M^2) = \int_{(m_1+m_2)^2}^{\infty} \frac{d\tilde{s}}{\pi} \frac{\rho(\tilde{s}) G^2(\tilde{s})}{(\tilde{s} - M^2)^2}. \quad (2.10)$$

The singular terms in Eqs (2.8) and (2.9) correspond to each other and hence

$$\chi_p(k_1, k_2) \rightarrow G_v(s) \equiv \frac{G(s)}{\sqrt{B'(M^2)}}. \quad (2.11)$$

Underline that among right-hand singularities only the two-particle cut is taken into account in the constructed dispersion amplitude.

Let us turn to the interaction of the two-constituent system with an external electromagnetic field. The amplitude of this process $T_\mu = \langle k'_1, k'_2 | J_\mu | k_1, k_2 \rangle$ in the case of a bound state takes the form

$$\begin{aligned} T_\mu &= \langle k'_1, k'_2 | p' \rangle \frac{1}{p'^2 - M^2} \langle p' | J_\mu | p \rangle \frac{1}{p^2 - M^2} \langle p | k_1, k_2 \rangle + \dots \\ &= \chi_p^*(k'_1, k'_2) \frac{1}{p'^2 - M^2} (p + p')_\mu F(q^2) \frac{1}{p^2 - M^2} \chi_p(k_1, k_2) + \dots \end{aligned} \quad (2.12)$$

where the bound state form factor is defined according to the relation

$$\langle p' | J_\mu | p \rangle = (p' + p)_\mu F(q^2). \quad (2.13)$$

The dispersion amplitude T_μ with only two-particle singularities in the p^2 - and p'^2 -channels taken into account is given [72] by the series of graphs in Fig.2.

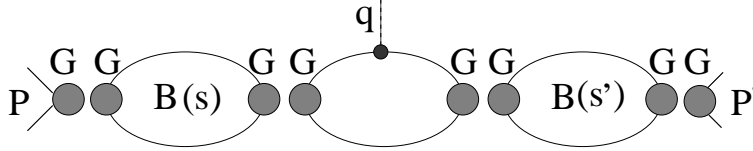


Fig. 2. One of the terms in the series for T_μ .

These graphs are obtained from the dispersion scattering amplitude series by inserting a photon line into constituent lines. The amplitude has the form

$$\begin{aligned} T_\mu(p', p, q) &= 2p_\mu(q) T(s', s, q^2) + \frac{q_\mu}{q^2} C, \\ p^2 &= s, \quad p'^2 = s', \quad q = p' - p, \quad p_\mu(q) = (p - \frac{qp}{q^2})_\mu \end{aligned} \quad (2.14)$$

The dispersion method allows one to determine the transverse part $T(s, s', q^2)$ of the amplitude. Summation of the series of dispersion graphs in Fig.2 gives

$$T(s', s, q^2) = \frac{G(s)}{1 - B(s)} \Gamma(s', s, q^2) \frac{G(s')}{1 - B(s')}. \quad (2.15)$$

Here

$$\Gamma(s', s, q^2) = \int \frac{d\tilde{s} G(\tilde{s})}{\pi(\tilde{s} - s)} \frac{d\tilde{s}' G(\tilde{s}')}{\pi(\tilde{s}' - s')} \Delta(\tilde{s}', \tilde{s}, q^2),$$

and $\Delta(\tilde{s}', \tilde{s}, q^2)$ is the double spectral density of the three-point Feynman graph with a pointlike vertex of the constituent interaction.

The longitudinal part C is determined by the Ward identity

$$C = \frac{G(s)}{1 - B(s)} \{B(s') - B(s)\} \frac{G(s')}{1 - B(s')}. \quad (2.16)$$

In the region $s \simeq s' \simeq M^2$, T_μ develops both s and s' poles, so we write

$$T_\mu(p', p, q) = \frac{G_v(M^2)}{M^2 - s} (p' + p)_\mu F(q^2) \frac{G_v(M^2)}{M^2 - s'} + \text{less singular terms} \quad (2.17)$$

where

$$F(q^2) = \int_{(m_1+m_2)^2}^{\infty} \frac{d\tilde{s} G_v(\tilde{s})}{\pi(\tilde{s} - M^2)} \frac{d\tilde{s}' G_v(\tilde{s}')}{\pi(\tilde{s}' - M^2)} \Delta(\tilde{s}', \tilde{s}, q^2). \quad (2.18)$$

is the bound-state form factor (see (2.11) and (2.12)). Thus, the quantity $\langle p' | J_\mu | p \rangle$ corresponds to the three-point dispersion graph with the vertices G_v . One can derive the following important relation

$$\Delta(\tilde{s}', \tilde{s}, 0) = \pi \delta(\tilde{s}' - \tilde{s}) \rho(\tilde{s}). \quad (2.19)$$

This is a consequence of the Ward identity which relates the three-point graph at zero momentum transfer to the loop graph. Making use of the relations (2.19) and (2.10), one obtains the normalization of the form factor at zero momentum

$$F(0) = 1, \quad (2.20)$$

which is just the charge conservation condition. The expression (2.18) gives the form factor in terms of the N -function of the constituent scattering amplitude and double spectral density of the Feynman graph.

If the constituent is a nonpoint particle, the expression (2.18) should be multiplied by form factor of an on-shell constituent.

In general, for constructing the spectral representation of the amplitude describing the bound state interaction within a two-particle approximation, the following prescription is valid: the spectral density of the amplitude is just the spectral density of the corresponding Feynman graph multiplied by G_v . The amplitude obtained through this procedure takes into account in a consistent relativistic-invariant way only two-particle singularities of the corresponding amplitude.

B. Quark structure of pseudoscalar mesons

The pseudoscalar meson P with the mass M is considered to be a bound state of the constituent quark with the mass m_1 and the antiquark with the mass m_2 . Therefore in order to derive the meson interaction amplitude for e.g. leptonic decay $P \rightarrow l\nu$, two-photon decay of the neutral pseudoscalar meson $P^0 \rightarrow \gamma\gamma$, and the elastic electromagnetic interaction $\langle P(p') | J_\mu | P(p) \rangle$, we start with the corresponding amplitudes of the constituent quark interactions $\langle l\nu | Q\bar{Q} \rangle$, $\langle \gamma\gamma | Q\bar{Q} \rangle$, and $\langle Q\bar{Q} | J_\mu | Q\bar{Q} \rangle$ and single out poles corresponding to the pseudoscalar meson. The amplitude of the $Q\bar{Q}$ interaction turns out to be the basic quantity for describing the bound state properties. Near the pole corresponding to the bound state with the quantum numbers $J^P = 0^-$, the amplitude is dominated by the S -wave partial amplitude. The latter can be expressed in the two-particle approximation through the dispersion loop graph B_{ps} with the vertex

$$\frac{\bar{Q}^a(k_1, m_1) i\gamma_5 Q^a(-k_2, m_2)}{\sqrt{N_c}} G(s) \quad (2.21)$$

with a a color index, $N_c = 3$ the number of quark colors, $k_1^2 = m_1^2$, $k_2^2 = m_2^2$, and $(k_1 + k_2)^2 = s \neq M^2$. For on-shell constituents, the expression (2.21) is the only independent spinorial structure.

The dispersion loop graph Fig. 3, which is connected with the meson vertex normalization, reads

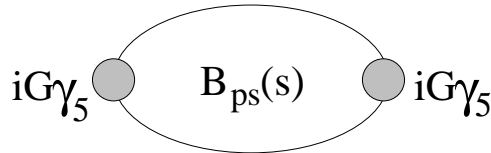


Fig. 3. Meson dispersion loop graph $B_{ps}(P^2)$.

$$B_{ps}(p^2) = \int_{(m_1+m_2)^2}^{\infty} \frac{ds G^2(s)}{\pi(s-p^2)} \rho_{ps}(s), \quad B_{ps}(M^2) = 1, \quad (2.22)$$

with $\rho_{ps}(s)$ the spectral density of the Feynman loop graph

$$\begin{aligned} \rho_{ps}(s, m_1, m_2) &= \frac{1}{8\pi^2} \int dk_1 dk_2 \delta(k_1^2 - m_1^2) \delta(k_2^2 - m_2^2) \delta(\tilde{p} - k_1 - k_2) \\ &\quad \times (-1) \text{Sp} \left((\hat{k}_1 + m_1) i\gamma_5 (m_2 - \hat{k}_2) i\gamma_5 \right) \\ &= \frac{\lambda^{1/2}(s, m_1^2, m_2^2)}{8\pi s} (s - (m_1 - m_2)^2) \theta(s - (m_1 + m_2)^2), \end{aligned} \quad (2.23)$$

where $s = \tilde{p}^2$ and

$$\lambda(s, m_1^2, m_2^2) \equiv (s + m_1^2 - m_2^2)^2 - 4sm_1^2.$$

Taking into account constituent-quark rescatterings leads to the renormalization of G (Section II A) and the soft constituent-quark structure of the pion is given by the vertex

$$\frac{\bar{Q}^a(k_1, m_1) i\gamma_5 Q^a(-k_2, m_2)}{\sqrt{N_c}} G_v(s) \quad (2.24)$$

where $G_v(s) = G(s)/B'(M^2)$, such that

$$\int \frac{G_v^2(s) \rho_{ps}(s, m_1, m_2) ds}{\pi(s - M^2)^2} = 1 \quad (2.25)$$

Once the soft vertex (2.24) is fixed, we can proceed with calculating meson interaction amplitudes.

1. Leptonic decay constant

Let us consider the decay $P \rightarrow l\nu$. The corresponding amplitude reads

$$\langle 0 | A_\mu(0) | P(p) \rangle = i p_\mu f_P. \quad (2.26)$$

In this expression $A_\mu = \bar{q}^a(0) \gamma_\mu \gamma_5 q^a(0)$ is the axial-vector current where summation over quark colours is implied and f_P is the meson axial-vector decay constant.

We must first take into account that the pion structure is described in terms of the constituent quarks whereas the current $A_\mu(0) = \bar{q} \gamma_\mu \gamma_5 q$ is given in terms of the current quarks. So let us consider the quantity

$$\langle 0 | A_\mu(0) | Q\bar{Q} \rangle. \quad (2.27)$$

The bare matrix element which emerges before we take into account the soft interactions of the constituent quarks has the structure

$$\begin{aligned} A_\mu^0 &= \langle 0 | A_\mu(0) | Q(k_1) \bar{Q}(k_2) \rangle_{bare} \\ &= \bar{Q}(-k_2) [\gamma_\mu \gamma_5 g_A^0(p^2) + p_\mu \gamma_5 h_+^0(p^2) + (k_1 - k_2)_\mu \gamma_5 h_-^0(p^2)] Q(k_1) \end{aligned} \quad (2.28)$$

If current quarks were identical to constituent ones we would have had

$$g_A^0(p^2) \equiv 1, \quad h_+^0(p^2) \equiv 0, \quad h_-^0(p^2) \equiv 0. \quad (2.29)$$

It is reasonable to assume that the form factors g^0 and h_\pm^0 are not far from these values [81,82].

Soft rescatterings of the constituent quarks lead to the series of the dispersion graphs of Fig. 4.

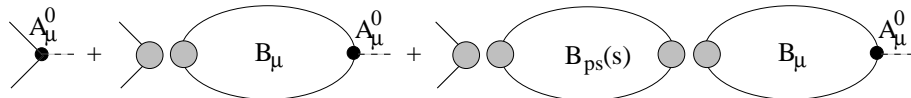


Fig. 4. The series of dispersion graphs for $\langle Q\bar{Q} | A_\mu(0) | 0 \rangle$.

The loop diagram B_{ps} is already known, so let us discuss $B_\mu(p)$. The latter contains the pseudoscalar vertex and the bare matrix element A_μ^0 . The spectral density of the corresponding Feynman graph reads ($\tilde{p}^2 = s$)

$$-\frac{\sqrt{N_c}}{8\pi^2} \int dk_1 dk_2 \delta(k_1^2 - m_1^2) \delta(k_2^2 - m_2^2) \delta(\tilde{p} - k_1 - k_2) \\ \times Sp \left(\left\{ \gamma_\mu \gamma_5 g_A^0(s) + P_\mu \gamma_5 h_+^0(s) + (k_1 - k_2)_\mu \gamma_5 h_-^0(s) \right\} (\hat{k}_1 + m_1) i \gamma_5 (m_2 - \hat{k}_2) \right). \quad (2.30)$$

The trace is equal to

$$-4i(k_{1\mu} m_2 + k_{2\mu} m_1) g_A^0(s) + 4i(k_1 + k_2)_\mu (k_1 k_2 + m_1 m_2) h_+^0(s) \\ + 4i(k_1 - k_2)_\mu (k_1 k_2 + m_1 m_2) h_-^0(s) \quad (2.31)$$

The expression for the loop graph B_μ takes the form

$$B_\mu(p) = 4ip_\mu \sqrt{N_c} \int_{(m_1+m_2)^2}^{\infty} \frac{ds G(s)}{\pi(s-p^2)} \frac{\lambda^{1/2}(s, m_1^2, m_2^2)}{16\pi s} \frac{s - (m_1 - m_2)^2}{2s} \\ \times [(m_1 + m_2) g_A^0(s) - s h_+^0(s) - (m_1^2 - m_2^2) h_-^0(s)]. \quad (2.32)$$

The amplitude with the quark rescatterings taken into account has the same spinorial structure as the bare amplitude

$$\langle 0 | A_\mu(0) | Q(k_1) \bar{Q}(k_2) \rangle = \bar{Q}(-k_2) [\gamma_\mu \gamma_5 g_A(p^2) + p_\mu \gamma_5 h_+(p^2) + (k_1 - k_2)_\mu \gamma_5 h_-(p^2)] Q(k_1) \quad (2.33)$$

with

$$g_A(p^2) = g_A^0(p^2) \\ h_-(p^2) = h_-^0(p^2) \\ h_+(p^2) = h_+^0(p^2) - \frac{G(p^2)}{1 - B_{ps}(p^2)} \int \frac{ds G(s)}{\pi(s-p^2)} \frac{\lambda^{1/2}(s, m_1^2, m_2^2)}{16\pi s} \frac{s - (m_1 - m_2)^2}{2s} \\ \times 4[(m_1 + m_2) g_A^0(s) - s h_+^0(s) - (m_1^2 - m_2^2) h_-^0(s)]$$

The form factor h_+ develops the pole at $p^2 = M^2$ since $B_{ps}(M^2) = 1$. Near $p^2 = M^2$ the pole dominates the amplitude

$$\langle 0 | A_\mu | \bar{Q} Q \rangle = \langle 0 | A_\mu | P(p) \rangle \frac{1}{M^2 - p^2} \langle P(p) | Q \bar{Q} \rangle + \text{regular terms}. \quad (2.34)$$

Comparing the pole terms in (2.33) and (2.34) and making use of the relation

$$\langle P(p) | Q \bar{Q} \rangle \rightarrow \frac{\bar{Q} i \gamma_5 Q}{\sqrt{N_c}} G_v \quad (2.35)$$

we find that

$$\langle 0 | A_\mu | P(p) \rangle = ip_\mu f_P \quad (2.36)$$

with

$$f_P = 4\sqrt{N_c} \int \frac{ds G_v(s)}{\pi(s-M^2)} \frac{\lambda^{1/2}(s, m_1^2, m_2^2)}{16\pi s} \frac{s - (m_1 - m_2)^2}{2s} \\ \times [(m_1 + m_2) g_A^0(s) - s h_+^0(s) - (m_1^2 - m_2^2) h_-^0(s)]. \quad (2.37)$$

Assuming that in reality g_A^0 and h^0 are not far from the limit (2.29), we come to the relation

$$f_P = \sqrt{N_c} (m_1 + m_2) g_A^0(M^2) \int_{(m_1+m_2)^2}^{\infty} \frac{ds G_v(s)}{\pi(s-M^2)} \frac{\lambda^{1/2}(s, m_1^2, m_2^2)}{8\pi s} \frac{(s - (m_1 - m_2)^2)}{s}. \quad (2.38)$$

2. Two-photon decay of a neutral pseudoscalar meson

Let us consider the two-photon decay of the neutral pseudoscalar meson P_0 . Its constituent quark structure is described by the vertex

$$\frac{\bar{Q}i\gamma_5 Q}{\sqrt{N_c}} G_v. \quad (2.39)$$

The rate of the decay $P_0(p) \rightarrow 2\gamma$ can be written as

$$\Gamma = \frac{\pi}{4} \alpha^2 M^3 g_{P\gamma\gamma}^2, \quad g_{P\gamma\gamma} = G_{P\gamma\gamma}(M^2, 0, 0), \quad (2.40)$$

where the form factor $G_{P\gamma\gamma}$ is connected with the amplitude

$$\langle 0 | J_{\alpha_2}^{em}(q_2) J_{\alpha_3}^{em}(q_3) | P(p) \rangle = 2\epsilon_{\alpha_2\alpha_3\beta_2\beta_3} q_2^{\beta_2} q_3^{\beta_3} G_{P\gamma\gamma}(M^2, q_2^2, q_3^2). \quad (2.41)$$

The electromagnetic current $J_\mu^{em}(0) = \bar{q}(0)\gamma_\mu q(0)$ is defined through current quarks, whereas the meson structure is described in terms of the constituent quarks. So, for calculating the meson amplitude the constituent quark amplitude of the electromagnetic current is necessary. The latter is assumed to have the following structure

$$\langle Q(k') | \bar{q}(0)\gamma_\mu q(0) | Q(k) \rangle = \bar{Q}(k')\gamma_\mu Q(k) f_c(q^2), \quad q = k' - k. \quad (2.42)$$

The constituent charge form factor $f_c(q^2)$ is normalized such that $f_c(0) = e_c$, the constituent charge. The anomalous magnetic moment of the constituent quark is neglected in the expression (2.42), but it can be included into consideration straightforwardly.

Hereafter we skip the intermediate steps and consider only the residue of the constituent interaction amplitude which determines the bound-state amplitude. From now on we shall use the following notations: \tilde{p} is the off-shell momentum $\tilde{p}^2 = s$ which is used for the calculation of the imaginary parts of the Feynman diagrams, p is the on-shell bound state momentum, $p^2 = M^2$.

The single dispersion representation for the form factor $G_{P\gamma\gamma}$ reads

$$G_{P\gamma\gamma}(M^2, q_2^2, q_3^2) = f_c(q_2^2) f_c(q_3^2) \int \frac{ds G_v(s)}{\pi(s - M^2)} \Delta_{P\gamma\gamma}(s, q_2^2, q_3^2). \quad (2.43)$$

Here $\Delta_{P\gamma\gamma}$ is the spectral of the triangle Feynman graph of Fig.5 and can be obtained from the following relation

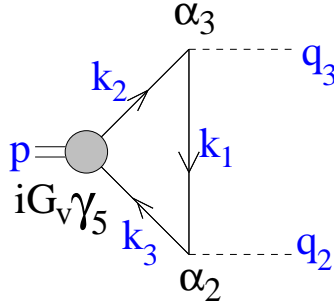


Fig. 5. The graph describing the decay $P^0 \rightarrow \gamma\gamma$.

$$\begin{aligned} & -\epsilon_{\alpha_2\alpha_3\beta_2\beta_3} q_2^{\beta_2} q_3^{\beta_3} \Delta_{P\gamma\gamma}(s, q_2^2, q_3^2) \\ &= -\frac{\sqrt{N_c}}{8\pi^2} \int dk_1 dk_2 dk_3 \delta(\tilde{p} - k_2 - k_3) \delta(k_2 - k_1 - q_3) \frac{\delta(k_2^2 - m^2) \delta(k_3^2 - m^2)}{m^2 - k_1^2} \\ & \times Sp \left(i\gamma_5 (m - \hat{k}_3) \gamma_{\alpha_2} (m + \hat{k}_1) \gamma_{\alpha_3} (m + \hat{k}_2) \right), \end{aligned} \quad (2.44)$$

where $\tilde{p}^2 = s$. The trace reads

$$Sp \left(i\gamma_5 (m - \hat{k}_3) \gamma_{\alpha_2} (m + \hat{k}_1) \gamma_{\alpha_3} (m + \hat{k}_2) \right) = 4m\epsilon_{\alpha_2\alpha_3\beta_2\beta_3} q_2^{\beta_2} q_3^{\beta_3}, \quad (2.45)$$

and we find

$$\Delta_{P\gamma\gamma}(s, q_2^2, q_3^2) = \frac{m\sqrt{N_c}}{4\pi} \frac{\theta(s - 4m^2)}{\lambda^{1/2}(s, q_2^2, q_3^2)} \log \left(\frac{s - q_2^2 - q_3^2 + \lambda^{1/2}(s, q_2^2, q_3^2) \sqrt{1 - 4m^2/s}}{s - q_2^2 - q_3^2 - \lambda^{1/2}(s, q_2^2, q_3^2) \sqrt{1 - 4m^2/s}} \right) \quad (2.46)$$

Substituting (2.46) into (2.43), one obtains $G_{P\gamma\gamma}$ for off-shell photons. For real photons one finds

$$g_{P\gamma\gamma} = \frac{m\sqrt{N_c}}{4\pi} e_c^2 \int_{4m^2}^{\infty} \frac{ds G_v(s)}{\pi(s - M^2)} \frac{1}{s} \log \left(\frac{1 + \sqrt{1 - 4m^2/s}}{1 - \sqrt{1 - 4m^2/s}} \right) \quad (2.47)$$

3. Elastic electromagnetic form factor

The elastic electromagnetic form factor of a pseudoscalar meson with the mass M is given by the following matrix element

$$\langle P(p') | J_\mu^{em}(0) | P(p) \rangle = (p' + p)_\mu F^{el}(q^2), \quad (2.48)$$

where $p^2 = p'^2 = M^2$, $q = p - p'$ and $q^2 < 0$. The form factor $F^{el}(q^2)$ describes the amplitude of the photon emission from the bound state which depends on the three independent Lorentz invariants. It is convenient to choose such invariants as the squares of the three external momenta p^2 , p'^2 , and q^2 . Therefore the form factor $F^{el}(q^2)$ is in fact the function of the three variables $F^{el}(p^2, p'^2, q^2)$, but considered for fixed values of the two invariants $p^2 = M^2$, $p'^2 = M^2$.

Assuming again the structure of the constituent quark matrix element of the the electromagnetic as given by Eq. (2.42), the meson elastic charge form factor can be written in the form

$$F^{el}(q^2) = f_1(q^2) H(q^2, m_1^2, m_2^2) + f_2(q^2) H(q^2, m_2^2, m_1^2) \quad (2.49)$$

in terms of the form factors H . The quantity $H(q^2, m_1^2, m_2^2)$ describes the subprocess when the constituent 1 interacts with the photon, while the constituent 2 remains spectator (Fig.6).

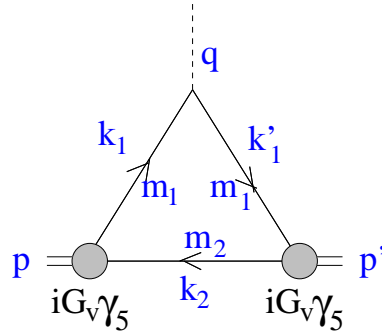


Fig. 6. Triangle diagram describing $H(q^2, m_1^2, m_2^2)$.

Clearly, the form factor $H(q^2, m_1^2, m_2^2)$ also implicitly depends on the invariant variables p^2 and p'^2 , such that $H(q^2, m_1^2, m_2^2) = H(q^2, p^2 = M^2, p'^2 = M^2, m_1^2, m_2^2)$. As well known [80] the form factor $H(q^2, p^2, p'^2, m_1^2, m_2^2)$ is an analytic function of the external mass variables p^2 and p'^2 and at $q^2 < 0$ satisfies the double spectral representation

$$H(q^2, m_1^2, m_2^2) = \int \frac{ds G_v(s)}{\pi(s - M^2)} \frac{ds' G_v(s')}{\pi(s' - M^2)} \Delta_V(s', s, q^2 | m_1, m_1, m_2). \quad (2.50)$$

Here Δ_V is the double spectral density of H over the variables P^2 and P'^2 . According to the Landau-Cutkosky rules, Δ_V can be calculated through the following procedure: one should place all internal particles on their mass shell, $k_1^2 = m_1^2$, $k_1'^2 = m_1^2$, $k_2^2 = m_2^2$ but go off the mass shell for the variables p^2 and p'^2 , i.e. instead of the on-shell external momenta p and p' consider off-shell external momenta \tilde{p} and \tilde{p}' , such that $\tilde{p}^2 = s$, $\tilde{p}'^2 = s'$, and $(\tilde{p}' - \tilde{p})^2 = q^2$, but $\tilde{p}' - \tilde{p} = \tilde{q} \neq q$. The double spectral density Δ is then determined from the following relation

$$\begin{aligned} & \frac{1}{8\pi} \int dk_1 dk'_1 dk_2 \delta(k_1^2 - m_1^2) \delta(k'_1{}^2 - m_1^2) \delta(k_2^2 - m_2^2) \delta(\tilde{p} - k_1 - k_2) \delta(\tilde{p}' - k'_1 - k_2) \\ & \times (-1) Sp \left((\hat{k}'_1 + m_1) \gamma_\mu (\hat{k}_1 + m_1) i \gamma_5 (m_2 - \hat{k}_2) i \gamma_5 \right) = 2\tilde{p}_\mu(q) \Delta_V(s', s, q^2 | m_1, m_1, m_2) \end{aligned} \quad (2.51)$$

with

$$\tilde{p}_\mu(q) = (\tilde{p} - \frac{\tilde{q}\tilde{p}}{\tilde{q}^2} \tilde{q})_\mu.$$

The trace reads

$$\begin{aligned} & \frac{1}{4} Sp \left((\hat{k}'_1 + m_1) \gamma_\mu (\hat{k}_1 + m_1) \gamma_5 (m_2 - \hat{k}_2) \gamma_5 \right) \\ & = 2k'_{1\mu}(s - (m_1 - m_2)^2) + 2k_{1\mu}(s' - (m_1 - m_2)^2) + 2k_{2\mu}q^2 \end{aligned} \quad (2.52)$$

Multiplying both sides of (2.51) by P_μ and using (2.52) one obtains for $q^2 < 0$

$$\begin{aligned} & \Delta_V(s', s, q^2 | m_1, m_1, m_2) \\ & = \frac{-q^2}{4\lambda^{3/2}(s', s, q^2)} (s's + (s' + s - q^2)m_2(m_1 - m_2) - (m_1 + m_2)(m_1 - m_2)^3) \\ & \quad \times \theta(s - (m_1 + m_2)^2) \theta(s' - (m_1 + m_2)^2) \\ & \quad \times \theta(-q^2(s' + s - q^2 + 2(m_1^2 - m_2^2))^2 + \lambda(s', s, q^2)(q^2 - 4m_1^2)) \end{aligned} \quad (2.53)$$

with $\lambda(s', s, q^2) = (s' + s - q^2)^2 - 4s's$.

At $q^2 = 0$ one finds

$$\Delta_V(s', s, q^2 = 0 | m_1, m_1, m_2) = \pi \rho_{ps}(s, m_1, m_2) \delta(s' - s), \quad (2.54)$$

and

$$\begin{aligned} F^{el}(0) &= (e_1 + e_2) \int_{(m_1+m_2)^2}^{\infty} \frac{ds G_v^2(s)}{\pi(s - M^2)^2} \rho_{ps}(s, m_1, m_2) \\ &= e_1 + e_2. \end{aligned} \quad (2.55)$$

This relation is the direct consequence of the Ward identity and corresponds to the electric charge conservation.

4. Dispersion approach in terms of the light-cone variable

For some applications and for comparison with the light-cone technique, it is convenient to rewrite our explicitly relativistic-invariant spectral representations in terms of the light-cone variables

$$k_- = \frac{1}{\sqrt{2}}(k_0 - k_z); \quad k_+ = \frac{1}{\sqrt{2}}(k_0 + k_z); \quad k^2 = 2k_+k_-k_\perp^2. \quad (2.56)$$

Most easily this can be done by introducing the light-cone variables directly into the integral representation for the form factor spectral density (2.51). The variables (2.56) should be connected with some specific reference frame, which can be specified by fixing components of the physical momenta p and q . It is convenient to choose the reference frame in which

$$p_\perp = 0, \quad q_+ = 0, \quad q_\perp^2 = -q^2. \quad (2.57)$$

Notice that this choice is only possible in the region $q^2 < 0$.

The choice of the reference frame in the form (2.57) allows us to choose components of the momenta in a convenient way. For the physical on-shell momenta¹

¹We use the notation $a_\mu = (a_+, a_-, a_\perp)$.

$$\begin{aligned}
p &= (p_+, \frac{M^2}{2p_+}, 0) \\
p' &= (p_+, \frac{M_2^2 + q_\perp^2}{2p_+}, -q_\perp) \\
q &= (0, \frac{-q_\perp^2}{2p_+}, q_\perp);
\end{aligned} \tag{2.58}$$

For the dispersion off-shell momenta:

$$\begin{aligned}
\tilde{p} &= (p_+, \frac{s}{2p_+}, 0) \\
\tilde{p}' &= (p_+, \frac{s' + q_\perp^2}{2p_+}, -q_\perp) \\
\tilde{q} &= (0, \frac{s - s' - q_\perp^2}{2p_+}, q_\perp).
\end{aligned} \tag{2.59}$$

A specific and good feature of this choice is that the (+) and (\perp) components of the on-shell vectors and the corresponding off-shell vectors are equal to each other, such that all off-shell effects in the description of a bound state are completely shifted to the (−) component of the momenta.

Now, let us consider (2.51) and set $\mu = +$ in both sides of this equation. Using the result for the trace (2.52) for $\mu = +$, and performing the k_- integration, we obtain

$$\begin{aligned}
\Delta_V(s', s, q^2 | m_1, m_1, m_2) &= \frac{1}{16\pi} \int \frac{dx d^2 k_\perp}{x(1-x)} \delta \left(s - \frac{m_1^2}{1-x} - \frac{m_2^2}{x} - \frac{k_\perp^2}{x(1-x)} \right) \\
&\times \delta \left(s' - \frac{m_1^2}{1-x} - \frac{m_2^2}{x} - \frac{(k_\perp + xq_\perp)^2}{x(1-x)} \right) (s' + s - 2(m_1 - m_2)^2 - \frac{x}{1-x} q^2)
\end{aligned} \tag{2.60}$$

Here $x = k_{2+}/p_+$ and $k_\perp = k_{2\perp}$.

Substituting (2.60) into (2.50) and performing s and s' integrations, one derives

$$H(q_\perp^2, m_1, m_2) = \int dx d^2 k_\perp \psi(x, k_\perp) \psi(x, k_\perp + xq_\perp) \beta(x, k_\perp, q_\perp) \tag{2.61}$$

where the radial light-cone wave function of a pseudoscalar meson is introduced

$$\begin{aligned}
\psi(x, k_\perp) &= \frac{G_v(s) \sqrt{s - (m_1 - m_2)^2}}{\pi^{3/2} \sqrt{8} (s - M^2) \sqrt{x(1-x)}}, \\
s &= \frac{m_1^2}{1-x} + \frac{m_2^2}{x} + \frac{k_\perp^2}{x(1-x)}
\end{aligned} \tag{2.62}$$

and

$$\beta = \frac{s - (m_1 - m_2)^2 + k_\perp q_\perp / (1-x)}{\sqrt{s - (m_1 - m_2)^2} \sqrt{s' - (m_1 - m_2)^2}}, \quad \beta(q_\perp = 0) = 1 \tag{2.63}$$

The function β accounts for the contribution of spins. It is different from unity at $q_\perp \neq 0$ because both the spin-nonflip and spin-flip amplitudes of the interacting quark contribute. The Eq.(2.55) is the normalization condition for the soft radial wave function

$$\int dx d^2 k_\perp |\psi(x, k_\perp)|^2 = 1. \tag{2.64}$$

In terms of this wave function, the pseudoscalar meson axial-vector decay constant f_P is represented as

$$f_P = g_A \frac{\sqrt{N_c}}{\sqrt{2}\pi^{3/2}} \int dx d^2 k_\perp \psi(x, k_\perp) \frac{m_2(1-x) + m_1 x}{\sqrt{s - (m_1 - m_2)^2}} \tag{2.65}$$

This expression can be easily deduced by introducing the light-cone variables into the dispersion representation (2.30), making use of (2.31) and examining the $\mu = +$ component of the axial current.

Similarly, introducing the light-cone variables into (2.44) yields the following expression for $g_{P\gamma\gamma}$

$$g_{P\gamma\gamma} = \frac{m\sqrt{N_c}}{\sqrt{2}\pi^{3/2}} \int \frac{dx d^2 k_\perp}{\sqrt{x(1-x)}} \psi(x, k_\perp) \frac{x}{(m^2 + k_\perp^2)\sqrt{s}} \quad (2.66)$$

The same expressions for the pseudoscalar meson elastic form factor, leptonic decay constant, and the two-photon decay constant as (2.61)-(2.66) were derived within the light-cone quark model in refs [14,23], with our $G_v(s)$ just equal to $h_0(P)$ of ref. [14]. As we see later, the light-cone quark model and the dispersion approach also lead to the same expression for the form factor F_+ describing weak transitions between pseudoscalar mesons at $q^2 < 0$. This is not at all strange as both of these approaches are based on the assumption of dominance of the $q\bar{q}$ components in the description of the meson properties.

However, the dispersion approach has several advantages compared to the light-cone quark model. In particular, the light-cone quark model faces at least two difficulties in applications to inelastic transitions: The first problem emerges already in the spacelike region of the momentum transfers in considering transitions induced by the current of higher spin. It is related to the proper choice of the current components to be used for the extraction of the form factors (so-called 'good' and 'bad' components and the problem to satisfy the angular condition, see [23] for discussion and references).

The second problem emerges for the description of hadron transition processes at $q^2 > 0$. The light-cone quark model can consistently take into account the spectator contribution, whereas contributions of the so-called Z-graphs (also called non-partonic, or pair-creation subprocesses) are in general beyond the scope of the light-cone treatment. The Z-graph can be calculated only for some exceptional simple forms of the light-cone wave functions. Unfortunately, in the light-cone treatment such contribution is inevitably present for processes in the region of timelike momentum transfers where it cannot be suppressed by an appropriate choice of the reference frame.

As we shall see, both of these problems find their solution in the dispersion approach.

C. Form factors of meson transitions

In this section we examine the electroweak transitions of pseudoscalar mesons. First, we derive the transition form factors at $q^2 < 0$ in the form of the relativistic dispersion representations. Second, these dispersion representations allow us to perform the analytic continuation in q^2 and derive the form factors of semileptonic decays of pseudoscalar mesons at $q^2 > 0$.

1. The pseudoscalar meson transition form factor at $q^2 < 0$

The amplitude of the weak transition of pseudoscalar mesons $M_1 \rightarrow M_2$ (Fig.7) is determined by the two form factors F_+ and F_-

$$\begin{aligned} \langle p_2, M_2 | V_\mu | p_1, M_1 \rangle &= (p_1 + p_2)_\mu F_+(q^2) + (p_1 - p_2)_\mu F_-(q^2) \\ \langle p_2, M_2 | A_\mu | p_1, M_1 \rangle &= 0, \\ p_1^2 &= M_1^2, \quad p_2^2 = M_2^2, \quad p_1 - p_2 = q. \end{aligned} \quad (2.67)$$

The weak currents are defined in terms of the current quarks

$$\begin{aligned} V_\mu &= \bar{q}_1^a(0) \gamma_\mu q_2^a(0), \\ A_\mu &= \bar{q}_1^a(0) \gamma_\mu \gamma_5 q_2^a(0). \end{aligned} \quad (2.68)$$

The structure of the mesons is described in terms of the constituent quarks by the vertices

$$\begin{aligned} M_1 : & \quad \frac{\bar{Q}_2(k_2) i \gamma_5 Q_3(-k_3)}{\sqrt{N_c}} G_{v1}(\tilde{p}_1^2), \\ M_2 : & \quad \frac{\bar{Q}_1(k_1) i \gamma_5 Q_3(-k_3)}{\sqrt{N_c}} G_{v2}(\tilde{p}_2^2) \end{aligned} \quad (2.69)$$

and $G_{v1,2}$ are normalized according to Eq. (2.25).

For calculating the transition amplitude (2.67) we again need the constituent quark matrix element of the weak current which is taken in the form

$$\langle Q_1(k_1) | \bar{q}_1(0) \gamma_\mu q_2(0) | Q_2(k_2) \rangle = \bar{Q}_1(k_1) \gamma_\mu Q_2(k_2) f_{21}(q^2) \quad (2.70)$$

As in the case of the elastic form factor, the transition form factors F_\pm can be treated as the functions of the three invariants p_1^2 , p_2^2 , and q^2 , taken at $p_1^2 = M_1^2$ and $p_2^2 = M_2^2$. The form factors are analytic functions of the external mass variables p_1^2 and p_2^2 and can be represented by the following double spectral representations

$$F_\pm(q^2) = f_{21}(q^2) \int \frac{ds_1 G_{v1}(s_1)}{\pi(s_1 - M_1^2)} \frac{ds_2 G_{v2}(s_2)}{\pi(s_2 - M_2^2)} \Delta_\pm(s_1, s_2, q^2 | m_1, m_2, m_3) \quad (2.71)$$

Here Δ_\pm are the double spectral densities of the triangle Feynman graph corresponding to Fig.7 in the p_1^2 and p_2^2 -channels

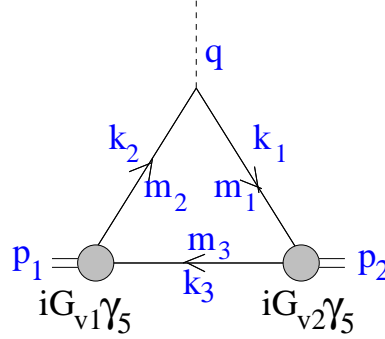


Fig. 7. The dispersion graph for the decay $\langle P_2 | V_\mu^{aa} | P_1 \rangle$.

To calculate Δ_\pm at $q^2 < 0$, we put internal particles on their mass shell, but consider external off-shell momenta $\tilde{p}_1 = \tilde{p}_2 + \tilde{q}$, $\tilde{p}_1^2 = s_1$, $\tilde{p}_2^2 = s_2$, $\tilde{q}^2 = q^2$. Then the double spectral densities can be obtained from the following equation

$$\begin{aligned} & \frac{1}{8\pi} \int dk_1 dk_2 dk_3 \delta(k_1^2 - m_1^2) \delta(k_2^2 - m_2^2) \delta(k_3^2 - m_3^2) \delta(\tilde{p}_1 - k_2 - k_3) \delta(\tilde{p}_2 - k_3 - k_1) \\ & \times (-1) Sp \left((\hat{k}_1 + m_1) \gamma_\mu (\hat{k}_2 + m_2) i \gamma_5 (m_3 - \hat{k}_3) i \gamma_5 \right) \\ & = (\tilde{p}_1 + \tilde{p}_2)_\mu \Delta_+(s_1, s_2, q^2 | m_1, m_2, m_3) + (\tilde{p}_1 - \tilde{p}_2)_\mu \Delta_-(s_1, s_2, q^2 | m_1, m_2, m_3) \end{aligned} \quad (2.72)$$

The trace has the following form

$$\begin{aligned} & -Sp \left((\hat{k}_1 + m_1) \gamma_\mu (\hat{k}_2 + m_2) i \gamma_5 (m_3 - \hat{k}_3) i \gamma_5 \right) \\ & = 2k_{1\mu} (s_1 - (m_2 - m_3)^2) + 2k_{2\mu} (s_2 - (m_3 - m_1)^2) + 2k_{3\mu} (q^2 - (m_1 - m_2)^2). \end{aligned} \quad (2.73)$$

Explicit calculations give

$$\Delta_\pm(s_1, s_2, q^2 | m_1, m_2, m_3) = \frac{B_\pm(s_1, s_2, q^2)}{\lambda(s_1, s_2, q^2)} \Delta(s_1, s_2, q^2 | m_1, m_2, m_3) \quad (2.74)$$

where B_\pm are the following polynomials

$$\begin{aligned} B_+(s_1, s_2, q^2) &= b_+(s_1, s_2, q^2) \{ a(s_1, m_2, m_3) + a(s_2, m_3, m_1) - a(q^2, m_1, m_2) \} \\ & \quad + a(q^2, m_1, m_2) \lambda(s_1, s_2, q^2), \\ B_-(s_1, s_2, q^2) &= b_-(s_1, s_2, q^2) \{ a(s_1, m_2, m_3) + a(s_2, m_3, m_1) - a(q^2, m_1, m_2) \}, \\ & \quad + (a(s_2, m_3, m_1) - a(s_1, m_2, m_3)) \lambda(s_1, s_2, q^2) \\ b_+(s_1, s_2, q^2) &= -q^2 (s_1 + s_2 - q^2 + m_1^2 + m_2^2 - 2m_3^2) - (m_1^2 - m_2^2)(s_1 - s_2), \\ b_-(s_1, s_2, q^2) &= (m_1^2 - m_2^2)(2s_1 + 2s_2 - q^2) - (s_1 - s_2)(s_1 + s_2 - q^2 + m_1^2 + m_2^2 - 2m_3^2), \\ a(s, \mu_1, \mu_2) &= s - (\mu_1 - \mu_2)^2. \end{aligned} \quad (2.75)$$

In the above relations we have introduced Δ , the double spectral density in p_1^2 and p_2^2 -channels of the Feynman triangle graph $\Gamma(p_1^2, p_2^2, q^2)$ with the scalar constituents defined according to the relation

$$\begin{aligned}\Gamma(p_1^2, p_2^2, q^2) &= \frac{1}{(2\pi)^4 i} \int \frac{dk_1 dk_2 dk_3 \delta(P_1 - k_2 - k_3) \delta(P_2 - k_3 - k_1)}{(m_1^2 - k_1^2 - i0)(m_2^2 - k_2^2 - i0)(m_3^2 - k_3^2 - i0)} \\ &= \int \frac{ds_1}{\pi(s_1 - p_1^2)} \frac{ds_2}{\pi(s_2 - p_2^2)} \Delta(s_1, s_2, q^2 | m_1, m_2, m_3).\end{aligned}\quad (2.76)$$

At $q^2 < 0$, Δ is given by the following integral

$$\begin{aligned}\Delta(s_1, s_2, q^2 | m_1, m_2, m_3) &= \frac{1}{8\pi} \int dk_1 dk_2 dk_3 \delta(\tilde{p}_1 - k_2 - k_3) \delta(\tilde{p}_2 - k_3 - k_1) \\ &\quad \times \delta(k_1^2 - m_1^2) \delta(k_2^2 - m_2^2) \delta(k_3^2 - m_3^2).\end{aligned}\quad (2.77)$$

Introducing the light-cone variables we derive a useful expression

$$\begin{aligned}\Delta(s_1, s_2, q^2 | m_1, m_2, m_3) &= \frac{1}{16\pi} \int \frac{dx_1 dx_2 dx_3}{x_1 x_2 x_3} d^2 k_{3\perp} \delta(x_1 - x_2) \delta(1 - x_1 - x_3) \\ &\quad \times \delta\left(s_1 - \frac{m_2^2}{x_2} - \frac{m_3^2}{x_3} - \frac{k_{3\perp}^2}{x_2 x_3}\right) \delta\left(s_2 - \frac{m_1^2}{x_1} - \frac{m_3^2}{x_3} - \frac{(k_{3\perp} + x_3 q_\perp)^2}{x_2 x_3}\right)\end{aligned}\quad (2.78)$$

Hereafter we denote $x_i = k_{i+}/p_+$, $p_{1+} = p_{2+} = p_+$, $-q_\perp^2 = q^2$, $x \equiv x_3$, $k_\perp \equiv k_{3\perp}$. For $q^2 < 0$ one obtains

$$\Delta(s_1, s_2, q^2 | m_1, m_2, m_3) = \frac{\theta(b_+^2(s_1, s_2, q^2) - \lambda(s_1, s_2, q^2)\lambda(q^2, m_1^2, m_2^2))}{16\lambda^{1/2}(s_1, s_2, q^2)}.\quad (2.79)$$

The solution of this θ -function gives the following allowed intervals for the integration variables s_1 and s_2

$$\begin{aligned}(m_1 + m_3)^2 &< s_2, \\ s_1^-(s_2, q^2) &< s_1 < s_1^+(s_2, q^2);\end{aligned}\quad (2.80)$$

where

$$\begin{aligned}s_1^\pm(s_2, q^2) &= \frac{s_2(m_1^2 + m_2^2 - q^2) + q^2(m_1^2 + m_3^2) - (m_1^2 - m_2^2)(m_1^2 - m_3^2)}{2m_1^2} \\ &\quad \pm \frac{\lambda^{1/2}(s_2, m_3^2, m_1^2)\lambda^{1/2}(q^2, m_1^2, m_2^2)}{2m_1^2}\end{aligned}\quad (2.81)$$

The final dispersion representation for the form factors at $q^2 < 0$ takes the form

$$F_\pm(q^2) = f_{21}(q^2) \int_{(m_1+m_3)^2}^{\infty} \frac{ds_2 G_{v2}(s_2)}{\pi(s_2 - M_2^2)} \int_{s_1^-(s_2, q^2)}^{s_1^+(s_2, q^2)} \frac{ds_1 G_{v1}(s_1)}{\pi(s_1 - M_1^2)} \frac{B_\pm(s_1, s_2, q^2)}{\lambda^{3/2}(s_1, s_2, q^2)}\quad (2.82)$$

This representation will be the starting point for the consideration of the meson decays in the next section.

The light-cone representation

For comparison with the light-cone quark model results it is convenient to represent the spectral representation (2.82) as the integral over the light-cone variables. Following the same lines for the elastic form factor, we turn back to the equation (2.72) and again make use of the light-cone variables (2.56), choosing the reference frame $q_+ = 0, p_{1\perp} = 0$ (see [69,73,75] for details). Setting $\mu = +$ and making use of the first line of (2.73) gives for Δ_+

$$\begin{aligned} \Delta_+(s_1, s_2, q^2 | m_1, m_2, m_3) &= \frac{1}{16\pi} \int \frac{dx_1 dx_2 dx_3}{x_1 x_2 x_3} d^2 k_{3\perp} \delta(x_1 - x_2) \delta(1 - x_1 - x_3) \\ &\times \delta \left(s_1 - \frac{m_2^2}{x_2} - \frac{m_3^2}{x_3} - \frac{k_{3\perp}^2}{x_2 x_3} \right) \delta \left(s_2 - \frac{m_1^2}{x_1} - \frac{m_3^2}{x_3} - \frac{(k_{3\perp} + x_3 q_\perp)^2}{x_2 x_3} \right) \\ &\times \{ x_1 (s_1 - (m_2 - m_3)^2) + x_2 (s_2 - (m_1 - m_3)^2) + x_3 (-q_\perp^2 - (m_1 - m_2)^2) \} \end{aligned} \quad (2.83)$$

Substituting (2.83) into (2.71) yields the following expression for the form factor F_+

$$\begin{aligned} F_+(q_\perp^2) &= f_{21}(q_\perp^2) \int \frac{dx d^2 k_\perp}{16\pi^3 x(1-x)} \frac{G_{v1}(s_1)}{\pi(s_1 - M_1^2)} \frac{G_{v2}(s_2)}{\pi(s_2 - M_2^2)} \\ &\times \left(s_1 + s_2 - (m_1 - m_3)^2 - (m_2 - m_3)^2 + \frac{x}{1-x} (-q_\perp^2 - (m_1 - m_2)^2) \right) \end{aligned} \quad (2.84)$$

Introducing the radial light-cone wave function according to (2.62) leads to the familiar light-cone expression (cf. [14])

$$F_+(q_\perp^2) = f_{21}(q_\perp^2) \int dx d^2 k_\perp \psi_1(x, k_\perp) \psi_2(x, k_\perp + x q_\perp) \beta_+(x, k_\perp, q_\perp), \quad (2.85)$$

with β_+ given by the expression

$$\begin{aligned} \beta_+ &= \frac{s_1 + s_2 - (m_1 - m_3)^2 - (m_2 - m_3)^2 + \frac{x}{1-x} (-q_\perp^2 - (m_1 - m_2)^2)}{2\sqrt{s_1 - (m_2 - m_3)^2} \sqrt{s_2 - (m_3 - m_1)^2}} \\ &= \frac{(m_1 x + m_3(1-x))(m_2 x + m_3(1-x)) + k_\perp(k_\perp + x q_\perp)}{x(1-x)\sqrt{s_1 - (m_2 - m_3)^2} \sqrt{s_2 - (m_3 - m_1)^2}} \end{aligned}$$

The same expression for $F_+(q_\perp^2)$ was obtained in [14] within the light-cone quark model. The (\perp) component in Eq. (2.72) allows to determine the form factor $F_-(q_\perp^2)$. The $(-)$ component of Eq. (2.72) cannot be used for isolating the form factor because of the difference between the $(-)$ components of the on-shell and the off-shell vectors as given by Eqs. (2.58) and (2.59).

2. Transition form factors at $q^2 > 0$

For the description of decay processes the form factors in the region $0 < q^2 < (M_1 - M_2)^2$ are necessary. For deriving the form factors at $q^2 > 0$ the dispersion representation (2.82) turns out to be a convenient starting point. In general, this representation has the following form

$$F(q^2) = f_{21}(q^2) \int \frac{ds_1 G_{v1}(s_1)}{\pi(s_1 - M_1^2)} \frac{ds_2 G_{v2}(s_2)}{\pi(s_2 - M_2^2)} \frac{B(s_1, s_2, q^2)}{\lambda(s_1, s_2, q^2)} \Delta(s_1, s_2, q^2 | m_1, m_2, m_3) \quad (2.86)$$

where Δ is the double spectral density of the Feynman graph Γ with scalar constituents Eq. (2.76). This double dispersion representation defines the analytic function of q^2 both at negative and positive values. It is important to point out that the functions $G_v(s)$ have no singularities in the right-hand side of the complex s -plane [72], and B and λ are polynomials. So the details of the dispersion integration at $q^2 > 0$ are determined by the behavior of the quantity Δ .

A detailed discussion of the double spectral representation and the anomalous singularities can be found in [80] in connection with the deuteron elastic form factor. Anomalous singularities in decay processes were considered in [28] for the case $m_1 = m_3 = 0$. We perform the analysis for arbitrary nonzero masses.

Let us start with the single dispersion representation for Γ in the variable p_2^2 . A standard calculation yields

$$\Gamma(p_1^2, p_2^2, q^2) = \int_{(m_1+m_3)^2}^{\infty} \frac{ds_2}{\pi(s_2 - p_2^2)} \sigma_2(p_1^2, s_2, q^2), \quad (2.87)$$

where

$$\begin{aligned} \sigma_2(p_1^2, s_2, q^2) &= \sigma_2^+(p_1^2, s_2, q^2) - \sigma_2^-(p_1^2, s_2, q^2), \\ \sigma_2^\pm(s_1, s_2, q^2) &= \frac{1}{16\pi\lambda^{1/2}(s_1, s_2, q^2)} \\ &\times \log \left(-s_2(s_1 + q^2 - s_2 + m_1^2 + m_3^2 - 2m_2^2) - (s_1 - q^2)(m_1^2 - m_3^2) \pm \lambda^{1/2}(s_2, m_1^2, m_3^2)\lambda^{1/2}(s_1, s_2, q^2) \right). \end{aligned}$$

Hereafter we assume $m_2 > m_1$. The single dispersion representation reproduces the exact value of the Feynman integral (2.76).

Let us consider the function $\sigma_2(p_1^2, s_2, q^2)$ as the analytic function of the variable $s_1 = p_1^2$ at fixed s_2 and $q^2 > 0$. As $s_2 < s_2^0$ such that

$$\sqrt{s_2^0} = -\frac{q^2 + m_1^2 - m_2^2}{2\sqrt{q^2}} + \sqrt{\left(\frac{q^2 + m_1^2 - m_2^2}{2\sqrt{q^2}}\right)^2 + (m_3^2 - m_1^2)}, \quad q^2 < (m_2 - m_1)^2, \quad (2.88)$$

both of the functions σ_2^+ and σ_2^- have square-root branch points on the physical sheet at $s_1^L = (\sqrt{s_2} - \sqrt{q^2})^2$ and $s_1^R = (\sqrt{s_2} + \sqrt{q^2})^2$, connected by the cut, see Fig.8.

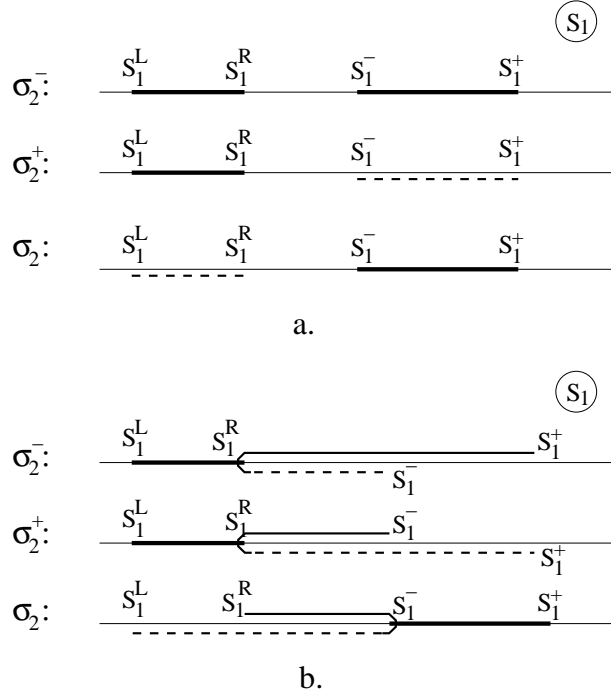


Fig. 8. The location of the singularities of σ_2 in the complex s_1 plane as a function of s_2 for $q^2 > 0$: a). $s_2 < s_2^0$; b). $s_2 > s_2^0$. Solid lines cuts located on the physical sheet, dashed lines - on the second sheet.

The function σ_2^- has in addition a logarithmic cut from s_1^- to s_1^+ on the physical sheet. Here s_1^\pm given by (2.80) are the zeros of the argument of the logarithm in σ_2^- . The function σ_2^+ also has a logarithmic cut from s_1^- to s_1^+ but on the second unphysical sheet of the Riemann surface of the square-root (dashed line in Fig.8a).

The square-root cuts cancel in $\sigma_2 = \sigma_2^+ - \sigma_2^-$, and the logarithmic cut is the only singularity of σ_2 on the physical sheet. Notice however that σ_2 has the two cuts from s_1^L to s_1^R and from s_1^- to s_1^+ of the second sheet.

The situation changes at $s_2 = s_2^0$ which is determined by the condition $s_1^R(s_2^0) = s_1^-(s_2^0)$. For this value of s_2 the logarithmic and square-root branch points coincide. As s_2 increases, $s_2 > s_2^0$, the branch point s_1^- of σ_2^+ moves up

through the square-root cut onto the physical sheet. At the same time the branch point s_1^- of σ_2^- moves onto the second sheet (Fig.8b). Hence, the function σ_2^+ acquires the logarithmic cut from s_1^R to s_1^- on the physical sheet, and σ_2^- still has the logarithmic cut which now lasts from s_1^R to s_1^+ . Both of the functions have also square-root cuts from s_1^L to s_1^R . In the difference $\sigma_2 = \sigma_2^+ - \sigma_2^-$ the square-root cuts cancel each other, but the logarithmic cuts add. The resulting expression for the double spectral density takes the form

$$\Delta(s_1, s_2, q^2 | m_1, m_2, m_3) = \frac{\theta(s_2 - (m_1 + m_3)^2) \theta(s_1^- < s_1 < s_1^+)}{16\lambda^{1/2}(s_1, s_2, q^2)} + \frac{2\theta(q^2) \theta(s_2 - s_2^0) \theta(s_1^R < s_1 < s_1^-)}{16\lambda^{1/2}(s_1, s_2, q^2)}. \quad (2.89)$$

One can check the double dispersion representation (2.76) with the spectral density Δ given by (2.89) to reproduce correctly the Feynman expression. The first term in (2.89) relates to the Landau-type contribution emerging when all intermediate particles go on mass shell, while the second term describes the *anomalous* contribution.

The expression (2.89) for Δ is derived for $m_2 > m_1$ implying the 'external' s_2 integration, and the 'internal' s_1 -integration. The location of the integration region for this case is shown in Fig. 9.

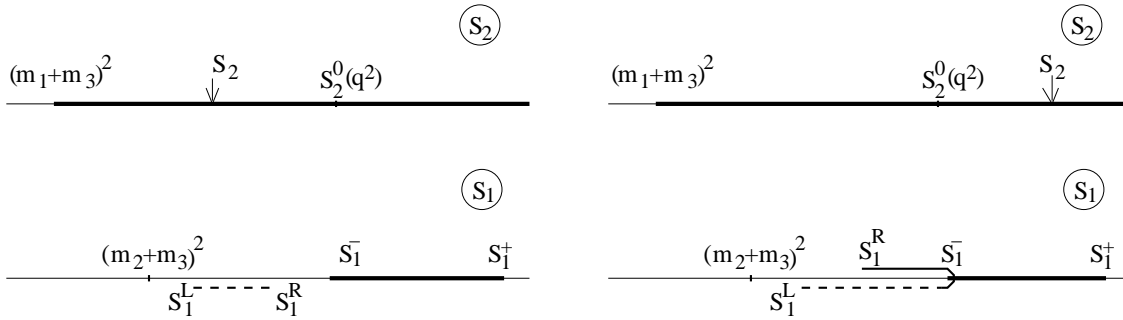


Fig. 9. The integration region for $m_2 > m_1$ and $q^2 > 0$ for the order of integration $\int ds_2 \int ds_1$: a. $s_2 < s_2^0$ b. $s_2 > s_2^0$. Solid lines - cuts on the physical sheet, dashed lines - cuts on the second sheet.

In addition to the quantity Δ , the spectral density of the representation (2.86) involves the factor $1/\lambda(s_1, s_2, q^2)$ which is singular at s_1^R , the lower integration limit in the anomalous term: because

$$\lambda(s_1, s_2, q^2) = (s - s_1^L)(s - s_1^R).$$

As it has been discussed in [28], in this case an accurate application of the Cauchy theorem yields the subtraction term in the non-Landau contribution. Representing σ_2 as a contour integral, we must take into account the nonvanishing contribution of the small circle around the point s_1^R . Underline once more that the presence of the factor $G_{v1}(s_1)$ does not change the argumentation as the function $G_v(s)$ has no singularities at $s_1 > (m_2 + m_3)^2$. The final properly regularized representation for the form factors at $0 < q^2 < (m_2 - m_1)^2$ takes the form (omitting the constituent transition form factor $f_{21}(q^2)$)

$$F(q^2) = \int_{(m_1+m_3)^2}^{\infty} \frac{ds_2 G_{v2}(s_2)}{\pi(s_2 - M_2^2)} \int_{s_1^-}^{s_1^+} \frac{ds_1 G_{v1}(s_1)}{\pi(s_1 - M_1^2)} \frac{B(s_1, s_2, q^2)}{16\lambda(s_1, s_2, q^2)} + 2\theta(q^2) \int_{s_2^0}^{\infty} \frac{ds_2 G_{v2}(s_2)}{\pi(s_2 - M_2^2)} \int_{s_1^R}^{s_1^-} \frac{ds_1}{16\pi(s_1 - s_1^R)^{3/2}} \left[\frac{G_{v1}(s_1) B(s_1, s_2, q^2)}{(s_1 - s_1^L)^{3/2} (s_1 - M_1^2)} - \frac{G_{v1}(s_1^R) B(s_1^R, s_2, q^2)}{(s_1^R - s_1^L)^{3/2} (s_1^R - M_1^2)} \right] \quad (2.90)$$

It should be pointed out, that although the representations (2.86) and (2.90) were derived for the case of pseudoscalar mesons, transition form factors of any hadrons have the similar structure. A particular choice of the initial and final hadrons yields a specific form of the function B . In the next chapter we shall calculate the double spectral densities for the form factors describing the pseudoscalar to vector meson transitions.

It is convenient to introduce the bound state wave function $\varphi(s)$ related to the bound state vertex as follows

$$\varphi(s) = G_v(s)/(s - M^2). \quad (2.91)$$

In the nonrelativistic limit one finds $\varphi(s) \simeq \Psi_{NR}(\vec{k})$, where the variable \vec{k} is connected with s

$$s = \sqrt{m_Q^2 + \vec{k}^2} + \sqrt{m_q^2 + \vec{k}^2}.$$

In the nonrelativistic limit the elastic electromagnetic form factor of a pseudoscalar meson takes a well-known form

$$F(\vec{q}^2) = \int \Psi_{NR}(\vec{k}) \Psi_{NR}(\vec{k} + \vec{q}) d\vec{k}, \quad \vec{q}^2 = -q^2. \quad (2.92)$$

The relationship between the bound state wave function $\varphi(s)$ and the light-cone wave function is given by the relation (2.62).

It should be pointed out that the analytic properties of $\varphi(s)$ in the region of s near the two-particle threshold are different for a truly bound state with a negative binding energy (like a deuteron as a two-nucleon system) and a bound state in a confined potential with a positive binding energy (like a meson as a $q\bar{q}$ bound state): in the deuteron case $G_v(s)$ is a smooth regular function near the threshold and the pole at $s = M^2$ is located only slightly below the two-particle threshold at $s = 4M_N^2$. Therefore $\varphi(s)$ is strongly peaked near the threshold and it is more convenient to analyse the deuteron form factors in terms of the vertex functions $G_v(s)$.

For the confined potential the situation is different: the pole at $s = M^2$ would have appeared in the physical region as the pole in $\varphi(s)$ at $s = M^2 > (m_Q + m_q)^2$. However this does not happen. As well known from e.g. the behaviour of the bound-state wave function in the harmonic oscillator potential, the function $\varphi(s)$ is a smooth exponential function of s above $s = (m_Q + m_q)^2$. This means that the would-be pole in $\varphi(s)$ at $s = M^2$ is completely washed out by the interaction. Therefore, for the analysis of the meson transitions $\varphi(s)$ turns out to be more appropriate than $G_v(s)$.

D. A simple model for pseudoscalar mesons

We are now in a position to apply the developed formalism to the analysis of the properties of pseudoscalar mesons and to the direct calculation of the decay form factors. To this end we must specify the parameters of the model, i.e. constituent quark masses and wave functions of pseudoscalar mesons.

We consider in this section a simple choice of quark model parameters for pseudoscalar mesons π , K , D , and B which gives a relativistic description of this sector and allows us to illustrate main features of the weak form factors and study the transition to the heavy-quark limit. We leave a detailed discussion of criteria for fixing parameters of the model, including also vector mesons, and analysis of the corresponding transition form factors for later sections.

For a pseudoscalar meson built up of quarks with the masses m_Q and m_q the wave function $\varphi(s) = G_v(s)/(s - M^2)$ can be written in the form

$$\varphi(s) = \frac{\pi}{\sqrt{2}} \frac{\sqrt{s^2 - (m_Q^2 - m_q^2)^2}}{\sqrt{s - (m_Q - m_q)^2}} \frac{1}{s^{3/4}} w(k), \quad k = \frac{\lambda^{1/2}(s, m_Q^2, m_q^2)}{2\sqrt{s}}. \quad (2.93)$$

The normalization condition (2.25) for G_v is equivalent to the following normalization condition for w

$$\int w^2(k) k^2 dk = 1. \quad (2.94)$$

The function w is the ground-state S -wave radial wave function of a pseudoscalar meson for which we choose in this section a simple exponential form

$$w(k) = \exp(-4\alpha k^2/\mu_P^2) \quad (2.95)$$

where $\mu_P = m_Q m_q / (m_Q + m_q)$ is the reduced mass. The parameterization of the wave function in the form (2.95) is inspired by the nonrelativistic quantum mechanics and is convenient for the analysis of the dependence of the observables on m_Q , in particular for analysing the case $m_Q \rightarrow \infty$.

In the nonrelativistic quantum mechanics a bound-state wave function is determined by the motion of the particle with the mass μ_P in the potential independent of masses, and thus α does not depend on the masses as well. Relativistic effects destroy this simple feature of the wave function. In QCD the situation is much more complicated because additional dimensional quantities such as Λ_{QCD} and the condensates appear. So, α should be considered as some unknown function of the quark masses. It is possible to obtain the information on the behavior of α as a function of m_Q at fixed $m_q = m_{u,d} = 0.25 \text{ GeV}$ in the two regions: at small m_Q and $m_Q \rightarrow \infty$.

Table 1. The constituent quark masses and the calculated f_P for $\alpha = 0.02$.

quark	quark mass, GeV	meson	meson mass, GeV	f_P, MeV
u,d	0.25	$\pi^+(ud)$	0.14	130
s	0.40	$K^+(u\bar{s})$	0.49	160
c	1.80	$D^+(c\bar{d})$	1.87	234
b	5.20	$B^+(u\bar{b})$	5.27	202

At $m_Q \leq 0.5 \text{ GeV}$ the value of α can be determined by describing the data in the light-meson sector. The light-quark masses given in Table 1 and $\alpha_\pi = \alpha_K = 0.02$ provide a good description of the data on f_π , f_K , and the elastic form factors, Fig. 10. The meson decay constants and form factors are calculated with the values $g_A^0(M^2) = 1$ and $f_c(q^2) = f_c(0)$, respectively.

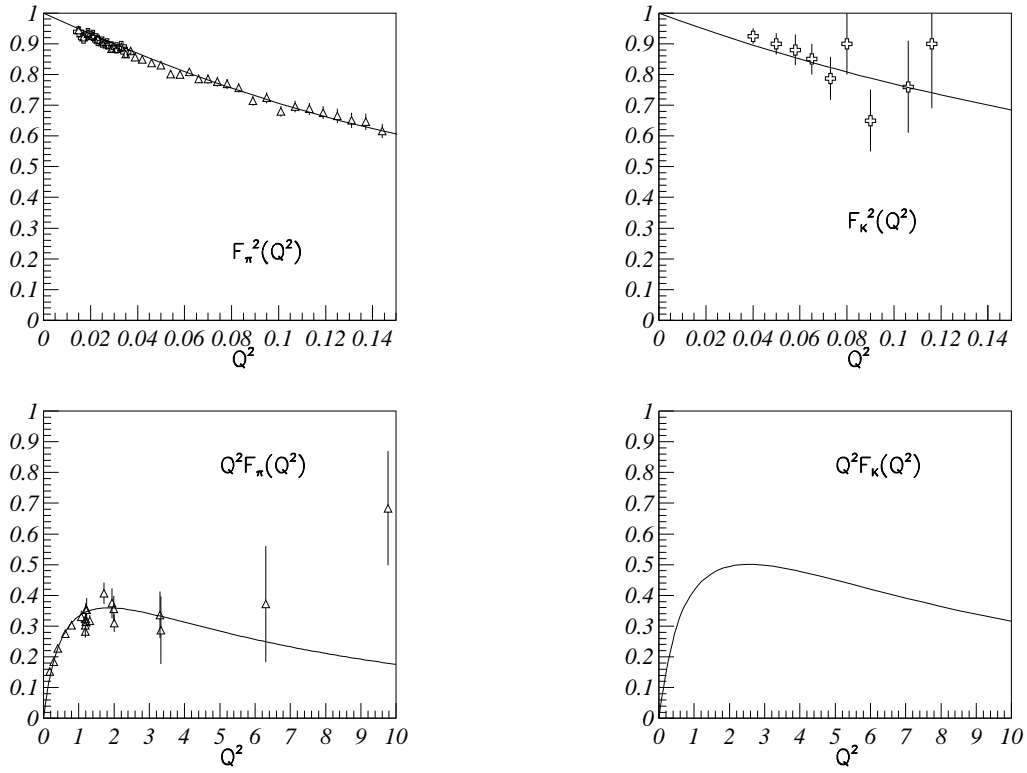


Fig. 10. The π^+ and K^+ elastic form factors evaluated for $\alpha_\pi = 0.02$.

In the region $m_Q \rightarrow \infty$ the behavior of α can be found on the basis of the heavy quark symmetry. To this end, let us consider the amplitudes of the elastic and inelastic transitions between pseudoscalar mesons consisting of heavy Q and light q quarks.

For the case of the transition between two heavy mesons it is convenient to introduce instead of q^2 the dimensionless recoil variable $\omega = vv'$, where v and v' are the 4-velocities of the initial and final mesons, respectively, and to analyse the transition in terms of the velocity-dependent form factors.

For the elastic-transition amplitude

$$\langle M, P' | \bar{Q} \gamma_\mu Q | M, P \rangle = (P' + P)_\mu F_{el}(q^2); \quad q^2 \leq 0 \quad (2.96)$$

the recoil takes the form

$$\omega = 1 - \frac{q^2}{2M^2} \geq 1, \quad (2.97)$$

and the velocity-dependent form factor just coincides with the elastic form factor

$$h_{el}(\omega) = F_{el}(q^2). \quad (2.98)$$

The function h_{el} can be expanded in powers of the variable $\omega - 1$ near zero recoil point $\omega = 1$ as follows

$$h_{el}(\omega) = 1 - \rho_{el}^2(\omega - 1) + O((\omega - 1)^2). \quad (2.99)$$

For the amplitude of the inelastic transition between two pseudoscalar mesons

$$\begin{aligned} \langle M_2, p_2 | \bar{Q}_2 \gamma_\mu Q_1 | M_1, p_1 \rangle &= (p_1 + p_2)_\mu F_+(q^2) + (p_1 - p_2)_\mu F_-(q^2); \\ 0 < q^2 < (M_1 - M_2)^2 \end{aligned} \quad (2.100)$$

the recoil reads

$$\omega = \frac{M_1^2 + M_2^2 - q^2}{2M_1 M_2} \geq 1, \quad (2.101)$$

and the velocity-dependent form-factors are related to the form factors F_\pm according to the relation

$$h_\pm(\omega) = \frac{M_1 \pm M_2}{2\sqrt{M_1 M_2}} F_+(q^2) + \frac{M_1 \mp M_2}{2\sqrt{M_1 M_2}} F_-(q^2). \quad (2.102)$$

In the limit of infinitely heavy quarks $Q_{1,2}$, both the elastic and inelastic amplitudes are expressed to a $1/m_Q$ accuracy in terms of the single universal Isgur-Wise (IW) function $\xi(\omega)$ [2]

$$\begin{aligned} h_+(\omega) &= h_{el}(\omega) = \xi(\omega) + O(1/m_Q), \\ h_-(\omega) &= O(1/m_Q). \end{aligned} \quad (2.103)$$

The Isgur-Wise function can be expanded near zero recoil as follows

$$\xi(\omega) = 1 - \rho^2(\omega - 1) + O((\omega - 1)^2). \quad (2.104)$$

It is important to stress, that the heavy-quark symmetry predicts the absolute normalization of the transition form factor in the heavy-quark limit.

In addition, the heavy-quark symmetry gives the universal relation for heavy-meson decay constants

$$\sqrt{M_P} f_Q = \text{const.} \quad (2.105)$$

The asymptotic relations (2.103) and (2.105) are the zero-order terms of the $1/m_Q$ -expansion which is calculable within the Heavy quark effective theory (HQET) [3]. A particular form of the IW function depends on the heavy meson wave function. In next Sections we discuss in detail the structure of this expansion for the transition of a heavy pseudoscalar meson into pseudoscalar and vector mesons.

The expressions (2.103) and (2.105) mean that the HQ symmetry restricts the possible behavior of the meson wave function at large m_Q .

Table 2 gives the results on f_P and ρ_{el}^2 vs m_Q at $m_q = 0.25 \text{ GeV}$, and Fig.11 presents the quantity $\sqrt{m_Q}f_P$ as the function of m_Q for various values of α .

Table 2. The decay constants f_P of pseudoscalar mesons built up of quarks with the masses m_Q and m_q and the slope of h_{el} at $\omega = 1$ calculated from $\langle M_Q | \bar{Q} \gamma_\mu Q | M_Q \rangle$ as functions of m_Q at $m_q = 0.25 \text{ GeV}$.

m_Q, GeV	$\alpha = 0.01$		$\alpha = 0.02$		$\alpha = 0.04$		$\alpha = 0.08$	
	f_P, MeV	ρ_{el}^2	f_P, MeV	ρ_{el}^2	f_P, MeV	ρ_{el}^2	f_P, MeV	ρ_{el}^2
0.25	151	0.04	130	0.06	104	0.08	80	0.1
0.4	190	0.25	160	0.35	128	0.5	97	0.65
1.8	324	0.6	234	0.65	163	0.82	110	1.0
5.2	308	0.75	202	1.0	132	1.05	85	1.1
10	254	1.0	162	1.05	102	1.1	64	1.25
20	195	1.0	122	1.1	76	1.23	48	1.45
40	143	1.0	89	1.11	55	1.25	34	1.66
80	103	1.0	63	1.11	39	1.25	24	1.66

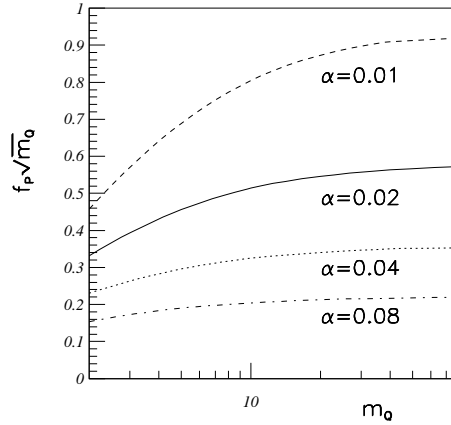


Fig. 11. The quantity $m_Q^{0.5} f_P$ as the function of m_Q at $m_q = 0.25 \text{ GeV}$.

In the HQ limit, for a finite binding energy of the meson the heavy meson and the heavy quark masses coincide, $M_Q/m_Q = 1$. So, the value of $\sqrt{m_Q}f_P$ should be independent of the heavy quark mass. Clearly, the asymptotic relations (2.103) and (2.105) are satisfied if the parameter α of the wave function (2.95) tends to a constant α_∞ as $m_Q \rightarrow \infty$.

Thus, the function $\alpha(m_Q)$ has the following behavior: it is equal to 0.02 at $m_Q \leq 0.5 \text{ GeV}$ and tends to a constant α_∞ as $m_Q \rightarrow \infty$. For investigating the B and D mesons and their decays we need the information on α in the region $m_Q = 2 \div 5 \text{ GeV}$.

The simplest way is to extract α at $m_Q = 2 \div 5 \text{ GeV}$ from the analysis of f_D and f_B as we have done for the light mesons. In the absence of the experimental data we refer to the results of other models. As one can see, the decay constants f_P calculated with α from the range $0.02 \leq \alpha_D, \alpha_B \leq 0.04$ cover the regions $160 \text{ MeV} \leq f_D \leq 230 \text{ MeV}$ and $130 \text{ MeV} \leq f_B \leq 200 \text{ MeV}$ which include the predictions of most of the models. Hence, the values of α_D and α_B related to the true wave functions of D and B mesons are expected to be inside the interval $0.02 \div 0.04$.

However, there is an attractive possibility to specify $\alpha_{D,B}$ more precisely. Namely, it seems reasonable to assume α to be approximately constant in the region $m_Q \geq 1 \div 2 \text{ GeV}$. There are at least two arguments behind this assumption. Firstly, a system consisting of a heavy and a light particles behaves like a quasinonrelativistic system. And secondly, there are no visible sources within QCD to yield step changes of α in this region. Then for the B and D mesons one expects $\alpha_D = \alpha_B = \alpha_\infty$. The next step is to estimate α_∞ . We consider the value $\alpha_\infty = 0.02$ to be both attractive and reasonable: on the one hand, the same parameter describes all ground-state mesons, and on the other hand, one finds for $\alpha_\infty = 0.02$

$$\sqrt{m_\infty} f_{P\infty} \simeq 5.8 \text{ GeV}^{3/2}$$

in agreement with the value $0.6 \div 0.7$ estimated in [32].

Assuming $\alpha_D = \alpha_B = \alpha_\infty$, we can estimate the magnitude of the higher order $1/m_Q$ corrections which determine the deviations of the calculated f_P and ρ_{el}^2 at finite m_Q from the asymptotic relations (2.103) and (2.105). Rather strong violation of the HQ symmetry for b - and c -quarks ($5 \div 15\%$ at $m_Q = 5 \text{ GeV}$ and $20 \div 30\%$ at $m_Q = 2 \text{ GeV}$) can be observed both in f_P and ρ_{el}^2 at $\alpha_\infty = 0.02 \div 0.04$.

We shall analyze the transition form factors obtained at $\alpha_{D,B} = 0.02$ and 0.04 . If our assumption $\alpha_D = \alpha_B = \alpha_\infty = 0.02$ does not work properly, the form factor calculations for $\alpha = 0.02$ and $\alpha = 0.04$ give an interval which is expected to include the true value. Table 1 gives the numerical parameters of the model.

The results on the axial-vector decay constant f_P are shown in Fig.11 and Table 2. Assuming $\alpha(m_Q) = \alpha_\infty$ at $m_Q \geq 2 \text{ GeV}$, one can see the asymptotic relation $\sqrt{m_Q} f_P = \text{const}$ to work perfectly at $m_Q > 40 - 50 \text{ GeV}$, and finds essential corrections to the asymptotic relations at lower m_Q . For $\alpha_\infty = 0.02$ one obtains $f_D = 234 \text{ MeV}$ and $f_B = 202 \text{ MeV}$ that confirms the expectation $f_D \simeq f_B$ [32]. These values for the decay constants correspond to the constituent quark leptonic decay constant $g_A^0 = 1$.

Figures 12, 13 and 14 present the form factors calculated with $\alpha_{D,B} = 0.02$ and 0.04 .

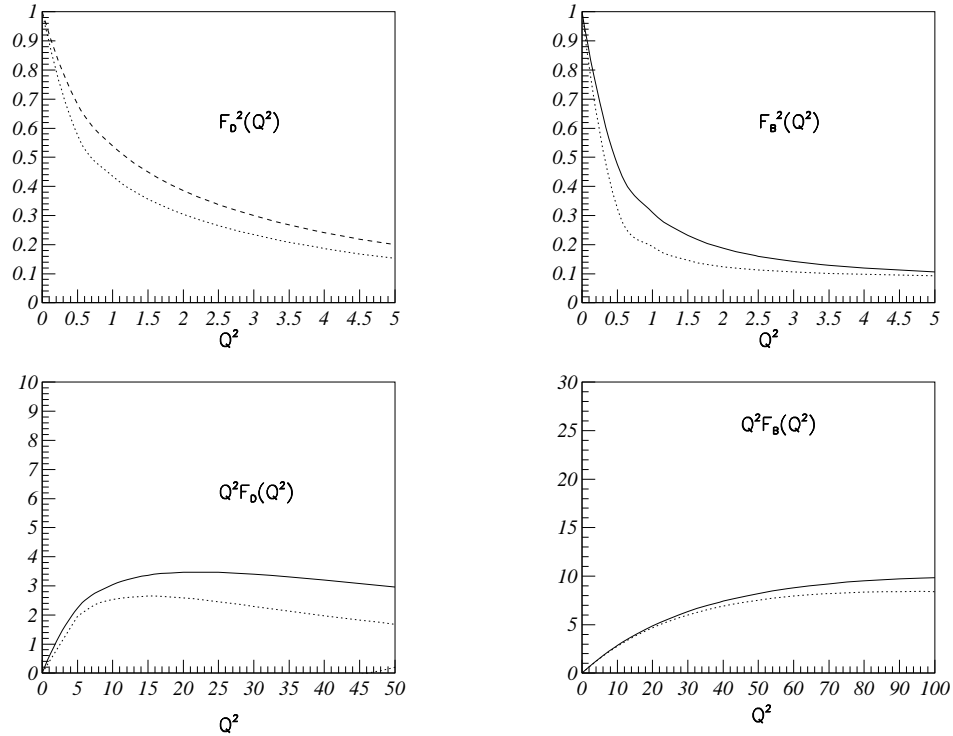


Fig. 12. The D and B elastic form factor F_+ . Solid line $\alpha = 0.02$, dashed line $\alpha = 0.04$.

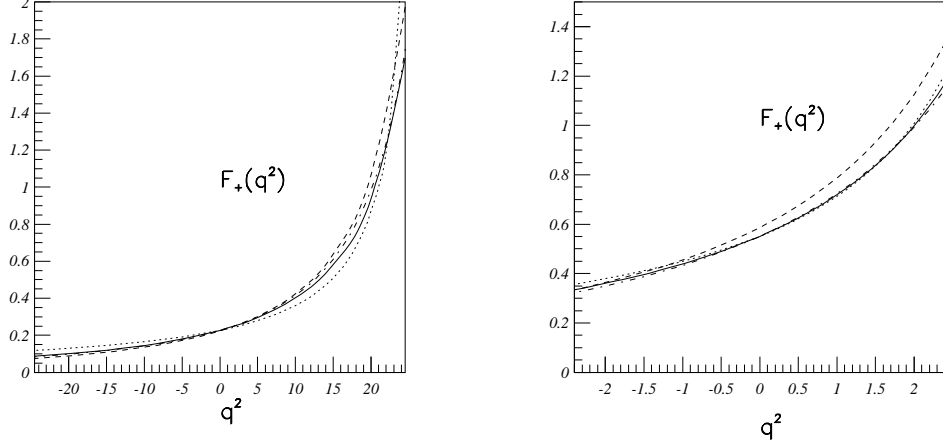


Fig. 13. The form factor F_+ for the $B \rightarrow \pi$ (left) and $D \rightarrow \pi$ (right) transitions. Solid - $\alpha_{B(D)} = 0.02$, dotted - the monopole fit, dash-dotted - the dipole fit. Dashed - $\alpha_{B(D)} = 0.04$.

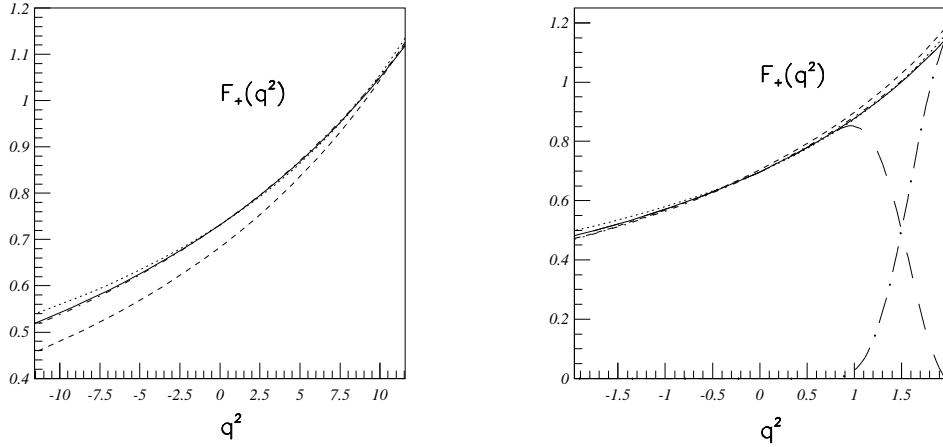


Fig. 14. (a) The form factor $F_+(q^2)$ for $B \rightarrow D$. Solid - $\alpha_D = \alpha_B = 0.02$, dotted - the monopole fit, dash-dotted - the dipole fit. Dashed - $\alpha_D = \alpha_B = 0.04$; (b) The form factor F_+ for the $D \rightarrow K$ decay. Solid - $\alpha_D = 0.02$, dotted - the monopole fit, dash-dotted - the dipole fit. Long-dashed - the Landau singularity contribution, long-dash-dotted - the non-Landau term. Dashed - $\alpha_D = 0.04$.

Figure 14 (b) shows the relative magnitude of the various contributions to the form factor F_+ , separately, as the function of q^2 for the $D \rightarrow K$ transition. Clearly, the full form factor is a monotonously-rising function of q^2 , whereas the behaviour of its normal and anomalous parts is rather specific:

The normal part rises up to some value of q^2 where it takes the maximal value, then it goes down rather steeply and vanishes at the maximal $q^2 = (m_2 - m_1)^2$ corresponding to 'quark zero recoil point'.

The anomalous part is identically zero at negative q^2 but comes into the game as q^2 goes into the positive region. It is small for small positive q^2 , but increases steeply as q^2 approaches its maximal value.

In other words, at $q^2 \leq 0$ the contribution of the non-Landau singularity (anomalous term) is absent, and the Landau-type singularity (normal term) determines the form factor; in the region $0 < q^2 < (m_2 - m_1)^2$ both of them are essential; at the point $q^2 = (m_2 - m_1)^2$ the contribution of the Landau singularity vanishes, and the non-Landau singularity determines the decay form factor at this 'quark zero recoil' point.

For heavy-to-heavy meson transitions, a specific relationship between the Landau and the non-Landau contributions to the dispersion representation is observed: the normal Landau contribution dominates the form factor at all $q^2 <$

$(m_2 - m_1)^2$, whereas the region where the anomalous singularity is essential shrinks to a very narrow vicinity of this point. So, effectively the transition form factor is determined by the contribution of the Landau singularity only. Thus, the HQ symmetry can be formulated in the language of the analytic properties of the transition form factors as the dominance of the Landau singularity in the almost whole kinematical region.

In the case of the meson decay related to a heavy-to-light quark transition, the anomalous non-Landau contribution is important in a broad kinematical region. So the relations suggested by the HQ symmetry would not work properly in this case.

Table 3 shows parameters of the monopole $F_+(q^2) = F_+(0)/(1 - q^2/M_{mon}^2)$ and the dipole $F_+(q^2) = F_+(0)/(1 - q^2/M_{dip}^2)$ fits to the calculated transition form factors. The dipole formula approximates the calculated form factors with better than 1% accuracy. Parameters of the monopole fit agree very well with the vector meson dominance.

The $K \rightarrow \pi$ transition form factor is well approximate by the linear function $F_+(q^2) = F_+(0) + aq^2$, $F_+(0) = 0.96$, $a = 1.27 \text{ GeV}^{-2}$ in agreement with the results of [49].

Table 3. Parameters of the monopole and dipole fits to the F_+ form factor. Masses of the lowest vector mesons which are expected to dominate the form factors are given in brackets.

Decay	$\alpha_B = \alpha_D = 0.02$			$\alpha_B = \alpha_D = 0.04$	
	$F_+(0)$	$M_{mon}, \text{ GeV}$	$M_{dip}, \text{ GeV}$	$F_+(0)$	$M_{dip}, \text{ GeV}$
$B \rightarrow D$	0.73	5.7	7.7	0.68	7.20
$B \rightarrow \pi$	0.23	5.2 [5.324]	6.2	0.22	6.08
$D \rightarrow K$	0.70	2.22 [2.11]	3.0	0.70	2.95
$D \rightarrow \pi$	0.55	2.1 [2.01]	2.8	0.59	2.68

E. Discussion

In this section we investigated form factors of hadron transitions within the relativistic dispersion approach based on the constituent quark picture and proposed a formalism for a direct calculation of hadron decay form factors. The developed approach was applied to the analysis of the electroweak properties and transitions of pseudoscalar mesons.

The main results of this chapter are as follows:

1. We analysed elastic and transition form factors for pseudoscalar mesons at spacelike momentum transfers, $q^2 < 0$, and obtained for them double spectral representations in the mass variables s_1 and s_2 , squares of the invariant masses of the initial and final $q\bar{q}$ pairs, respectively. These representations involve double spectral densities of the corresponding triangle Feynman diagrams and wave functions of the participating mesons.
2. We performed the analytic continuation of the form factors to timelike momentum transfers. We observed the appearance of the anomalous cut and, respectively, the appearance of the anomalous contribution to the form factor for $q^2 > 0$. The anomalous cut appears due to the motion of the singularities of the Feynman triangle graph from the second sheet onto the physical sheet through the normal cut. The normal cut is related to the Landau-Cutkosky singularities of the Feynman graphs, whereas the anomalous cut is related to the non-Landau type singularities which come into the game in the region of timelike momentum transfers. It is important to emphasise that both the normal and anomalous contributions to the form factors are expressed in terms of the wave functions of the initial and final mesons only in the physical region above the threshold, $s_1 > (m_2 + m_3)^2$ and $s_2 > (m_1 + m_3)^2$.
3. We demonstrated the equivalence of our approach based on spectral representations with the light-cone constituent quark model for the description of leptonic decays and for transition form factors between pseudoscalar mesons at *spacelike momentum transfers*. It should be noticed that the dispersion approach has important advantages compared to the light-cone approach in the region $q^2 > 0$, where the direct application of the latter is hampered by the contribution of pair-creation subprocesses.

4. For meson decays related to heavy-to-heavy quark transitions a dominance of the normal contribution over the anomalous contribution for almost all q^2 from the decay region except for the very vicinity of the zero-recoil point has been observed. This allows a formulation of the heavy-quark symmetry in the language of the analytic properties of the decay form factors as the dominance of the normal Landau contribution in the almost whole kinematic region of momentum transfers.

5. Electroweak properties and form factors of pseudoscalar mesons have been analysed using a simple parametrization of the meson wave function based on the heavy quark symmetry. We have examined the dependence of the axial-vector decay constant on the heavy-quark mass, and found $f_D \simeq 235 \text{ MeV}$ and $f_B \simeq 200 \text{ MeV}$.

Analysing the dependence of f_P and the heavy meson form factor on the heavy quark mass we have found that the violation of the HQ symmetry relations can be expected at the 10-20% level for the b and c -quark masses.

In the next Chapter we consider the $1/m_Q$ expansion of the transition form factors given by the double spectral representations and match this expansion to the heavy quark expansion in QCD. In particular, we demonstrate that the heavy quark expansion of the $P \rightarrow P$ transition form factors is fully compatible with the $1/m_Q$ expansion in QCD in the leading and subleading $1/m_Q$ orders.

III. HEAVY QUARK EXPANSION AND UNIVERSAL FORM FACTORS IN THE DISPERSION APPROACH

This Chapter presents a detailed discussion of form factors for weak meson decays within the dispersion approach following the analysis of Ref. [27].

We calculate the double spectral densities for the form factors describing the transition of a pseudoscalar (P) meson to pseudoscalar (P) and vector (V) mesons induced by the vector, axial-vector and tensor currents. These spectral densities are given in terms of the soft wave functions of the participating mesons and the double spectral densities of the corresponding triangle Feynman graphs.

We then analyse the spectral representations for the form factors in the two specific cases of the heavy-to-heavy and heavy-to-light transitions.

- (i) The *heavy-to-heavy* transition means that the masses of the initial quark m_2 and the final quark m_1 participating in the weak transition are much larger than the confinement scale Λ

$$m_2 > m_1, \quad m_2 \sim m_1 \sim m_Q \gg \Lambda. \quad (3.1)$$

In this case the meson transition can be analysed using the formalism of Heavy quark effective theory (HQET) [6], an effective theory obtained from QCD for heavy quarks. Expansions of the form factors in powers of $1/m_Q$ can be obtained in terms of the universal form factors which appear in each order of $1/m_Q$. These process-independent form factors contain the information about the long-distance dynamics in the heavy-quark limit and can be calculated only within some nonperturbative approach.

We studied the form factors of the dispersion approach for the quark masses satisfying the relation (3.1). We perform the $1/m_Q$ expansion of our spectral representations and require its structure to match to the known structure of the $1/m_Q$ expansion in HQET.

- (ii) The *heavy-to-light* transition means that

$$m_2 = m_Q \gg m_1 \simeq \Lambda. \quad (3.2)$$

In this case the explicit structure of the $1/m_Q$ expansion cannot be obtained directly from QCD by the existing methods, but QCD provides relations between the form factors in the region of large q^2 near zero recoil [8]. We therefore require the form factors of our dispersion approach to obey these relations.

The conditions (i) and (ii) allow us to determine the necessary subtraction terms in the spectral representations for the form factors. As prompted by the structure of the $1/m_Q$ expansion of the dispersion form factors, no subtractions are necessary for $P \rightarrow P$ transition form factors, but subtractions for some of the $P \rightarrow V$ form factors are necessary.

Section III A gives the definitions of all the necessary form factors for $P \rightarrow P$ and $P \rightarrow V$ weak transitions. The structure of the $1/m_Q$ expansion of the transition form factor induced by the vector and axial-vector current has been calculated within HQET in [6]. We apply the formalism of HQET to transitions induced by the tensor current and report the $1/m_Q$ expansion of the form factors h_{g_+} , h_{g_-} , h_{g_0} , and h_s (the definitions are given in the next section) in the leading (LO) and next-to-leading (NLO) orders in $1/m_Q$. In particular, we find the $1/m_Q$ correction to the value of the form factor h_{g_+} at zero recoil to vanish exactly as for the form factors h_{f_+} and h_f (the Luke theorem).

We later use the $1/m_Q$ expansion of the weak form factors from HQET as a benchmark for testing the $1/m_Q$ expansion of the form factors of our dispersion approach.

In section III B we calculate the double spectral densities for form factors and give results for the necessary subtraction terms which are explained later in the sections III C and III D.

In section III C we consider the case of the heavy-to-heavy meson transition and perform the expansion of the spectral representations for the transition form factors in the LO and NLO in $1/m_Q$.

The spectral representations without subtractions are found to agree with HQET in the LO for all $P \rightarrow P$ and $P \rightarrow V$ form factors. The next-to-leading order analysis shows the necessity of subtractions in the spectral representations for some of the $P \rightarrow V$ form factors in order to match to the structure of the HQET. The matching condition provides constraints on the subtraction terms.

Assuming the strong peaking of the meson soft wave functions in terms of the relative quark momenta with a width of order of the confinement scale, we calculate the Isgur-Wise function and the NLO universal form factors in terms of the wave function of the infinitely heavy meson. Our dispersion approach leads to the following relations for the universal NLO form factors:

$$\begin{aligned}\chi_2(\omega) &= 0; \\ \chi_3(\omega) &= 0; \\ \xi_3(\omega) &> 0, \quad \xi_3(1) = \langle z \rangle / 3,\end{aligned}\tag{3.3}$$

where $\langle z \rangle$ is an average kinetic energy of the light quark in the heavy meson rest frame.

In section III D we discuss heavy-to-light quark transitions and consider the $1/m_Q$ expansion for the wave functions and the form factors in this case. We then consider the heavy-to-light meson transitions in which case a small parameter Λ_{QCD}/m_Q emerges and analyse the form factors in the leading Λ_{QCD}/m_Q order. Requiring the fulfillment of the Isgur-Wise relations for the heavy-to-light transitions [8] further constrains the subtraction terms providing explicit spectral representations with subtractions for the form factors of interest.

Section III E illustrates the main results with numerical estimates and evaluate the universal form factors for various quark model parameters.

A. Meson transition amplitudes and heavy-quark expansion in QCD

The amplitudes of meson decays induced by the quark transition $q_2 \rightarrow q_1$ through the vector $V_\mu = \bar{q}_1 \gamma_\mu q_2$, axial-vector $A_\mu = \bar{q}_1 \gamma_\mu \gamma_5 q_2$, tensor $T_{\mu\nu} = \bar{q}_1 \sigma_{\mu\nu} q_2$, and pseudo-tensor $T_{\mu\nu}^5 = \bar{q}_1 \sigma_{\mu\nu} \gamma_5 q_2$ currents have the following structure [8]

$$\begin{aligned}\langle P(M_2, p_2) | V_\mu(0) | P(M_1, p_1) \rangle &= f_1(q^2) p_{1\mu} + f_2(q^2) p_{2\mu}, \\ \langle V(M_2, p_2, \epsilon) | V_\mu(0) | P(M_1, p_1) \rangle &= 2g(q^2) \epsilon_{\mu\nu\alpha\beta} \epsilon^{*\nu} p_1^\alpha p_2^\beta, \\ \langle V(M_2, p_2, \epsilon) | A_\mu(0) | P(M_1, p_1) \rangle &= i\epsilon^{*\alpha} [f(q^2) g_{\mu\alpha} + a_1(q^2) p_{1\alpha} p_{1\mu} + a_2(q^2) p_{1\alpha} p_{2\mu}], \\ \langle P(M_2, p_2) | T_{\mu\nu}(0) | P(M_1, p_1) \rangle &= -2i s(q^2) (p_{1\mu} p_{2\nu} - p_{1\nu} p_{2\mu}), \\ \langle V(M_2, p_2, \epsilon) | T_{\mu\nu}(0) | P(M_1, p_1) \rangle &= i\epsilon^{*\alpha} [g_1(q^2) \epsilon_{\mu\nu\alpha\beta} p^{1\beta} + g_2(q^2) \epsilon_{\mu\nu\alpha\beta} p^{2\beta} \\ &\quad + g_0(q^2) p_{1\alpha} \epsilon_{\mu\nu\beta\gamma} p_1^\beta p_2^\gamma], \\ \langle P(M_2, p_2) | T_{\mu\nu}^5(0) | P(M_1, p_1) \rangle &= s(q^2) \epsilon_{\mu\nu\alpha\beta} P^\alpha q^\beta, \\ \langle V(M_2, p_2, \epsilon) | T_{\mu\nu}^5(0) | P(M_1, p_1) \rangle &= g_1(q^2) (\epsilon_\nu^* p_{1\mu} - \epsilon_\mu^* p_{1\nu}) + g_2(q^2) (\epsilon_\nu^* p_{2\mu} - \epsilon_\mu^* p_{2\nu}) \\ &\quad + g_0(q^2) (\epsilon^* p_1) (p_{1\nu} p_{2\mu} - p_{1\mu} p_{2\nu}),\end{aligned}\tag{3.4}$$

with $q = p_1 - p_2$, $P = p_1 + p_2$. Also the following linear combinations of the form factors will be used

$$\begin{aligned}f_\pm &= \frac{1}{2}(f_1 \pm f_2), \\ a_\pm &= \frac{1}{2}(a_1 \pm a_2), \\ g_\pm &= \frac{1}{2}(g_1 \pm g_2).\end{aligned}\tag{3.5}$$

The matrix element of the penguin operator relevant for rare decays has the following structure

$$\begin{aligned}\langle V(M_2, p_2, \epsilon) | \bar{q}_1 \sigma_{\mu\nu} q^\nu (1 + \gamma_5) q_2 | P(M_1, p_1) \rangle &= -i\epsilon_{\mu\nu\alpha\beta} \epsilon^{*\nu} p_1^\alpha p_2^\beta 2g_+ \\ &\quad - (g_{\mu\nu} \cdot qP - q_\nu P_\mu) \epsilon^{*\nu} \left(g_+ - \frac{q^2}{qP} g_- \right) + (\epsilon^* q) \left(q_\mu - \frac{q^2}{qP} P_\mu \right) \left(g_- - \frac{1}{2} qP g_0 \right).\end{aligned}\tag{3.6}$$

We use the following conventions:

$$\gamma^5 = i\gamma^0 \gamma^1 \gamma^2 \gamma^3, \quad \sigma_{\mu\nu} = \frac{i}{2} [\gamma_\mu, \gamma_\nu], \quad \epsilon^{0123} = -1.\tag{3.7}$$

Accordingly,

$$Sp(\gamma^5 \gamma^\mu \gamma^\nu \gamma^\alpha \gamma^\beta) = 4i\epsilon^{\mu\nu\alpha\beta}, \quad \sigma_{\mu\nu} \gamma^5 = -\frac{i}{2} \epsilon_{\mu\nu\alpha\beta} \sigma^{\alpha\beta}. \quad (3.8)$$

The relativistic-invariant form factors contain the dynamical information on the process and should be calculated within a nonperturbative approach for any particular initial and final mesons.

For analysing the transition in the case when both the parent and the daughter quarks inducing the meson transition are heavy, i.e. $m_1 \simeq m_2 \gg \Lambda_{QCD}$ it is convenient to introduce a new dimensionless variable

$$\omega = v_1 v_2 = \frac{M_1^2 + M_2^2 - q^2}{M_1 M_2} \quad (3.9)$$

and velocity-dependent form factors $h(\omega)$ connected with 4-velocities and not 4-momenta as in (3.4) in the following way

$$\begin{aligned} \langle P(M_2, p_2) | V_\mu(0) | P(M_1, p_1) \rangle &= \sqrt{M_1 M_2} [h_{f+}(\omega)(v_1 + v_2)_\mu + h_{f-}(\omega)(v_1 - v_2)_\mu], \\ \langle V(M_2, p_2, \epsilon) | V_\mu(0) | P(M_1, p_1) \rangle &= \sqrt{M_1 M_2} h_g(\omega) \epsilon_{\mu\nu\alpha\beta} \epsilon^{*\nu} v_1^\alpha v_2^\beta, \\ \langle V(M_2, p_2, \epsilon) | A_\mu(0) | P(M_1, p_1) \rangle &= i\epsilon^{*\alpha} \sqrt{M_1 M_2} [h_f(\omega)(1 + \omega)g_{\mu\alpha} \\ &\quad - h_{a_1}(\omega)v_{1\alpha}v_{1\mu} \\ &\quad - h_{a_2}(\omega)v_{1\alpha}v_{2\mu}], \\ \langle P(M_2, p_2) | T_{\mu\nu}(0) | P(M_1, p_1) \rangle &= -2i \sqrt{M_1 M_2} h_s(\omega) (v_{1\mu}v_{2\nu} - v_{1\nu}v_{2\mu}), \\ \langle V(M_2, p_2, \epsilon) | T_{\mu\nu}(0) | P(M_1, p_1) \rangle &= i\epsilon^{*\alpha} \sqrt{M_1 M_2} [h_{g+}(\omega) \epsilon_{\mu\nu\alpha\beta} (v_1 + v_2)^\beta \\ &\quad + h_{g-}(\omega) \epsilon_{\mu\nu\alpha\beta} (v_1 - v_2)^\beta \\ &\quad + h_{g_0}(\omega) v_{1\alpha} \epsilon_{\mu\nu\beta\gamma} v_1^\beta v_2^\gamma], \\ \langle P(M_2, p_2) | T_{\mu\nu}^5(0) | P(M_1, p_1) \rangle &= 2 \sqrt{M_1 M_2} h_s(\omega) \epsilon_{\mu\nu\alpha\beta} v_1^\alpha v_2^\beta, \\ \langle V(M_2, p_2, \epsilon) | T_{\mu\nu}^5(0) | P(M_1, p_1) \rangle &= \sqrt{M_1 M_2} [h_{g+}(\omega) (\epsilon_\nu^*(v_1 + v_2)_\mu - \epsilon_\mu^*(v_1 + v_2)_\nu) \\ &\quad + h_{g-}(\omega) (\epsilon_\nu^*(v_1 - v_2)_\mu - \epsilon_\mu^*(v_1 - v_2)_\nu) \\ &\quad + h_{g_0}(\omega) (\epsilon^* v_1)(v_{1\nu}v_{2\mu} - v_{1\mu}v_{2\nu})]. \end{aligned} \quad (3.10)$$

These form factors are related to the form factors introduced by the relations (3.4) as follows

$$\begin{aligned} f_1 &= \frac{M_2}{\sqrt{M_1 M_2}} [h_{f+} + h_{f-}], \\ f_2 &= \frac{M_1}{\sqrt{M_1 M_2}} [h_{f+} - h_{f-}], \\ s &= \frac{1}{2\sqrt{M_1 M_2}} h_s, \\ g &= \frac{1}{2\sqrt{M_1 M_2}} h_g, \\ a_1 &= -\frac{1}{\sqrt{M_1 M_2}} \frac{M_2}{M_1} h_{a_1}, \\ a_2 &= -\frac{1}{\sqrt{M_1 M_2}} h_{a_2}, \\ f &= \sqrt{M_1 M_2} (1 + \omega) h_f, \\ g &= \frac{1}{2\sqrt{M_1 M_2}} h_g, \\ g_1 &= \frac{M_2}{\sqrt{M_1 M_2}} [h_{g+} + h_{g-}], \\ g_2 &= \frac{M_1}{\sqrt{M_1 M_2}} [h_{g+} - h_{g-}], \\ g_0 &= \frac{1}{\sqrt{M_1 M_2}} \frac{1}{M_1} h_{g_0} \end{aligned} \quad (3.11)$$

The form factors h are convenient quantities as in the leading $1/m_Q$ order all of them are expressed through a single universal function of the dimensionless variable ω – the Isgur–Wise function. A consistent heavy–quark expansion of the form factors, i.e. expansion in inverse powers of the heavy–quark mass, can be constructed within the Heavy Quark Effective Theory based on QCD with heavy quarks.

The general structure of the $1/m_Q$ expansion of the heavy quark form factors in QCD for the meson transition $M_1 \rightarrow M_2$ induced by heavy quark transition $m_2 \rightarrow m_1$ have the form (omitting corrections $O(\alpha_s, \alpha_s/m_Q, 1/m_Q^2)$):

$$\begin{aligned}
h_{f_+} &= \xi + \left(\frac{1}{m_1} + \frac{1}{m_2} \right) \rho_1, \\
h_{f_-} &= \left(\frac{1}{m_1} - \frac{1}{m_2} \right) \left(-\frac{\bar{\Lambda}}{2} \xi + \xi_3 \right), \\
h_g &= \xi + \left(\frac{1}{m_1} + \frac{1}{m_2} \right) \frac{\bar{\Lambda}}{2} \xi + \frac{1}{m_1} \rho_2 + \frac{1}{m_2} (\rho_1 - \xi_3), \\
h_f &= \xi + \left(\frac{1}{m_1} + \frac{1}{m_2} \right) \frac{\omega - 1}{\omega + 1} \frac{\bar{\Lambda}}{2} \xi + \frac{1}{m_1} \rho_2 + \frac{1}{m_2} \left(\rho_1 - \frac{\omega - 1}{\omega + 1} \xi_3 \right), \\
h_{a_1} &= \frac{1}{m_1} \frac{1}{\omega + 1} (-\bar{\Lambda} \xi + 2(\omega + 1) \chi_2 - \xi_3), \\
h_{a_2} &= \xi + \left(\frac{\omega - 1}{\omega + 1} \frac{1}{m_1} + \frac{1}{m_2} \right) \frac{\bar{\Lambda}}{2} \xi + \frac{1}{m_1} \left(\rho_2 - 2\chi_2 - \frac{1}{\omega + 1} \xi_3 \right) + \frac{1}{m_2} (\rho_1 - \xi_3). \\
h_s &= \xi + \left(\frac{1}{m_1} + \frac{1}{m_2} \right) \left(\frac{\bar{\Lambda}}{2} \xi - \xi_3 + \rho_1 \right), \\
h_{g_+} &= -\xi - \frac{1}{m_2} \rho_1 - \frac{1}{m_1} \rho_2, \\
h_{g_-} &= \left(\frac{1}{m_1} - \frac{1}{m_2} \right) \frac{\bar{\Lambda}}{2} \xi + \frac{1}{m_2} \xi_3, \\
h_{g_0} &= \frac{1}{m_1} \left(\frac{\bar{\Lambda} \xi + \xi_3}{\omega + 1} + 2\chi_2 \right). \tag{3.12}
\end{aligned}$$

In the leading $1/m_Q$ order (LO) all the form factors are represented through the single universal Isgur–Wise function $\xi(\omega)$, whereas in the next-to-leading order (NLO) the 4 new form factors ρ_1, ρ_2, χ_2 , and ξ_3 appear. The universal form factors are functions of a single variable ω .

The form factor ξ_3 originates from the expansion of the transition quark current, and the form factors ρ_1, ρ_2, χ_2 are connected with the nontrivial relationship between the mesonic states in the full and the effective theory. The universal form factors satisfy the conditions

$$\begin{aligned}
\xi(1) &= 1, \\
\rho_1(1) &= 0, \\
\rho_2(1) &= 0, \tag{3.13}
\end{aligned}$$

whereas no constraints on ξ_3 and χ_2 are imposed by the heavy quark symmetry. As found by Luke [6], the $1/m_Q$ corrections to the form factors h_f and h_{f_+} vanish due to kinematical or dynamical reasons:

$$\begin{aligned}
h_f(1) &= 1 + O(1/m_Q^2), \\
h_{f_+}(1) &= 1 + O(1/m_Q^2). \tag{3.14}
\end{aligned}$$

The same is found to be true also for the form factor h_{g_+} : namely,

$$h_{g_+}(1) = -1 + O(1/m_Q^2). \tag{3.15}$$

The parameter $\bar{\Lambda}$ in (3.12) comes from the $1/m_Q$ expansion of the mass of a meson consisting of the heavy quark and light degrees of freedom

$$M_Q = m_Q + \bar{\Lambda} + O(1/m_Q). \tag{3.16}$$

In our notations for heavy quarks and mesons, this gives

$$\begin{aligned} M_1 &= m_2 + \bar{\Lambda} + \dots, \\ M_2 &= m_1 + \bar{\Lambda} + \dots, \end{aligned} \quad (3.17)$$

for the parent and daughter particles, respectively.

It is straightforward to derive the following useful relations

$$\begin{aligned} \frac{M_1 + M_2}{\sqrt{M_1 M_2}} &= \frac{m_2 + m_1}{\sqrt{m_1 m_2}} \left[1 - \left(\frac{1}{m_1} + \frac{1}{m_2} \right) \left(\frac{m_2 - m_1}{m_2 + m_1} \right)^2 \frac{\bar{\Lambda}}{2} + \dots \right] \\ \frac{M_1 - M_2}{\sqrt{M_1 M_2}} &= \frac{m_2 - m_1}{\sqrt{m_1 m_2}} \left[1 - \left(\frac{1}{m_1} + \frac{1}{m_2} \right) \frac{\bar{\Lambda}}{2} + \dots \right] \\ \sqrt{M_1 M_2} &= \sqrt{m_1 m_2} \left[1 + \left(\frac{1}{m_1} + \frac{1}{m_2} \right) \frac{\bar{\Lambda}}{2} + \dots \right], \end{aligned} \quad (3.18)$$

where the dots denote higher order terms.

Using the relations (3.11) and (3.18), we obtain for the form factors (3.4) the following expansions

$$f_1 = \frac{m_1}{\sqrt{m_1 m_2}} \left[\xi + \frac{1}{m_1} (\rho_1 + \xi_3) + \frac{1}{m_2} (\rho_1 - \xi_3) \right], \quad (3.19)$$

$$f_2 = \frac{m_2}{\sqrt{m_1 m_2}} \left[\xi + \frac{1}{m_1} (\rho_1 - \xi_3) + \frac{1}{m_2} (\rho_1 + \xi_3) \right], \quad (3.20)$$

$$s = \frac{1}{2\sqrt{m_1 m_2}} \left[\xi + \frac{1}{m_1} (\rho_1 - \xi_3) + \frac{1}{m_2} (\rho_1 - \xi_3) \right], \quad (3.21)$$

$$g_1 = -\frac{m_1}{\sqrt{m_1 m_2}} \left[\xi + \frac{1}{m_1} \rho_2 + \frac{1}{m_2} (\rho_1 - \xi_3) \right], \quad (3.22)$$

$$g_2 = -\frac{m_2}{\sqrt{m_1 m_2}} \left[\xi + \frac{1}{m_1} \rho_2 + \frac{1}{m_2} (\rho_1 + \xi_3) \right], \quad (3.23)$$

$$g = \frac{1}{2\sqrt{m_1 m_2}} \left[\xi + \frac{1}{m_1} \rho_2 + \frac{1}{m_2} (\rho_1 - \xi_3) \right], \quad (3.24)$$

$$a_1 = -\frac{1}{\sqrt{m_1 m_2}} \frac{1}{m_2} \frac{1}{\omega + 1} [-\bar{\Lambda} \xi + 2(\omega + 1) \chi_2 - \xi_3], \quad (3.25)$$

$$\begin{aligned} a_2 = -\frac{1}{\sqrt{m_1 m_2}} \left[\xi + \frac{1}{m_1} (\rho_1 - \xi_3) + \frac{1}{m_2} (\rho_1 - \xi_3) - \frac{\bar{\Lambda}}{m_1} \frac{1}{\omega + 1} \xi \right. \\ \left. - \frac{2\chi_2}{m_1} + \frac{1}{m_1} \frac{\omega}{\omega + 1} \xi_3 \right], \end{aligned} \quad (3.26)$$

$$f = \sqrt{m_1 m_2} (\omega + 1) \left[\xi + \frac{\bar{\Lambda} \xi \omega}{\omega + 1} \left(\frac{1}{m_1} + \frac{1}{m_2} \right) + \frac{1}{m_1} \rho_2 + \frac{1}{m_2} \left(\rho_1 - \frac{\omega - 1}{\omega + 1} \xi_3 \right) \right] \quad (3.27)$$

$$g_0 = \frac{1}{(m_1 m_2)^{3/2}} \left[\frac{\bar{\Lambda} \xi + \xi_3}{\omega + 1} + 2\chi_2 \right] \quad (3.28)$$

For the following analysis it is worth noting that the behavior of the combination $2p_1 p_2 \cdot g - m_1 \cdot g_2$ and f in LO and NLO coincide, namely

$$f \simeq 2p_1 p_2 \cdot g - m_1 \cdot g_2. \quad (3.29)$$

It is also convenient to introduce the form factor a'_2 such that

$$a'_2 = a_2 + 2s. \quad (3.30)$$

In what follows we need the expansions of the following linear combinations of the form factors a'_2 and a_1

$$a_1 m_2 - a'_2 m_1 = -\frac{1}{\sqrt{m_1 m_2}} [4\chi_2 - \xi_3], \quad (3.31)$$

$$a_1 m_2 + a'_2 m_1 = -\frac{1}{\sqrt{m_1 m_2}} \left[-\frac{2\bar{\Lambda} \xi}{\omega + 1} + \xi_3 \frac{\omega - 1}{\omega + 1} \right]. \quad (3.32)$$

B. Transition form factors in the dispersion approach

The results presented in the previous section are strict consequences of QCD in the heavy-quark limit. The universal form factors ξ and $\rho_1, \rho_2, \chi_2, \xi_3$ can be calculated within a nonperturbative dynamical approach.

We study the form factors within the dispersion approach based of the constituent quark picture which turns out to be an efficient framework for describing meson decays. We start with $q^2 < 0$ and represent the form factors as double spectral representations in the invariant masses of the initial and final $q\bar{q}$ pairs. The form factors at $q^2 > 0$ are derived by performing the analytical continuation.

The transition of the initial meson $q(m_2)\bar{q}(m_3)$ with the mass M_1 to the final meson $q(m_1)\bar{q}(m_3)$ with the mass M_2 induced by the quark transition $m_2 \rightarrow m_1$ through the current $\bar{q}(m_1)J_\mu q(m_2)$ is described by the triangle diagram of Fig.15. As explained in the previous section, for constructing the double spectral representation we must consider a double-cut graph where all intermediate particles go on mass shell but the initial and final mesons have the off-shell momenta \tilde{p}_1 and \tilde{p}_2 such that $\tilde{p}_1^2 = s_1$ and $\tilde{p}_2^2 = s_2$ with $(\tilde{p}_1 - \tilde{p}_2)^2 = q^2$ kept fixed.

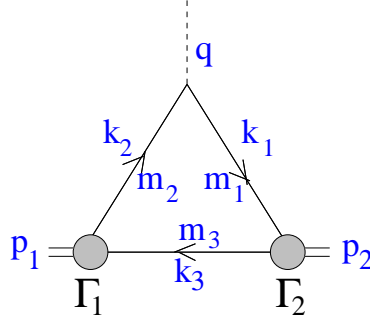


Fig. 15. One-loop graph for the meson transition.

For the transition $B \rightarrow D, D^*$ we have $m_2 = m_b, m_1 = m_c$, and $m_3 = m_u$. The constituent quark structure of the initial and final mesons is given in terms of the vertices Γ_1 and Γ_2 , respectively. The vertex describing the initial pseudoscalar meson has the spinorial structure

$$\Gamma_1 = i\gamma_5 G_1 / \sqrt{N_c}. \quad (3.33)$$

The vertex for the final pseudoscalar state reads

$$\Gamma_2 = i\gamma_5 G_2 / \sqrt{N_c}. \quad (3.34)$$

The final vector meson is described by the vertex

$$\Gamma_{2\mu} = [A\gamma_\mu + B(k_1 - k_3)_\mu] G_2 / \sqrt{N_c}, \quad (3.35)$$

where for an S -wave vector meson

$$A = -1, \quad B = 1/(\sqrt{s_2} + m_1 + m_3). \quad (3.36)$$

As explained above, the double spectral densities \tilde{f} of the form factors are obtained by calculating the relevant traces and isolating the Lorentz structures depending on \tilde{p}_1 and \tilde{p}_2 . The invariant factors of such Lorentz structures provide the double spectral densities \tilde{f} corresponding to contributions of the two-particle singularities in the Feynman graph. Let us point out that this procedure allows one to obtain double spectral densities, whereas subtraction terms should be determined independently. We determine the subtraction terms from matching the $1/m_Q$ expanded form factors of the quark model to the heavy-quark expansion in QCD.

Recall that at $q^2 < 0$ the spectral representations of the form factors have the form

$$f_i(q^2) = \frac{1}{16\pi^2} \int_{(m_1+m_3)^2}^{\infty} ds_2 \varphi_2(s_2) \int_{s_1^-(s_2, q^2)}^{s_1^+(s_2, q^2)} ds_1 \varphi_1(s_1) \frac{\tilde{f}_i(s_1, s_2, q^2)}{\lambda^{1/2}(s_1, s_2, q^2)}, \quad (3.37)$$

where the wave function $\varphi_i(s_i) = G_i(s_i)/(s_i - M_i^2)$ and

$$s_1^\pm(s_2, q^2) = \frac{s_2(m_1^2 + m_2^2 - q^2) + q^2(m_1^2 + m_3^2) - (m_1^2 - m_2^2)(m_1^2 - m_3^2)}{2m_1^2} \\ \pm \frac{\lambda^{1/2}(s_2, m_3^2, m_1^2)\lambda^{1/2}(q^2, m_1^2, m_2^2)}{2m_1^2}.$$

Here $\lambda(s_1, s_2, q^2) = (s_1 + s_2 - q^2)^2 - 4s_1s_2$ is the triangle function.

Calculating the necessary traces and isolating the coefficients of the relevant Lorentz structures, we come to the following expressions for the double spectral densities $\tilde{f}_i(s_1, s_2, q^2)$ of the form factors [27]:

$$\tilde{s} = 2[m_1\alpha_2 + m_2\alpha_1 + m_3(1 - \alpha_1 - \alpha_2)], \quad (3.38)$$

$$\tilde{f}_1 = 2m_1\tilde{s} + 4\alpha_2[s_2 - (m_1 - m_3)^2] - 2m_3\tilde{s}, \quad (3.39)$$

$$\tilde{f}_2 = 2m_2\tilde{s} + 4\alpha_1[s_1 - (m_2 - m_3)^2] - 2m_3\tilde{s}, \quad (3.40)$$

$$\tilde{g} = -A\tilde{s} - 4B\beta, \quad (3.41)$$

$$\tilde{g}_1 = A\tilde{f}_1 - 8\beta + 8B(m_1 + m_3)\beta, \quad (3.42)$$

$$\tilde{g}_2 = A\tilde{f}_2 + 8B(m_2 - m_3)\beta, \quad (3.43)$$

$$\tilde{a}_{2D} = -2\tilde{s} + 4BC_2\alpha_1 + \alpha_{12}C_0, \quad (3.44)$$

$$\tilde{a}_{1D} = -4A(2m_3 + BC_1)\alpha_1 + \alpha_{11}C_0, \quad (3.45)$$

$$\tilde{f}_D = -4A[m_1m_2m_3 + \frac{m_2}{2}(s_2 - m_1^2 - m_3^2) + \frac{m_1}{2}(s_1 - m_2^2 - m_3^2) - \frac{m_3}{2}(q^2 - m_1^2 - m_2^2)] \\ + C_0\beta, \quad (3.46)$$

$$\tilde{g}_{0D} = -8A\alpha_{12} - 8B[-m_3\alpha_1 + (m_3 - m_2)\alpha_{11} + (m_3 + m_1)\alpha_{12}], \quad (3.47)$$

where

$$C_0 = -8A(m_2 - m_3) + 4BC_3, \quad (3.48)$$

$$C_1 = s_2 - (m_1 + m_3)^2, \quad (3.49)$$

$$C_2 = s_1 - (m_2 - m_3)^2, \quad (3.50)$$

$$C_3 = q^2 - (m_1 + m_2)^2 - C_1 - C_2. \quad (3.51)$$

The coefficients α_1 , α_2 , α_{11} , α_{12} , and β are defined according to the relations

$$\frac{1}{8\pi} \int dk_1 dk_2 dk_3 \delta(\tilde{p}_1 - k_2 - k_3) \delta(\tilde{p}_2 - k_3 - k_1) \delta(k_1^2 - m_1^2) \delta(k_2^2 - m_2^2) \delta(k_3^2 - m_3^2) k_{3\mu} \\ = (\alpha_1 \tilde{p}_{1\mu} + \alpha_2 \tilde{p}_{2\mu}) \Delta(s_1, s_2, q^2), \\ \frac{1}{8\pi} \int dk_1 dk_2 dk_3 \delta(\tilde{p}_1 - k_2 - k_3) \delta(\tilde{p}_2 - k_3 - k_1) \delta(k_1^2 - m_1^2) \delta(k_2^2 - m_2^2) \delta(k_3^2 - m_3^2) k_{3\mu} k_{3\nu} \\ = (\alpha_{11} \tilde{p}_{1\mu} \tilde{p}_{1\nu} + \alpha_{12} (\tilde{p}_{1\mu} \tilde{p}_{2\nu} + \tilde{p}_{1\nu} \tilde{p}_{2\mu}) + \alpha_{22} \tilde{p}_{2\mu} \tilde{p}_{2\nu} + \beta g_{\mu\nu}) \Delta(s_1, s_2, q^2),$$

with $\Delta(s_1, s_2, q^2)$ given by Eq. (2.79). Explicitly, they read

$$\alpha_1 = [(s_1 + s_2 - q^2)(s_2 - m_1^2 + m_3^2) - 2s_2(s_1 - m_2^2 + m_3^2)] / \lambda(s_1, s_2, q^2), \quad (3.52)$$

$$\alpha_2 = [(s_1 + s_2 - q^2)(s_1 - m_2^2 + m_3^2) - 2s_1(s_2 - m_1^2 + m_3^2)] / \lambda(s_1, s_2, q^2), \quad (3.53)$$

$$\beta = \frac{1}{4} [2m_3^2 - \alpha_1(s_1 - m_2^2 + m_3^2) - \alpha_2(s_2 - m_1^2 + m_3^2)], \quad (3.54)$$

$$\alpha_{11} = \alpha_1^2 + 4\beta s_2 / \lambda(s_1, s_2, q^2), \quad (3.55)$$

$$\alpha_{12} = \alpha_1\alpha_2 - 2\beta(s_1 + s_2 - q^2) / \lambda(s_1, s_2, q^2), \quad (3.56)$$

In Eqs (3.44-3.47) we label with a subscript 'D' the true double spectral densities obtained from the Feynman graph for those form factors which require subtractions. We fix this subtraction procedure by requiring the $1/m_Q$ expansion of the form factors to have a proper form in accordance with QCD in leading and next-to-leading orders for the case of a meson transition caused by heavy-to-heavy quark transition. It is convenient to introduce for such form factors the modified double spectral densities which include properly defined subtraction terms as follows

$$\tilde{f} = \tilde{f}_D + [(M_1^2 - s_1) + (M_2^2 - s_2)]\tilde{g}, \quad (3.57)$$

$$\tilde{a}_1 = \tilde{a}_{1D} + \frac{1}{(\bar{\omega} + 1)m_2} \left(\frac{M_1^2 - s_1}{\sqrt{s_1}} + \frac{M_2^2 - s_2}{\sqrt{s_2}} \right) \frac{\tilde{g}}{2}, \quad (3.58)$$

$$\tilde{a}_2 = \tilde{a}_{2D} + \frac{1}{(\bar{\omega} + 1)m_1} \left(\frac{M_1^2 - s_1}{\sqrt{s_1}} + \frac{M_2^2 - s_2}{\sqrt{s_2}} \right) \frac{\tilde{g}}{2}, \quad (3.59)$$

$$\tilde{g}_0 = \tilde{g}_{0D} + \frac{1}{(\bar{\omega} + 1)m_1 m_2} \left(\frac{M_1^2 - s_1}{\sqrt{s_1}} + \frac{M_2^2 - s_2}{\sqrt{s_2}} \right) \frac{\tilde{g}}{2}. \quad (3.60)$$

As the analytical continuation to the timelike region is performed, in addition to the normal contribution which is just the expression (3.37) taken at $q^2 > 0$, anomalous contribution emerges. As we have shown in the previous section, the origin of the anomalous contribution is connected with the motion of the zero of the triangle function $\lambda(s_1, s_2, q^2)$ located at $s_1^R = (\sqrt{s_2} - \sqrt{q^2})^2$ from the unphysical sheet at $q^2 < 0$ onto the physical sheet at $q^2 > 0$ through the normal cut between the points $s_1^-(s_2, q^2)$ and $s_1^+(s_2, q^2)$. Pinching of the points s_1^R and s_1^- occurs at s_2^0 given by Eq. (2.88). The spectral representation of the form factor at $q^2 > 0$ takes the form

$$\begin{aligned} f(q^2) = & \frac{1}{16\pi^2} \int_{(m_1+m_3)^2}^{\infty} \varphi_2(s_2) \int_{s_1^-}^{s_1^+} \varphi_1(s_1) \frac{\tilde{f}(s_1, s_2, q^2)}{\lambda^{1/2}(s_1, s_2, q^2)} \\ & + \theta(q^2) \frac{1}{8\pi^2} \int_{s_2^0}^{\infty} \varphi_2(s_2) \int_{s_1^R}^{s_1^-} ds_1 \varphi_1(s_1) \frac{\tilde{f}(s_1, s_2, q^2)}{\lambda^{1/2}(s_1, s_2, q^2)}, \end{aligned} \quad (3.61)$$

One should also take into account that if the double spectral density \tilde{f} is singular at the point s_1^R , which is the case for the form factors describing transitions to vector meson, then a properly defined anomalous part contains subtraction terms which appear as the contribution of a small circle around s_1^R . Obviously, these subtractions have quite different nature from subtractions in the spectral representations at $q^2 < 0$ performed to match the structure of the heavy quark expansion in QCD. The corresponding expression was derived and can be found in [26].

The normal contribution dominates the form factor at small timelike and vanishes as $q^2 = (m_2 - m_1)^2$ while the anomalous contribution is negligible at small q^2 and steeply rises as $q^2 \rightarrow (m_2 - m_1)^2$.

Both for pseudoscalar and vector mesons with the mass M built up of the constituent quarks m_Q and m_q , the function φ is normalized according to the relation

$$\frac{1}{8\pi^2} \int ds \varphi^2(s) \frac{\lambda^{1/2}(s, m_Q^2, m_q^2)}{s} [s - (m_Q - m_q)^2] = 1. \quad (3.62)$$

This equation corresponds to the normalization of the elastic charge form factor at $q^2 = 0$.

Recall the spectral representation for the leptonic decay constant of the pseudoscalar meson f_P

$$f_P = \sqrt{N_c}(m_Q + m_q) \int ds \varphi(s) \frac{\lambda^{1/2}(s, m_Q^2, m_q^2)}{8\pi^2 s} \frac{s - (m_Q - m_q)^2}{s}. \quad (3.63)$$

In the subsequent sections we analyse the form factors given by the dispersion representation (3.61) with the spectral densities (3.38–3.43) and (3.57–3.60) and demonstrate them to have the following properties in the case of a heavy parent meson: for the transition induced by the heavy-to-heavy quark transition they satisfy the LO and NLO relations [6] of the $1/m_Q$ expansion in accordance with QCD provided the functions φ_i are localized near the $q\bar{q}$ threshold with the width of order Λ_{QCD} . For the meson decay induced by the heavy-to-light quark transition they satisfy the LO relations between the form factors of the vector, axial-vector and tensor currents [8].

C. Heavy-quark expansion in the dispersion approach for heavy-to-heavy transitions

In this section we consider the form factors of the dispersion quark model in the case when both m_2 and m_1 are large. We calculate the universal form factors and demonstrate that requiring the structure of the $1/m_Q$ expansion in the quark model to be consistent with the structure of such expansion in QCD allows us to determine the subtraction terms.

Soft wave function and normalization condition

First, we need to specify the properties of the soft wave function of a heavy meson. A basic property of such soft wave function $\varphi(s, m_Q, m_q, \bar{\Lambda})$ is a strong peaking near the $q\bar{q}$ threshold. For elaborating the $1/m_Q$ expansion, it is convenient to formulate such peaking in terms of the variable z such that $s = (m_Q + m_3 + z)^2$ (hereafter we denote the mass of the light quark as m_3). The region above the $q\bar{q}$ threshold which contributes to the spectral representation corresponds to $z > 0$. A localization of the soft wave function in terms of z means that the wave function is nonzero as $z \leq \Lambda_{QCD}$. In the heavy meson case $m_Q \gg m_3 \simeq z \simeq \bar{\Lambda}$. Let us notice that for a heavy meson the localization in terms of z is equivalent to the localization in terms of the relative momentum in the meson rest frame

$$\vec{k}^2 = z(z + 2m_3) + O(1/m_Q). \quad (3.64)$$

The normalization condition (3.62) which is a consequence of the vector current conservation in the full theory provides an (infinite) chain of relations in the effective theory. Namely, expanding the soft wave function in $1/m_Q$ as follows

$$\varphi(s, m_Q, m_3, \bar{\Lambda}) = \frac{\pi}{\sqrt{m_Q}} \phi_0(z, m_3, \bar{\Lambda}) \left[1 + \frac{m_3}{4m_Q} \chi_1(z, m_3, \bar{\Lambda}) + O(1/m_Q^2) \right], \quad (3.65)$$

we come to the normalization condition in the form

$$\int dz \phi_0^2(z) \sqrt{z}(z + 2m_3)^{3/2} \left[1 + \frac{m_3}{2m_Q} \chi_1(z) - \frac{m_3}{2m_Q} + \dots \right] = 1. \quad (3.66)$$

This exact relation is equivalent to an infinite chain of equations in different $1/m_Q$ orders. Lowest order relations take the form

$$\int dz \phi_0^2(z) \sqrt{z}(z + 2m_3)^{3/2} = 1, \quad (3.67)$$

$$\int dz \phi_0^2(z) \sqrt{z}(z + 2m_3)^{3/2} \chi_1(z) = 1. \quad (3.68)$$

The variables ω and $\bar{\omega}$

In the description of the transition processes the dispersion formulation of the quark model has the following feature: since the underlying process is the quark transition, the relevant kinematical variable for the description of the dynamics of the process is the quark recoil $\bar{\omega}$ which is defined as follows

$$q^2 = (m_2 - m_1)^2 - 2m_1 m_2 (\bar{\omega} - 1). \quad (3.69)$$

The relationship between ω and $\bar{\omega}$ is given by the condition that the spectral representation for the form factor is written at fixed value of q^2 and hence

$$q^2 = (M_1 - M_2)^2 - 2M_1 M_2 (\omega - 1) = (m_2 - m_1)^2 - 2m_1 m_2 (\bar{\omega} - 1). \quad (3.70)$$

In the case of heavy particle transitions these quantities are related to each other as

$$\bar{\omega} = \omega + \bar{\Lambda} \left(\frac{1}{m_1} + \frac{1}{m_2} \right) (\omega - 1) + O(1/m_Q^2). \quad (3.71)$$

We shall obtain the representations of the form factors as functions of the variable $\bar{\omega}$. The variables ω and $\bar{\omega}$ are different by the terms of order $1/m_Q$ at nonzero recoil. On the other hand, the quark and meson zero recoil points coincide with $1/m_Q^2$ accuracy. This means that in the analyses of the $1/m_Q$ expansion at nonzero recoil the difference between the ω and $\bar{\omega}$ might be ignored in the Isgur–Wise function, but gives nontrivial contribution to the NLO form factors. At the same time, at zero recoil the difference between ω and $\bar{\omega}$ might be neglected both in the leading and next-to-leading orders. Namely, the quark model provides the expansion of the form factor in the following form

$$h = h_0(\bar{\omega}) + \frac{1}{m_1} h_1^{(1)}(\bar{\omega}) + \frac{1}{m_2} h_1^{(2)}(\bar{\omega}) + \dots \quad (3.72)$$

$$= h_0(\omega) + h_0'(\omega) \bar{\Lambda} \left(\frac{1}{m_1} + \frac{1}{m_2} \right) (\omega - 1) + \frac{1}{m_1} h_1^{(1)}(\bar{\omega}) + \frac{1}{m_2} \bar{h}_1^{(2)}(\bar{\omega}) + \dots \quad (3.73)$$

As we shall see later, among the NLO form factors only $\rho_{1,2}$ are affected by the the difference between ω and $\bar{\omega}$ whereas ξ, ξ_3, χ_2 are not.

Relative magnitudes of the normal and the anomalous contributions

We are going now to demonstrate that the anomalous contribution comes into the game only in close vicinity of the zero recoil point whereas beyond this region is negligible.

Let us study the behavior of the anomalous contribution in the region

$$\bar{\omega} - 1 \simeq m_Q^{-(2+\varepsilon)}. \quad (3.74)$$

Introducing the variables z_1 and z_2 such that $s_1 = (m_2 + m_3 + z_1)^2$ and $s_2 = (m_1 + m_3 + z_2)^2$ we find that the magnitude of the anomalous contribution is controlled by the value of $z_2^0(\bar{\omega})$ such that $s_2^0 = (m_1 + m_3 + z_2^0(\bar{\omega}))^2$ which is the lower boundary of the z_2 integration. If $z_2^0(\bar{\omega})$ becomes large, i.e. of the order m_Q , the anomalous contribution is suppressed by the fall-down of the soft wave function. This suppression is at least stronger than $1/m_Q^2$. This means that the anomalous contribution is nonvanishing only if

$$z_2^0(\bar{\omega}) = \frac{m_1 m_2 \sqrt{\bar{\omega}^2 - 1} + m_1 m_2 \bar{\omega} - m_1^2}{\sqrt{m_1^2 + m_2^2 - 2m_1 m_2 \bar{\omega}}} - m_1 + O(m_3) \simeq \bar{\Lambda}. \quad (3.75)$$

In the region $\bar{\omega} - 1 \simeq m_Q^{-(2+\varepsilon)}$, one finds $z_2^0(\bar{\omega}) \simeq m_Q^{-\varepsilon/2}$. Hence the anomalous contribution comes actually into the game only in the $O(1/m_Q^2)$ vicinity of the zero recoil point but otherwise might be neglected. On the other hand, at the quark zero recoil point $\bar{\omega} = 1$, the normal contribution vanishes and the form factor is given by the anomalous contribution.

We shall calculate the form factors in the region $\bar{\omega} - 1 = O(1)$ where only the normal contribution should be taken into account in leading and subleading orders.

The LO analysis

To perform the LO analysis of the form factors let us start with the integration measure. With $1/m_Q$ accuracy it can be represented in the form

$$\frac{1}{16\pi^2} \frac{ds_1 ds_2 \theta(s_2 \geq (m_1 + m_3)^2) \theta(s_1^- \leq s_1 \leq s_1^+)}{\lambda^{1/2}(s_1, s_2, q^2)} \simeq \frac{1}{4\pi^2} dz_2 \sqrt{z_2(z_2 + 2m_3)} \frac{d\eta}{2} \theta(z_2) \theta(\eta^2 < 1), \quad (3.76)$$

and the expression for z_1 reads

$$z_1 = z_2 \bar{\omega} + m_3(\bar{\omega} - 1) + \eta \sqrt{z_2(z_2 + 2m_3)} \sqrt{\bar{\omega}^2 - 1} + O(1/m_Q). \quad (3.77)$$

Let us point out that the LO integration measure is symmetric in z_1 and z_2 .

Next, we need expanding the spectral densities (3.38)-(3.47). To this end we must take into account that under the integral sign z_1 and z_2 are localized in the region $z \leq \bar{\Lambda}$ due to the soft wave functions $\phi(z)$.

In LO the kinematical coefficients (3.48)-(3.52) in the region $\bar{\omega} - 1 = O(1)$ simplify to

$$\lambda(s_1, s_2, q^2) = 4m_1^2 m_2^2 (\bar{\omega}^2 - 1), \quad (3.78)$$

$$\alpha_1 = \frac{1}{m_2(\bar{\omega} + 1)} \left[m_3 + z_2 + \frac{z_2 - z_1}{\bar{\omega} - 1} \right], \quad (3.79)$$

$$\alpha_2 = \frac{1}{m_1(\bar{\omega} + 1)} \left[m_3 + z_1 + \frac{z_1 - z_2}{\bar{\omega} - 1} \right], \quad (3.80)$$

$$\beta = \frac{1}{2} \left[m_3^2 - \frac{2}{\omega + 1} (m_3 + z_1)(m_3 + z_2) + \frac{(z_1 - z_2)^2}{\bar{\omega}^2 - 1} \right], \quad (3.81)$$

$$\alpha_{11} = \alpha_1^2 + \frac{\beta}{m_2^2(\bar{\omega}^2 - 1)}, \quad (3.82)$$

$$\alpha_{12} = \alpha_1 \alpha_2 - \frac{\beta \bar{\omega}}{m_1 m_2 (\bar{\omega}^2 - 1)}, \quad (3.83)$$

$$B = \frac{1}{2m_1}, \quad (3.84)$$

$$C_0 = -4m_2(\bar{\omega} - 1), \quad (3.85)$$

$$C_1 = 2m_1z_2, \quad (3.86)$$

$$C_2 = 2m_2(z_1 + 2m_3). \quad (3.87)$$

One finds the LO behavior of the form factor densities (3.38–3.44) is determined by the term proportional to \tilde{s} . The latter reads in the LO

$$\tilde{s} \simeq 2 \left(m_3 + \frac{z_1 + z_2 + 2m_3}{\bar{\omega} + 1} \right). \quad (3.88)$$

The LO expression for \tilde{f} takes the form

$$\tilde{f}_D = (\bar{\omega} + 1) \left(m_3 + \frac{z_1 + z_2 + 2m_3}{\bar{\omega} + 1} \right). \quad (3.89)$$

The spectral densities \tilde{a}_1 and \tilde{g}_{0D} vanish in the leading order.

Hence the LO relations (3.19–3.28) are fulfilled with the Isgur–Wise (IW) function

$$\xi(\omega) = \int dz_2 \phi_0(z_2) \sqrt{z_2(z_2 + 2m_3)} \int_{-1}^1 \frac{d\eta}{2} \phi_0(z_1) \left(m_3 + \frac{2m_3 + z_1 + z_2}{1 + \omega} \right). \quad (3.90)$$

In (3.90) we used the equality of $\bar{\omega}$ and ω with $1/m_Q$ accuracy. The normalization condition of the LO wave functions (3.67) yields $\xi(1) = 1$. For the slope of the IW function at zero recoil, $\rho^2 = -\xi'(1)$, one finds

$$\rho^2 = \frac{1}{3} \int dz \sqrt{z} (z + 2m_3)^{3/2} (\phi'_0(z))^2 z (z + 2m_3) \quad (3.91)$$

Let us point out that the subtraction terms in the spectral densities do not contribute in the LO relations. As we shall see later, they are important in the NLO analysis.

The NLO analysis of the form factors s , f_1 , f_2 , g_1 , g_2 , and g

First, let us concentrate on the NLO relations (3.19–3.24). It is convenient to analyze the linear combinations of the form factors which do not contain the LO contribution. These combinations are

$$g - s = \frac{1}{2\sqrt{m_1 m_2}} \frac{1}{m_1} [\rho_2 - \rho_1 + \xi_3], \quad (3.92)$$

$$g_1 + f_1 = \frac{1}{\sqrt{m_1 m_2}} [-\rho_2 + \rho_1 + \xi_3], \quad (3.93)$$

$$g_2 + f_2 = -\frac{m_2}{m_1} \frac{1}{\sqrt{m_1 m_2}} [\rho_2 - \rho_1 + \xi_3], \quad (3.94)$$

$$f_1 - 2m_1 s = \frac{2\xi_3}{\sqrt{m_1 m_2}}. \quad (3.95)$$

The spectral densities of the form factor combinations in the l.h.s. of eqs. (3.92–3.94) read

$$\tilde{g} - \tilde{s} = -\frac{2}{m_1} \beta, \quad (3.96)$$

$$\tilde{g}_1 + \tilde{f}_1 = -4\beta, \quad (3.97)$$

$$\tilde{g}_2 + \tilde{f}_2 = 4\frac{m_2}{m_1} \beta, \quad (3.98)$$

Comparison with the eqs. (3.92–3.94) leads to the relation

$$\rho_1(\omega) = \rho_2(\omega), \quad (3.99)$$

For the form factor ξ_3 we come to the representation

$$\begin{aligned}\xi_3(\omega) = & - \int dz_2 \phi_0(z_2) \sqrt{z_2(z_2 + 2m_3)} \\ & \times \int_{-1}^1 \frac{d\eta}{2} \phi_0(z_1) \frac{1}{2} \left[m_3^2 - \frac{2}{\omega + 1} (m_3 + z_1)(m_3 + z_2) + \frac{(z_1 - z_2)^2}{\omega^2 - 1} \right],\end{aligned}\quad (3.100)$$

with z_1 given by the expression (3.77). In (3.100) we have neglected the $O(1/m_Q)$ difference between ω and $\bar{\omega}$.

On the other hand, the equation (3.95) yields the representation for the form factor ξ_3 in a different form

$$\begin{aligned}\xi_3(\omega) = & \int dz_2 \phi_0(z_2) \sqrt{z_2(z_2 + 2m_3)} \int_{-1}^1 \frac{d\eta}{2} \phi_0(z_1) \\ & \times \left[\frac{z_2 + 2m_3}{\omega + 1} \left(z_2 + m_3 + \frac{(z_1 - z_2)\omega}{\omega - 1} \right) - \frac{m_3}{2} \left(m_3 + \frac{2m_3 + z_1 + z_2}{1 + \omega} \right) \right].\end{aligned}\quad (3.101)$$

One can check that for the soft wave functions providing convergency of the integrals and nonsingular at $z = 0$ the representations (3.100) and (3.101) are equivalent. At zero recoil one finds

$$\begin{aligned}\xi_3(1) &= \int dz_2 \sqrt{z_2}(z_2 + 2m_3)^{3/2} \phi_0^2(z_2) \frac{z_2}{3} \\ &\equiv \frac{\langle z \rangle}{3},\end{aligned}\quad (3.102)$$

where $\langle z \rangle$ is an average kinetic energy of the light constituent quark inside an (infinitely) heavy meson in its rest frame. It is worth noting that the function ξ_3 is positive for all ω .

The universal form factor $\rho_1 = \rho_2$ can be found from the expansion of $s(\omega)$ with a NLO accuracy. In this case the NLO terms in the $1/m_Q$ expansions of the integration measure, the wave function, and the spectral density \tilde{s} contribute. Namely, we can write for the form factor h_s the expression

$$\begin{aligned}h_s(\omega) &= \int \left[d\mu_0 + \frac{d\mu_1^{(1)}}{m_1} + \frac{d\mu_1^{(2)}}{m_2} \right] \left[\tilde{s}(\bar{\omega}) + \frac{S_1}{m_1} + \frac{S_2}{m_2} \right] \\ &\quad \times \phi_0(z_1) \left(1 + \frac{m_3}{4m_1} \chi_1(z_1) \right) \phi_0(z_2) \left(1 + \frac{m_3}{4m_2} \chi_1(z_2) \right) \\ &= \xi(\bar{\omega}) + \left(\frac{1}{m_1} + \frac{1}{m_2} \right) \xi^{(1)}(\bar{\omega}) + \dots \\ &= \xi(\omega) + \left(\frac{1}{m_1} + \frac{1}{m_2} \right) [\xi^{(1)}(\omega) + \xi'(\omega) \bar{\Lambda}(\omega - 1)] + \dots,\end{aligned}\quad (3.103)$$

and hence $\rho_1(\omega) = \xi^{(1)}(\omega) + \xi'(\omega) \bar{\Lambda}(\omega - 1) - \xi_3(\omega) - \frac{\bar{\Lambda}}{2} \xi(\omega)$. We do not present explicit expression for ρ_1 . However, let us consider ρ_1 at zero recoil. The analysis of the anomalous contribution at $\bar{\omega} = 1$ gives

$$h_s(\bar{\omega} = 1) = 1 + \left(\frac{1}{m_1} + \frac{1}{m_2} \right) \left(\frac{\bar{\Lambda}}{2} - \frac{\langle z \rangle}{3} \right) + \dots\quad (3.104)$$

Using the relations $h_s(\omega = 1) = h_s(\bar{\omega} = 1) + O(1/m_Q^2)$ and $\xi_3(1) = \langle z \rangle/3$ we obtain $\rho_1(1) = 0$ just as required by HQET.

First, let us demonstrate that the dispersion representation of the form factor f requires subtraction. To this end consider the anomalous contribution at $\bar{\omega} = 1$. For the form factor f_D constructed from the spectral density \tilde{f}_D through the double dispersion representation without subtractions we find ²

$$f_D(1) = 2\sqrt{M_1 M_2} \left[1 + \frac{1}{2} \left(\frac{1}{m_1} + \frac{1}{m_2} \right) (\langle z \rangle + m_3 - \bar{\Lambda}) + \dots \right] \quad (3.105)$$

This value contradicts the Luke theorem which requires the $1/m_Q$ corrections to vanish at zero recoil. Let us demonstrate that the form factor f constructed from the spectral density with the included subtraction term

$$\begin{aligned} \tilde{f} &= \tilde{f}_D + (M_1^2 - s_1 + M_2^2 - s_2) \tilde{g} \\ &= \tilde{f}_D + (2p_1 p_2 - 2\tilde{p}_1 \tilde{p}_2) \tilde{g}, \end{aligned} \quad (3.106)$$

satisfies the NLO relation (3.27). Here $2\tilde{p}_1 \tilde{p}_2 = s_1 + s_2 - q^2$.

We have noticed above that to LO and NLO the expansion of the form factor f and the combination $2p_1 p_2 \cdot g - m_1 \cdot g_2$ coincide (3.29). Hence checking the NLO relations for the form factor f is equivalent to checking with the NLO accuracy the relation

$$f_D \simeq f_{2\tilde{p}_1 \tilde{p}_2 \cdot \tilde{g} - m_1 \cdot g_2}. \quad (3.107)$$

The spectral density of the r.h.s. of eq. (3.107) can be written as

$$\begin{aligned} 2\tilde{p}_1 \tilde{p}_2 \cdot \tilde{g} - m_1 \cdot \tilde{g}_2 &\simeq 2m_1 m_2 (\bar{\omega} + 1) \tilde{s} + [2m_1(z_2 + m_3) + 2m_2(z_1 + m_3)] \tilde{s} \\ &\quad - 8(m_1 + m_2)\beta - 4m_2(\bar{\omega} - 1)\beta. \end{aligned} \quad (3.108)$$

For checking the expression (3.107) in NLO we need the expansion of the spectral density \tilde{s} in LO and NLO which has the structure

$$\begin{aligned} \frac{1}{2} \tilde{s} &= m_1 \alpha_2 + m_2 \alpha_1 + m_3 (1 - \alpha_1 - \alpha_2) \\ &\equiv m_3 + \frac{z_1 + z_2 + 2m_3}{\bar{\omega} + 1} + \frac{S_1}{m_1} + \frac{S_2}{m_2} + \dots, \end{aligned} \quad (3.109)$$

with

$$S_1 = \frac{1}{2} z_2 (z_2 + 2m_3) - z_1 m_3 - (z_2 + 2m_3) \frac{z_1 - z_2}{\bar{\omega} - 1} - \frac{(z_1 + z_2 + 2m_3)^2}{\bar{\omega} + 1}, \quad (3.110)$$

and S_2 is obtained from S_1 by replacing z_1 and z_2 . The spectral density \tilde{f}_D reads

$$\tilde{f}_D = 4m_1 m_2 (\bar{\omega} + 1) \left(m_3 + \frac{z_1 + z_2 + 2m_3}{\bar{\omega} + 1} \right) + 2m_2 z_2 (z_2 + 2m_3) + 2m_1 z_1 (z_1 + 2m_3) - 4m_2 (\bar{\omega} - 1) \beta. \quad (3.111)$$

Notice that for checking the NLO relation (3.107) between the form factors we do not need explicit expression for the integration measure in the NLO: in the LO the spectral densities are equal and hence the NLO contributions from the integration measure into both sides of the eq (3.107) are equal too. Finally, Eq. (3.107) is satisfied if the following relation is valid

$$\begin{aligned} &\int dz_2 \sqrt{z_2(z_2 + 2m_3)} \phi_0(z_2) \int_{-1}^1 \frac{d\eta}{2} \phi_0(z_1) \\ &\quad \times \left[-z_2(z_2 + 2m_3) + 2(z_1 + m_3) \left(m_3 + \frac{z_1 + z_2 + 2m_3}{\bar{\omega} + 1} \right) - 4\beta + 2(\bar{\omega} + 1)S_1 \right] = 0, \end{aligned} \quad (3.112)$$

²Hereafter we denote as a_D a form factor reconstructed from its double discontinuity through dispersion representation without subtractions.

with z_1 given by (3.77). One can check this relation to be true for any function $\phi_0(z)$ regular at $z = 0$. Hence, the form factor f calculated with the subtracted double spectral density (3.106) satisfies the HQET relations in LO and NLO at all ω .

Strictly speaking, the NLO analysis does not allow us to uniquely specify the subtraction term: namely, any spectral density of the form

$$\tilde{f} = \tilde{f}_D + (M_1^2 - s_1 + M_2^2 - s_2)\tilde{\rho}_f \quad (3.113)$$

has a proper NLO behavior in accordance with (3.27) provided the spectral density $\tilde{\rho}_f$ behaves in the LO as

$$\tilde{\rho}_f \simeq 2 \left(m_3 + \frac{z_1 + z_2 + 2m_3}{\bar{\omega} + 1} \right).$$

As we demonstrate in the next section, the analysis of the heavy-to-light LO relations requires the identification $\tilde{\rho}_f = \tilde{g}$.

Let us notice that the form factor obtained within the light-cone approach [14] can be represented as dispersion representation with the spectral density [27]

$$\tilde{f}_{LC} = \frac{M_2}{\sqrt{s_2}} \tilde{f}_D + M_2 \left(\frac{s_1 - s_2 - q^2}{2\sqrt{s_2}} - \frac{M_1^2 - M_2^2 - q^2}{2M_2} \right) \frac{\tilde{a}_1 + \tilde{a}_2}{2}. \quad (3.114)$$

At zero recoil one finds

$$f_{LC}(1) = 2\sqrt{M_1 M_2} \left[1 - \frac{1}{2} \left(\frac{1}{m_1} - \frac{1}{m_2} \right) (\langle z \rangle + m_3 - \bar{\Lambda}) + \dots \right] \quad (3.115)$$

that contradicts the Luke theorem.

The NLO analysis of the form factors $a_{1,2}$ and χ_2

The double spectral densities of the form factors a_1 and $a'_2 \equiv a_2 - 2s$ in the LO read

$$\tilde{a}_{1D} = 4 [(z_2 + 2m_3)\alpha_1 - m_2\alpha_{11}(\bar{\omega} - 1)], \quad (3.116)$$

$$\tilde{a}'_{2D} = 4 \left[\frac{m_2}{m_1} (z_2 + 2m_3)\alpha_1 - m_2\alpha_{12}(\bar{\omega} - 1) \right]. \quad (3.117)$$

The quantity a'_2 is more convenient than a_2 for calculations because the LO term of the heavy quark expansion of a'_2 is zero.

The unsubtracted spectral representation for $a_1(\omega)m_2 - a_2(\omega)m_1$ in combination with eq (3.31) gives

$$\chi_2(\omega) = \xi_3(\omega) - \frac{1}{4} \int dz_2 \phi_0(z_2) \sqrt{z_2(z_2 + 2m_3)} \int_{-1}^1 \frac{d\eta}{2} \phi_0(z_1) [\tilde{a}_1 m_2 - \tilde{a}_2 m_1]. \quad (3.118)$$

Substituting the representation (3.100) for ξ_3 we find

$$\chi_2(\omega) = 0. \quad (3.119)$$

Let us now consider the linear combination $a_1(\omega)m_2 + a'_2(\omega)m_1$. As a first step, show that the unsubtracted dispersion representation is not compatible with HQET. To this end calculate the unsubtracted form factors a_{1D} and a'_{2D} at zero recoil:

$$a_{1D}(1) = \frac{1}{\sqrt{m_1 m_2}} \frac{1}{m_2} \left[\frac{2}{3} \langle z \rangle + \frac{m_3}{2} \right], \quad (3.120)$$

$$a'_{2D}(1) = \frac{1}{\sqrt{m_1 m_2}} \frac{1}{m_1} \left[\frac{1}{3} \langle z \rangle + \frac{m_3}{2} \right], \quad (3.121)$$

and hence

$$a_{1D}(1)m_2 + a'_{2D}(1)m_1 = \frac{1}{\sqrt{m_1 m_2}} [\langle z \rangle + m_3] \quad (3.122)$$

in contradiction with the HQET result eq. (3.32)

$$\frac{\bar{\Lambda}}{\sqrt{m_1 m_2}}. \quad (3.123)$$

This fact suggests a necessity of subtraction in the quantity $a_1 m_2 + a'_2 m_1$. Let us write the spectral density with subtraction in the form

$$\tilde{a}_1 m_2 + \tilde{a}'_2 m_1 = \tilde{a}_{1D} m_2 + \tilde{a}'_{2D} m_1 + \frac{\kappa}{\bar{\omega} + 1} \left(\frac{M_1^2 - s_1}{2\sqrt{s_1}} + \frac{M_2^2 - s_2}{2\sqrt{s_2}} \right) \frac{\tilde{\rho}_a}{2} \quad (3.124)$$

with

$$\tilde{\rho}_a \simeq 2 \left(m_3 + \frac{z_1 + z_2 + 2m_3}{\bar{\omega} + 1} \right). \quad (3.125)$$

Then corresponding representation for the form factor reads

$$\begin{aligned} a_1(\omega)m_2 + a'_2(\omega)m_1 &= \frac{1}{4\sqrt{m_1 m_2}} \int dz_2 \phi_0(z_2) \sqrt{z_2(z_2 + 2m_3)} \int_{-1}^1 \frac{dn}{2} \phi_0(z_1) \\ &\times \left[\tilde{a}_{1D} m_2 + \tilde{a}'_{2D} m_1 - \frac{2\kappa}{\omega + 1} (z_1 + z_2 + 2m_3) \left(m_3 + \frac{z_1 + z_2 + 2m_3}{\omega + 1} \right) \right] + \frac{\kappa \bar{\Lambda}}{2\sqrt{m_1 m_2}} \frac{\xi(\omega)}{\omega + 1}. \end{aligned} \quad (3.126)$$

According to the HQET relation (3.32) this quantity should be equal to

$$\frac{1}{\sqrt{m_1 m_2}} \left[\frac{2\bar{\Lambda}}{\omega + 1} \xi(\omega) - \xi_3(\omega) \frac{\omega - 1}{\omega + 1} \right] \quad (3.127)$$

The term proportional $\xi(\omega)$ yields $\kappa = 4$. One can check that this value also makes other parts of both expressions equal. Hence we arrive at the subtracted spectral density

$$\tilde{a}_1 m_2 + \tilde{a}'_2 m_1 = \tilde{a}_{1D} m_2 + \tilde{a}'_{2D} m_1 + \frac{1}{\bar{\omega} + 1} \left(\frac{M_1^2 - s_1}{\sqrt{s_1}} + \frac{M_2^2 - s_2}{\sqrt{s_2}} \right) \tilde{\rho}_a. \quad (3.128)$$

The resulting spectral densities of the form factors a_1 and a_2 with the built-in subtraction terms take the form

$$\tilde{a}_1 = \tilde{a}_{1D} + \frac{1}{(\bar{\omega} + 1)m_2} \left(\frac{M_1^2 - s_1}{\sqrt{s_1}} + \frac{M_2^2 - s_2}{\sqrt{s_2}} \right) \frac{\tilde{\rho}_a}{2}, \quad (3.129)$$

$$\tilde{a}_2 = \tilde{a}_{2D} + \frac{1}{(\bar{\omega} + 1)m_1} \left(\frac{M_1^2 - s_1}{\sqrt{s_1}} + \frac{M_2^2 - s_2}{\sqrt{s_2}} \right) \frac{\tilde{\rho}_a}{2}. \quad (3.130)$$

The NLO analysis of g_0 .

The unsubtracted spectral density \tilde{g}_{0D} has the form

$$\tilde{g}_{0D} \simeq \frac{4}{\sqrt{m_1 m_2}} \left[m_2 \alpha_1 (m_3 + m_2 \alpha_1 + m_1 \alpha_2) - \frac{\beta}{\bar{\omega} + 1} \right]. \quad (3.131)$$

At zero recoil one finds

$$g_{0D}(1) = \frac{1}{(m_1 m_2)^{3/2}} \left[\frac{\langle z \rangle + m_3}{2} + \frac{\langle z \rangle}{6} \right]. \quad (3.132)$$

On the other hand, taking into account our earlier finding $\chi_2 = 0$, the HQET result (3.28) reads

$$g_{0D}(1) = \frac{1}{(m_1 m_2)^{3/2}} \left[\frac{\bar{\Lambda}}{2} + \frac{\langle z \rangle}{6} \right]. \quad (3.133)$$

Our experience obtained in considering $a_1 m_2 + a'_2 m_1$ hints that the subtraction procedure adds a term proportional at zero recoil to $\bar{\Lambda} - \langle z \rangle - m_3$, and hence we expect subtraction to work properly also in the case of g_0 .

As a matter of fact, the spectral density

$$\tilde{g}_0 = \tilde{g}_{0D} + \frac{1}{(\bar{\omega} + 1)m_1 m_2} \left(\frac{M_1^2 - s_1}{\sqrt{s_1}} + \frac{M_2^2 - s_2}{\sqrt{s_2}} \right) \frac{\tilde{\rho}_{g_0}}{2} \quad (3.134)$$

satisfies the HQ expansion (3.28) provided the function $\tilde{\rho}_{g_0}$ behaves in the LO as

$$\tilde{\rho}_{g_0} \simeq 2 \left(m_3 + \frac{z_1 + z_2 + 2m_3}{\bar{\omega} + 1} \right). \quad (3.135)$$

The scalar form factor

Let us consider the form factor of the transition between two pseudoscalar mesons induced by the scalar current

$$\langle P(M_2, p_2) | \bar{q}_1 q_2 | P(M_1, p_1) \rangle = f_s(q^2) \quad (3.136)$$

For the analysis of the heavy-quark transition we introduce the velocity-dependent form factor as follows

$$\langle P(M_2, p_2) | \bar{q}_1 q_2 | P(M_1, p_1) \rangle = \sqrt{M_1 M_2} (1 + \omega) h_{f_s}(\omega) \quad (3.137)$$

such that

$$f_s(q^2) = \sqrt{M_1 M_2} (1 + \omega) h_{f_s}(\omega). \quad (3.138)$$

From HQET we find the following expansion

$$h_{f_s} = \xi + \left(\frac{1}{m_1} + \frac{1}{m_2} \right) \left[\frac{\omega - 1}{\omega + 1} \left(\frac{\bar{\Lambda}}{2} \xi - \xi_3 \right) + \rho_1 \right]. \quad (3.139)$$

An important consequence of this expansion is the relation

$$h_{f_s}(1) = 1 + O(1/m_Q^2), \quad (3.140)$$

which shows that the deviation of $h_{f_s}(1)$ from unity emerges only at the $1/m_Q^2$ order, as well as for the form factors h_f , h_{f_+} , and h_{g_+} (3.14).

Notice that in the leading and subleading orders in $1/m_Q$ the following quantities have the same expansion

$$\begin{aligned} f_s &\sim 2(p_1 p_2 - m_1 m_2)s + m_2 f_1 + m_1 f_2 \\ &\sim 2(p_1 p_2 - M_1 M_2)s + M_1 f_1 + M_2 f_2. \end{aligned} \quad (3.141)$$

The form factor can be obtained according to the relation

$$f_s(q^2) = \frac{1}{m_2 - m_1} q^\mu \langle P(M_2, p_2) | \bar{q}_1 \gamma_\mu q_2 | P(M_1, p_1) \rangle, \quad (3.142)$$

which follows from the equations of motion for quark fields. We then find

$$f_s(q^2) = \frac{1}{m_2 - m_1} [(M_1^2 - M_2^2) f_+(q^2) + q^2 f_-(q^2)] \quad (3.143)$$

and

$$h_{f_s} = \frac{1}{m_2 - m_1} [h_{f_+}(M_1 - M_2)(\omega + 1) - h_{f_-}(M_1 + M_2)(\omega - 1)]. \quad (3.144)$$

In this case the structure of the expansion (3.139) is satisfied automatically.

In the dispersion approach the double discontinuity of the form factor f_s is found from the Feynman graph

$$\tilde{f}_s^D = 2m_3 ((m_1 - m_2)^2 - q^2) + 2m_2 (s_2 - (m_1 - m_3)^2) + 2m_1 (s_1 - (m_2 - m_3)^2) - 4m_1 m_2 m_3. \quad (3.145)$$

The double discontinuities of the form factors f_+ , f_- and f_s obey the classical equation of motion

$$\tilde{f}_s^D(s_1, s_2, q^2) = \frac{1}{m_2 - m_1} \left[(s_1 - s_2) \tilde{f}_+(s_1, s_2, q^2) + q^2 \tilde{f}_-(s_1, s_2, q^2) \right]. \quad (3.146)$$

As becomes clear from comparing Eqs.(3.142) and (3.146), in order to satisfy the structure of the expansion (3.139) the form factor requires subtraction. The spectral density which includes the proper subtraction term reads

$$\tilde{f}_s = \tilde{f}_s^D + [(M_1^2 - s_1) - (M_2^2 - s_2)] \frac{\tilde{f}_+}{m_2 - m_1}. \quad (3.147)$$

Equivalently, the behavior of the form factor f_s can be brought in accordance with HQET in the NLO by defining the subtraction as follows

$$\tilde{f}_s = \tilde{f}_s^D + [(M_1^2 - s_1) + (M_2^2 - s_2)] \tilde{\rho}_{f_s}, \quad (3.148)$$

provided $\tilde{\rho}_{f_s} \sim \tilde{\rho}_{g_0} \sim \tilde{\rho}_a$, Eqs. (3.125) and (3.135).

Concluding this section let us summarize our main results: we have calculated the universal form factors and demonstrated the dispersion representations with relevant subtractions in the case of heavy-to-heavy transitions to reproduce the structure of the heavy-quark expansion in QCD in the leading and next-to-leading orders. However, we have not been able to fix uniquely these subtractions. As we shall see in the next section, the heavy-to-light transitions provide further restrictions on the form of the subtraction terms.

D. Heavy-to-light meson transitions

In this section we discuss meson decays induced by the heavy-to-light quark transitions in which case $M_1 = m_2 + O(1)$ is large, while $M_2 \simeq m_1$ is kept finite. As found by Isgur and Wise [8], in the region $\omega - 1 = O(1)$ the form factors of the tensor current can be expressed through the form factors of the vector and axial-vector currents in the leading $1/m_2$ order as follows

$$s(q^2) = \frac{1}{2M_1} f_1(q^2), \quad (3.149)$$

$$g_2(q^2) = -2M_1 g(q^2), \quad (3.150)$$

$$g_0(q^2) = \frac{1}{M_1} [2g(q^2) + a_2(q^2)], \quad (3.151)$$

$$g_1(q^2) = \frac{1}{M_1} [-f(q^2) + 2p_1 p_2 \cdot g(q^2)]. \quad (3.152)$$

We address the two issues: (i) perform the leading order $1/m_2$ expansion of the form factors and show the fulfillment of the relations (3.149–3.152) and (ii) discuss the scaling behavior of the form factors of the transition of different heavy mesons into a fixed final light state.

The LO $1/m_Q$ expansion of the form factors in the quark model

In the case of heavy-light transitions one observes the appearance of the two scales: the light scale $M_2 \simeq m_1 \simeq m_3 \simeq \bar{\Lambda}$, and the heavy scale $M_2 \simeq m_1$, and we may expand the form factors in inverse powers of the small parameter $\bar{\Lambda}/m_2$. The kinematical coefficients in the leading $\bar{\Lambda}/m_2$ order in the region $\bar{\omega} - 1 = O(1)$ simplify to

$$\lambda(s_1, s_2, q^2) \simeq 4m_2^2 [(z_1 + m_3 + \bar{\omega}m_1)^2 - s_2], \quad (3.153)$$

$$\beta = O(1), \quad (3.154)$$

$$\alpha_1 \simeq \frac{1}{m_2} \frac{(z_1 + m_3 + \bar{\omega}m_1)(s_2 - m_1^2 + m_3^2)/2 - s_2(z_1 + m_3)}{(z_1 + m_3 + \bar{\omega}m_1)^2 - s_2}$$

$$= O\left(\frac{1}{m_2}\right), \quad (3.155)$$

$$\alpha_2 \simeq \frac{(z_1 + m_3 + \bar{\omega}m_1)(z_1 + m_3) - (s_2 - m_1^2 + m_3^2)/2}{(z_1 + m_3 + \bar{\omega}m_1)^2 - s_2} \\ = O(1), \quad (3.156)$$

$$\alpha_{12} \simeq \alpha_1 \alpha_2 - \frac{\beta(z_1 + m_3 + \bar{\omega}m_1)}{2m_2[(z_1 + m_3 + \bar{\omega}m_1)^2 - s_2]} \\ = O\left(\frac{1}{m_2}\right), \quad (3.157)$$

$$\alpha_{11} \simeq \alpha_1^2 + \frac{1}{m_2^2} \frac{\beta s_2}{[(z_1 + m_3 + \bar{\omega}m_1)^2 - s_2]} \\ = O\left(\frac{1}{m_2^2}\right). \quad (3.158)$$

For the double spectral densities \tilde{f}_i these expressions yield the following LO relations

$$\tilde{s} = \frac{1}{2m_2} \tilde{f}_2, \quad (3.159)$$

$$\tilde{g}_2 = 2m_2 \tilde{g}, \quad (3.160)$$

$$\tilde{g}_{0D} = \frac{1}{m_2} (2\tilde{g} + \tilde{a}_{2D}), \quad (3.161)$$

$$\tilde{g}_1 = \frac{1}{m_2} [-\tilde{f}_D + 2\tilde{p}_1 \tilde{p}_2 \cdot \tilde{g}], \quad (3.162)$$

with $2\tilde{p}_1 \tilde{p}_2 = s_1 + s_2 - q^2$. Notice that these relations hold also for $\bar{\omega} = O(m_2)$.

First two equations directly give the LO equality of the corresponding form factors. The relation (3.161) between the unsubtracted spectral densities is more interesting and requires the LO identity of the subtraction terms

$$\tilde{\rho}_a \simeq \tilde{\rho}_{g_0}. \quad (3.163)$$

The choice $\tilde{\rho}_a = \tilde{\rho}_{g_0} = \tilde{g}$ is acceptable although there are no firm backgrounds to justify this very choice.

The most informative is the relation (3.162): this relation not only suggests a necessity of subtraction in the form factor f but also determines the subtraction term. When considering the heavy-to-heavy transitions we have found that the subtracted spectral density of the form (3.106)

$$\tilde{f} = \tilde{f}_D + (M_1^2 - s_1 + M_2^2 - s_2) \tilde{\rho}_f \quad (3.164)$$

matches the HQET expansion if $\tilde{\rho}_f \simeq \tilde{g}$ in LO. The eq. (3.162) prescribes $\tilde{\rho}_f = \tilde{g}$.

Scaling of the form factors with m_Q

Let us point out that in the case of the heavy-to-light transition there is no parametrical suppression of the anomalous contribution to the form factors compared with the normal one as it was in heavy-to-heavy transitions and both parts contribute on equal footings. We shall present all the results for the normal part but the same holds also for the anomalous part.

In the region $\bar{\omega} = O(1)$ one finds for the normal contribution

$$f_i(\bar{\omega}) = \frac{1}{\sqrt{m_2}} \int \frac{ds_2 \varphi(s_2) \lambda^{1/2}(s_2, m_1^2, m_3^2)}{16\pi m_1} \int_{-1}^1 \frac{d\eta \sqrt{\bar{\omega}^2 - 1} \phi_0(z_1) \tilde{f}_i(z_1, z_2, m_1, m_2, m_3, \bar{\omega})}{\sqrt{(m_1(\bar{\omega} + 1) + z_1 + z_2 + 2m_3)(m_1(\bar{\omega} - 1) + z_1 - z_2)}} \quad (3.165)$$

where

$$s_2 = (m_1 + m_3 + z_2)^2, \\ z_1 = z_2 \bar{\omega} \left(1 + \frac{2m_3 + z_2}{m_1}\right) + m_3(\bar{\omega} - 1) + \eta \sqrt{\bar{\omega}^2 - 1} \frac{\lambda^{1/2}(s_2, m_1^2, m_3^2)}{2m_1} + O(1/m_2).$$

Using the relations (3.153) one finds that the spectral densities scale at large m_2 as

$$\tilde{f}_i = m_2^{n_i} \rho_i(\bar{\omega}, m_1, m_3, z_1, z_2). \quad (3.166)$$

Namely,

$$\begin{aligned} \tilde{f}_1 &= O(1), \\ \tilde{f}_2 &= O(m_2), \\ \tilde{g} &= O(1), \\ \tilde{a}_1 &= O(1/m_2), \\ \tilde{a}_2 &= O(1), \\ \tilde{f} &= O(m_2), \\ \tilde{g}_1 &= O(1), \\ \tilde{g}_2 &= O(m_2), \\ \tilde{g}_0 &= O(1/m_2), \\ \tilde{s} &= O(1). \end{aligned}$$

Hence, the form factors have the scaling behaviour of the form

$$f_i = m_2^{n_i-1/2} r_i(\bar{\omega}; m_1, m_3; \varphi_2, \phi_0). \quad (3.167)$$

The variables ω and $\bar{\omega}$ are connected with each other as follows

$$\bar{\omega} = \frac{M_2}{m_1} \omega - \frac{\bar{\Lambda}}{m_1} + O(1/m_2), \quad (3.168)$$

and hence the ratio

$$f_i(\omega)/m_Q^{n_i+1/2} \quad (3.169)$$

is universal for the transition of any heavy meson into a fixed light state. This behaviour reproduces the results of [8] up to the logarithmic corrections which arise from the anomalous scaling of the quark currents in QCD.

To summarize, matching the LO $1/m_2$ relations between the form factors in the quark model to the corresponding relations of [8] allowed us to determine the subtraction term in the form factor f and equated to each other subtraction terms in the form factors $a_{1,2}$ and g_0 .

E. Numerical estimates for the universal form factors

In this section we apply the derived results to the model-dependent estimates of the universal form factors.

1. First, let us study the dependence of the IW function on the parameters of the quark model. We adopt the exponential parametrization of the radial wave functions in the form $w(\vec{k}^2) \simeq \exp(-\vec{k}^2/2\beta^2)$. For obtaining the LO wave function ϕ_0 we must take into account the relationship between the parameters z and \vec{k}^2 which is found from the following equation

$$\sqrt{s} = \sqrt{\vec{k}^2 + m_Q^2} + \sqrt{\vec{k}^2 + m_3^2} = m_Q + m_3 + z. \quad (3.170)$$

This yields the relation

$$\vec{k}^2 = z(z + 2m_3) + O(1/m_Q). \quad (3.171)$$

Using the eq. (2.93) we come to the following form of the LO wave function

$$\phi_0(z) \simeq \sqrt{\frac{z + m_3}{z + 2m_3}} \exp\left(-\frac{z(z + 2m_3)}{2\beta_0^2}\right), \quad (3.172)$$

where β_0 is the LO harmonic oscillator parameter

$$\beta(m_Q) = \beta_0 + O(1/m_Q). \quad (3.173)$$

For calculations we need to specify β_0 . The exact value of β_0 is not known but extrapolating the known values of β_D , β_B , and β_{D^*} we find $\beta_0 \simeq 0.4$ both in the WSB [10] and the ISGW2 [13] models. In the model for pseudoscalar mesons discussed in the previous Chapter we have found the following approximate relation

$$\beta(m_Q) \simeq 2.5 \frac{m_Q m_3}{m_Q + m_3}, \quad (3.174)$$

which gives $\beta_0 \simeq 2.5 m_3$. Table 4 presents the relevant numerical parameters. The results of calculating the IW function through the eq. (3.90) are shown in Fig. 16. Table 4 demonstrates the values $\xi'(1)$ calculated with the eq. (3.91) and the parameters of the quadratic fit of the form

$$\xi(\omega) = 1 - \rho_i^2(\omega - 1) + \delta_i(\omega - 1)^2, \quad (3.175)$$

obtained by interpolating the results of calculations in the range $1 \leq \omega \leq 1.5$. One can observe the value of $-\xi'(1)$ to be considerably larger than the parameter ρ^2 obtained by the interpolation procedure.

Table 4. Parameters of the quadratic fit to the IW function and the NLO form factor ξ_3 in various quark-model versions.

Ref.	m_3	β_0	$-\xi'(1)$	ρ^2	δ	$\xi_3(1)$	$\rho_{\xi_3}^2$	δ_{ξ_3}
Set 1 [10]	0.35	0.4	1.47	1.34	0.78	0.077	1.49	0.88
Set 2 [13]	0.33	0.4	1.43	1.31	0.76	0.08	1.4	0.84
Set 3 [24]	0.25	0.63	1.37	1.12	0.62	0.17	1.2	0.65

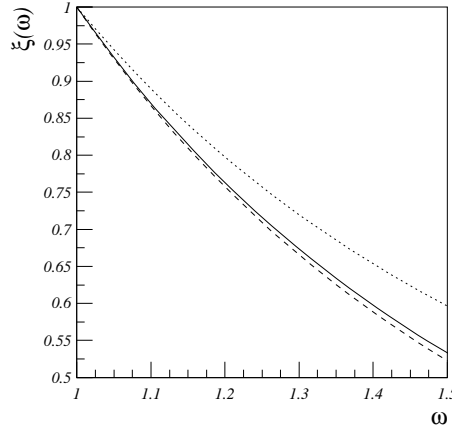


Fig. 16. The Isgur-Wise function calculated with various quark-model parameters: dashed line – set 1, solid line – set 2, dotted line – set 3.

The IW function obtained from the dispersion quark model agrees with the results of the light-cone quark model applied to the elastic $P \rightarrow P$ transition for (infinitely) heavy mesons [22] $\xi(1.5) = 0.62$ and turns out to be a bit smaller than the SR result $\xi(1.5) = 0.66$ [33].

The NLO form factor $\xi_3(\omega)$ is found to be very sensitive to the light-quark mass. The parameters of the quadratic fit to $\xi_3(\omega)$ calculated through eq. (3.100) in the form

$$h_i(\omega) = h_i(1) [1 - \rho_i^2(\omega - 1) + \delta_i(\omega - 1)^2] \quad (3.176)$$

for various sets of the quark-model parameters are shown in Table 4. One can observe an approximate relation $\xi_3(\omega)/\xi(\omega) \simeq 0.08 \text{ GeV}$ for the light quark mass $m_3 \simeq 0.35 \text{ GeV}$ and $\xi_3(\omega)/\xi(\omega) \simeq 0.17 \text{ GeV}$ for the light quark mass $m_3 \simeq 0.25 \text{ GeV}$ in the whole region $1 \leq \omega \leq 1.5$. This ratio is to be compared with the SR result with the $O(\alpha_s)$ corrections omitted [7]

$$\xi_3(\omega)/\xi(\omega) = \bar{\Lambda}/3 \simeq 0.16 \text{ GeV}, \quad \bar{\Lambda} \simeq 0.5 \text{ GeV}. \quad (3.177)$$

2. We are in a position to estimate the higher order corrections as we can calculate the form factors at finite masses and the leading-order contribution separately. For the ISGW2 parameter set ($m_c = 1.82$, $m_b = 5.2$, $\beta_D = 0.45$, $\beta_B = 0.43$, and $\beta_{D^*} = 0.38$), the results on h_{f_+} and h_f are shown in Fig. 17, and Table 5 presents the results of interpolating in the range $1 \leq \omega \leq 1.5$ with a quadratic fit (3.176).

Table 5. The form factors calculated with the parameters of ISGW2 model.

	h_{f_+}	h_f	ξ
$h(1)$	0.93	0.96	1.0
ρ^2	0.87	1.06	1.25
δ	0.37	0.53	0.7

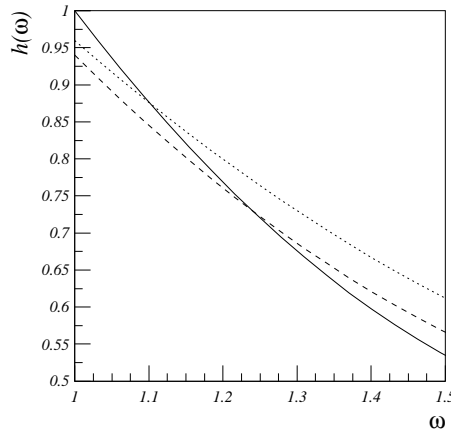


Fig. 17. The velocity-dependent form factors calculated for the ISGW2 parameters: solid line – the IW function, dashed line – $h_f(\omega)$, dotted line – $h_{f_+}(\omega)$.

The form factor h_f can be seen to agree with the results of a combined fit to the ALEPH, ARGUS, CLEO, DELPHI, and OPAL data [27]

$$\rho_f^2 = 1.07 \pm 0.20. \quad (3.178)$$

One observes sizeable difference between the form factors h_f and h_{f_+} and the Isgur–Wise function both in the value at zero recoil and the slope parameter. This indicates sizeable higher order corrections. At zero recoil the $1/m_Q$ corrections to h_f vanish and writing [7]

$$h_f(1) = 1 + \delta_{1/m^2} \quad (3.179)$$

we find $\delta_{1/m^2} = -0.04$ that agrees well with the value -0.055 ± 0.025 [7]. At the nonzero recoil the higher-order corrections yield a more flat ω -dependence of the form factor h_f compared with the IW function such that the slope of the IW function in our model turns out to be considerably larger compared with the slope of h_f : An approximate relation $\rho_{IW}^2 \simeq \rho_{h_f}^2 + 0.2$ is found. This is different from the sum-rules result $\rho_{IW}^2 \simeq \rho_{h_f}^2 - 0.2$ [7]. Let us also point out that $h'(1)$ obtained by the direct calculation (the theoretical value) turns out to be considerably larger than the parameter ρ^2 of the quadratic fit obtained by the interpolation over the range $1 \leq \omega \leq 1.5$ which could be measured experimentally. The same happens for the Isgur–Wise function.

F. Discussion

A detailed analysis of our dispersion approach to meson transition form factors was performed in this chapter. We calculated the double spectral densities of the form factors at spacelike momentum transfers from the Feynman graphs, and determined the necessary subtractions by considering the two following cases:

- (i) by performing the $1/m_Q$ expansion of the form factors in the case of heavy-to-heavy transitions and matching them to HQET, and
- (ii) by considering the relations between the form factors of the vector, axial-vector and tensor currents in the case of the heavy-to-light transition and matching them to the general relations in QCD obtained in ref. [8].

This procedure led to the spectral representations with appropriate subtractions at spacelike momentum transfers.

The form factors at timelike momentum transfers were then obtained by performing the analytical continuation in q^2 . The analytical continuation yielded the appearance of the anomalous contribution to the form factors at $q^2 > 0$. As a result, we have come to an explicit model of the form factors describing the weak meson transitions which develops the correct structure of the heavy-quark expansion in agreement with HQET.

Let us emphasize that the obtained representations allow to calculate form factors both at spacelike and timelike momentum transfers in terms of the wave functions of the participating mesons.

The following results were obtained in this chapter:

1. Applying the method of ref. [6] to meson amplitudes induced by the heavy-quark tensor current we have found the expansions of the relevant form factors in LO and NLO in HQET. The $1/m_Q$ corrections in the form factor h_{g+} vanish at zero recoil just as in h_{f+} and h_f .
2. The $1/m_Q$ expansion of the soft wave function was constructed. The normalization condition of the wave function yields an infinite chain of normalization conditions for wave function components emerging in various $1/m_Q$ orders. The LO normalization condition provides the proper normalization of the Isgur-Wise function at zero recoil.
3. Form factors of *heavy-to-heavy* meson transitions were considered.

First, the leading $1/m_Q$ -order analysis of the spectral representations for the form factors was performed. It was shown that to this accuracy all the transition form factors are represented through the Isgur-Wise function in accordance with HQET. The Isgur-Wise function was calculated in terms of the leading-order component of the heavy meson wave function. Subtraction terms in the spectral representations for the form factors do not contribute to this accuracy.

The anomalous contribution which emerges when the analytical continuation to the timelike region is performed comes into the game only in the $1/m_Q^2$ vicinity of the zero recoil point. It is otherwise suppressed by at least the second inverse power of the heavy-quark mass.

We then analysed spectral representations for the form factors with next-to-leading order accuracy.

We found that the $P \rightarrow P$ form factors do not require any subtractions to this accuracy and calculated the universal form factor ξ_3 in terms of the LO wave function.

In the case of the $P \rightarrow V$ transition the representations without subtractions perfectly match HQET for the form factors g , g_1 , g_2 , and $m_1 a_2 - m_2 a_1$ and leads to the relation $\rho_1 = \rho_2$ (or $\chi_3 = 0$) and $\chi_2 = 0$. At the same time, spectral representations without subtractions for the form factors f , g_0 , and $m_1 a_2 + m_2 a_1$ do not agree with HQET to this order.

Matching of the dispersion representations for these form factors to HQET shows the necessity of subtractions and restricts the form of the subtraction terms.

For performing the heavy-quark expansion only a strong localization of the meson momentum distribution with a width of order of the confinement scale was necessary. No other constraints on the soft wave functions or numerical parameters of the model have emerged.

4. We analysed *heavy-to-light* meson transitions and found that the Isgur-Wise relations between the form factors of the tensor and vector and axial-vector currents [8] further constrain subtraction terms in the spectral representations for the form factors.

5. We observed a discrepancy between the predictions of the various versions of the quark model on the NLO universal form factors : Namely, the analysis of the Wirbel-Stech-Bauer model [10] performed in [6] resulted in $\rho_1 \neq \rho_2 \neq 0$ and

$\rho_3 \neq 0$, but $\rho_4 = 0$; the quasipotential quark model [18] predicts all the NLO form factors to be nonzero; a consistent relativistic treatment of the $q\bar{q}$ intermediate states in Feynman graphs performed in this paper gives $\rho_1 = \rho_2$, $\rho_3=0$, and $\rho_4 \neq 0$.

The disagreement between our relativistic approach and the WSB model [10] can be traced back to the not fully consistent treatment of the quark spins in the latter. On the other hand, the origin of the discrepancy between the relativistic quasipotential approach of [18] and our dispersion approach is not fully understood and should be considered in more detail.

6. Numerical results from our dispersion approach using several parameter sets (i.e. constituent quark masses and wave functions) demonstrate only a moderate dependence of the Isgur-Wise functions on the value of the light-quark mass and the shape of the soft wave function.

Namely, the light-quark mass $m_3 = 0.25 \div 0.35$ and the wave-function width $\beta_0 = 0.4 \div 0.65$ give $\xi(1.5) = 0.55 \div 0.6$ that is a bit smaller than the SR result $\xi(1.5) = 0.66$ [33].

The form factor h_f is found to behave in agreement with predictions of other models and experimental results.

We observed a sizeable difference between the form factor h_f and the Isgur-Wise function both in the value at zero recoil and the slope parameter. This difference might be important for the analysis of the experimental data for the $B \rightarrow (D, D^*)l\nu$ decays.

The size of the higher-order $1/m_Q$ -corrections to $h_f(1)$, $\delta_{1/m^2} = -0.04$, obtained using the ISGW2 parameters agrees favorably with the sum rule estimates.

The slope of the Isgur-Wise function in our model turns out to be considerably larger compared with the slope of h_f : An approximate relation $\rho_{IW}^2 \simeq \rho_{h_f}^2 + 0.2$ (see Fig. 17) is found. This is opposite to the sum-rules result $\rho_{IW}^2 \simeq \rho_{h_f}^2 - 0.2$ [7]. We would like to notice that the slope parameter is very sensitive to the interpolation procedure: namely, the value $h'(1)$ turns out to be considerably larger than the result of the quadratic interpolation over the range $1 \leq \omega \leq 1.5$.

Our dispersion approach to the transition form factors can be further improved by performing the heavy-quark expansion in higher orders and matching to HQET order by order. It should be taken into account that the quark model effectively describes the whole $1/m_Q$ series, but the short-distance corrections are not contained in the model and should be considered separately.

IV. CALCULATION OF THE WEAK FORM FACTORS

In this Chapter the dispersion approach developed in previous sections is applied to form factors of weak transitions of heavy mesons. This issue was studied in [25,26,59–61]. We present form factors for weak decays of $B_{(s)}$ and $D_{(s)}$ mesons to light pseudoscalar and vector mesons obtained by the recent detailed analysis [61].

The use of this dispersion approach based on the constituent quark picture allows us to reveal the intimate connection between different decay modes and to perform the calculations in the full physical q^2 -region. In fact quark models provide for the only approach which leads to relations between the decays of various mesons through the meson wave functions and gives the form factors in the full q^2 range. However, quark models are not closely related to the QCD Lagrangian (or at least this relationship is not well understood yet) and therefore have input parameters which are not directly measurable and may not be of fundamental significance.

We reduce the usual disadvantages of quark models related to ill-defined effective quark masses and not precisely known meson wave functions by fitting the quark model parameters to lattice QCD results for the $B \rightarrow \rho$ transition form factors at large momentum transfers and to the measured total $D \rightarrow (K, K^*)l\nu$ decay rates. This allows us to predict numerous form factors for various decay channels and for all kinematically accessible q^2 values.

As demonstrated in the previous Section, the calculated form factors have the correct structure of the long-distance corrections in accordance with QCD in the leading and next-to-leading $1/m_Q$ orders, if the radial wave functions $w(k^2)$ are localized in a region of the order of the confinement scale, $k^2 \leq \Lambda^2$. We assume a simple gaussian parametrization of the radial wave function

$$w(k^2) \propto \exp(-k^2/2\beta^2), \quad (4.1)$$

which satisfies the localization requirement for $\beta \simeq \Lambda_{QCD}$.

A. Parameters of the model

We consider the slope parameter β of the meson wave function (4.1) and the constituent quark masses as fit parameters. The relevant values for the B , ρ , and π mesons are determined [59] from the requirement to reproduce the observed value of the pion decay constant $f_\pi = 130 \text{ MeV}$ and from the fit to the lattice results on the form factors $T_2(q^2)$ and $A_1(q^2)$ (see Eq. (4.3) below) at $q^2 = 19.6$ and 17.6 GeV^2 [52]. The spectral representations for the decay constants (3.63) and for the form factors (3.37) are used for calculations.

The values obtained for m_b , m_u , and β_B , β_ρ , β_π are displayed in Table 6.

Table 6. Constituent quark masses and slope parameters of the exponential wave function (in GeV).

m_u	m_s	m_c	m_b	β_π	β_K	β_D	β_B	β_{η_s}	β_{D_s}	β_{B_s}	β_ρ	β_{K^*}	β_{D^*}	β_ϕ
0.23	0.35	1.45	4.85	0.36	0.42	0.46	0.54	0.45	0.48	0.56	0.31	0.42	0.46	0.45

A few comments are in order:

- As it was already noticed, the spectral representation (3.37) takes into account the long-distance contributions connected with the structure of the initial and final mesons. To describe additional long-distance effects in the q^2 channel, Eq. (3.37) should be multiplied by the constituent quark form factor $f_{q_2 \rightarrow q_1}(q^2)$ which contributes to the resonance structure in the q^2 channel. However, in the region of calculation $q^2 < (m_2 - m_1)^2$, the wave functions provide already for a rise of the form factors with q^2 which is well compatible with a properly located meson pole. Thus an additional quark form factor is not needed there, but we shall use a proper extrapolation formula when considering the vicinity of the poles.
- The quark model double spectral representations take into account long-range QCD effects but not the short-range perturbative corrections. However, by fitting the wave functions and masses to reproduce the lattice points, these corrections are effectively taken care of: Corrections to the quark propagators correspond to the appearance of the effective quark masses. Corrections to the vertices at the relevant values of the recoil variable $\omega = (M_B^2 + m_\pi^2 - q^2)/2M_B M_\pi$ should be small as found in form factors of other meson transitions [69].
- The value obtained for the b -quark mass $m_b = 4.85 \text{ GeV}$ is close to the one-loop pole mass which in fact is the relevant mass for quark model calculations.

We now need to fix the parameters describing the strange and charmed mesons. The charm quark mass can be determined from the well-known $1/m_Q$ expansion of the heavy meson mass in terms of the heavy quark mass and the hadronic parameters $\bar{\Lambda}$, λ_1 and λ_2 . Using the recent estimates of these parameters [83] one finds

$$m_b - m_c \simeq 3.4 \text{ GeV}. \quad (4.2)$$

This provides $m_c \simeq 1.45 \text{ GeV}$. For m_s one expects $m_s \simeq 350 - 370 \text{ MeV}$ taking into account that $m_u = 230 \text{ MeV}$.

A stringent way to constrain the parameters m_s , β_K , β_{K^*} , and β_D is provided by the measured integrated rates of the semileptonic decays $D \rightarrow (K, K^*)l\nu$. In addition we apply the relation (3.63) which connects β_K with m_s by using the known value of the K -meson leptonic decay constant $f_K = 160 \text{ MeV}$. The parameter values found this way are displayed in Table 6³. The corresponding form factors and decay rates are given in Tables 9 and 11.

The polarization of the K^* in the $D \rightarrow K^*l\nu$ decays turns out to be in good agreement with the experimental result (Table 11), and the calculated D meson decay constant $f_D = 200 \text{ MeV}$ corresponds to the expectation for the magnitude of this quantity.

The parameter β_{D^*} cannot be found this way, but it should be close to β_D because of the heavy quark symmetry requirements. We therefore set $\beta_{D^*} = \beta_D$.

Also listed in Table 6 are the parameters which describe strange heavy mesons. They are discussed in subsection D.

Table 7. Leptonic decay constants of pseudoscalar mesons in MeV calculated via (3.63) for the quark-model parameters of Table 6.

f_π	f_K	f_D	f_B	f_{η_s}	f_{D_s}	f_{B_s}
132	160	200	180	183	220	200

Table 8. Meson masses in GeV from PDG [84]

M_π	M_K	M_η	$M_{\eta'}$	M_D	M_{D_s}	M_B	M_{B_s}	M_ρ	M_{K^*}	M_ϕ	M_{D^*}	$M_{D_s^*}$
0.14	0.49	0.547	0.958	1.87	1.97	5.27	5.37	0.77	0.89	1.02	2.01	2.11

The knowledge of the wave functions and the quark masses allows the calculation of the form factors in Eq. (3.4). It is however more convenient to present our results in terms of the dimensionless form factors F_+ , F_0 , F_T , V , A_0 , A_1 , A_2 , T_1 , T_2 , T_3 [10] which are the following linear combinations of the form factors given in Eq. (3.4):

$$\begin{aligned}
F_+ &= f_+, \\
F_0 &= f_+ + \frac{q^2}{Pq} f_-, \\
F_T &= (M_1 + M_2)s, \\
V &= (M_1 + M_2)g, \\
A_1 &= \frac{1}{M_1 + M_2} f, \\
A_2 &= -(M_1 + M_2)a_+, \\
A_0 &= \frac{1}{2M_2} (f + q^2 \cdot a_- + Pq \cdot a_+), \\
T_1 &= -g_+, \\
T_2 &= -g_+ - \frac{q^2}{Pq} g_-, \\
T_3 &= g_- - \frac{Pq}{2} g_0.
\end{aligned} \quad (4.3)$$

³In [27] a different set of the parameters was used which also provided a good description of the available experimental data on semileptonic B and D decays. However, the corresponding form factors have a rather flat q^2 -dependence and do not match the lattice results at large q^2 .

Each of these form factors contains contributions of q^2 -channel resonances only of the same spin. This is the advantage of the form factors of the set (4.3) compared with the form factors defined by the Eq. (3.4), some of which contain contributions of resonances with different spins.

1. The form factors F_+ , F_T , V , T_1 , and A_0

The form factors F_+ , F_T , V , T_1 contain a pole at $q^2 = M_V^2 \equiv M_{1-}^2$ and A_0 contains a pole at $q^2 = M_B \equiv M_{0-}^2$. The residues of the form factors at these poles are given in terms of the product of the weak and strong coupling constants. These coupling constants therefore determine the behavior of the form factors at q^2 near the resonance poles (beyond the decay region). We consider as an example the case of the $B \rightarrow \pi, \rho$ transition.

Weak decay constants

Weak decay constants of mesons are defined by the following relations

$$\begin{aligned}\langle 0 | \bar{q} \gamma_\mu \gamma_5 b | B(q) \rangle &= i f_P^{(B)} q_\mu \\ \langle 0 | \bar{q} \gamma_\mu b | B^*(q) \rangle &= \epsilon_\mu^{*(B^*)} M_{B^*} f_V^{(B^*)} \\ \langle 0 | \bar{q} \sigma_{\mu\nu} b | B^*(q) \rangle &= i (\epsilon_\mu^{*(B^*)} q_\nu - \epsilon_\nu^{*(B^*)} q_\mu) f_T^{(B^*)},\end{aligned}\tag{4.4}$$

where $\epsilon_\mu^{(B^*)}$ is the B^* polarization vector. In the heavy quark limit one has

$$f_P^{(B)} = f_V^{(B^*)} = f_T^{(B^*)}.$$

Strong coupling constants

Strong coupling constants are connected with the three-meson amplitudes as follows

$$\begin{aligned}\langle \pi(p_2) B^*(q) | B(p_1) \rangle &= -\frac{1}{2} g_{B^* B \pi} P_\mu \epsilon_\mu^{(B^*)} \\ \langle \rho(p_2) B^*(q) | B(p_1) \rangle &= \frac{1}{2} \epsilon_{\alpha\beta\mu\nu} \epsilon_\alpha^{(\rho)} \epsilon_\beta^{(B^*)} P_\mu q_\nu \frac{g_{BB\rho}}{M_B^*} \\ \langle \rho(p_2) B(q) | B(p_1) \rangle &= \frac{1}{2} g_{BB\rho} P_\mu \epsilon_\mu^{(\rho)},\end{aligned}\tag{4.5}$$

where $q = p_1 - p_2$, $P = p_1 + p_2$ and ϵ_μ is the polarization vector of the vector meson.

In the heavy quark limit

$$g_{B^* B \rho} = g_{BB\rho}.$$

The form factors F_+ , F_T , V , T_1 contain pole at $q^2 = M_{B^*}^2$ due to the contribution of the intermediate B^* (1^- state) in the q^2 channel. The residue of this pole is given in terms of the product of the weak and strong coupling constants such that in the region $q^2 \simeq M_{B^*}^2$ the form factors read

$$\begin{aligned}F_+ &= \frac{g_{B^* B \pi} f_V^{(B^*)}}{2M_{B^*}^*} \frac{1}{1 - q^2/M_{B^*}^2} + \dots, \\ F_T &= \frac{g_{B^* B \pi} f_T^{(B^*)}}{2M_{B^*}^*} \frac{M_B + M_\pi}{M_{B^*}^*} \frac{1}{1 - q^2/M_{B^*}^2} + \dots, \\ V &= \frac{g_{B^* B \rho} f_V^{(B^*)}}{2M_{B^*}^*} \frac{M_B + M_\rho}{M_{B^*}^*} \frac{1}{1 - q^2/M_{B^*}^2} + \dots, \\ T_1 &= \frac{g_{B^* B \rho} f_T^{(B^*)}}{2M_{B^*}^*} \frac{1}{1 - q^2/M_{B^*}^2} + \dots\end{aligned}\tag{4.6}$$

Here ... stand for the terms non-singular at $q^2 = M_{B^*}^2$.

Similarly, A_0 contains the contribution of the B (0^- state). In the region of $q^2 \simeq M_B^2$ it can be represented as follows

$$A_0 = \frac{g_{BB\rho} f_P^{(B)}}{2M_B} \frac{M_B}{2M_\rho} \frac{1}{1 - q^2/M_B^2} + \dots \quad (4.7)$$

Let us notice that the residues of the form factors are not all independent and are connected with each other as follows:

$$\frac{Res(F_T)Res(V)}{Res(F_+)Res(T_1)} = \frac{M_B + M_\rho}{M_{B^*}} \frac{M_B + M_\pi}{M_{B^*}}. \quad (4.8)$$

This relation can be used as a cross-check of the consistency of the extrapolation for the form factors.

The coupling constants are related to the residues of the form factors according to the relations

$$\begin{aligned} \frac{g_{B^*B\pi} f_V^{(B^*)}}{2M_{B^*}} &= Res(F_+), \\ \frac{g_{BB\rho} f_P^{(B)}}{2M_\rho} &= 2Res(A_0), \\ \frac{f_T^{(B^*)}}{f_V^{(B^*)}} &= \frac{Res(F_T)}{Res(F_+)} \frac{M_{B^*}}{M_B + M_\pi}, \\ \frac{g_{B^*B\rho}}{g_{B^*B\pi}} &= \frac{Res(V)}{Res(F_+)} \frac{M_{B^*}}{M_B + M_\rho}. \end{aligned} \quad (4.9)$$

2. The form factors F_0 , A_1 , A_2 , T_2 and T_3

The remaining form factors, F_0 , A_1 , A_2 , T_2 and T_3 , do not contain contributions of the lowest lying negative parity states (for instance, F_0 contains a contribution of the 0^+ state, and A_1 contains that of the 1^+ which have considerably higher masses). As a result they have a rather flat q^2 behaviour in the decay region, whereas the form factors F_+ , F_T , V , T_1 , A_0 are rising more steeply.

From the spectral representations (3.37) together with the parameter values of Table I the form factors are obtained numerically. For the applications it is convenient, however, to represent our results by simple fit formulas which interpolate these numerical values within a 1% accuracy for all q^2 values in the region $0 < q^2 < (m_2 - m_1)^2$. Also, they should be appropriate for a simple extrapolation to the resonance region.

Let us start with the form factors F_+ , F_T , V , T_1 , A_0 . If we interpolate the results of the calculation with the simple three-parameter fit formula

$$f(q^2) = \frac{f(0)}{(1 - q^2/M^2)(1 - q^2/(\alpha M^2))}, \quad (4.10)$$

the least- χ^2 interpolation procedure leads in all cases to a value of the parameter M which is within 3% equal to the lowest resonance mass. We consider this fact to be an important indication for the proper choice of the quark-model parameters and for the reliability of our calculations. We therefore prefer to fix the pole mass M to its physical value. The fit functions (4.10) represent the results now with an accuracy of less than 2%. To achieve the accuracy of less than 1% in all cases we take the form [59]:

$$f(q^2) = \frac{f(0)}{(1 - q^2/M^2)[1 - \sigma_1 q^2/M^2 + \sigma_2 q^4/M^4]}, \quad (4.11)$$

where $M = M_P$ for the form factor A_0 and $M = M_V$ for the form factors F_+ , F_T , V , T_1 . In the Tables below we quote numerical values of σ_2 only if an accuracy of better than 1% cannot be achieved with $\sigma_2 = 0$, and take $\sigma_2 = 0$ if this accuracy can already be achieved with the two parameters $f(0)$ and σ_1 .

For the heavy-to-light meson transitions the masses of the lowest resonances are not very much different from the highest q^2 values in the decay. Eq. (4.11) then allows an estimate of the residues of these poles. These residues can be expressed in terms of products of weak and strong coupling constants. The errors for these constants induced

by changing σ_1 and σ_2 in our fitting procedure (keeping to the 1% requirement) do not exceed 10%. Moreover, the residues of the form factors at the meson pole are not independent and satisfy certain constraint (4.8), which provides a consistency check of the extrapolations. The mismatch in (4.8) is always below 10%, and in most of the cases much lower.

For the form factors F_0 , A_1 , A_2 , T_2 and T_3 the contributing resonances (0^+ , 1^+ , etc) lie farther away from the physical decay region and the effect of any particular resonance is smeared out. For these form factors the interpolation formula taken is⁴

$$f(q^2) = f(0)/[1 - \sigma_1 q^2/M_V^2 + \sigma_2 q^4/M_V^4]. \quad (4.12)$$

If setting $\sigma_2 = 0$ allows us to describe the calculation results with better than 1% accuracy for all q^2 , a simple monopole two-parameter formula is used.

The values of $f(0)$, σ_1 , and σ_2 are given for each decay mode in the relevant sections.

⁴ One should note that the parameters σ_1 and σ_2 in the fit formula (4.12) for the form factors F_0 , A_1 , A_2 , T_2 , and T_3 are introduced in a different way than in the fit formula (4.11) for the form factors F_+ , F_T , V , T_1 , and A_0 .

B. Charmed meson decays

1. $D \rightarrow K, K^*$

The $D \rightarrow K, K^*$ decays are induced by the charged current $c \rightarrow s$ quark transition. As described in the previous section, the measured total rates of these decays are used for a precise fit of the parameters of our model. With the parameters of Table 6 we obtain the form factors listed in Table 9. Table 10 compares the form factors at $q^2 = 0$ with the results of other approaches and Table 11 presents the decay rates.

Table 9. The $D \rightarrow K, K^*$ transition form factors. $M_V = M_{D_s^*} = 2.11 \text{ GeV}$, $M_P = M_{D_s} = 1.97 \text{ GeV}$. For the form factors F_+, F_T, V, A_0, T_1 the fit formula Eq. (4.11) is used, for the other form factors - Eq. (4.12)

	$D \rightarrow K$			$D \rightarrow K^*$						
	F_+	F_0	F_T	V	A_0	A_1	A_2	T_1	T_2	T_3
$f(0)$	0.78	0.78	0.75	1.03	0.76	0.66	0.49	0.78	0.78	0.45
σ_1	0.24	0.38	0.27	0.27	0.17	0.30	0.67	0.25	0.02	1.23
σ_2		0.46				0.20	0.16		1.80	0.34

Table 10. Comparison of the results of different approaches for the semileptonic $D \rightarrow K, K^*$ form factors at $q^2 = 0$.

Ref.	$F_+(0)$	$F_T(0)$	$V(0)$	$A_1(0)$	$A_2(0)$
This work	0.78	0.75	1.03	0.66	0.49
WSB [10]	0.76	—	1.3	0.88	1.2
Jaus'96 [14]	0.78	—	1.04	0.66	0.43
SR [29]	0.60(15)	—	1.10(25)	0.50(15)	0.60(15)
Lat(average) [45]	0.73(7)	—	1.2(2)	0.70(7)	0.6(1)
Lat [46]	0.71(3)	0.66(5)	—	—	—
Exp [85]	0.76(3)	—	1.07(9)	0.58(3)	0.41(5)

Table 11. The $D \rightarrow (K, K^*)l\nu$ decay rates in 10^{10} s^{-1} obtained within different approaches, $|V_{cs}| = 0.975$.

Ref.	$\Gamma(D \rightarrow K)$	$\Gamma(D \rightarrow K^*)$	$\Gamma(K^*)/\Gamma(K)$	Γ_L/Γ_T
This work	9.7	6.0	0.63	1.28
Jaus'96 [14]	9.6	5.5	0.57	1.33
SR [29]	6.5(1.5)	3.8(1.5)	0.50(15)	0.86(6)
Exp [86]	9.3(4)	5.7(7)	0.61(7)	1.23(13) [84]

Extrapolating the form factors to $q^2 = M_{D^*}^2$ (or $q^2 = M_D^2$ for A_0) gives the following estimates of the coupling constants

$$\begin{aligned}
\frac{g_{D_s^* DK} f_V^{(D_s^*)}}{2M_{D_s^*}} &= 1.05 \pm 0.05, \\
\frac{g_{D_s DK^*} f_P^{(D_s)}}{2M_{K^*}} &= 1.7 \pm 0.1, \\
\frac{f_T^{(D_s^*)}}{f_V^{(D_s^*)}} &= 0.95 \pm 0.05, \\
\frac{g_{D_s^* DK^*}}{g_{D_s^* DK}} &= 1.1 \pm 0.1.
\end{aligned}$$

2. $D \rightarrow \pi, \rho$

These decays are induced by the $c \rightarrow d$ charged current. Since all the necessary parameters have already been fixed, this mode allows for parameter-free predictions. Table 12 presents the results of our calculations. In Tables 13 and 14 we compare our results with different approaches and with experimental data.

Table 12. The calculated $D \rightarrow \pi, \rho$ transition form factors. $M_V = M_{D^*} = 2.01 \text{ GeV}$, $M_P = M_D = 1.87 \text{ GeV}$. For the form factors F_+, F_T, V, A_0, T_1 the fit formula Eq. (4.11) is used, for the other form factors - Eq. (4.12).

	$D \rightarrow \pi$			$D \rightarrow \rho$						
	F_+	F_0	F_T	V	A_0	A_1	A_2	T_1	T_2	T_3
$f(0)$	0.69	0.69	0.60	0.90	0.66	0.59	0.49	0.66	0.66	0.31
σ_1	0.30	0.54	0.34	0.46	0.36	0.50	0.89	0.44	0.38	1.10
σ_2		0.32							0.50	0.17

Table 13. Comparison of the results of different approaches for the semileptonic $D \rightarrow \pi, \rho$ form factors at $q^2 = 0$.

Ref.	$F_+(0)$	$F_T(0)$	$V(0)$	$A_1(0)$	$A_2(0)$
This work	0.69	0.60	0.90	0.59	0.49
WSB [10]	0.69	—	1.23	0.78	0.92
Jaus'96 [14]	0.67	—	0.93	0.58	0.42
SR [29]	0.50(15)	—	1.0(2)	0.5(2)	0.4(2)
Lat(ave) [45]	0.65(10)	—	1.1(2)	0.65(7)	0.55(10)
Lat [46]	0.64(5)	0.60(7)	—	—	—

Table 14. The $D \rightarrow (\pi, \rho) l \nu$ decay rates in 10^{10} s^{-1} , $|V_{cd}| = 0.22$.

Ref.	$\Gamma(D \rightarrow \pi)$	$\Gamma(D \rightarrow \rho)$	$\Gamma(\rho)/\Gamma(\pi)$	Γ_L/Γ_T
This work	0.95	0.42	0.45	1.16
WSB [10]	0.68	0.67	1.0	0.91
Jaus'96 [14]	0.8	0.33	0.41	1.22
SR [29]	0.39(8)	0.12(4)	—	1.31(11)
Melikhov'97 [27]	0.62	0.26	0.41	1.27
Exp [87–89]	0.92(45)	0.45(22)	0.50(35)	—

The form factors at $q^2 = 0$ are close to the predictions of the relativistic quark model of Ref. [14], but the q^2 dependence is different such that our model and [14] predict different decay rates. Although the experimental errors are very large and nearly all theoretical results agree with experiment, we notice perfect agreement of our decay rates with the central values.

For the coupling constants we get the following relations

$$\frac{g_{D^* D \pi} f_V^{(D^*)}}{2M_{D^*}} = 1.05 \pm 0.05, \quad \frac{g_{D D \rho} f_P^{(D)}}{2M_\rho} = 2.1 \pm 0.2, \quad \frac{f_T^{(D^*)}}{f_V^{(D^*)}} = 0.9 \pm 0.1, \quad \frac{g_{D^* D \rho}}{g_{D^* D \pi}} = 1.3 \pm 0.2.$$

Taking $f_V^{(D^*)} \simeq 220 \text{ MeV}$, we find

$$g_{D^* D \pi} = 18 \pm 3$$

in good agreement with a calculation of $g_{D^* D \pi}$ based on combining PCAC with the dispersion approach [60]. This value also compares very well with the first recent measurement of $g_{D^* D \pi}$ reported by CLEO [90]

$$g_{D^* D \pi} = 17.9 \pm 0.3 \pm 1.9.$$

Notice a serious disagreement between our result and the sum rule estimate [91]

$$g_{D^* D \pi}^{SR} = 12.5 \pm 1.0.$$

The experimental result clearly speaks in favour of our prediction.

C. Beauty meson decays

1. $B \rightarrow D, D^*$

These decays arise from the heavy-quark $b \rightarrow c$ transition. Here one has rigorous predictions for the expansion of the form factors in terms of the heavy-quark mass [6]. Namely, the main part of the form factors can be expressed through the universal form factor - the Isgur-Wise function. However, different models provide different q^2 -dependences of the Isgur-Wise function as well as different subleading $1/m_Q$ corrections.

We recall that our spectral representations of the form factors explicitly respect the structure of the long-distance QCD corrections in the leading and the subleading orders of the heavy-quark expansion. Thus, we expect reliable predictions for the form factors. Our numerical results are summarized in Tables 15, 16, and 17.

Table 15. The $B \rightarrow D, D^*$ transition form factors. $M_V = M_{B_c^*} \simeq M_P = M_{B_c} = 6.4 \text{ GeV}$. For the form factors F_+, F_T, V, A_0, T_1 the fit formula Eq. (4.11) is used, for the other form factors - Eq. (4.12).

	$B \rightarrow D$			$B \rightarrow D^*$						
	F_+	F_0	F_T	V	A_0	A_1	A_2	T_1	T_2	T_3
$f(0)$	0.67	0.67	0.69	0.76	0.69	0.66	0.62	0.68	0.68	0.33
σ_1	0.57	0.78	0.56	0.57	0.58	0.78	1.40	0.57	0.64	1.46
σ_2							0.41			0.50

Table 16. Comparison of the results of different approaches for the semileptonic $B \rightarrow D, D^*$ form factors at $q^2 = 0$.

Ref.	$F_+(0)$	$A_1(0)$	$R_1(0) = V(0)/A_1(0)$	$R_2(0) = A_2(0)/A_1(0)$
This work	0.67	0.66	1.15	0.94
Jaus'96 [14]	0.69	0.69	1.17	0.93
Neubert [7]			1.3	0.8
Exp [92]			$1.18 \pm 0.15 \pm 0.16$	$0.71 \pm 0.22 \pm 0.07$

Table 17. The $B \rightarrow (D, D^*) l \nu$ decay rates in $|V_{cb}|^2 \text{ ps}^{-1}$.

Ref.	$\Gamma(B \rightarrow D)$	$\Gamma(B \rightarrow D^*)$	$\Gamma(D^*)/\Gamma(D)$	Γ_L/Γ_T
This work	8.57	22.82	2.66	1.11
Jaus'96 [14]	9.6	25.33	2.64	
Mel'97 [26]	8.7	21.0	2.65	1.28
Exp	$(1.34 \pm 0.15)10^{-2} \text{ ps}^{-1}$ [93]	$(2.98 \pm 0.17)10^{-2} \text{ ps}^{-1}$ [94]	2.35(1.3)	1.24(0.16) [95]

For the coupling constants we find

$$\begin{aligned}
\frac{g_{B_c^* BD} f_V^{(B_c^*)}}{2M_{B_c^*}} &= 1.56 \pm 0.15, \\
\frac{g_{B_c BD^*} f_P^{(B_c)}}{2M_{D^*}} &= 3.3 \pm 0.3, \\
\frac{f_T^{(B_c^*)}}{f_V^{(B_c^*)}} &= 0.9 \pm 0.1, \\
\frac{g_{B_c^* BD^*}}{g_{B_c^* BD}} &= 1.05 \pm 0.05.
\end{aligned}$$

2. $B \rightarrow K, K^*$

These decays are induced by the $b \rightarrow s$ Flavor Changing Neutral Current (FCNC). We recall that the $B \rightarrow \pi, \rho$ form factors at large q^2 have been used to fix the parameters of the model. Thus we expect that the predictions for the $B \rightarrow K, K^*$ form factors which in fact differ from the former mode only by SU(3) violating effects should be particularly reliable. Table 18 presents the calculated form factors and Fig 18 exhibits our predictions together with the available lattice results at large q^2 . The good agreement shows that the size and the sign of the SU(3) violating effects are correctly accounted for.

Table 18. The calculated $B \rightarrow K, K^*$ transition form factors. $M_V = M_{B_s^*} = 5.42 \text{ GeV}$, $M_P = M_{B_s} = 5.37 \text{ GeV}$. For the form factors F_+, F_T, V, A_0, T_1 the fit formula Eq. (4.11) is used, for the other form factors - Eq. (4.12).

	$B \rightarrow K$			$B \rightarrow K^*$						
	F_+	F_0	F_T	V	A_0	A_1	A_2	T_1	T_2	T_3
$f(0)$	0.36	0.36	0.35	0.44	0.45	0.36	0.32	0.39	0.39	0.27
σ_1	0.43	0.70	0.43	0.45	0.46	0.64	1.23	0.45	0.72	1.31
σ_2		0.27				0.36	0.38		0.62	0.41

Table 19. Comparison of the results of different approaches for the $B \rightarrow K, K^*$ form factors at $q^2 = 0$.

Ref.	$F_+(0)$	$F_T(0)$	$V(0)$	$A_1(0)$	$A_2(0)$	$A_0(0)$	$T_1(0)$	$T_3(0)$
This work	0.36	0.35	0.44	0.36	0.32	0.45	0.39	0.27
SR [34]	0.25	-	0.47	0.37	0.40	0.30	0.38	-
Lat+Stech [52]	-	-	0.38	0.28	-	0.32	0.32	-
LCSR'98 [36]	0.34	0.374	0.46	0.34	0.28	0.47	0.38	0.26
Lat [46]	0.30(4)	0.29(6)	-	-	-	-	-	-

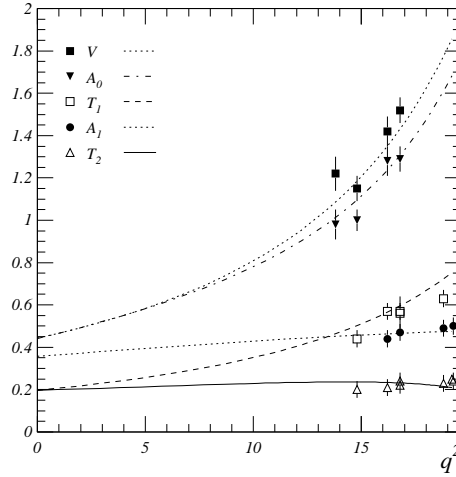


Fig. 18. Form factors of the $B \rightarrow K^*$ transition vs the lattice results.

For the coupling constants we obtain

$$\begin{aligned} \frac{g_{B_s^*BK} f_V^{(B_s^*)}}{2M_{B_s^*}} &= 0.65 \pm 0.05, & \frac{g_{B_sBK^*} f_P^{(B_s)}}{2M_{K^*}} &= 1.65 \pm 0.1, \\ \frac{f_T^{(B_s^*)}}{f_V^{(B_s^*)}} &= 0.95 \pm 0.05 & \frac{g_{B_s^*BK^*}}{g_{B_s^*BK}} &= 1.15 \pm 0.05. \end{aligned}$$

3. $B \rightarrow \pi, \rho$

The $B \rightarrow \rho$ transition has been used for determining the parameters of our quark model in the u, d and b sectors by fitting the quark-model form factors to available lattice results on T_2 and A_1 at large q^2 [59], see Figure 19. The parametrizations for the $B \rightarrow \pi, \rho$ form factors are given in Table 20.

The form factor F_0 at large q^2 lies below the central lattice values but nevertheless agrees with lattice results within the given error bars. Notice however that in our model the form factor F_0 is calculated as a difference of f_+ and f_- and at large q^2 turns out to be much more sensitive to the subtle details of the pion wave function, than f_+ and f_- separately. A simple Gaussian wave function which works quite well for f_+ and f_- , might not be sufficiently accurate for F_0 .

Table 20. The calculated $B \rightarrow \pi, \rho$ transition form factors. $M_V = M_{B^*} = 5.32 \text{ GeV}$, $M_P = M_B = 5.27 \text{ GeV}$. For the form factors F_+, F_T, V, A_0, T_1 the fit formula Eq. (4.11) is used, for the other form factors - Eq. (4.12).

	$B \rightarrow \pi$			$B \rightarrow \rho$						
	F_+	F_0	F_T	V	A_0	A_1	A_2	T_1	T_2	T_3
$f(0)$	0.29	0.29	0.28	0.31	0.30	0.26	0.24	0.27	0.27	0.19
σ_1	0.48	0.76	0.48	0.59	0.54	0.73	1.40	0.60	0.74	1.42
σ_2		0.28				0.10	0.50		0.19	0.51

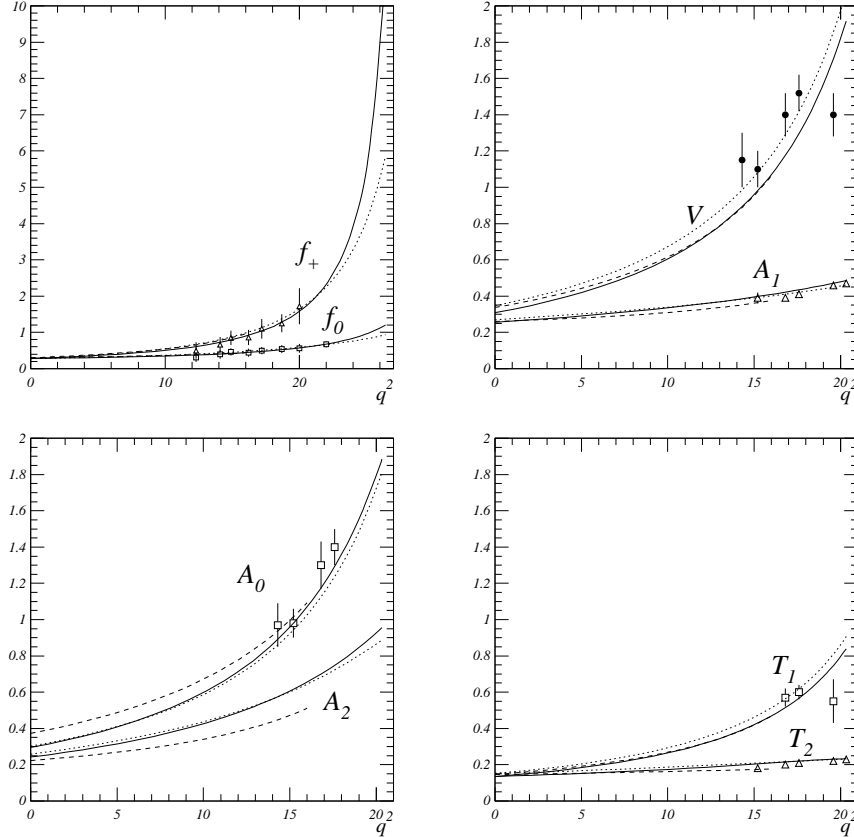


Fig. 19. The $B \rightarrow \pi$ and $B \rightarrow \rho$ form factors vs lattice results. Solid lines - results from the dispersion approach obtained in Ref. [59], dotted lines - lattice-constrained parametrizations of Ref. [52], dashed lines - results from light-cone sum rules [36]

Table 21. Comparison of the results of different approaches on weak $B \rightarrow \pi, \rho$ form factors at $q^2 = 0$.

Ref.	$F_+(0)$	$F_T(0)$	$V(0)$	$A_1(0)$	$A_2(0)$	$A_0(0)$	$T_1(0)$	$T_3(0)$
This work	0.29	0.28	0.31	0.26	0.24	0.29	0.27	0.19
Jaus'96 [14]	0.27	-	0.35	0.26	0.24	-	-	-
LCSR'98 [36]	0.305	0.296	0.34	0.26	0.22	0.37	0.29	0.20
Lat [46]	0.28(4)	0.28(7)	-	-	-	-	-	-

Table 21 compares the results obtained from the quark model of Ref. [59] with results from the quark model of Jaus [14] and latest light-cone sum rule (LCSR) results [36]. One observes very good agreement between the quark model of Jaus, LCSRs, and our approach. The only visible difference with the LCSR method occurs in the form factor $A_0(0)$, which is caused by small differences of the two methods in $A_1(0)$ and $A_2(0)$ (recall that $A_0(0) = ((M_1 + M_2)A_1(0) - (M_1 - M_2)A_2(0))/2M_2$). This discrepancy exceeds the 15% error bar quoted for the LCSR results only marginally. If the LCSR results at small q^2 and lattice results at large q^2 are correct, our approach surely provides a realistic description of the form factors at all kinematically accessible q^2 values.

Extrapolating the form factors to the poles, we obtain

$$\begin{aligned}
 \frac{g_{B^*B\pi}f_V^{(B^*)}}{2M_{B^*}} &= 0.6 \pm 0.05, \\
 \frac{g_{BB\rho}f_P^{(B)}}{2M_\rho} &= 1.4 \pm 0.2, \\
 \frac{f_T^{(B^*)}}{f_V^{(B^*)}} &= 0.97 \pm 0.03, \\
 \frac{g_{B^*B\rho}}{g_{B^*B\pi}} &= 1.2 \pm 0.1.
 \end{aligned}$$

It is convenient to define the quantity \hat{g} according to the relation

$$\hat{g} = \frac{f_\pi}{2\sqrt{M_B M_{B^*}}} g_{BB^*\pi}. \quad (4.13)$$

Using $f_V^{B^*} \simeq 200 \text{ MeV}$ gives the estimate

$$\begin{aligned}
 g_{BB^*\pi} &= 32 \pm 5, \\
 \hat{g} &= 0.4 \pm 0.06
 \end{aligned} \quad (4.14)$$

The latter value is in good agreement with the lattice result $\hat{g} = 0.42 \pm 0.04 \pm 0.08$ [48] and is only slightly smaller than $\hat{g} = 0.5 \pm 0.02$ [60] based on combining PCAC with our dispersion approach.

Table 22 compares the calculated semileptonic decay rates from different theoretical approaches.

 Table 22. The $B \rightarrow (\pi\rho)l\nu$ Decay rates in units $|V_{ub}|^2 \text{ps}^{-1}$.

Ref.	$\Gamma(B \rightarrow \pi\ell\nu)$	$\Gamma(B \rightarrow \rho\ell\nu)$	Γ_L/Γ_T
This work	$8.0^{+0.8}_{-0.2}$	15.8 ± 2.3	0.88 ± 0.08
ISGW2 QM [12]	9.6	14.2	0.3
Lat [52]	$8.5^{+3.4}_{-0.9}$	$16.5^{+3.5}_{-2.3}$	$0.80^{+0.04}_{-0.03}$
LCSR [37]	—	13.5 ± 4.0	0.52 ± 0.08
LCSR [31]	8.85	17.7	1.12

Combining the experimental data reported by CLEO $\mathcal{B}(B^0 \rightarrow \rho^- l^+ \nu) = (2.57 \pm 0.29_{-0.46}^{0.33} \pm 0.41) \cdot 10^{-4}$ [96] with our prediction for $\Gamma(B \rightarrow \rho l \nu)$ leads to the following estimate for the central value of V_{ub} :

$$|V_{ub}| = 3.25 \cdot 10^{-3}. \quad (4.15)$$

Using the $B^0 \rightarrow \pi^- l^+ \nu$ measurement from Belle $\mathcal{B}(B^0 \rightarrow \pi^- l^+ \nu) = (1.28 \pm 0.20 \pm 0.26) \cdot 10^{-4}$ [97] and our prediction for $\Gamma(B \rightarrow \pi l \nu)$ leads to the central value

$$|V_{ub}| = 3.22 \cdot 10^{-3}. \quad (4.16)$$

The perfect agreement between these values speaks in favour of the reliability of our predictions for the form factors.

Summing up our results on the decays of the nonstrange heavy mesons, we found no disagreement neither with the existing experimental data nor with the available results of the lattice QCD or sum rules in their specific regions of validity. The only exception is the form factor F_0 at large q^2 in $B \rightarrow \pi$ and $D \rightarrow \pi$ decays, where our results are lying slightly below the lattice points. However, this disagreement can be related to a strong sensitivity of F_0 at large q^2 to the details of the pion wave function. Small changes in the pion wave function, which only marginally affect f_+ and f_- , can change the form factor F_0 . But such subtle effects are beyond the scope of our present analysis.

In the next section we apply our model to the decays of strange heavy mesons for which a few new parameters have to be introduced which are specific to the description of weak decays of strange heavy mesons to light mesons.

D. Decays of the strange mesons D_s and B_s

Before dealing with these decays, we must first specify the slope parameters of the B_s and the D_s wave function. We obtain these parameters by applying (3.63) and using $f_{B_s}/f_B = 1.1$ and $f_{D_s}/f_D = 1.1$ in agreement with the lattice estimates for these quantities [45]. The resulting values of the slope parameters are listed in Table 6. Since all other parameters have already been fixed the calculation of the form factors is straight forward. The only exceptions are the decays into the η, η', ϕ final states. For these decays we need to know the ϕ wave function, the mixing angle and the slope of the radial wave function of the $s\bar{s}$ component in η and η' . Our procedure of fixing these parameters are discussed in the relevant subsection.

1. $D_s \rightarrow K, K^*$

These meson transition are driven by the charged-current $c \rightarrow d$ quark transition. The results of the calculation are given in Table 23. The predictions for the semileptonic decay rates are displayed in Table 24.

Table 23. The calculated $D_s \rightarrow K, K^*$ transition form factors. $M_V = M_{D^*} = 2.01 \text{ GeV}$, $M_P = M_D = 1.87 \text{ GeV}$. For the form factors F_+, F_T, V, A_0, T_1 the fit formula Eq. (4.11) is used, for the other form factors - Eq. (4.12).

	$D_s \rightarrow K$			$D_s \rightarrow K^*$						
	F_+	F_0	F_T	V	A_0	A_1	A_2	T_1	T_2	T_3
$f(0)$	0.72	0.72	0.77	1.04	0.67	0.57	0.42	0.71	0.71	0.45
σ_1	0.20	0.41	0.24	0.24	0.20	0.29	0.58	0.22	-0.06	1.08
σ_2		0.70				0.42			0.44	0.68

Table 24. The $D_s \rightarrow (K, K^*)l\nu$ decay rates in 10^{10} s^{-1} , $|V_{cd}| = 0.22$.

Ref	$\Gamma(D_s \rightarrow K)$	$\Gamma(D_s \rightarrow K^*)$	$\Gamma(K^*)/\Gamma(K)$	Γ_L/Γ_T
This work	0.63	0.38	0.6	1.21

For the coupling constants we obtain

$$\begin{aligned}
\frac{g_{D^* D_s K} f_V^{(D^*)}}{2M_{D^*}} &= 0.95 \pm 0.05, \\
\frac{g_{D D_s K^*} f_P^{(D)}}{2M_{K^*}} &= 1.85 \pm 0.15, \\
\frac{f_T^{(D^*)}}{f_V^{(D^*)}} &= 0.9 \pm 0.1, \\
\frac{g_{D^* D_s K^*}}{g_{D^* D_s K}} &= 1.15 \pm 0.15.
\end{aligned}$$

2. $D_s \rightarrow \eta, \eta', \phi$

These decay modes are induced by the charged current $c \rightarrow s$ quark transition. The pseudoscalar mesons η and η' are mixtures of the nonstrange and the strange components with the flavour wave functions $\eta_n \equiv \frac{\bar{u}u + \bar{d}d}{\sqrt{2}}$ and $\eta_s = \bar{s}s$, respectively,

$$\begin{aligned}\eta &= \cos(\varphi) \eta_n - \sin(\varphi) \eta_s \\ \eta' &= \sin(\varphi) \eta_n + \cos(\varphi) \eta_s,\end{aligned}\tag{4.17}$$

with the angle $\varphi \simeq 40^\circ$ [69].

The decay rates of interest are

$$\begin{aligned}\Gamma(D_s \rightarrow \eta l \nu) &= \sin^2(\varphi) \Gamma(D_s \rightarrow \eta_s(M_\eta) l \nu) \\ \Gamma(D_s \rightarrow \eta' l \nu) &= \cos^2(\varphi) \Gamma(D_s \rightarrow \eta_s(M_{\eta'}) l \nu).\end{aligned}\tag{4.18}$$

Let us give a brief explanation of these formulas: The semileptonic decay rates are determined by the form factor f_+ . The spectral representation of this form factor does not involve the final meson mass explicitly. This means that for the $\bar{s}s$ component of both η and η' we have to deal with the same form factor, which can be expressed through the radial wave function of this component. On the other hand, the phase-space volume of the decay process is determined by the physical meson masses, as indicated in (4.18). It should be clear, however, that the η_s is not an eigenstate of the Hamiltonian and does not have a definite mass.

Assuming universality of the wave functions of the ground state pseudoscalar 0^- nonet, the radial wave function of the nonstrange component Ψ_{η_n} coincides with the pion radial wave function [69]. The radial wave function Ψ_{η_s} should be determined independently. From the analysis of a broad set of processes the leptonic decay constant f_s of the strange component η_s , has been found to lie in the interval $f_s = (1.36 \pm 0.04) f_\pi$ [98]. This allows us to determine the slope parameter β_{η_s} in such a way that the calculated value of f_s lies in this interval, and the calculated ratio $\Gamma(D_s \rightarrow \eta)/\Gamma(D_s \rightarrow \eta')$ agrees with the experimental data for $\varphi = 40^\circ$. This procedure yields for the slope parameter $\beta_{\eta_s} = 0.45$ ⁵. For the slope parameter β_ϕ of the wave function of the ϕ -meson, which is the vector $\bar{s}s$ state, we expect a value close to β_{η_s} .

In fact, $\beta_\phi = 0.45 \text{ GeV}$ leads to the $B_s \rightarrow \phi$ transition form factors which agree well with the LCSR results at $q^2 = 0$ (see subsection 4). With all other quark model parameters fixed from the description of the nonstrange heavy meson decays and by taking a simple Gaussian form of the radial wave function, the decay rate $\Gamma(D_s \rightarrow \phi l \nu)$ is a function of β_ϕ . This function has a minimum at the value $\beta_\phi = 0.45 \text{ GeV}$; nevertheless, the corresponding value of the decay rate is 1σ above the central experimental value.

The results of our calculations are given in Tables 25 and 26.

Table 25. The calculated $D_s \rightarrow \eta_s, \phi$ transition form factors. $M_V = M_{D_s^*} = 2.11 \text{ GeV}$, $M_P = M_{D_s} = 1.97 \text{ GeV}$. For the form factors F_+, F_T, V, A_0, T_1 the fit formula Eq. (4.11) is used, for the other form factors - Eq. (4.12).

	$D_s \rightarrow \eta_s(M_\eta)$			$D_s \rightarrow \eta_s(M_{\eta'})$		$D_s \rightarrow \phi$						
	F_+	F_0	F_T	F_0	F_T	V	A_0	A_1	A_2	T_1	T_2	T_3
$f(0)$	0.78	0.78	0.80	0.78	0.94	1.10	0.73	0.64	0.47	0.77	0.77	0.46
σ_1	0.23	0.33	0.24	0.21	0.24	0.26	0.10	0.29	0.63	0.25	0.02	1.34
σ_2		0.38		0.76							2.01	0.45

⁵Another procedure of taking into account the SU(3) breaking effects to obtain Ψ_{η_s} from Ψ_{η_n} has been proposed in [69].

Table 26. The $D_s \rightarrow (\eta, \eta', \phi) l \nu$ decay rates in 10^{10} s^{-1} , $|V_{cs}| = 0.975$. The experimental rates are obtained from the corresponding branching ratios using the D_s lifetime $\tau_{D_s} = 0.495 \pm 0.013 \text{ ps}$ from the 1999 update [84]

Ref	$\Gamma(D_s \rightarrow \eta)$	$\Gamma(D_s \rightarrow \eta')$	$\Gamma(D_s \rightarrow \phi)$
This work	5.0	1.85	5.1
Exp [99]	5.2 ± 1.3	2.0 ± 0.8	4.04 ± 1.01

For the coupling constants we obtain

$$\begin{aligned}
\frac{g_{D_s^* D_s \eta_s} f_V^{(D_s^*)}}{2M_{D_s^*}} &= 1.0 \pm 0.1, \\
\frac{g_{D_s D_s \phi} f_P^{(D_s)}}{2M_\phi} &= 1.6 \pm 0.3, \\
\frac{f_T^{(D_s^*)}}{f_V^{(D_s^*)}} &= 0.93 \pm 0.03, \\
\frac{g_{D_s^* D_s \phi}}{g_{D_s^* D_s \eta_s}} &= 1.08 \pm 0.04.
\end{aligned}$$

3. $B_s \rightarrow K, K^*$

This mode is driven by the $b \rightarrow u$ charged current transition. The only additional new parameter needed here is the slope of the B_s wave function. We obtain it by using (3.63) and taking $f_{B_s}/f_B = 1.1$. The results of our calculation are given in Table 27.

Table 27. The calculated $B_s \rightarrow K, K^*$ transition form factors. $M_V = M_{B^*} = 5.32 \text{ GeV}$, $M_P = M_B = 5.27 \text{ GeV}$. For the form factors F_+, F_T, V, A_0, T_1 the fit formula Eq. (4.11) is used, for the other form factors - Eq. (4.12).

	$B_s \rightarrow K$			$B_s \rightarrow K^*$						
	F_+	F_0	F_T	V	A_0	A_1	A_2	T_1	T_2	T_3
$f(0)$	0.31	0.31	0.31	0.38	0.37	0.29	0.26	0.32	0.32	0.23
σ_1	0.63	0.93	0.61	0.66	0.60	0.86	1.32	0.66	0.98	1.42
σ_2	0.33	0.70	0.30	0.30	0.16	0.60	0.54	0.31	0.90	0.62

These form factors lead to the following relations

$$\begin{aligned}
\frac{g_{B^* B_s K} f_V^{(B^*)}}{2M_{B^*}} &= 0.44 \pm 0.04, \\
\frac{g_{B B_s K^*} f_P^{(B)}}{2M_{K^*}} &= 1.3 \pm 0.1, \\
\frac{f_T^{(B^*)}}{f_V^{(B^*)}} &= 0.95 \pm 0.05, \\
\frac{g_{B^* B_s K^*}}{g_{B^* B_s K}} &= 1.2 \pm 0.1.
\end{aligned}$$

The form factors at $q^2 = 0$ are compared with the LCSR predictions in Table 28. We observe some disagreement between our predictions and the LCSR calculation which gives smaller values for all the form factors. A closer look at the origin of this discrepancy shows that its source is the strength and sign of the SU(3)-breaking effects. They lead to opposite corrections in the two approaches.

Table 28. Comparison of the QM and LCSR results on the $B_s \rightarrow K, K^*$ form factors at $q^2 = 0$.

Ref.	$V(0)$	$A_1(0)$	$A_2(0)$	$A_0(0)$	$T_1(0)$	$T_3(0)$
This work	0.38	0.29	0.26	0.37	0.32	0.23
LCSR'98 [36]	0.262	0.19	0.164	0.254	0.22	0.16

To discuss these SU(3) breaking effects, let us start with $B \rightarrow \rho$, which in fact differs from the $B_s \rightarrow K^*$ only by the flavour of the spectator quark, and move to $B_s \rightarrow K^*$ by accounting for the SU(3) violating effects:

Within the LCSR method there are two changes which affect the form factors: first, the change $f_{B_s} \rightarrow f_B$ leads to an increase of the $B_s \rightarrow K^*$ form factors; second, the change of the symmetric twist-two distribution amplitude of the ρ -meson to the asymmetric one of the K^* meson leads to a decrease of the form factors. The second effect turns out to be much stronger than the first one with the result of an overall decrease of the form factors.

In the quark model, the same SU(3) breaking effects take place: The change of the spectator mass (it determines the increase of f_{B_s}/f_B) and the change of the K^* meson wave function (due to the change of both the quark mass and the slope parameter of the light meson wave function). Here the influence of the slope of the heavy meson wave function upon the form factor is only marginal. Therefore, the resulting effect of these changes leads to an increase of the form factors.

We want to point out that the difference between the results of the two approaches does not arise from specific effects (higher twists, higher radiative corrections etc) which are present in the LCSRs but absent in the quark model. The observed difference is only due to the different strength of the SU(3) violating effects at the level of the twist-2 distribution amplitude. As was discussed in [69], this distribution amplitude can be expressed through the radial soft wave function of the meson. The change of the quark-model wave function caused by SU(3) violating effects does not induce a strong asymmetry in the leading twist-2 distribution amplitude.

In view of the discrepancy between our results and the LCSR it would be interesting to have independent calculations of the $B_s \rightarrow K^*$ form factors at small q^2 from the 3-point sum rules, as well as a lattice calculation for large q^2 .

4. $B_s \rightarrow \eta, \eta', \phi$

These weak meson transitions are induced by the FCNC $b \rightarrow s$ quark transition. The results of the form factor calculation are given in Table 29 and compared with the LCSR predictions at $q^2 = 0$ in Table 30. The agreement between the two values is satisfactory at least within the declared 15% accuracy of the LCSR predictions. This allows us to expect that also the $D_s \rightarrow \phi, \eta, \eta'$ form factors and the corresponding decay rates (given earlier in subsection 2) are calculated reliably.

Table 29. The calculated $B_s \rightarrow \eta_s, \phi$ transition form factors. $M_V = M_{B_s^*} = 5.42 \text{ GeV}$, $M_P = M_{B_s} = 5.37 \text{ GeV}$. For the form factors F_+, F_T, V, A_0, T_1 the fit formula Eq. (4.11) is used, for the other form factors - Eq. (4.12).

	$B_s \rightarrow \eta_s(M_\eta)$			$B_s \rightarrow \eta_s(M_{\eta'})$		$B_s \rightarrow \phi$						
	F_+	F_0	F_T	F_0	F_T	V	A_0	A_1	A_2	T_1	T_2	T_3
$f(0)$	0.36	0.36	0.36	0.36	0.39	0.44	0.42	0.34	0.31	0.38	0.38	0.26
σ_1	0.60	0.80	0.58	0.80	0.58	0.62	0.55	0.73	1.30	0.62	0.83	1.41
σ_2	0.20	0.40	0.18	0.45	0.18	0.20	0.12	0.42	0.52	0.20	0.71	0.57

Table 30. Comparison of the QM and LCSR results on the $B_s \rightarrow \phi$ form factors at $q^2 = 0$.

Ref.	$V(0)$	$A_1(0)$	$A_2(0)$	$A_0(0)$	$T_1(0)$	$T_3(0)$
This work	0.44	0.34	0.31	0.42	0.38	0.26
LCSR'98 [36]	0.433	0.296	0.255	0.382	0.35	0.25

For the coupling constants we obtain

$$\begin{aligned}
\frac{g_{B_s^* B_s \eta_s} f_V^{(B_s^*)}}{2M_{B_s^*}} &= 0.6 \pm 0.05, \\
\frac{g_{B_s B_s \phi} f_P^{(B_s)}}{2M_\phi} &= 1.5 \pm 0.1, \\
\frac{f_T^{(B_s^*)}}{f_V^{(B_s^*)}} &= 0.95 \pm 0.05, \\
\frac{g_{B_s^* B_s \phi}}{g_{B_s^* B_s \eta_s}} &= 1.13 \pm 0.06.
\end{aligned}$$

E. Discussion

In this Chapter we have calculated numerous form factors of heavy meson transitions to light mesons which are relevant for the semileptonic (charged current) and penguin (flavor-changing neutral current) decay processes. Our approach is based on evaluating the triangular decay graph within a relativistic quark model which has the correct analytical properties and satisfies all known general requirements of long-distance QCD.

The model connects different decay channels in a unique way and gives the form factors for all relevant q^2 values. The disadvantage of the constituent quark model connected with its dependence on ill-defined parameters such as the effective constituent quark masses, have been reduced by using several constraints: the quark masses and the slope parameters of the wave functions are chosen such that the calculated form factors reproduce the lattice results for the $B \rightarrow \rho$ form factors at large q^2 and the observed integrated rates of the semileptonic $D \rightarrow K, K^*$ decays.

Our main results from this Chapter are as follows:

- In spite of the rather different masses and properties of mesons involved in weak transitions, all existing data on the form factors, both from theory and experiment, can be understood in our quark picture. Namely, all the form factors are essentially described by the few degrees of freedom of constituent quarks, i.e. their wave functions and their effective masses. Details of the soft wave functions are not crucial; only the spatial extension of these wave functions of order of the confinement scale is important. In other words, only the meson radii are essential.
- The calculated transition form factors are in all cases in good agreement with the results available from lattice QCD and from sum rules in their specific regions of validity. The only exception is a disagreement with the LCSR results for the $B_s \rightarrow K^*$ transition where we predict larger form factors. This disagreement is caused by a different way of taking into account the SU(3) violating effects when going from $B \rightarrow \rho$ to $B_s \rightarrow K^*$ and is not related to specific details of the dynamics of the decay process. We suspect that the LCSR method overestimates the SU(3) breaking in the long-distance region but this problem deserves further clarification.
- We have estimated the products of the meson weak and strong coupling constants by using the fit formulas for the form factors for the extrapolation to the meson pole. The error of such estimates connected with the errors in the extrapolation procedure is found to be around 5-10%.

We cannot provide for definite error estimates of our predictions for the form factors because of the approximate character of the constituent quark model. However from the fine agreement obtained in cases where checks are possible, we believe that the actual accuracy of our predictions for the form factors is around 10%. Since some parameters have been fixed by using lattice results and have also been tested using the sum rule predictions, further improvements of the accuracy of our predictions will follow if these approaches attain smaller errors. Of course, each precisely measured decay will also allow a more accurate determination of the parameters of the model and thus can be used to diminish the errors at least for closely related decays.

V. WEAK ANNIHILATION IN THE RARE RADIATIVE $B \rightarrow \rho\gamma$ DECAY AND THE $B \rightarrow \gamma\ell\nu$ FORM FACTORS

Results obtained in the previous Chapter allow us to fully describe semileptonic $B_{(s)}$ and $D_{(s)}$ decays. We now discuss rare radiative decays of heavy mesons induced by the flavour-changing neutral currents (FCNC) such as $B \rightarrow K^*\gamma$ and $B \rightarrow \rho\gamma$ decays. This Chapter is based on Refs. [64,65].

The investigation of rare semileptonic B decays induced by the flavour-changing neutral current transitions $b \rightarrow s$ and $b \rightarrow d$ represents an important test of the standard model or its extensions. Rare decays are forbidden at the tree level in the standard model and occur at the lowest order only through loop diagrams. This fact opens the possibility to probe the structure of the electroweak sector at large mass scales due to contributions of virtual particles in the loop diagrams. Interesting information about the structure of the theory is contained in the Wilson coefficients in the effective Hamiltonian which describes the $b \rightarrow s, d$ transition at low energies. These Wilson coefficients take different values in different theories with testable consequences in rare B decays [100–107].

Among rare B decays the radiative decays $b \rightarrow s\gamma$ and $b \rightarrow d\gamma$ have the largest probabilities. The $b \rightarrow s\gamma$ transitions are CKM favoured and have larger branching ratios than the $b \rightarrow d\gamma$ transitions. The $b \rightarrow s\gamma$ transition has been observed by CLEO in the exclusive channel $B \rightarrow K^*\gamma$ in 1993 [108] and measured inclusively in 1995 [109]. The $B \rightarrow \rho\gamma$ decay will be extensively studied by BaBar and BELLE.

Any reliable extraction of the perturbative (short-distance) effects encoded in the Wilson coefficients of the effective Hamiltonian requires an accurate separation of the nonperturbative (long-distance) contributions, which therefore should be known with high accuracy.

In rare exclusive semileptonic decays one faces several types of long-distance contributions which arise in the meson transition amplitude of the effective Hamiltonian, which contains penguin and 4-quark operators (see [110] for more details).

The dominant long-distance effects for the radiative decays arise from the electromagnetic penguin operator and is given in terms of the form factor $T_1(q^2 = 0)$.

The 4-quark operators generate many different contributions:

One of them is the so-called long-range charming penguins, i.e. intermediate $c\bar{c}$ states in the q^2 -channel which include the $c\bar{c}$ resonances (ψ, ψ', \dots) and the charmed hadronic continuum. The charming penguins are crucial for rare semileptonic decays $b \rightarrow (s, d)l^+l^-$, but provide only a small contribution for the radiative decays $b \rightarrow (s, d)\gamma$ [111–113]: In the factorization approximation the $c\bar{c}$ contribution precisely vanishes due to the gauge invariance [113], whereas the nonfactorizable effects turn out to be only at the level of few percent [112].

Another effect of the 4-quark operators is the so-called weak annihilation which corresponds to the annihilation of quarks in the channel of the initial or final mesons.

In the $B \rightarrow K^*\gamma$ decay the weak annihilation is negligible compared to the penguin effect: it is suppressed by two powers of the small parameter $\lambda \simeq 0.2$ of the Cabibbo-Kobayashi-Maskawa (CKM) matrix. In $B \rightarrow \rho\gamma$ both effects have the same order in λ and must be taken into account.

The penguin contribution is known rather well. On the other hand, the WA in $B \rightarrow \rho\gamma$ has been studied in less detail: the relevant form factors were analysed within sum rules [114,115] and perturbative QCD [116]. However, some contributions to these form factors were neglected. These contributions may be relevant if precise measurements become available.

We now apply the dispersion approach to the weak annihilation in the $B^- \rightarrow \rho^- \gamma$ decay.

In the factorization approximation [117] the weak-annihilation amplitude can be represented as the product of meson leptonic decay constants and matrix elements of the weak current between meson and photon. The latter contain the meson-photon transition form factors and contact terms which are determined by the equations of motion. The photon can be emitted from the loop containing the b quark which is described by $B\gamma$ transition form factors. It can also be emitted from the loop containing only light quarks described by the $\rho\gamma$ transition form factors (Fig 20).

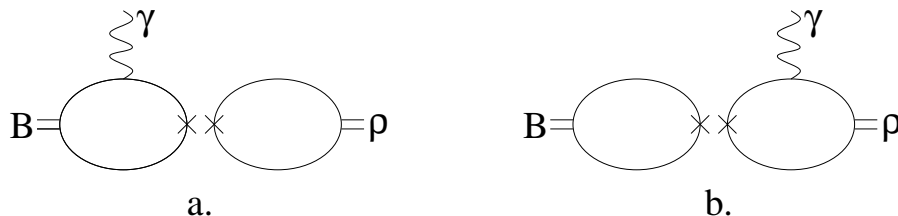


Fig. 20. Diagrams describing the weak annihilation process for $B \rightarrow \rho\gamma$ in the factorization approximation: (a) The photon is emitted from the loop containing the b quark, (b) The photon is emitted from the loop containing only light quarks.

We calculate the $B\gamma$ form factors within our relativistic dispersion approach which expresses these form factors in terms of the B meson wave function. We demonstrate that the form factors calculated by the dispersion approach behave in the limit $m_b \rightarrow \infty$ in agreement with perturbative QCD. The B meson wave function was previously tested in the $B \rightarrow$ light meson weak decays and is known quite well, allowing us to provide reliable numerical estimates for the $B\gamma$ form factors.

The $\rho\gamma$ transition form factor is related to the divergence of the vector and axial-vector currents. In the case of the axial-vector current it is proportional to the light-quark masses if the classical equation of motion is applied. Because the quark momenta in the loop are high, these masses have to be identified with current quark masses. For this reason the corresponding $\rho\gamma$ form factor was neglected in previous analyses [114,115]. We find however that this argument is not correct: this form factor remains finite in the limit of vanishing light quark mass $m \rightarrow 0$ and behaves like $\sim M_\rho f_\rho / M_B^2$ which means the violation of the classical equation of motion. Here we present the result for the $\rho\gamma$ transition form factor. A detailed discussion of the anomaly appearing for the matrix element $\langle \rho\gamma | \partial_\nu A_\nu | 0 \rangle$ can be found in Ref. [65]

Finally, we provide numerical estimates of the weak-annihilation amplitude taking into account the $B\gamma$, $\rho\gamma$ transition form factors, and the contact term contributions.

In section V A the effective Hamiltonian for the $b \rightarrow d$ transition and the general structure of the amplitude are presented. In Section V B we discuss the photon emission from the B meson loop and obtain the $B\gamma$ transition form factors within the dispersion approach. Section V C contains results for the $\rho\gamma$ transition form factors. In Section V D the numerical estimates are given. The concluding Section V E summarises our results for the weak annihilation.

A. The effective Hamiltonian, the amplitude and the decay rate

The amplitude of the weak radiative $B \rightarrow \rho$ transition is given by the matrix element of the effective Hamiltonian for the $b \rightarrow d$ transition

$$A(B \rightarrow \rho\gamma) = \langle \gamma(q_1) \rho(q_2) | H_{\text{eff}}(b \rightarrow d) | B(p) \rangle, \quad (5.1)$$

where p is the B momentum, q_2 is the ρ momentum, and q_1 is the photon momentum, $p = q_1 + q_2$, $q_1^2 = 0$, $q_2^2 = M_\rho^2$, $p^2 = M_B^2$. The effective weak Hamiltonian has the structure [118–121]:

$$H_{\text{eff}}(b \rightarrow d) = \frac{G_F}{\sqrt{2}} \xi_t C_{7\gamma}(\mu) \mathcal{O}_{7\gamma} - \frac{G_F}{\sqrt{2}} \xi_u (C_1(\mu) \mathcal{O}_1 + C_2(\mu) \mathcal{O}_2), \quad (5.2)$$

where only operators relevant for the penguin and weak annihilation effects are listed. G_F is the Fermi constant, $\xi_q = V_{qd}^* V_{qb}$, C_i 's are the Wilson coefficients and \mathcal{O}_i 's are the basis operators

$$\mathcal{O}_{7\gamma} = \frac{e}{8\pi^2} \bar{d}_\alpha \sigma_{\mu\nu} m_b(\mu) (1 + \gamma_5) b_\alpha F_{\mu\nu}, \quad (5.3)$$

$$\begin{aligned} \mathcal{O}_1 &= \bar{d}_\alpha \gamma_\nu (1 - \gamma_5) u_\alpha \bar{u}_\beta \gamma_\nu (1 - \gamma_5) b_\beta, \\ \mathcal{O}_2 &= \bar{d}_\alpha \gamma_\nu (1 - \gamma_5) u_\beta \bar{u}_\beta \gamma_\nu (1 - \gamma_5) b_\alpha. \end{aligned} \quad (5.4)$$

with $e = \sqrt{4\pi\alpha_{\text{em}}}$. Other notations are given in Eq. (3.7).

The amplitude can be parametrized as follows

$$A(B^- \rightarrow \rho^- \gamma) = \frac{eG_F}{\sqrt{2}} [\epsilon_{q_1 \epsilon_1^* q_2 \epsilon_2^*} F_{\text{PC}} + i\epsilon_2^{*\nu} \epsilon_1^{*\mu} (g_{\nu\mu} p q_1 - p_\mu q_{1\nu}) F_{\text{PV}}], \quad (5.5)$$

where F_{PC} and F_{PV} are the parity-conserving and parity-violating invariant amplitudes, respectively. $\epsilon_2(\epsilon_1)$ is the ρ -meson (photon) polarization vector. We use the short-hand notation $\epsilon_{abcd} = \epsilon_{\alpha\beta\mu\nu} a^\alpha b^\beta c^\mu d^\nu$ for any 4-vectors a, b, c, d .

For the decay rate one finds

$$\Gamma(B^- \rightarrow \rho^- \gamma) = \frac{G_F^2 \alpha_{\text{em}}}{16} M_B^3 (1 - M_\rho^2/M_B^2)^3 (|F_{\text{PC}}|^2 + |F_{\text{PV}}|^2). \quad (5.6)$$

1. The penguin amplitude

The main contribution to the amplitude is given by the electromagnetic penguin operator $O_{7\gamma}$:

$$A_{\text{peng}}(B \rightarrow \rho\gamma) = -\frac{eG_F}{\sqrt{2}}\xi_t C_7 \frac{m_b}{2\pi^2} T_1(0) (\epsilon_{q_1\epsilon_1^*q_2\epsilon_2^*} + i\epsilon_2^{*\nu}\epsilon_1^{*\mu}(g_{\nu\mu}pq_1 - p_\mu q_{1\nu})), \quad (5.7)$$

where T_1 is the form factor of the $B \rightarrow \rho$ transition through the tensor current [10,24,27,61]. The corresponding contribution to the invariant amplitudes is therefore

$$F_{\text{PC}}^{\text{peng}} = F_{\text{PV}}^{\text{peng}} = -\xi_t C_7 \frac{m_b}{2\pi^2} T_1(0). \quad (5.8)$$

2. The weak annihilation amplitude

The radiative $B \rightarrow \rho\gamma$ transition also receives contribution from the 4-fermion operators \mathcal{O}_1 and \mathcal{O}_2 . For the charged $B^- \rightarrow \rho^-(q_2)\gamma(q_1)$ transition the corresponding amplitude reads

$$A_{\text{WA}}(B^- \rightarrow \rho^-\gamma) = -\frac{G_F}{\sqrt{2}}\xi_u \langle \rho(q_2)\gamma(q_1) | \bar{d}\gamma_\nu(1-\gamma_5)u \cdot \bar{u}\gamma_\nu(1-\gamma_5)b | B(p) \rangle, \quad (5.9)$$

In what follows we suppress the label WA. Neglecting the nonfactorizable soft-gluon exchanges, i.e. assuming vacuum saturation, the complicated matrix element in Eq. (5.9) is reduced to simpler quantities - the meson-photon matrix elements of the bilinear quark currents and the meson decay constants. The latter are defined as usual

$$\begin{aligned} \langle \rho(q_2) | \bar{d}\gamma_\nu u | 0 \rangle &= \epsilon_{2\nu}^* M_\rho f_\rho, & f_\rho > 0, \\ \langle 0 | \bar{u}\gamma_\nu \gamma_5 b | B(p) \rangle &= i p_\nu f_B, & f_B > 0. \end{aligned} \quad (5.10)$$

It is convenient to isolate the parity-conserving contribution which emerges from the product of the two equal-parity currents, and the parity-violating contribution which emerges from the product of the two opposite-parity currents.

The parity-violating contribution

The parity-violating contribution to the weak annihilation amplitude has the form

$$A_{\text{PV}}(B \rightarrow \rho\gamma) = \frac{G_F}{\sqrt{2}}\xi_u a_1 \{ \langle \rho\gamma | \bar{d}\gamma_\nu u | 0 \rangle \langle 0 | \bar{u}\gamma_\nu \gamma_5 b | B \rangle + \langle \rho | \bar{d}\gamma_\nu u | 0 \rangle \langle \gamma | \bar{u}\gamma_\nu \gamma_5 b | B \rangle \}. \quad (5.11)$$

Here a_1 is an effective Wilson coefficient, which we take as $a_1 = C_1 + C_2/N_c$ at the scale ~ 5 GeV.

It is convenient to denote

$$A_1^{\text{PV}} = \langle \rho^-(q_2) | \bar{d}\gamma_\nu u | 0 \rangle \langle \gamma(q_1) | \bar{u}\gamma_\nu \gamma_5 b | B^-(p) \rangle \quad (5.12)$$

and

$$A_2^{\text{PV}} = \langle \rho^-(q_2)\gamma(q_1) | \bar{d}\gamma_\nu u | 0 \rangle \langle 0 | \bar{u}\gamma_\nu \gamma_5 b | B^-(p) \rangle. \quad (5.13)$$

1. Let us start with A_1^{PV} . One can write

$$\langle \gamma(q_1) | \bar{u}\gamma_\nu \gamma_5 b | B^-(p) \rangle = e \epsilon_1^{*\mu} T_{\mu\nu}^B \quad (5.14)$$

where

$$T_{\mu\nu}^B(p, q_1) = i \int dx e^{iq_1 x} \langle 0 | T(J_\mu(x), \bar{u}\gamma_\nu \gamma_5 b) | B^-(p) \rangle, \quad (5.15)$$

and

$$J_\mu(x) = \frac{2}{3} \bar{u}\gamma_\mu u - \frac{1}{3} \bar{d}\gamma_\mu d - \frac{1}{3} \bar{b}\gamma_\mu b \quad (5.16)$$

is the electromagnetic quark current.

The amplitude $T_{\mu\nu}^B$ in general contains 5 independent Lorentz structures and can be parametrised in various ways.

A possible way is to write $T_{\mu\nu}^B$ as follows

$$T_{\mu\nu}^B = T_{\mu\nu}^\perp + \frac{ip_\mu p_\nu}{pq_1} C_1 + \frac{ip_\mu q_\nu}{pq_1} C_2, \quad (5.17)$$

where

$$\begin{aligned} T_{\mu\nu}^\perp = & i (g_{\mu\nu} pq_1 - p_\mu q_{1\nu}) F_{1A}(q_1^2) \\ & + i (q_1^2 p_\mu - pq_1 q_{1\mu}) q_{1\nu} F_{2A}(q_1^2) \\ & + i (q_1^2 p_\mu - pq_1 q_{1\mu}) p_\nu F_{3A}(q_1^2). \end{aligned} \quad (5.18)$$

is transverse with respect to $q_{1\mu}$,

$$q_1^\mu T_{\mu\nu}^\perp = 0. \quad (5.19)$$

The Lorentz structures in this expansion are chosen such that they contain no singularity for $q_1^2 \rightarrow 0$.

The invariant amplitudes C_1 and C_2 in the longitudinal structure can be determined using the conservation of the electromagnetic current $\partial_\mu J_\mu = 0$, which leads to the relation

$$\begin{aligned} q_{1\mu} T_{\mu\nu}^B(p, q_1) &= -\langle 0 | [\hat{Q}, \bar{d} \gamma_\nu \gamma_5 u] | B^-(p) \rangle \\ &= i Q_B f_B p_\nu. \end{aligned} \quad (5.20)$$

This gives

$$\begin{aligned} C_1 &= Q_B f_B, \\ C_2 &= 0. \end{aligned} \quad (5.21)$$

In particular, $C = -f_B$ for the B^- meson. Notice however, that the longitudinal part of the amplitude in this form is *not a contact term*.⁶ This means that some of the invariant amplitudes in the transverse part are mixtures of the true form factors (i.e. quantities with definite and known analytic properties) and remnants of the contact terms.

After setting $q_1^2 = 0$ and multiplying by $\epsilon_1^{*\mu}$ (this very combination is needed for A_1^{PV}) only some of the Lorentz structures contribute and we find

$$\epsilon_1^{*\mu} T_{\mu\nu}^B|_{q_1^2=0} = i \epsilon_1^{*\mu} \left\{ (g_{\mu\nu} pq_1 - p_\mu q_{1\nu}) F_{1A}(0) - p_\mu p_\nu \frac{2f_B}{M_B^2 - M_\rho^2} \right\}, \quad (5.22)$$

where we have used the relation $q_1 p = \frac{1}{2}(M_B^2 - M_\rho^2)$ for $q_1^2 = 0$.

The parametrization of Eq. (5.17) is of course not unique and there are other possibilities. There is however only one choice when the longitudinal part is a pure contact term. Such a choice, which is also the most natural one, is prompted by the structure of the Feynman diagram:

Let us rewrite the usual electromagnetic coupling of the quark as follows ($q_1 = k' - k$):

$$(m + \hat{k}') \gamma_\mu (m + \hat{k}) = (m + \hat{k}') \left\{ \gamma_\mu - \hat{q}_1 \frac{q_{1\mu}}{q_1^2} \right\} (m + \hat{k}) + \frac{q_{1\mu}}{q_1^2} \left[(k'^2 - m^2)(m + \hat{k}) - (k^2 - m^2)(m + \hat{k}') \right]. \quad (5.23)$$

The first term is explicitly transverse with respect to $q_{1\mu}$ and leads to $T_{\mu\nu}^\perp$.

The second term, containing the factors $(k^2 - m^2)$ and $(k'^2 - m^2)$, leads to the contact term

$$ip_\nu \frac{q_{1\mu}}{q_1^2} f_B.$$

⁶We recall that according to the usual definition, a contact term is a quantity which is represented by the delta-function and its derivatives in the coordinate space. One can then easily check, that the Fourier transform of the expression $\frac{ip_\mu p_\nu}{pq_1}$ is not a contact term.

Finally, we come to the following parametrization

$$T_{\mu\nu}^B = T_{\mu\nu}' + \frac{iq_{1\mu}p_\nu}{q_1^2}C_1' + \frac{iq_{1\mu}q_{1\nu}}{q_1^2}C_2', \quad (5.24)$$

with

$$\begin{aligned} T_{\mu\nu}' &= i \left(g_{\mu\nu} - \frac{q_{1\mu}q_{1\nu}}{q_1^2} \right) p q_1 F_{1A}'(q_1^2) \\ &+ i \left(p_\mu - \frac{p q_1}{q_1^2} q_{1\mu} \right) q_{1\nu} F_{2A}'(q_1^2) \\ &+ i \left(p_\mu - \frac{p q_1}{q_1^2} q_{1\mu} \right) p_\nu F_{3A}'(q_1^2). \end{aligned} \quad (5.25)$$

Notice, that this is the only parametrization of the amplitude, which provides a distinct separation of the amplitude: form factors in the gauge-invariant transverse part of the amplitude, and contact terms in the longitudinal part of the amplitude.

Clearly, $F_{1A}' = F_{1A}$, whereas other form factors of the sets F and F' are different. Now the Lorentz structures contain explicit singularities for $q_1^2 = 0$ which must cancel each other in the amplitude $T_{\mu\nu}^B$. This leads to the constraints on the form factors at $q_1^2 = 0$

$$\begin{aligned} -q_1 p F_{1A}'(0) - q_1 p F_{2A}'(0) + C_2' &= 0, \\ -q_1 p F_{3A}'(0) + C_1' &= 0. \end{aligned} \quad (5.26)$$

Equation (5.20) gives

$$\begin{aligned} C_1' &= -f_B, \\ C_2' &= 0, \end{aligned} \quad (5.27)$$

and hence

$$\begin{aligned} F_{1A}'(0) &= -F_{2A}'(0), \\ F_{3A}'(0) &= -\frac{2f_B}{M_B^2 - M_\rho^2}. \end{aligned} \quad (5.28)$$

By virtue of the relations (5.26), for the amplitude A_1^{PV} at $q_1^2 = 0$ we find

$$\begin{aligned} A_1^{\text{PV}} &= ie f_\rho M_\rho \epsilon_1^{*\mu} \epsilon_2^{*\nu} \{ g_{\mu\nu} p q_1 F_{1A}(0) + p_\mu q_{1\nu} F_{2A}(0) - p_\mu p_\nu F_{3A}(0) \} \\ &= ie f_\rho M_\rho \epsilon_1^{*\mu} \epsilon_2^{*\nu} \left\{ (g_{\mu\nu} p q_1 - p_\mu q_{1\nu}) F_{1A}(0) - p_\mu q_{1\nu} \frac{2f_B}{M_B^2 - M_\rho^2} \right\}. \end{aligned} \quad (5.29)$$

Notice that the contact term does not contribute to the amplitude *directly*, but *indirectly* determines the value of the form factor $F_{3A}(0)$.

2. Let us now turn to A_2^{PV} .

Using the equation of motion for the quark fields ($Q_u = 2/3 e$, $Q_d = -1/3 e$)

$$\begin{aligned} i\gamma_\nu \partial^\nu q(x) &= m q(x) - Q_q A_\nu \gamma^\nu q(x), \\ i\partial^\nu \bar{q}(x) \gamma_\nu &= -m \bar{q}(x) + Q_q A_\nu \bar{q}(x) \gamma^\nu, \end{aligned} \quad (5.30)$$

one obtains for A_2^{PV}

$$\begin{aligned} A_2^{\text{PV}} &= ip_\nu f_B \langle \rho^- \gamma | \bar{d} \gamma_\nu u | 0 \rangle \\ &= f_B \langle \rho^- \gamma | \partial_\nu (\bar{d} \gamma_\nu u) | 0 \rangle \\ &= -(Q_d - Q_u) e \langle \rho^- \gamma | A^\nu \bar{d} \gamma_\nu u | 0 \rangle \\ &= e \epsilon_1^{*\mu} \epsilon_2^{*\nu} g_{\mu\nu} f_\rho M_\rho f_B + O(m_u, m_d). \end{aligned} \quad (5.31)$$

Now the full contribution is due to the contact terms only, since the transverse form-factor part of the amplitude $\langle \rho^- \gamma | \bar{d} \gamma_\nu u | 0 \rangle$ vanishes after the multiplication by p_ν .

3. For the sum we find

$$A_1^{\text{PV}} + A_2^{\text{PV}} = ie f_\rho M_\rho \epsilon_1^{*\mu} \epsilon_2^{*\nu} (g_{\mu\nu} p q_1 - p_\mu q_{1\nu}) \left[F_{1A}(0) + \frac{2f_B}{M_B^2 - M_\rho^2} \right] \quad (5.32)$$

Summing the contributions of the photon emission from the B -meson loop and the ρ -meson loop gives the amplitude A_{PV} which can be represented in the form $A_{\text{PV}} = \epsilon_1^{*\mu} T_\mu$ with $q_1^\mu T_\mu = 0$ as required by gauge invariance. The weak-annihilation contribution to the form factor F_{PV} for the $B^- \rightarrow \rho^- \gamma$ decay takes the form (after redefining $F_{1A} = 2F_A/M_B$)

$$F_{\text{PV}}^{\text{WA}} = \xi_u a_1 f_\rho M_\rho \left[\frac{2F_A}{M_B} + \frac{2f_B}{M_B^2 - M_\rho^2} \right]. \quad (5.33)$$

Notice that in addition to the form factor contribution $\sim F_A$, there is a contribution proportional to f_B . The latter is determined by the contact terms: namely, the contact terms which are present in the amplitudes of the photon emission from the B meson loop and from the ρ -meson loop do not cancel each other, but lead to a nonvanishing contribution.⁷ In the amplitude of the $B^+ \rightarrow \rho^+ \gamma$ decay the contact term proportional to f_B changes sign, and also $F_A^{B^+} = -F_A^{B^-}$ as can be obtained from charge conjugation of the amplitude A_{PV} . For the $B^0 \rightarrow \rho^0 \gamma$ decay the contact term proportional to f_B is absent.

The parity-conserving amplitude

This amplitude reads

$$A_{\text{PC}}(B \rightarrow \rho \gamma) = -\frac{G_F}{\sqrt{2}} \xi_u a_1 \left\{ \langle \rho | \bar{d} \gamma_\nu u | 0 \rangle \langle \gamma | \bar{u} \gamma_\nu b | B \rangle + \langle \gamma \rho | \bar{d} \gamma_\nu \gamma_5 u | 0 \rangle \langle 0 | \bar{u} \gamma_\nu \gamma_5 b | B \rangle \right\}. \quad (5.34)$$

The $B \rightarrow \gamma$ amplitude from the first term in the brackets contains the form factor $F_V(q_2^2 = M_\rho^2)$:

$$\langle \gamma(q_1) | \bar{u} \gamma_\nu b | B(p) \rangle = e \epsilon_{\nu\mu p q_1} \epsilon_1^{*\mu} \frac{2F_V}{M_B}. \quad (5.35)$$

The second term in (5.34) can be reduced to the divergence of the axial-vector current and contains another form factor, G_V : namely,

$$\begin{aligned} \langle 0 | \bar{u} \gamma_\nu \gamma_5 b | B \rangle \langle \gamma \rho | \bar{d} \gamma_\nu \gamma_5 u | 0 \rangle &= f_B \langle \gamma \rho | \partial_\nu \bar{d} \gamma_\nu \gamma_5 u | 0 \rangle \\ &= e f_B G_V \epsilon_{q_1 \epsilon_1^* q_2 \epsilon_2^*}. \end{aligned} \quad (5.36)$$

Thus, the weak annihilation contribution to F_{PC} reads

$$F_{\text{PC}}^{\text{WA}} = \xi_u a_1 M_\rho f_\rho \left[\frac{2F_V}{M_B} - \frac{f_B G_V}{M_\rho f_\rho} \right]. \quad (5.37)$$

Summing up, within the factorization approximation the weak annihilation amplitude can be expressed in terms of the three form factors F_A , F_V , and G_V .

⁷ Here we disagree with the recent statement of [122] that contact terms cancel each other and do not contribute to the final amplitude. The conclusion of [122] is based on choosing the longitudinal part of the amplitude in the form $\left\{ g_{\mu\nu} + \frac{q_{2\mu} q_{2\nu}}{q_2^2 q_1^2} \right\} f_B$ which is *not a contact term* according to the usual definition of the latter. As a result, the invariant amplitude of [114,115,122] at $q_1^2 = 0$ corresponds to the combination $F_A + \frac{M_B f_B}{M_B^2 - M_\rho^2}$. We take this relationship into account when comparing numerical results from different approaches later in this section.

B. Form factors for the $B \rightarrow \gamma \ell \nu$ transition

In this section we derive formulas for the form factors $F_{A,V}$ describing the weak transition $B \rightarrow \gamma \ell \nu$ within the dispersion approach to the transition form factors. Recall that the form factors $F_{A,V}$ describe the transition of the B -meson to the photon with the momentum q_1 , $q_1^2 = 0$, induced by the axial-vector (vector) current with the momentum transfer q_2 , $q_2^2 = M_\rho^2$. For technical reasons, it is convenient to treat the form factor $F_{A(V)}$ as describing the amplitude of the photon-induced transition of the B -meson into a $b\bar{u}$ axial-vector (vector) virtual particle with the corresponding factor $1/(s - q_2^2)$ in the dispersion integral. Then we can directly apply the equations obtained in Chapter II for meson-to-meson transition form factors.

1. The form factor F_A

The form factor F_A is given by the diagrams of Fig 21. Fig 21a shows $F_A^{(b)}$, the contribution to the form factor of the process when the b quark interacts with the photon; Fig 21b describes the contribution of the process when the quark u interacts while b remains a spectator. One has

$$F_A = F_A^{(b)} + F_A^{(u)}. \quad (5.38)$$

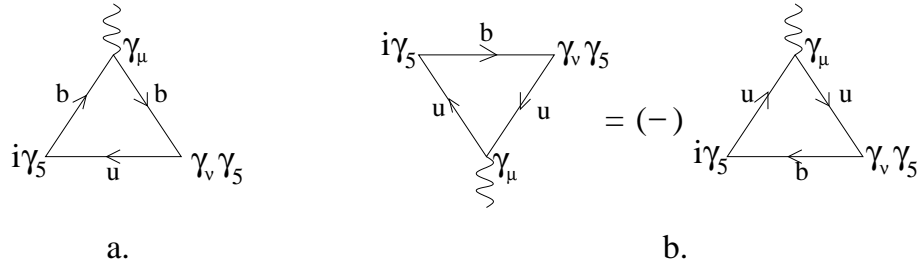


Fig. 21. Diagrams for the form factor F_A : a) $F_A^{(b)}$, b) $F_A^{(u)}$.

The B^- meson is described by the vertex $\bar{b}(k_b) i\gamma_5 u(k_u) G(s)/\sqrt{N_c}$, with $G(s) = \varphi_B(s)(s - M_B^2)$. The B -meson wave function φ_B is normalized according to the relation (3.62).

It is convenient to change the direction of the quark line in the loop diagram of Fig 21b. This is done by performing the charge conjugation of the matrix element and leads to a sign change for the $\gamma_\nu \gamma_5$ vertex.

Now both diagrams in Fig 21 a,b are reduced to the diagram of Fig 22 which defines the form factor $F_A^{(1)}(m_1, m_2)$: Setting $m_1 = m_b$, $m_2 = m_u$ gives $F_A^{(b)}$:

$$F_A^{(b)} = Q_b F_A^{(1)}(m_b, m_u).$$

Similarly, setting $m_1 = m_u$, $m_2 = m_b$ gives $F_A^{(u)}$,

$$F_A^{(u)} = -Q_u F_A^{(1)}(m_u, m_b).$$

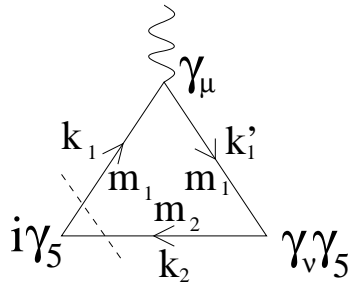


Fig. 22. The triangle diagram for $F_A^{(1)}(m_1, m_2)$. The cut corresponds to calculating the imaginary part in the variable p^2 .

For the diagram of Fig 22 (quark 1 emits the photon, quark 2 is the spectator) the trace reads

$$\begin{aligned} & -\text{Sp } i\gamma_5(m_2 - \hat{k}_2)\gamma_\nu\gamma_5(m_1 + \hat{k}'_1)\gamma_\mu(m_1 + \hat{k}_1) \\ & = 4i(k_1 + k'_1)_\mu(m_1k_2 + m_2k_1)_\nu + 4i(g_{\mu\nu}q_\alpha - g_{\mu\alpha}q_\nu)(m_1k_2 + m_2k_1)_\alpha. \end{aligned} \quad (5.39)$$

The spectral density of the form factor $F_A^{(1)}(m_1, m_2)$ in the variable p^2 , $p = k_1 + k_2$, is the coefficient of the structure $g_{\mu\nu}$ obtained after the integration of the trace over the quark phase space. Performing necessary calculations, we arrive at the following single dispersion integral

$$\begin{aligned} \frac{2}{M_B}F_A^{(1)} &= \frac{\sqrt{N_c}}{4\pi^2} \int_{(m_b+m_u)^2}^{\infty} \frac{ds \varphi_B(s)}{(s - M_\rho^2)} \\ &\times \left\{ \left(m_1 \log \left(\frac{s + m_1^2 - m_2^2 + \lambda^{1/2}(s, m_1^2, m_2^2)}{s + m_1^2 - m_2^2 - \lambda^{1/2}(s, m_1^2, m_2^2)} \right) + (m_2 - m_1) \frac{\lambda^{1/2}(s, m_b^2, m_u^2)}{s} \right) \right. \\ &\left. + \frac{1}{pq_1} \left(\frac{\lambda^{1/2}(s, m_b^2, m_u^2)}{2s} - m_1^2 \log \left(\frac{s + m_1^2 - m_2^2 + \lambda^{1/2}(s, m_1^2, m_2^2)}{s + m_1^2 - m_2^2 - \lambda^{1/2}(s, m_1^2, m_2^2)} \right) \right) \right\}. \end{aligned} \quad (5.40)$$

For $q_1^2 = 0$ one has $pq_1 = (M_B^2 - M_\rho^2)/2$.

Now, let us analyse the behaviour of the form factor in the limit $m_b \rightarrow \infty$. To this end it is convenient to rewrite the spectral representation (5.40) in terms of the light-cone variables as follows (see [69] for details)

$$\begin{aligned} \frac{2}{M_B}F_A^{(1)}(m_1, m_2) &= \frac{\sqrt{N_c}}{4\pi^2} \int \frac{dx_1 dx_2 dk_\perp^2}{x_1^2 x_2} \delta(1 - x_1 - x_2) \frac{\varphi_B(s)}{s - M_\rho^2} \\ &\times \{m_1 x_2 + m_2 x_1 - (m_1 - m_2)k_\perp^2/pq_1\}. \end{aligned} \quad (5.41)$$

Here x_i is the fraction of the B -meson light-cone momentum carried by the quark i , and

$$s = m_1^2/x_1 + m_2^2/x_2 + k_\perp^2/x_1 x_2.$$

For the form factors $F_A^{(u)}$ and $F_A^{(b)}$ one obtains

$$\begin{aligned} \frac{2}{M_B}F_A^{(u)} &= -Q_u \frac{\sqrt{N_c}}{4\pi^2} \int \frac{dx dk_\perp^2}{x_u^2 x_b} \frac{\varphi_B(s)}{s - M_\rho^2} \left\{ m_u x_b + m_b x_u + \frac{2(m_b - m_u)k_\perp^2}{M_B^2 - M_\rho^2} \right\}, \\ \frac{2}{M_B}F_A^{(b)} &= Q_b \frac{\sqrt{N_c}}{4\pi^2} \int \frac{dx dk_\perp^2}{x_b^2 x_u} \frac{\varphi_B(s)}{s - M_\rho^2} \left\{ m_b x_u + m_u x_b + \frac{2(m_u - m_b)k_\perp^2}{M_B^2 - M_\rho^2} \right\}, \end{aligned}$$

with

$$s = \frac{m_b^2}{x_b} + \frac{m_u^2}{x_u} + \frac{k_\perp^2}{x_u x_b}. \quad (5.42)$$

Recall that the B -meson decay constant is given in terms of the wave function by Eq. (3.63). Due to the wave function $\varphi_B(s)$, the integral in the heavy quark limit is dominated by the region $x_u = \bar{\Lambda}/m_b$, $x_b = 1 - \bar{\Lambda}/m_b$, where $\bar{\Lambda}$ is a constant of order $M_B - m_b$. This leads to the following expansion of the form factors in the $1/m_b$ series

$$\begin{aligned} \frac{2}{M_B}F_A^{(u)} &= -Q_u \frac{f_B}{\bar{\Lambda} m_b} + \dots \\ \frac{2}{M_B}F_A^{(b)} &= Q_b \frac{f_B}{m_b^2} + \dots \end{aligned} \quad (5.43)$$

Clearly, the dominant contribution in the heavy quark limit comes from the process when the light quark emits the photon, whereas the emission of the photon from the heavy quark gives only a $1/m_b$ correction. The expressions (5.43) for the form factor $F_A^{(u)}$ agrees with the result of Ref. [116], while we have found a different sign for $F_A^{(b)}$.

2. The form factor F_V

The consideration of the form factor F_V is very similar to the form factor F_A . F_V is determined by the two diagrams shown in Fig 23: Fig 23a gives $F_V^{(b)}$, the contribution of the process when the b quark interacts with the photon; Fig 23b describes the contribution of the process when the quark u interacts. One has

$$F_V = F_V^{(b)} + F_V^{(u)}. \quad (5.44)$$

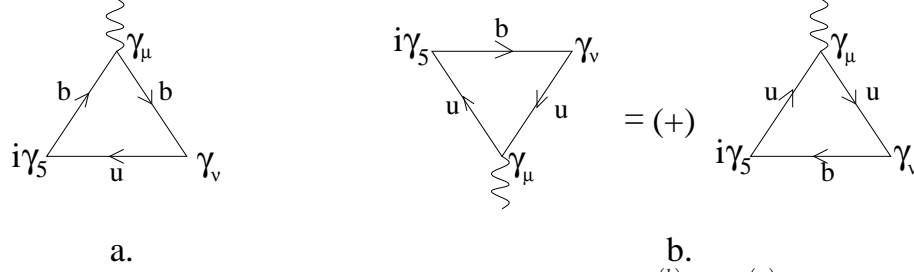


Fig. 23. Diagrams for the form factor F_V : a) $F_V^{(b)}$, b) $F_V^{(u)}$.

It is again convenient to change the direction of the quark line in the loop diagram of Fig 23b describing $F_V^{(u)}$ by performing the charge conjugation of the matrix element. For the vector current γ_ν in the vertex the sign does not change (in contrast to the $\gamma_\nu \gamma_5$ case considered above).

Then both diagrams in Fig 23 a, b are reduced to the diagram of Fig 24 which gives the form factor $F_V^{(1)}(m_1, m_2)$: Setting $m_1 = m_b$, $m_2 = m_u$ gives $F_V^{(b)}$:

$$F_V^{(b)} = Q_b F_V^{(1)}(m_b, m_u).$$

Setting $m_1 = m_u$, $m_2 = m_b$ gives $F_V^{(u)}$

$$F_V^{(u)} = Q_u F_V^{(1)}(m_u, m_b).$$

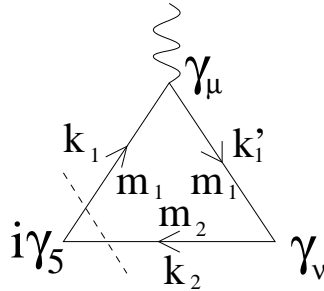


Fig. 24. The triangle diagram for $F_V^{(1)}(m_1, m_2)$. The cut corresponds to calculating the imaginary part in the variable p^2 .

The trace corresponding to the diagram of Fig 4 (1 - active quark, 2 - spectator) reads

$$-\text{Sp} \left[i\gamma_5(m_2 - \hat{k}_2)\gamma_\nu(m_1 + \hat{k}'_1)\gamma_\mu(m_1 + \hat{k}_1) \right] = -4\epsilon_{\nu\mu\alpha q_1}(m_1 k_2 + m_2 k_1)_\alpha.$$

The spectral representation for the form factor takes the form

$$\begin{aligned} \frac{2}{M_B} F_V^{(1)} &= \frac{\sqrt{N_c}}{4\pi^2} \int_{(m_b+m_u)^2}^{\infty} \frac{ds \varphi_B(s)}{(s - M_\rho^2)} \\ &\times \left\{ (m_2 - m_1) \frac{\lambda^{1/2}(s, m_b^2, m_u^2)}{s} + m_1 \log \left(\frac{s + m_1^2 - m_2^2 + \lambda^{1/2}(s, m_1^2, m_2^2)}{s + m_1^2 - m_2^2 - \lambda^{1/2}(s, m_1^2, m_2^2)} \right) \right\}. \end{aligned} \quad (5.45)$$

To analyse the heavy quark limit $m_b \rightarrow \infty$ we again represent the form factor in terms of the light-cone variables

$$\frac{2}{M_B} F_V^{(1)} = -\frac{\sqrt{N_c}}{4\pi^2} \int \frac{dx_1 dx_2 dk_\perp^2}{x_1^2 x_2} \delta(1 - x_1 - x_2) \frac{\varphi_B(s)}{s - M_\rho^2} (m_1 x_2 + m_2 x_1). \quad (5.46)$$

For $F_V^{(u)}$ and $F_V^{(b)}$ the corresponding expressions read

$$\begin{aligned} \frac{2}{M_B} F_V^{(u)} &= -Q_u \frac{\sqrt{N_c}}{4\pi^2} \int \frac{dx dk_\perp^2}{x_u^2 x_b} \frac{\varphi_B(s)}{s - M_\rho^2} \{m_u x_b + m_b x_u\}, \\ \frac{2}{M_B} F_V^{(b)} &= -Q_b \frac{\sqrt{N_c}}{4\pi^2} \int \frac{dx dk_\perp^2}{x_b^2 x_u} \frac{\varphi_B(s)}{s - M_\rho^2} \{m_b x_u + m_u x_b\}, \end{aligned}$$

By the same procedure as used for F_A , we obtain in the limit $m_b \rightarrow \infty$

$$\begin{aligned} \frac{2}{M_B} F_V^{(u)} &= -Q_u \frac{f_B}{\Lambda m_b} + \dots \\ \frac{2}{M_B} F_V^{(b)} &= -Q_b \frac{f_B}{m_b^2} + \dots \end{aligned} \quad (5.47)$$

The dominant contribution in the heavy quark limit again comes from the process when the light quark emits the photon. Now both form factors $F_V^{(u)}$ and $F_V^{(b)}$ in (5.47) perfectly agree with the expansions obtained in [116].

As seen from Eqs. (5.43) and (5.47), one finds $F_A = F_V$ in the heavy quark limit, in agreement with the large-energy effective theory [9].

C. The form factor G_V

The form factor G_V is determined by the divergence of the matrix element of the charged current between the vacuum and the $\rho^- \gamma$ state,

$$ip_\nu \langle \gamma(q_1) \rho^-(q_2) | \bar{d} \gamma_\nu \gamma_5 u | 0 \rangle = e G_V \epsilon_{q_1 \epsilon_1^* q_2 \epsilon_2^*}. \quad (5.48)$$

The corresponding diagrams are shown in Fig 25.

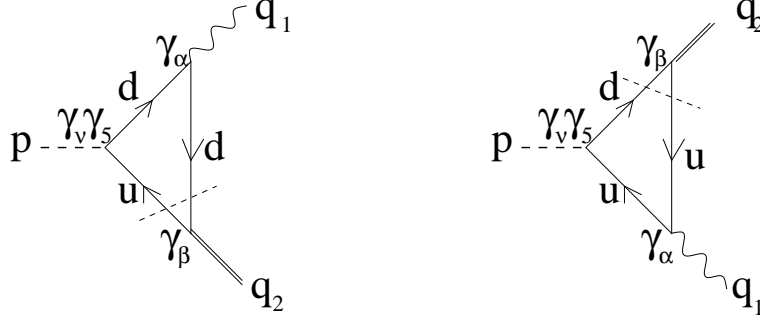


Fig. 25. Diagrams describing the amplitude $\langle \gamma(q_1) \rho^-(q_2) | \bar{d} \gamma_\nu \gamma_5 u | 0 \rangle$, $p = q_1 + q_2$, $p^2 = M_B^2$. The diagram (a) is multiplied by the d -quark charge, and the diagram (b) is multiplied by the u -quark charge. The cut corresponds to the calculation of the imaginary part in the variable q_2^2 .

If the classical equations of motion are applied, the form factor G_V is proportional to the light-quark masses. This is the reason why this form factor was neglected in previous analyses [28,110]. However, a proper calculation shows that this argument is not correct: in fact the classical equations of motions do not hold and the divergence contains the anomaly.

The anomalous behavior of the divergence of the axial-vector current in the chiral limit is a well-known phenomenon discovered in the two-photon amplitude $\langle \gamma \gamma | \partial_\nu \bar{q} \gamma_\nu \gamma_5 q | 0 \rangle$ [123]. A very clear way to demonstrate the anomaly is to start with the matrix element of the axial vector current and to calculate the spectral representations for the relevant form factors. The anomaly is then obtained by performing the divergence at the final stage of the calculation [124]. A similar treatment applied to the matrix element $\langle \gamma \rho^- | \bar{d} \gamma_\nu \gamma_5 u | 0 \rangle$ leads to the form factor G_V which does not vanish in the limit $m \rightarrow 0$. We will present a detailed discussion of the anomaly in radiative B decays in a separate publication [65]. Here we only quote the final result: considering the spectral representation in the variable q_2^2 and introducing the appropriate ρ -meson radial wave function $\psi_\rho(s)$, one finds the following expression for the form factor G_V

$$G_V = \sqrt{N_c} (Q_u + Q_d) \left[-\frac{M_B^2}{4\pi^2} \int \frac{ds \psi_\rho(s) (s - M_\rho^2)}{(s - M_B^2 - i0)^2} \right]. \quad (5.49)$$

$\psi_\rho(s)$ is normalized according to the relation (for massless quarks)

$$\frac{1}{8\pi^2} \int_0^\infty ds s |\psi_\rho(s)|^2 = 1. \quad (5.50)$$

Clearly, G_V is finite for $m = 0$ which means a violation of the classical equations of motion for the axial-vector current. Eq. (5.49) describes the anomaly which takes place for the $\gamma \rho$ final state as well as for the $\gamma \gamma$ one. There is however an important difference between the two cases: For the $\gamma \gamma$ final state the divergence remains finite in the limit $m \rightarrow 0$ and $p^2 = M_B^2 \rightarrow \infty$. For the $\rho \gamma$ final state the divergence is finite for $m \rightarrow 0$ but decreases as $1/p^2$ for $p^2 \rightarrow \infty$. It is convenient to introduce the parameter κ such that

$$G_V = (Q_u + Q_d) \kappa \frac{M_\rho f_\rho}{M_B^2}, \quad (5.51)$$

with κ staying finite for $m = 0$ and $M_B \rightarrow \infty$.

D. Numerical estimates

Table 31 presents formulas for the penguin and the weak-annihilation invariant amplitudes for the $B^- \rightarrow \rho^- \gamma$ and $B^0 \rightarrow \rho^0 \gamma$ decays.

Before giving numerical estimates, let us look at the scaling behavior of the form factors in the limit $M_B \rightarrow \infty$:

$$T_1(0) \sim M_B^{-3/2} [35], \quad F_{A,B} \sim M_B^{-1/2}, \quad G_V \sim M_B^{-2} \quad (5.52)$$

such that

$$F^{\text{peng}} \sim M_B^{-1/2}, \quad F_{\text{PV,PC}}^{\text{WA}} \sim M_B^{-3/2}. \quad (5.53)$$

The terms proportional to f_B ($f_B \sim 1/\sqrt{M_B}$) are $1/M_B$ -suppressed compared with the terms containing the form factors $F_{A,V}$. As we see below numerically this leads to a suppression by a factor of 4 – 5.

Table 31. The penguin and the weak-annihilation invariant amplitudes for the $B^- \rightarrow \rho^- \gamma$ and $B^0(b\bar{d}) \rightarrow \rho^0 \gamma$ decays.

Quantity	$B^- \rightarrow \rho^- \gamma$	$B^0 \rightarrow \rho^0 \gamma$
F^{peng}	$-\xi_t C_7 \frac{m_b}{2\pi^2} T_1^{B^- \rightarrow \rho^-}(0)$	$-\xi_t C_7 \frac{m_b}{2\pi^2} T_1^{B^0 \rightarrow \rho^0}(0)$
$F_{\text{PV}}^{\text{WA}}$	$\xi_u a_1 M_\rho f_\rho \left(\frac{2F_A^{B^-}}{M_B} + \frac{2f_B}{M_B^2 - M_\rho^2} \right)$	$\xi_u a_2 M_\rho f_{\rho^0} \left(\frac{2F_A^{B^0}}{M_B} \right)$
$F_{\text{PC}}^{\text{WA}}$	$\xi_u a_1 M_\rho f_\rho \left(\frac{2F_V^{B^-}}{M_B} - (Q_u + Q_d) \kappa \frac{f_B}{M_B^2} \right)$	$\xi_u a_2 M_\rho f_{\rho^0} \left(\frac{2F_V^{B^0}}{M_B} - 2 Q_u \kappa \frac{f_B}{M_B^2} \right)$

We now proceed to numerical estimates for the B -meson decay. The scale-dependent Wilson coefficients $C_i(\mu)$ and $a_1(\mu)$ take the following values at the renormalization scale $\mu \simeq 5$ GeV [121]:

$$C_1 = 1.1, \quad C_2 = -0.241, \quad C_{7\gamma} = -0.312, \quad a_1 = C_1 + C_2/N_c \simeq 1.02, \quad a_2 = C_2 + C_1/N_c \simeq 0.27 \pm 0.1. \quad (5.54)$$

The penguin form factor was previously calculated within the dispersion approach with the result $T_1^{B^- \rightarrow \rho^-}(0) = 0.27 \pm 0.3$, see Table 20 in Chapter IV. Using the same parameters and the B meson wave function as in Chapter IV, we obtain the form factors $F_{A,B}$ shown in Table 32. Our result for the form factor F_V is in good agreement with the estimates from other approaches. The form factor F_A agrees well with the constraints from perturbative QCD and turns out to be considerably larger than the corresponding sum rule estimate.

The value of the G_V is sensitive to the details of the ρ meson wave function ψ_ρ . The reason for that is the presence of the term $(s - M_\rho^2)$ in the integrand in Eq. (5.49) which changes sign in the integration region. Assuming $\psi_\rho(s) \simeq \beta^2/(\beta^2 + s)^2$ and setting $\beta = 0.8$ GeV, which gives a good description of the ρ meson radius, leads to $\kappa = -1.8$. Conservatively, we take $-\kappa < 2.0$ and use this result for further estimates. The form factor G_V does not contribute more than a few % to the full amplitude, but can sizeably correct the weak-annihilation part, especially for the $B^0 \rightarrow \rho^0 \gamma$ decay.

Table 32. The weak-annihilation form factors F_A , F_V and G_V . The accuracy of our estimates is about 10%. The sum rule results are recalculated from [115] according to the relation $-F_A^{SR} = F_1^{SR} M_B/f_{\rho^-} + f_B/M_B$ and $-F_V^{SR} = F_2^{SR} M_B/f_{\rho^-}$. The results from [116] are recalculated according to $-F_{A,V} = \frac{1}{2} f_{A,V}^{[116]}$ for $\bar{\Lambda} = 0.5$ GeV. According to our estimates, κ related to G_V is found in the range $-\kappa < 2.0$.

	Disp Approach	SR [115]	pQCD [116]
$-F_A^{B^-}$	0.120	0.110	≥ 0.09
$-F_V^{B^-}$	0.092	0.091	≥ 0.09
G^{ρ^-}	0.002κ		
$F_A^{B^0}$	0.055	0.037	
$F_V^{B^0}$	0.043	0.046	
G^{ρ^0}	0.0055κ		

Using the obtained form factors and the decay constants $f_B = 180$ MeV, $f_\rho = 210$ MeV, $f_\rho^0 = 210$ MeV, we arrive at the results for the penguin and weak annihilation invariant amplitudes shown in Table 33.

Our results for F^{peng} and $F_{\text{PV}}^{\text{WA}}$ amplitudes agree with the sum rule results [115]. We would like to notice, however, that the anatomy of F^{WA} in our analysis is different. Namely, we have found F_A considerably larger than the sum rule result. But after including the contact term $\sim f_B$ which we have come to $F_{\text{PV}}^{\text{WA}}$ close to the sum rule estimate [115].

If the form factor G_V is not taken into account, our estimate for $F_{\text{PC}}^{\text{WA}}$ agrees with the sum rules. Notice, however, that the contribution of G_V is enhanced for the B^0 decay compared to the B^- decay. Therefore, if the value $\kappa \simeq -1 \div -2$ is confirmed by the future analysis, the $F_{\text{PC}}^{\text{WA}}$ for the $B^0 \rightarrow \rho^0 \gamma$ decay might appear sizeably increased. For a definite conclusion a more accurate study of the form factor G_V is necessary.

Table 33. Results for the invariant amplitudes and their ratios for the $B^- \rightarrow \rho^- \gamma$ and $B^0 \rightarrow \rho^0 \gamma$ decays. In the Standard Model $|\xi_u/\xi_t| \simeq 0.4$. According to our estimates $-\kappa \leq 2$.

Quantity	$B^- \rightarrow \rho^- \gamma$	$B^0 \rightarrow \rho^0 \gamma$
F^{peng} , in MeV	$20 \xi_t$	$14 \xi_t$
$F_{\text{PC}}^{\text{WA}}$, in MeV [this work]	$-5.6 a_1 \xi_u$	$1.9 a_2 \xi_u$
$F_{\text{PV}}^{\text{WA}}$, in MeV [this work]	$-6.0 (1 + 0.06 \kappa) a_1 \xi_u$	$2.5 (1 - 0.3 \kappa) a_2 \xi_u$
$F_{\text{PV}}^{\text{WA}}/F^{\text{peng}}$ [this work]	$-0.28 a_1 \xi_u/\xi_t$	$0.14 a_2 \xi_u/\xi_t$
$F_{\text{PC}}^{\text{WA}}/F^{\text{peng}}$ [this work]	$-0.33 (1 + 0.06 \kappa) a_1 \xi_u/\xi_t$	$0.18 (1 - 0.33 \kappa) a_2 \xi_u/\xi_t$
$F_{\text{PV}}^{\text{WA}}/F^{\text{peng}}$ [125,115]	$-0.3 a_1 \xi_u/\xi_t$	$0.15 a_2 \xi_u/\xi_t$
$F_{\text{PC}}^{\text{WA}}/F^{\text{peng}}$ [125,115]	$-0.3 a_1 \xi_u/\xi_t$	$0.15 a_2 \xi_u/\xi_t$

The calculated form factors and the ratios of the weak-annihilation to the penguin amplitudes is one of the necessary ingredients for the calculation of the branching ratios of the $B \rightarrow \rho \gamma$ decays, Isospin and CP Asymmetries. In addition to the above ratios, these quantities contain the phase induced by the strong interactions and the CP-violating phase of the CKM matrix (see [125] for details). The corresponding analysis was done recently in [125] using the value $F^{\text{WA}}/F^{\text{peng}} \simeq -0.3 \xi_u/\xi_t$ and $F^{\text{WA}}/F^{\text{peng}} \simeq 0.03 \xi_u/\xi_t$ for $B^- \rightarrow \rho^- \gamma$ and $B^0 \rightarrow \rho^0 \gamma$ decays, respectively.

E. Discussion

We have analysed the weak annihilation for the radiative decay $B \rightarrow \rho \gamma$ in the factorization approximation.

1. Making use of the dispersion approach, we have calculated the form factors F_A and F_V describing the radiative semileptonic weak transition $B \rightarrow \gamma l \nu$. They are given by the diagrams with photon emitted from the B meson loop. We have performed the $1/m_b$ expansion of the spectral representations for these form factors and demonstrated them to exhibit a behaviour in agreement with the large-energy limit of QCD.
2. We have analysed the contribution to the weak annihilation amplitude from the diagram when the photon is emitted from the loop containing only light quarks. For the parity-conserving process this quantity is related to the divergence of the axial-vector current

$$\langle \gamma(q_1) \rho^-(q_2) | \partial_\nu \bar{d} \gamma_\nu \gamma_5 u | 0 \rangle = e \epsilon_{q_1 \epsilon_1^* q_2 \epsilon_2^*} (Q_u + Q_d) \kappa f_\rho M_\rho / M_B^2. \quad (5.55)$$

with κ staying finite in the chiral limit $m \rightarrow 0$ and estimated to be $-\kappa \leq 2$. The anomalous behavior of this amplitude has the similar origin as the anomalous behaviour of the matrix element $\langle \gamma(q_1) \gamma(q_2) | \partial_\mu A_\mu | 0 \rangle$. Let us stress this important result: the axial-vector current *is not conserved in the chiral limit* opposite to the common belief.

3. We have also included contact terms which were missed in some of the previous analyses. Numerical estimates for the weak annihilation contribution to the $B \rightarrow \rho \gamma$ amplitude are given in Table 32.

VI. NONFACTORIZABLE EFFECTS IN THE $B^0 - \bar{B}^0$ MIXING

In this Chapter we analyse corrections to factorization for the $B - \bar{B}$ mixing amplitude assuming that non-factorizable soft gluon exchanges can be described in terms of the local gluon condensate. The Chapter is based on Ref. [66].

Within this approximation the $\langle \alpha_s GG \rangle$ -correction to the mixing amplitude can be expressed through specific B -meson transition form factors at zero momentum transfer. First, the correction is demonstrated to be strictly *negative* independent of the particular values of the form factors.

As a next step, we study these form factors making use of the relativistic dispersion approach.

The study of the oscillations in the system of neutral B mesons provides important information on the pattern of the CP violation in the Standard model and its extensions (a detailed discussion can be found in [126]). The main uncertainty in the theoretical description of the process arises from the nonperturbative long-distance contributions to the mixing amplitude. In the $B - \bar{B}$ mixing there are two kinds of such contributions: first, effects related to the presence of the B -mesons in the initial and final states, and, second, corrections to the weak 4-quark amplitude due to the soft gluon exchanges between quarks of the initial B and the final \bar{B} meson. By neglecting the second contribution the amplitude factorizes. In this case all nonperturbative effects connected with the meson formation are reduced to only one quantity - the leptonic decay constant f_B .

Soft-gluon corrections to the weak 4-quark amplitude give rise to non-factorizable contributions, such that the influence of the B -meson structure is no longer described by the decay constant only. The understanding of the actual size of the non-factorizable effects and their adequate description in the heavy quark systems is an important and challenging task.

The theoretical analysis of $B - \bar{B}$ mixing was first performed within the QCD sum rules [127–129] and later using lattice QCD, see [130,131] and refs therein. The results from the sum rules are in all cases well compatible with factorization (vacuum saturation), within rather large errors. Recent lattice analyses definitely reported negative non-factorizable effects, around 5-10% for the central values at the scale $\mu \simeq m_b$. Still, the errors of the calculations have a similar size. Results from these approaches are shown in Table 34.

Table 34. Comparison of results from various approaches

Ref.	$B_{B_d}(m_b)$	$B_{B_s}(m_b)$	\hat{B}_{B_d}	$\hat{B}_{B_s}/\hat{B}_{B_d}$
SR [127,128]	1.0 ± 0.15			
SR [129]	0.95 ± 0.1			
Lat [130]	$0.92(4)^{+3}_0$	$0.91(2)^{+3}_{-0}$	$1.41(6)^{+5}_0$	$0.98(3)$
Lat [131]	$0.93(8)$	$0.92(6)$	$1.38(11)$	$0.98(5)$
This work	0.94 ± 0.035	0.95 ± 0.03	1.4 ± 0.05	1.01 ± 0.01

We analyse corrections to factorization in the $B - \bar{B}$ mixing due to soft gluon exchanges in the leading α_s -order, assuming the main effect of such exchanges to be described by the local gluon condensate introduced in Ref. [132]. Then the parameter ΔB_B which describes correction to factorization, is determined by the meson transition form factors at zero momentum transfer.

We demonstrate that in the local gluon condensate approximation the value of ΔB_B turns out to be *negative*, independently of the particular values of these form factors.

As a next step we calculate the relevant form factors making use of the dispersion approach. We obtain spectral representations for the form factors in terms of the B -meson wave function and the propagator of the color-octet $b\bar{q}$ -system.

Parameters of the model, such as the quark masses and the wave function have been fixed, but for numerical estimates we also need the propagator of the color-octet $q\bar{b}$ -system in the nonperturbative region, so we discuss the possible form of this propagator. The lack of reliable information about its details in the nonperturbative region leads to the main uncertainties in our numerical estimates.

The Chapter is organised as follows: The next Section presents basic formulas for the $B - \bar{B}$ mixing. In Section VIB we calculate the non-factorizable contribution to the mixing amplitude induced by the local gluon condensate and show that the correction is negative. In Section VIC we calculate the B -meson transition form factors within the dispersion approach. Section VID gives numerical estimates.

A. Effective Hamiltonian and the structure of the amplitude

The effective Hamiltonian which summarizes the perturbative QCD corrections for the $B^0 - \bar{B}^0$ mixing has the following form [133]

$$H_{eff}^{\Delta B=2} = \frac{G_F^2 M_W^2}{\sqrt{2}} (V_{tb}^* V_{td})^2 C(\mu) \bar{d} O_\sigma b \cdot \bar{d} O_\sigma b + h.c. \quad (6.1)$$

where G_F is the Fermi constant and $O_\sigma = \gamma_\sigma(1 - \gamma_5)$.

The parameter μ stands for the renormalization scale which separates the hard region taken into account perturbatively and the soft region. The Wilson coefficient $C(\mu)$ includes perturbative corrections above the scale μ . The explicit expression for $C(\mu)$ can be taken from [133]. The soft contributions are contained in the B -meson matrix elements of the operators in the effective Hamiltonian

$$A = \langle \bar{B}^0 | \bar{d} O_\sigma b \cdot \bar{d} O_\sigma b | B^0 \rangle. \quad (6.2)$$

The diagrammatic representation for the amplitude A of Eq. (6.2) is shown in Fig. 26.

$$\begin{aligned} A &= 2 \times \left[\text{Diagram 1} \right] + 2 \times \left[\text{Diagram 2} \right] \\ &= \frac{8}{3} \times \left[\text{Diagram 1} \right] + 4 \times \left[\text{Diagram 3} \right] \end{aligned}$$

Fig. 26. Different representations for the $B^0 - \bar{B}^0$ mixing amplitude. The enclosed quark lines show the order of contraction of the spinorial indices. The circles stand for the initial (final) B (\bar{B}) meson. The second line is obtained from the first line by performing the combined color and spinorial Fierz rearrangements.

Using the language of the hadronic intermediate states one finds that the contribution of the hadronic vacuum to this amplitude gives

$$\langle \bar{B}^0 | H_{eff}^{\Delta B=2} | B^0 \rangle = \frac{8}{3} \frac{G_F^2 M_W^2 M_B^2}{\sqrt{2}} (V_{tb}^* V_{td})^2 C(\mu) f_B^2, \quad (6.3)$$

with f_B the leptonic decay constant of the B meson defined according to the relation

$$\langle 0 | \bar{d} \gamma_\mu \gamma_5 b | B(p) \rangle = i f_B p_\mu, \quad \langle \bar{B}(p) | \bar{d} \gamma_\mu \gamma_5 b | 0 \rangle = -i f_B p_\mu. \quad (6.4)$$

It is convenient to parametrize the full amplitude as follows

$$\langle \bar{B}^0 | H_{eff}^{\Delta B=2} | B^0 \rangle = \frac{8}{3} \frac{G_F^2 M_W^2 M_B^2}{\sqrt{2}} (V_{tb}^* V_{td})^2 C(\mu) f_B^2 B_B, \quad (6.5)$$

such that the quantity $B_B - 1 \equiv \Delta B_B$ measures contributions of the non-vacuum intermediate hadronic states.

Using the language of quarks and gluons, the corrections to the amplitude of Fig. 26 due to soft gluon exchanges are obtained by inserting the (soft) gluons between the quark lines in Fig. 26. Soft gluon exchanges between the quarks of the same loop lead to the α_s -corrections either to the meson vertices or to the quark propagators. They only contribute to the leptonic decay constant f_B but do not lead to non-factorizable effects.

The non-factorizable effects originate from the soft gluon exchanges between quarks of different loops. To lowest α_s -order these effects are described by the 4 diagrams shown in Fig. 27.

Fig. 27. Soft-gluon exchanges leading to the non-factorizable effects.

We assume that the main effect of the soft gluon exchange can be described by the local gluon condensate. In the next section we demonstrate that in this approximation the $\langle \alpha_s GG \rangle$ -correction to the factorization is *negative*.

B. ΔB in terms of the local gluon condensate

Let us consider the exchange of a soft gluon between different quark loops assuming the dominance of the local gluon condensate [132]. In this case a typical graph of Fig. 27 describing the soft-gluon contribution is reduced to the product of the three-point diagrams as shown in Fig. 28.

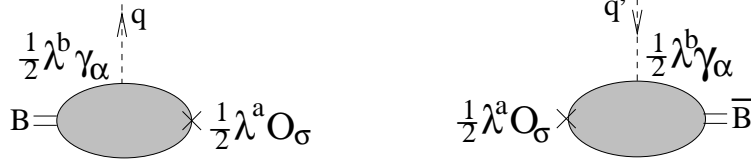


Fig. 28. Diagrams for $T_{\sigma\alpha}^{ab(l)}(p, q)$ (a) and $T_{\sigma\alpha}^{ab(r)}(p, q)$ (b).

The corresponding amplitude has the form

$$A^{(1)} = g^2 \int dq dq' T_{\sigma\alpha}^{ab(l)}(p, q) T_{\sigma\alpha'}^{ab'(r)}(p, q) \frac{dx}{(2\pi)^4} \frac{dx'}{(2\pi)^4} e^{-iqx + iq'x'} \langle A_\alpha^b(x) A_{\alpha'}^{b'}(x') \rangle, \quad (6.6)$$

where $T_{\sigma\alpha}^{ab(l)}(p, q)$ with the superscript l stands for the amplitude of Fig. 28a with the B in the initial state, and $T_{\sigma\alpha'}^{ab'(r)}(p, q')$ with the superscript r for the amplitude of Fig. 28b with the \bar{B} in the final state.

It is convenient to use the fixed-point gauge $x_\mu A_\mu(x) = 0$ [134]. In this case the gluon potential reads

$$A_\alpha^b(x) = \frac{1}{2} x_\beta G_{\alpha\beta}^b + \dots, \quad (6.7)$$

where dots stand for terms with higher order derivatives. The average over the hadronic vacuum is performed according to the relation

$$\langle G_{\alpha\beta}^b G_{\alpha'\beta'}^{b'} \rangle = \frac{\delta^{bb'}}{96} (g_{\alpha\alpha'} g_{\beta\beta'} - g_{\alpha\beta'} g_{\alpha'\beta}) \langle GG \rangle, \quad (6.8)$$

with $\delta^{aa} = N_c^2 - 1$. Here $\langle GG \rangle$ is the positive-valued gluon condensate $\langle \frac{\alpha_s}{\pi} GG \rangle = 0.012 \text{ GeV}^4$ [132].

The amplitude of Fig. 28 then takes the form

$$\begin{aligned} A^{(1)} &= \frac{g^2}{4} \int dq dq' T_{\sigma\alpha}^{ab(l)}(p, q) \frac{\partial}{\partial q_\beta} \delta(q) T_{\sigma\alpha'}^{ab'(r)}(p, q') \frac{\partial}{\partial q'_{\beta'}} \delta(q') \langle G_{\alpha\beta}^b G_{\alpha'\beta'}^{b'} \rangle \\ &= \frac{g^2}{4} \langle G_{\alpha\beta}^b G_{\alpha'\beta'}^{b'} \rangle \frac{\delta^{ab}}{2\sqrt{N_c}} T_{\sigma\alpha,\beta}^{(l)}(p) \frac{\delta^{ab'}}{2\sqrt{N_c}} T_{\sigma\alpha',\beta'}^{(r)}(p), \end{aligned} \quad (6.9)$$

where we have denoted

$$\frac{\partial}{\partial q_\beta} T_{\sigma\alpha}^{ab(l,r)}(p, q)|_{q=0} \equiv \frac{\delta^{ab}}{2\sqrt{N_c}} T_{\sigma\alpha,\beta}^{(l,r)}(p). \quad (6.10)$$

Notice that only the parts of the amplitudes $T^{(l,r)}$ antisymmetric in indices α and β give a nonvanishing contribution. These antisymmetric parts have the following general Lorentz structure:

$$\begin{aligned} T_{\sigma\alpha,\beta}^{A(l,q)} &= 4p^\nu [f_1^q \epsilon_{\alpha\beta\sigma\nu} + i f_2^q (g_{\alpha\nu} g_{\beta\sigma} - g_{\beta\nu} g_{\alpha\sigma})], \\ T_{\sigma\alpha,\beta}^{A(l,\bar{q})} &= 4p^\nu [f_1^{\bar{q}} \epsilon_{\alpha\beta\sigma\nu} + i f_2^{\bar{q}} (g_{\alpha\nu} g_{\beta\sigma} - g_{\beta\nu} g_{\alpha\sigma})], \\ T_{\sigma\alpha,\beta}^{A(r,q)} &= T_{\sigma\alpha,\beta}^{A(l,\bar{q})}, \\ T_{\sigma\alpha,\beta}^{A(r,\bar{q})} &= T_{\sigma\alpha,\beta}^{A(l,q)}, \\ f_1^q &= f_1^{\bar{q}}, \quad f_2^q = -f_2^{\bar{q}}. \end{aligned} \quad (6.11)$$

The superscript $q(\bar{q})$ in these expressions denotes the flavour of the quark (antiquark) to which the soft external gluon is attached in diagrams of Fig. 28. The quantities $f_{1,2}^{q,\bar{q}}$ are real constants. The last three lines in Eq. (6.11) are the consequence of the C -invariance of the strong interaction S -matrix. As we discuss in the next section, the constants $f_{1,2}^{q,\bar{q}}$ can be represented as specific B -meson transition form factors at zero momentum transfer.

We have to collect now contributions of the four diagrams in Fig. 27. For instance, the contribution to the amplitude of the subprocess in which the soft gluons are attached to the b quark in the left loop and the \bar{b} quark in the right loop reads

$$T_{\sigma\alpha;\beta}^{A(l,b)}(p)T_{\sigma\alpha';\beta'}^{A(r,\bar{b})}(p)(g_{\alpha\alpha'}g_{\beta\beta'} - g_{\alpha\beta'}g_{\alpha'\beta}) = -192M_B^2((f_1^b)^2 + (f_2^b)^2). \quad (6.12)$$

Similar expressions are easily obtained for other diagrams using the relations (6.11). Taking into account the relevant symmetry factors as shown in Fig. 26, we finally arrive at the following expressions for the factorizable and nonfactorizable contributions to the mixing amplitude:

$$\begin{aligned} A^{(0)} &\simeq \frac{8}{3}M_B^2 f_B^2 \\ A^{(1)} &\simeq -8C_F M_B^2 \left\langle \frac{\alpha_s}{\pi} GG \right\rangle \pi^2 [(f_1^b + f_1^d)^2 + (f_2^b - f_2^d)^2], \end{aligned} \quad (6.13)$$

with the color factor $C_F = \frac{N_c^2 - 1}{4N_c}$. Finally, for ΔB_B we find the expression

$$\Delta B_B(\mu) = -\frac{\left\langle \frac{\alpha_s}{\pi} GG \right\rangle}{f_B^2} 2\pi^2 [(f_1^b + f_1^d)^2 + (f_2^b - f_2^d)^2]. \quad (6.14)$$

The quantities f_1 and f_2 depend on the renormalization scale μ .

Obviously, the correction to the factorizable amplitude due to the local gluon condensate is *negative*. Let us point out that the relation (6.14) is the direct consequence of the only assumption of the locality of the gluon condensate, dominating the nonfactorizable correction. It is completely independent of any details of the B -meson structure.

C. Form factors in the dispersion approach

We now proceed to the calculation of the form factors f_1 and f_2 . We start with the amplitude $T_{\sigma\alpha}^{(l)ab}(p, q)$. It is diagonal in color indices, so we write $T_{\sigma\alpha}^{(l)ab}(p, q) = \frac{\delta^{ab}}{\sqrt{N_c}} T_{\sigma\alpha}^{(l)}(p, q)$. The triangle diagram for $T_{\sigma\alpha}^{(l)}(p, q)$ is shown in Fig. 29a. Throughout this section we shall omit the superscript l . The quark structure of the B -meson is described by the vertex $i\bar{q}_1\gamma_5 q_2 G(s)/\sqrt{N_c}$. One should set $m_1 = m_b$, $m_2 = m_d$ for the calculation of $f^{(b)}$, and $m_1 = m_d$, $m_2 = m_b$ for $f^{(d)}$.

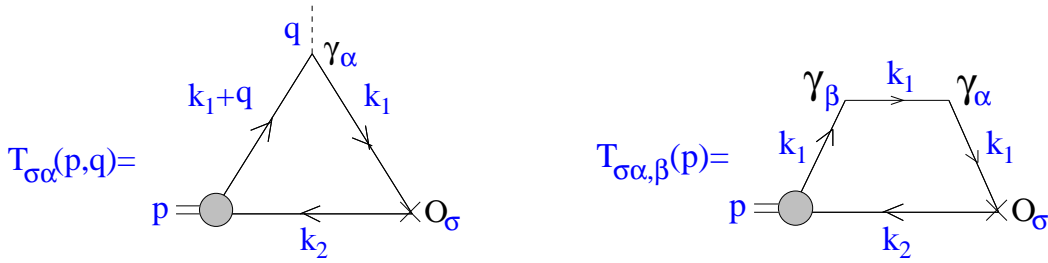


Fig. 29. Diagrams for $T_{\sigma\alpha}(p, q)$ (a) and $T_{\sigma\alpha,\beta}(p) = \frac{\partial}{\partial q^{\beta}} T_{\sigma\alpha}(p, q)|_{q=0}$ (b).

We need to calculate $T_{\sigma\alpha,\beta}(p) = \frac{\partial}{\partial q^{\beta}} T_{\sigma\alpha}(p, q)|_{q=0}$ (6.10). For the $T_{\sigma\alpha}(p, q)$ shown in Fig. 29a, its derivative $T_{\sigma\alpha,\beta}(p)$ is given by the diagram in Fig. 29b. The trace corresponding to the Feynman diagram of Fig. 29b reads:

$$S_{\sigma\alpha;\beta} = \text{Sp} \left[i\gamma_5(m_2 - \hat{k}_2)O_{\sigma}(m_1 + \hat{k}_1)\gamma_{\alpha}(m_1 + \hat{k}_1)\gamma_{\beta}(m_1 + \hat{k}_1) \right], \quad (6.15)$$

where $O_{\sigma} = \gamma_{\sigma}(1 - \gamma_5)$. Since this expression is further multiplied by $G_{\alpha\beta}$, only its antisymmetric part in α and β is necessary. The latter reads

$$\begin{aligned}
S_{\sigma\alpha;\beta}^A &= (m_1^2 - k_1^2) \text{Sp} \left(i\gamma_5(m_2 - \hat{k}_2)\gamma_\sigma(1 - \gamma_5)\gamma_\beta(m_1 - \hat{k}_1) \right) \\
&= (m_1^2 - k_1^2) [4\epsilon_{\beta\alpha\sigma\nu}(m_2 k_1^\nu + m_1 k_2^\nu) + 4im_1 k_2^\nu (g_{\alpha\sigma}g_{\beta\nu} - g_{\beta\sigma}g_{\alpha\nu})].
\end{aligned} \tag{6.16}$$

The corresponding expression for the Feynman amplitude takes the form

$$\begin{aligned}
T_{\sigma\alpha;\beta}^A(p) &= \frac{1}{(2\pi)^4 i} \int dk_1 dk_2 \delta(p - k_1 - k_2) \frac{-1}{(m_1^2 - k_1^2)^2 (m_2^2 - k_2^2)} \\
&\quad \times [4\epsilon_{\beta\alpha\sigma\nu}(m_2 k_1^\nu + m_1 k_2^\nu) + 4im_1 k_2^\nu (g_{\alpha\sigma}g_{\beta\nu} - g_{\beta\sigma}g_{\alpha\nu})].
\end{aligned} \tag{6.17}$$

We define f_v and f_s by the relations

$$\begin{aligned}
\frac{1}{(2\pi)^4 i} \int dk_1 dk_2 \delta(p - k_1 - k_2) \frac{k_1^\nu}{(m_1^2 - k_1^2)^2 (m_2^2 - k_2^2)} &= p^\nu f_v(p^2), \\
\frac{1}{(2\pi)^4 i} \int dk_1 dk_2 \delta(p - k_1 - k_2) \frac{1}{(m_1^2 - k_1^2)^2 (m_2^2 - k_2^2)} &= f_s(p^2).
\end{aligned} \tag{6.18}$$

After the k -integration in Eq. (6.17) one recovers the structure of the amplitude from Eq. (6.11)

$$T_{\sigma\alpha;\beta}^A(p) = -4p^\nu [f_1 \epsilon_{\beta\alpha\sigma\nu} + i f_2 (g_{\alpha\sigma}g_{\beta\nu} - g_{\beta\sigma}g_{\alpha\nu})], \tag{6.19}$$

with

$$\begin{aligned}
f_1 &= (m_2 - m_1)f_v + m_1 f_s, \\
f_2 &= m_1(f_s - f_v).
\end{aligned} \tag{6.20}$$

Let us obtain now spectral representations for the form factors f_v^F and f_s^F . We first notice that the expressions (6.18) correspond to the triangle Feynman diagram at zero momentum transfer $q = 0$. This condition means that both $q^2 = 0$ and $p^2 = p'^2$, where $p' = p - q$, so we can write $f_i^F(p^2) = f_i^F(q^2 = 0, p^2, p'^2 = p^2)$, with $i = v, s$.

It is convenient to start with the case $q^2 \neq 0$ and $p^2 \neq p'^2$. Then the form factors f_i can be written in the form of the double spectral representation:

$$f_i^F(q^2, p^2, p'^2) = \int \frac{ds}{s - p^2} \frac{ds'}{s' - p'^2} \Delta_i(s, s', q^2), \tag{6.21}$$

where the double spectral density Δ_i can be calculated for any of the form factors from the Feynman integral.

As the next step, we set $q^2 = 0$, but still treat p^2 and p'^2 as independent variables. In this case the double spectral representations of the form (6.21) simplify to the following single spectral representations

$$\begin{aligned}
f_s^F(p^2, p'^2) &= \frac{1}{16\pi^2} \int ds \frac{1}{s - p^2} \frac{1}{s - p'^2} \log \left(\frac{s + m_1^2 - m_2^2 + \lambda^{1/2}(s, m_1^2, m_2^2)}{s + m_1^2 - m_2^2 - \lambda^{1/2}(s, m_1^2, m_2^2)} \right), \\
f_v^F(p^2, p'^2) &= \frac{1}{16\pi^2} \int ds \frac{1}{s - p^2} \frac{1}{s - p'^2} \frac{\lambda^{1/2}(s, m_1^2, m_2^2)}{s}.
\end{aligned} \tag{6.22}$$

The representations for the form factors in the form (6.22) are valid however only in the region of p^2 and p'^2 (far) below the threshold. The reason for that is the following: the representations (6.21) and (6.22) are based on the Feynman form of the quark propagators. This form is however valid only for highly virtual particles, while in the soft region it is strongly distorted by nonperturbative effects. In particular, the pole at $k^2 = m^2$ in the propagator of a color object, like quark and gluon, is absent. Recently, this was confirmed in a lattice study of the gluon propagator [135].

The modification of the quark propagator in the soft region leads to the change of the spectral representation for the form factors in the region of p^2 and p'^2 near and above the $b\bar{q}$ threshold.

Notice that the quantities $1/(s - p^2)$ and $1/(s' - p'^2)$ in Eq. (6.21) are the propagators of the initial and final $b\bar{q}$ states with virtualities s and s' , and the squared masses p^2 and p'^2 , respectively. The nonperturbative effects which modify the quark and gluon propagators in the soft region, modify the propagators of the $b\bar{q}$ states as well.

We know the character of these changes in the p^2 -channel corresponding to the B -meson: soft interaction of quarks effectively replace the factor $1/(s - M_B^2)$ with a regular B -meson soft wave function $\varphi_B(s)$ in the integrand of (6.22).

In the color-octet p'^2 -channel the Feynman propagator $1/(s - p'^2)$ in Eq (6.22) is replaced by the propagator $D(s, p'^2)$ which involves proper modifications in the soft region. We therefore find the following representation for the form factors $f_i(p'^2) \equiv f_i(q^2 = 0, p^2 = M_B^2, p'^2)$

$$\begin{aligned}
f_v(p'^2) &= \frac{1}{16\pi^2} \int ds \phi_B(s) D(s, p'^2) \frac{\lambda^{1/2}(s, m_1^2, m_2^2)}{s}, \\
f_s(p'^2) &= \frac{1}{16\pi^2} \int ds \phi_B(s) D(s, p'^2) \log \left(\frac{s + m_1^2 - m_2^2 + \lambda^{1/2}(s, m_1^2, m_2^2)}{s + m_1^2 - m_2^2 - \lambda^{1/2}(s, m_1^2, m_2^2)} \right).
\end{aligned} \tag{6.23}$$

We know that $D(s, p'^2) \sim 1/(s - p'^2)$ at large values of $s - p'^2$, and also that $D(s, p'^2)$ is finite at $s = p'^2$. However, we do not know details of $D(s, p'^2)$ in the soft region. Motivated by the discussion in [136], we assume here that the nonperturbative effects can be described by the following modification of the propagator

$$D(s, p'^2) = \frac{1}{s - p'^2 + M_0^2} \tag{6.24}$$

where M_0 is a mass parameter. In order to guarantee the absence of the pole in $D(s, p'^2)$ in the heavy quark limit, M_0 should scale with the heavy quark mass as follows: $M_0^2 = O(\Lambda_{QCD} m_Q)$. So it is convenient to write M_0 in the form

$$M_0^2 = w m_d m_b, \tag{6.25}$$

where $m_d \simeq \Lambda_{QCD}$ is the constituent mass of the light quark, and w is a parameter of order unity.⁸

In the next section we make use of Eqs. (6.23) and (6.24) to analyse $f_{v,s}(p'^2)$ for B_d and B_s mesons.

D. Numerical results.

The parametrization for the B -meson wave function and values of the quark masses have been already fixed. Recall that we have determined the wave function by fitting the lattice data on the weak transition form factors for large momentum transfers at the normalization point $\mu \simeq 5$ GeV. Therefore, the B -meson soft wave function and the form factors $f_{s,v}(p'^2)$ at this scale are determined.

Whereas the B -meson wave function is known quite well, good information about the details of $D(s, p'^2)$ is lacking. We therefore use the simple Ansatz (6.24) for $D(s, p'^2)$ in the full range of s and p'^2 and treat w as a free parameter of order unity. We expect that the variation of w in the interval $w = 0.5 \div 2$ provides reasonable error estimates for the form factors and ΔB . Notice that the value of ΔB corresponding to $w = 1$ agrees favourably with the recent lattice estimates, see Table 34.

The form factor $f_s^{(d)}$ which gives the main contribution to ΔB_B is shown in Fig. 30 vs p'^2 .

Table 35 gives numerical results for the form factors at $q^2 = 0$. The relative magnitudes of these form factors can be easily understood taking into account their scaling properties in the heavy quark limit: $f_s^{(d)} \sim m_b^{-1/2}$, $f_s^{(b)} \sim m_b^{-3/2}$, $f_v^{(b)}/f_s^{(b)} \sim 1$.

Table 35. Form factors and ΔB_{B_q} with $q = d$ for B_d , and $q = s$ for B_s . The factors $f_{1,2}(p'^2)$ are calculated at $p'^2 = M_{B_d}^2$ for B_d and at $p'^2 = M_{B_s}^2$ for B_s . The errors correspond to the interval $w=0.5 \div 2$.

	B_d	B_s
$f_v^{(b)} = f_v^{(q)}$	$9 \pm 3 \times 10^{-3}$	$8 \pm 3 \times 10^{-3}$
$f_s^{(b)}$	$1.1 \pm 0.2 \times 10^{-2}$	$9 \pm 3 \times 10^{-3}$
$f_s^{(d)}$	$1.4 \pm 0.5 \times 10^{-1}$	$1.0 \pm 0.4 \times 10^{-1}$
$f_1^{(b)}$	$7 \pm 1.5 \times 10^{-3}$	$8 \pm 3 \times 10^{-3}$
$f_2^{(b)}$	$5.5 \pm 1.5 \times 10^{-3}$	$5.5 \pm 2.0 \times 10^{-3}$
$f_1^{(d)}$	$7.5 \pm 2.5 \times 10^{-2}$	$7.5 \pm 2.5 \times 10^{-2}$
$f_2^{(d)}$	$3.5 \pm 1.0 \times 10^{-2}$	$3.0 \pm 1.5 \times 10^{-2}$
ΔB_{B_q}	-0.06 ± 0.035	-0.05 ± 0.03

⁸ Assuming that for the color-octet light $q\bar{q}$ system Eq (6.24) remains valid with $M_0^2 = w m_d^2$, we find $D(k^2 = 0) \simeq 15 \text{ GeV}^{-2}$ for $w = 1$. This is close to the value of the gluon propagator $D(k^2 = 0) \simeq 18 \text{ GeV}^{-2}$ as found in [135]. This agreement seems to be reasonable since one can expect the propagator of the light $q\bar{q}$ color-octet system to have a structure in the nonperturbative region similar to the structure of the gluon propagator.

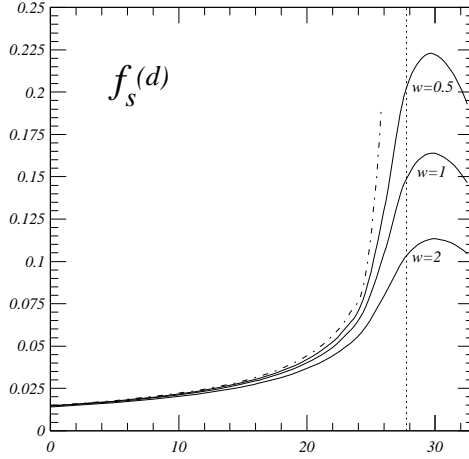


Fig. 30. The form factor $f_s(p'^2)$ for the B_d meson vs p'^2 . Solid curves are results of the calculation via the Eqs. (6.23) and (6.24) for various values of the parameter w : upper curve - $w = 0.5$, middle curve - $w = 1.0$, lower curve - $w = 2$. The dash-dotted curve in the region $p'^2 < (m_b + m_d)^2$ corresponds to $w = 0$. The vertical dotted line corresponds to $p'^2 = M_B^2$.

Fig. 30 shows the form factor $f_s^{(d)}$ which gives the main contribution to ΔB_B .

The value of ΔB is obtained from Eq. (6.14) taking $\langle \frac{\alpha_s}{\pi} GG \rangle = 0.012 \text{ GeV}^4$ from [132]. Using the Wilson coefficient at the scale $\mu = m_b$ we obtain the renorm-invariant factors \hat{B}_{B_d} and \hat{B}_{B_s} (the definition are given in [131]) listed in Table 34.

Our results are in good agreement with the lattice results, except for a slightly different estimate of the SU(3) violating effects in the $B_d - \bar{B}_d$ and $B_s - \bar{B}_s$ cases. This nice agreement gives support to our Ansatz for the description of the nonperturbative effects in the propagator of the color-octet $q\bar{q}$ system.

We would like to notice that taking the Ansatz (6.24) and (6.25) for the propagator of the $s\bar{q}$ system and setting $M_0^2 = w m_s m_{\bar{q}}$, with $w \simeq 1$ allows a parameter-free estimate of the $K^0 - \bar{K}^0$ mixing. In this case the result is much more stable with respect to the particular value of w and therefore to the details of the propagator in the nonperturbative region. We obtained this way $\Delta B_K(1 \text{ GeV}) = -0.21 \pm 0.04$.

E. Discussion.

In this Chapter we have considered corrections to factorization in the $B\bar{B}$ mixing amplitude due to soft-gluon exchanges, assuming that the main effect of such exchanges can be described in terms of the local gluon condensate.

1. We have proved that within this approximation the correction of order $\alpha_s \langle GG \rangle$ to factorization is *negative*. It can be expressed through the specific B -meson transition form factors at zero momentum transfer.
2. We calculated these form factors within our dispersion approach. Spectral representations for the form factors in terms of the B -meson soft wave function and the propagator of the color-octet $q\bar{b}$ system were obtained. The behaviour of this propagator in the nonperturbative region was discussed. The obtained numerical estimates for ΔB_B favourably compare with the recent lattice calculations.

Let us point out that the proposed approach can be extended to the description of more complicated problems. In particular, it can be applied to the analysis of the non-factorizable effects in non-leptonic B decays.

VII. QUARK-BINDING EFFECTS IN INCLUSIVE DECAYS OF HEAVY MESONS

As we have discussed in Chapter II, the dispersion approach allows us to represent amplitudes of the hadron interactions as relativistic spectral representations in terms of the hadron wave function. In previous Chapters we analysed in detail form factors of meson decays and meson wave functions.

In this Chapter we apply the dispersion approach to the analysis of quark-binding effects in inclusive semileptonic decays of heavy mesons. We derive spectral representations for various differential distributions, such as electron energy spectrum, q^2 - and M_X -distributions, in terms of the same meson wave function [67].

Using the quark-model parameters determined in the previous Chapters, we provide numerical estimates for various distributions describing inclusive $B \rightarrow X_c \ell \bar{\nu}_\ell$ decays.

Inclusive decays provide a promising possibility to determine those CKM matrix elements which describe the mixing of b quark. This is due to the fact that a rigorous theoretical treatment of these decays, including nonperturbative effects, is possible. The consideration based on the Operator Product Expansion (OPE) and the Heavy Quark (HQ) expansion [4] allows to connect the rate of the inclusive B meson decay with the rate of the b quark decay. An important consequence of the OPE is the appearance of quark-binding effects in the integrated rates (both total and semileptonic) of heavy meson decays only in the second order of the $1/m_Q$ expansion [5]. These second order corrections are expressed in terms of the two hadronic parameters, λ_1 and λ_2 . The latter are the mesonic matrix elements of operators of dimension 5 which appear in the OPE of the product of two weak currents. The differential distributions can be obtained in the form of expansions in inverse powers of the heavy-quark mass m_Q [137–139].

Whereas providing quite reliable results for the integrated semileptonic decay rate, the OPE method encounters difficulties in calculating various differential distributions. For instance, before comparing the OPE-based results for the differential distributions with the true distributions a proper smearing over duality interval is necessary.

There are several reasons for complications arising in the calculation of differential distributions in the resonance region near zero recoil, namely:

1. duality-violating $1/m_Q$ effects (i.e. the difference between the true distributions and the smeared OPE results) in the differential distributions near zero recoil which originate from the delay in opening different hadronic channels, as noticed in [140]. Although these effects are cancelled in the integrated semileptonic rate, they can considerably influence the kinematical distributions near the zero recoil point;
2. the convergence of the OPE series for the differential distributions persists only in the region where the quark produced in the semileptonic decay is sufficiently fast. This means that the OPE cannot directly predict distributions in some kinematical regions, such as:

- the photon energy spectrum $d\Gamma/dE_\gamma$ in the radiative $B \rightarrow X_s \gamma$: the window in the photon energy between $m_Q/2$ and $M_Q/2$ turns out to be completely inaccessible within the OPE formalism [139];
- the lepton energy spectrum $d\Gamma/dE_\ell$ at large values of E_ℓ in semileptonic or rare semileptonic decays;
- the lepton q^2 -distributions in semileptonic $B \rightarrow X_c$ (X_u) and rare $B \rightarrow X_s$ decays at large q^2 near zero recoil; in this region one encounters both the quark-binding and duality-violating effects.

Problems related to the quark-binding effects can be solved in principle by performing proper resummation of the nonperturbative corrections which in practice however leads to the appearance of *a priori* unknown distribution functions [141,142].

The inclusion of the quark-binding effects in heavy meson decays was first done in [143], where an unknown distribution function of a heavy quark inside the heavy meson was introduced. Evidently, this distribution function is connected with the wave function of the heavy meson which also determines the exclusive transition form factors. To put this connection on a more solid basis, it is reasonable to consider the inclusive and exclusive processes within the same approach.

We show in this Chapter that the dispersion approach based on the constituent quark picture can be used as an efficient tool for calculating differential distributions in inclusive decays of heavy mesons, covering also kinematical regions where OPE cannot provide a rigorous treatment. Our dispersion approach allows one to take into account quark-binding effects in inclusive heavy meson decays in terms of the meson soft wave function. The latter describes the heavy meson properties both in exclusive and inclusive processes and thus allows one to consider on the same ground long-distance effects in various kinds of hadronic processes.

Quark-model calculations of inclusive distributions are essentially based on the evaluation of the box diagram (see Fig. 31 later on) by introducing the heavy meson wave function in one way or another. To illustrate the basic features of such an approach as well as its advantages and limitations it suffices to consider the case of a nonrelativistic potential model with scalar currents. Inclusion of relativistic effects can be then performed.

Let us consider a weak transition induced by the scalar current $J = \bar{c}b$, where both b and c are heavy. To make the nonrelativistic treatment consistent we assume that

$$m_b, m_c \gg \delta m \equiv m_b - m_c \gg \Lambda, \quad (7.1)$$

where Λ is the typical scale of the quark binding effects in the heavy meson. In the nonrelativistic theory the general expression for the hadronic tensor

$$W(q_0, \vec{q}) = \frac{1}{\pi} \text{Im} \int \langle B | T(J(x) J^\dagger(0)) | B \rangle e^{-iqx} dx \quad (7.2)$$

is reduced to the form

$$W(q_0, \vec{q}) = \frac{1}{\pi} \text{Im} \langle B | G_{c\bar{d}}(M_B - q^0 - i0, \vec{q}) | B \rangle. \quad (7.3)$$

Here

$$G_{c\bar{d}}(E, \vec{q}) = (\hat{H}_{c\bar{d}}(\vec{q}) - E)^{-1} \quad (7.4)$$

is the full Green function corresponding to the full Hamiltonian operator of the $c\bar{d}$ system with the total momentum \vec{q}

$$\hat{H}_{c\bar{d}}(\vec{q}) = m_c + m_d + \frac{(\hat{\vec{k}} + \vec{q})^2}{2m_c} + \frac{\hat{\vec{k}}^2}{2m_d} + V_{c\bar{d}}(\hat{r}). \quad (7.5)$$

Thus, the hadronic tensor is the average of the full $c\bar{d}$ Green function over the ground state of the full $b\bar{d}$ Hamiltonian

$$\hat{H}_{b\bar{d}}|B\rangle = M_B|B\rangle = (m_b + m_d + \epsilon_B)|B\rangle. \quad (7.6)$$

In the rest frame of the B -meson one has

$$\begin{aligned} \hat{H}_{b\bar{d}} &= m_b + m_d + \frac{\hat{\vec{k}}^2}{2m_b} + \frac{\hat{\vec{k}}^2}{2m_d} + V_{b\bar{d}}(\hat{r}) \\ &\equiv m_b + m_d + \hat{h}_{b\bar{d}} \end{aligned} \quad (7.7)$$

The following relation provides a basis for performing the OPE in the nonrelativistic potential model [144]

$$\begin{aligned} \hat{H}_{c\bar{d}} - (M_B - q^0) &= -(\delta m - \frac{q^2}{2m_c} - q^0) + (\hat{h}_{b\bar{d}} - \epsilon_B) \\ &+ \frac{\hat{\vec{k}}^2 + \hat{V}_1}{2} \left(\frac{1}{m_c} - \frac{1}{m_b} \right) - \frac{\hat{\vec{k}}\vec{q}}{m_c} + O\left(\frac{\gamma^3 \delta m}{m_c^3}\right) \end{aligned} \quad (7.8)$$

where $\gamma \sim \Lambda_{QCD}$ and we have assumed the following expansion of the potential

$$\hat{V}_{Q\bar{q}} = \hat{V}_0 + \frac{\hat{V}_1}{2m_Q} + \frac{\hat{V}_2}{2m_Q^2} + \dots \quad (7.9)$$

Starting with (7.8) one constructs an OPE series using the amplitude of the free $b \rightarrow c$ quark transition as a zero-order approximation (hereafter referred to as the standard OPE). By virtue of the equations of motion,

$$(\hat{h}_{b\bar{d}} - \epsilon_B)|B\rangle = 0, \quad (7.10)$$

one observes the absence of $1/m_Q$ corrections to the leading order (LO) $b \rightarrow c$ amplitude, so that the corrections emerge only at the $1/m_Q^2$ order. A detailed analysis of the duality in the nonrelativistic potential model can be found in [144]. Being completely reliable for the calculation of the integrated decay rate, the choice of the free-quark decay as the zero-order approximation turns out to be inconvenient however for calculating differential distributions. In particular, the distribution in the invariant mass of the produced hadronic system, M_X , becomes very singular and

is represented via $\delta(M_X - m_c)$ and its derivatives, such that the $1/m_Q$ corrections are even more singular than the leading-order result. This is the price one pays for the choice of the zero-order term.

It is clear that the free-quark transition amplitude is not the unique choice of the zero-order approximation, at least in quantum mechanics. For instance, another structure of the expansion can be obtained if the free $c\bar{d}$ Green function is used as the zero-order approximation.

In the nonrelativistic quantum mechanics the relation between the full $G(E)$ and the free $G_0(E)$ Green functions is well known and reads

$$G^{-1}(E) = H - E, \quad G_0^{-1}(E) = H_0 - E, \quad G^{-1}(E) - G_0^{-1}(E) = V, \quad (7.11)$$

or, equivalently,

$$\begin{aligned} G(E) &= G_0(E) - G_0(E)VG(E) \\ &= G_0(E) - G_0(E)VG_0(E) + G_0(E)VG_0(E)VG_0(E) + \dots \end{aligned} \quad (7.12)$$

For the heavy quark decay, in most of the kinematical q^2 -region except for a vicinity of the zero recoil point, the Green function G_0 behaves as $1/m_Q$, and, since the matrix elements of the operator V remain finite as $m_Q \rightarrow \infty$, the series (7.12) is an expansion in powers of $1/m_Q$. Notice that in the nonrelativistic potential model the expansion (7.12) is fully equivalent to the OPE series obtained from (7.8). Inserting the expansion (7.12) into the expression for the hadronic tensor W given by eq. (7.3), we come to the series shown in Fig 31.

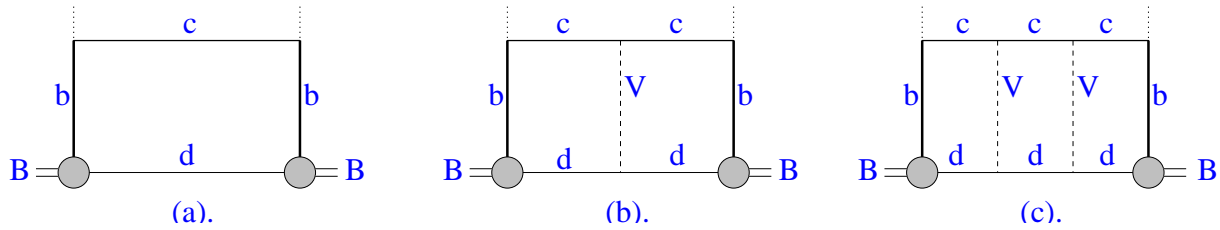


Fig. 31. Expansion of the hadronic tensor in the quark model: (a) - the box diagram which provides the LO free-quark contribution, (b,c) - diagrams contributing in subleading $1/m_Q$ orders and containing the final state interaction $V \equiv V_{c\bar{d}}$. The short-dashed lines represent W bosons.

The leading contribution in the heavy quark limit is given by the box diagram of Fig. 31a with the free c and \bar{d} quarks in the intermediate state. The corresponding analytical expression reads

$$W^{\text{QM}} = \frac{1}{\pi} \text{Im} \langle B | G_{c\bar{d}}^0(M_B - q^0, \vec{q}) | B \rangle. \quad (7.13)$$

This is the quantity usually taken into account in quark-model calculations. It is easy to see, that the semileptonic decay rate calculation based on the box diagram of Fig. 31 only, reproduces the free quark semileptonic decay rate in the heavy-quark limit, but should contain also $1/m_Q$ corrections (see also the general structure of the quark-model results of Ref. [145]). Namely, the next-to-leading order (NLO) term in the expansion (7.12) is the diagram with a single insertion of the potential between the free c and \bar{d} quarks (the diagram of Fig. 31b). It has the order $1/m_Q$ and precisely cancels the $1/m_Q$ contribution of the quark-model box diagram, yielding in this way the absence of the $1/m_Q$ correction in the difference between the decay rates of bound and free heavy quarks.

In other words, the quark-model box-diagram calculation is just the first term in an alternative expansion of the full Green function: unlike the standard OPE series which starts with a single c -quark in the intermediate state, the quark-model starts with the free $c\bar{d}$ pair which is the eigenstate of the Hamiltonian

$$H_{c\bar{d}}^0(\vec{q}) = m_c + m_d + \frac{(\vec{k} + \vec{q})^2}{2m_c} + \frac{\vec{k}^2}{2m_d}. \quad (7.14)$$

Hereafter we refer to the expansion of the decay rate based on the expansion (7.12) of the Green function as the quark-model (QM) expansion.

Summing up, the quark model provides an alternative $1/m_Q$ expansion with the following properties:

1. the box diagram of Fig. 31a provides the LO $1/m_Q$ term and reproduces the free-quark decay in the limit $m_Q \rightarrow \infty$. All other terms contribute only in subleading $1/m_Q$ orders;
2. the differential distributions in any $1/m_Q$ order are convergent for almost all allowed q^2 , except for the region close to zero recoil;
3. before comparing the calculated differential distributions based on the expansion (7.12) with the true distributions in the resonance region a proper smearing over some duality interval is required;
4. the $1/m_Q$ correction to the LO term is nonvanishing.

Clearly, the properties 1-3 are completely equivalent to the standard OPE, while the property 4 makes the quark-model expansion much less convenient than the standard OPE, at least for the calculation of the semileptonic decay rate. However:

5. the expansion (7.12) turns out to be more suitable for the calculation of the differential distributions, e.g. for the calculation of $d\Gamma/dM_X$: in this case the LO result (the box diagram of Fig. 31a) is well-defined in the whole kinematical region as well as the higher order corrections to it. Thus already the box diagram is appropriate for comparison with the experimental $d\Gamma/dM_X$ at all M_X apart from the resonance region. Beyond the resonance region no additional smearing of the calculated $d\Gamma/dM_X$ is required.

In full QCD the situation is of course much more complicated. Hadrons are coherent states of infinite number of quarks and gluons. Nevertheless, many applications of the constituent quark model have proved the treatment of mesons as bound states of two constituent quarks to provide a reasonable description of their properties. From this viewpoint the arguments given above remain valid. Namely, the box diagram represents the main contribution to the hadronic tensor which reproduces the free-quark decay in the infinite quark mass limit. However the hadronic tensor calculated from the box diagram contains $1/m_Q$ term compared with the free-quark decay tensor. This linear $1/m_Q$ term is known to be cancelled by the $1/m_Q$ contributions of higher order diagrams. In practice, however the $1/m_Q$ term of the box diagram is not so dangerous: namely, the hadronic tensor calculated from the box diagram, as well as all corrections given by the other graphs, are regular in the whole kinematical region. Thus *the box diagram should provide a reasonable description appropriate for comparison with experiment*. Moreover, the box-diagram result can be further improved by effectively taking into account the higher order term which kills the $1/m_Q$ correction contained in the box diagram. We follow this strategy in our analysis and perform a relativistic treatment of quark-binding effects within a constituent quark picture.

Our consideration of the quark binding effects in inclusive semileptonic decays is based on the relativistic dispersion formulation of the quark model discussed in detail in the previous chapters.

The inclusive decay rates as well as the exclusive hadron transition form factors are given by double spectral representations in terms of the soft meson wave functions. Recall, that the double spectral densities of these spectral representations are obtained from the corresponding Feynman graphs, whereas subtraction terms should be fixed independently. Such subtraction terms in the spectral representations for exclusive transition form factors were fixed by requiring the structure of the heavy quark expansion in our approach to match the structure of the heavy quark expansion in QCD. In this Chapter we proceed along the same lines in inclusive processes.

- We construct the double spectral representation of the hadronic tensor within the constituent quark model starting with $q^2 < 0$. The hadronic tensor is represented in terms of the soft wave function of the B meson and the double spectral density of the box diagram. The hadronic tensor at $q^2 > 0$ is obtained by the analytical continuation. Then the $1/m_Q$ expansion of the spectral representation of the decay rate is performed and the LO term is shown to reproduce the free quark decay rate. The subtraction is defined in such a way that the $1/m_Q$ correction to the semileptonic decay rate is absent. This corresponds to effectively taking into account other terms beyond the box-diagram approximation which contribute in subleading $1/m_Q$ orders. Moreover an account of the $1/m_Q^2$ effects of the whole series within the box-diagram expression is possible. This is done by introducing a phenomenological cut in the double spectral representation of the box-diagram which affects only the differential distributions at large q^2 . This cut brings the size of the $1/m_Q^2$ corrections in the $\Gamma(B \rightarrow X_c \ell \bar{\nu}_\ell)$ in full agreement with the OPE result and keeps the LO and $1/m_Q$ correction unchanged. The cut yields differential distributions which are finite also in the endpoint q^2 -region where the HQ expansion series is not properly convergent;
- We calculate various differential distributions in terms of the B -meson soft wave function. These distributions are regular in the whole kinematically accessible region and, apart from the resonance region (where the exact

distributions are dominated by single resonances and a proper smearing over the duality intervals is necessary), can be directly compared with the observable values. The main effect of quark-binding upon these distributions is determined unambiguously through the soft wave function, while the $1/m_Q^2$ corrections depend on the particular details of an account of the higher-order terms in the series (7.12). However, in practice these details are not essential due to the following two reasons: first they are numerically small, and second, the size of the $1/m_Q^2$ corrections in the integrated semileptonic rate is close to the OPE result. So we expect that the size of the $1/m_Q^2$ corrections is reasonably reproduced also in other quantities;

- We perform numerical estimates of various differential distributions in inclusive decays in terms of the B -meson wave function determined from the description of the exclusive processes.

In the next section we present necessary formulas for the free-quark decay and also the OPE prediction for the total integrated rate to $1/m_Q^2$ accuracy. In Section VII B we construct the dispersion representation for the box diagram at $q^2 < 0$ and discuss its analytical continuation to $q^2 > 0$. Section VII C gives the $1/m_Q$ expansion of the hadronic tensor in the quark model, and Sections VII D and VII D present numerical results for the differential distributions.

A. Free quark decay and OPE

The semileptonic weak decay $Q_2 \rightarrow Q_1$ is governed by the effective Hamiltonian

$$H_{\text{eff}} = \frac{G_F}{\sqrt{2}} V_{21} \cdot \bar{Q}_1(x) \gamma_\mu (1 - \gamma_5) Q_2 \cdot \bar{l}_1 \gamma_\mu (1 - \gamma_5) l_2, \quad (7.15)$$

where V_{21} is the corresponding matrix element of the Cabibbo-Kabayashi-Maskawa quark mixing matrix. In what follows we assume both leptons to be massless. We imply $Q_2 = b$ and $Q_1 = c$, and therefore use both notations throughout this section.

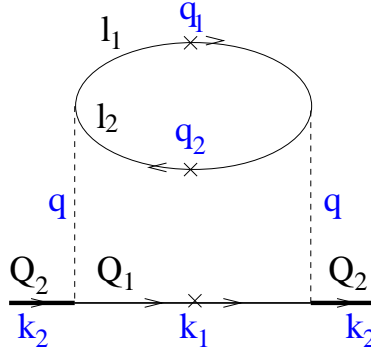


Fig. 32. The cut Feynman diagram corresponding to the free quark semileptonic decay $Q_2(k_2) \rightarrow Q_1(k_1) l_1(q_1) \bar{l}_2(q_2)$. Crossed lines mean that the corresponding particles are on the mass shell.

A tree-level decay rate of the free-quark semileptonic decay averaged over the polarizations of the initial quark Q_2 and summed over the polarizations of the final quark Q_1 is given the cut Feynman diagram of Fig. 32 and has the form

$$\begin{aligned} \Gamma_0(Q_2 \rightarrow Q_1 l_1 \bar{l}_2) &= \frac{G_F^2}{2} |V_{21}|^2 \frac{(2\pi)^4}{2m_2} \int \frac{dk_1 dq_1 dq_2}{(2\pi)^9} \delta(k_2 - k_1 - q_1 - q_2) \\ &\times \frac{1}{2} \text{Sp} \left(\gamma_\mu (1 - \gamma_5) (m_1 + \hat{k}_1) \gamma_\nu (1 - \gamma_5) (m_2 + \hat{k}_2) \right) \theta(k_1^0) \delta(k_1^2 - m_1^2) \\ &\times \text{Sp} (\gamma_\mu (1 - \gamma_5) \hat{q}_2 \gamma_\nu (1 - \gamma_5) \hat{q}_1) \theta(q_1^0) \delta(q_1^2) \theta(q_2^0) \delta(q_2^2) \end{aligned} \quad (7.16)$$

It is convenient to introduce additional integration by inserting the unity factor

$$\int dq \delta(q - q_1 - q_2) d\mu^2 \delta(q^2 - \mu^2) = 1 \quad (7.17)$$

in the integrand. Then we can rewrite the decay rate as follows

$$\Gamma_0(Q_2 \rightarrow Q_1 l_1 \bar{l}_2) = \frac{G_F^2 |V_{21}|^2 (2\pi)^4}{2} \frac{1}{2m_2} \int \frac{dk_1 dq}{(2\pi)^9} d\mu^2 \theta(q^0) \delta(q^2 - \mu^2) \theta(k_1^0) \delta(k_1^2 - m_1^2) \\ \times \delta(k_2 - k_1 - q) w_{\mu\nu}^0(k_1, k_2) l_{\mu\nu}(q). \quad (7.18)$$

Here we have introduced the following quantities:

The leptonic tensor $l_{\mu\nu}(q)$

$$l_{\mu\nu}(q) = \int dq_1 dq_2 \delta(q - q_1 - q_2) \theta(q_1^0) \delta(q_1^2) \theta(q_2^0) \delta(q_2^2) \text{Sp}(\gamma_\mu (1 - \gamma_5) \hat{q}_1 \gamma_\nu (1 - \gamma_5) \hat{q}_2) \\ = \frac{4\pi}{3} (q_\mu q_\nu - g_{\mu\nu} q^2). \quad (7.19)$$

The free-quark tensor

$$w_{\mu\nu}^0(k_1, k_2) = \frac{1}{2} \text{Sp}(\gamma_\mu (1 - \gamma_5) (m_1 + \hat{k}_1) \gamma_\nu (1 - \gamma_5) (m_2 + \hat{k}_2)) \\ = 4(k_{1\mu} k_{2\nu} + k_{2\mu} k_{1\nu} - g_{\mu\nu} k_1 k_2 + i\epsilon_{\mu\nu\alpha\beta} k_{2\alpha} k_{1\beta}). \quad (7.20)$$

We also denote

$$C_{SL}(m_2^2, m_1^2, q^2) = \frac{1}{2} w_{\mu\nu}^0(k_1, k_2) (q_\mu q_\nu - g_{\mu\nu} q^2) \\ = 2k_1 q \cdot 2k_2 q + q^2 \cdot 2k_1 k_2 \\ = (m_2^2 - m_1^2)^2 + q^2(m_2^2 + m_1^2) - 2q^4. \quad (7.21)$$

By virtue of these formulas we come to the representation

$$\Gamma_0(Q_2 \rightarrow Q_1 l_1 \bar{l}_2) = \frac{G_F^2 |V_{bc}|^2}{96\pi^3} \frac{1}{m_2^3} \int d\mu^2 \lambda^{1/2}(m_2^2, m_1^2, \mu^2) C_{SL}(m_2^2, m_1^2, \mu^2), \quad (7.22)$$

Switching to $m_b = m_2$ and $m_c = m_1$, the differential decay rate takes the familiar form

$$\frac{d\Gamma_0(b \rightarrow cl\nu)}{dq^2} = \frac{G_F^2 |V_{bc}|^2}{96\pi^3} \frac{1}{m_b^3} \lambda^{1/2}(m_b^2, m_c^2, q^2) C_{SL}(m_b^2, m_c^2, q^2). \quad (7.23)$$

The integrated semileptonic decay rate is then given by the expression

$$\Gamma_0(b \rightarrow cl\nu) = \int_0^{(m_b - m_c)^2} dq^2 \frac{d\Gamma_0}{dq^2} = \frac{G_F^2 |V_{bc}|^2}{192\pi^3} \cdot m_b^5 \cdot I_0(r) \quad (7.24)$$

with

$$I_0(r) = 1 - 8r + 8r^3 - r^4 - 12r^2 \ln(r), \quad r \equiv (m_c/m_b)^2. \quad (7.25)$$

The operator product expansion in QCD predicts the absence of the $1/m_b$ corrections to the ratio of the bound to free quark decay rates [4,5]. With the $1/m_b^2$ accuracy the integrated rate of the inclusive semileptonic $B \rightarrow X_c$ decay is given by the expression

$$\Gamma(B \rightarrow X_c l \nu) = \Gamma_0(b \rightarrow cl\nu) \cdot \left(1 + \frac{\lambda_1 + 3\lambda_2}{2m_b^2} - 6 \frac{\lambda_2}{m_b^2} \frac{(1-r)^4}{I_0(r)} \right). \quad (7.26)$$

In this expression λ_1 and λ_2 are the hadronic matrix elements of the operators of dimension 5 appearing in the OPE of the product of the two weak currents. The value $\lambda_2 = 0.12 \text{ GeV}^2$ is well known from the $B - B^*$ mass splitting, whereas the knowledge of λ_1 is loose and present estimates range from -0.6 GeV^2 to 0. Note that in the nonrelativistic quark potential model one has $\lambda_1 = -\langle \vec{k}^2 \rangle$, where \vec{k} is the relative momentum of the constituent $Q\bar{q}$ pair. Typically, the nonrelativistic quark model estimates of λ_1 range from -0.6 to -0.4 GeV^2 .

B. Inclusive meson decay in the dispersion approach

We now proceed to the inclusive rate for the decay of a pseudoscalar meson with mass M_1 containing a heavy quark Q_2 , which we refer to as P_{Q_2} , induced by the quark semileptonic transition $Q_2 \rightarrow Q_1 l_1 \bar{l}_2$.

As discussed above, within the quark model the dominant contribution to the inclusive decay rate of any process for $m_Q \rightarrow \infty$ is given by the box diagram of Fig. 31a. For semileptonic inclusive decay the corresponding diagram is shown in Fig. 33. We start with this diagram and discuss the relevant modifications due to the other terms presented in Fig. 31b,c later.

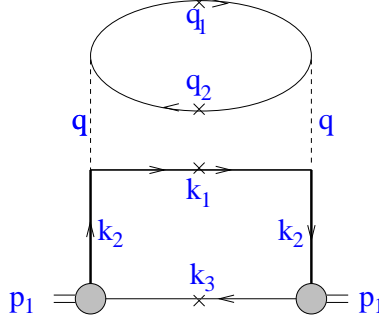


Fig. 33. The cut Feynman diagram corresponding to the decay $P_{Q_2} \rightarrow X_{Q_1} l_1(q_1) \bar{l}_2(q_2)$. Crossed lines mean that the corresponding particles are on the mass shell. We denote $p_2 = k_1 + k_3$. Our notations follow those of Chapter 3 where transition form factors have been considered.

Recall that the quark structure of the pseudoscalar meson transition into two real quarks is described by the vertex (3.33)

$$\frac{G(s_1)}{\sqrt{N_c}} \bar{Q}_2(k_2) i \gamma_5 q_3(k_3) \delta(\tilde{p}_1 - k_2 - k_3), \quad (7.27)$$

where $\tilde{p}_1^2 = s_1, k_2^2 = m_2^2, k_3^2 = m_3^2$.

Notice that the upper leptonic block of the diagram in Fig. 33 is exactly the same block $l_{\mu\nu}$ as for the free quark decay. The leptonic tensor $l_{\mu\nu}$ is given by Eq. (7.19).

Within the dispersion approach the differential decay rate reads ⁹

$$\begin{aligned} \frac{d\Gamma(P_{Q_2} \rightarrow X_{Q_1} l_1 \bar{l}_2)}{dq^2} &= \frac{G_F^2 |V_{21}|^2 (2\pi)^4}{2} \frac{1}{2M_1 (2\pi)^{12}} \\ &\times \int \frac{ds_1 G(s_1)}{s_1 - M_1^2} \frac{ds'_1 G(s'_1)}{s'_1 - M_1^2} \frac{\pi \lambda^{1/2}(s_1, s_2, q^2)}{2s_1} l_{\mu\nu}(q) \tilde{w}_{\mu\nu}(\tilde{p}_1, \tilde{p}_2, \kappa) |_{\kappa^2 \rightarrow 0}. \end{aligned} \quad (7.28)$$

The hadronic tensor $\tilde{w}_{\mu\nu}(\tilde{p}_1, \tilde{p}_2, \kappa)$ represents the full double spectral density of the Feynman box diagram $w_{\mu\nu}(p_1, p_2, \kappa)$ of Fig. 34 a. This quantity is constructed from the double discontinuity $\tilde{w}_{\mu\nu}^D(\tilde{p}_1, \tilde{p}_2, \kappa)$

$$\tilde{w}_{\mu\nu}^D(\tilde{p}_1, \tilde{p}_2, \kappa) = \text{disc}_{s_1} \text{disc}_{s'_1} w_{\mu\nu}(\tilde{p}_1, \tilde{p}_2, \kappa), \quad (7.29)$$

by applying the appropriate subtraction prescription. Fig. 34b shows the momenta in the integrand of Eq. (7.28). They satisfy the following relations

⁹This representation is appropriate for the calculation of the q^2 -distribution. A more detailed formula is necessary for the lepton energy spectrum. It will be considered later in this Chapter.

$$\begin{aligned}
\tilde{p}'_1 &= \tilde{p}_1 + \kappa, \\
\tilde{q}' &= \tilde{q} + \kappa, \\
\tilde{p}_2 &= \tilde{p}_1 - \tilde{q}, \\
\tilde{p}_1^2 &= s_1, \\
\tilde{p}_1'^2 &= s'_1, \\
\tilde{p}_2^2 &= s_2, \\
\tilde{q}^2 &= \tilde{q}'^2 = q^2,
\end{aligned} \tag{7.30}$$

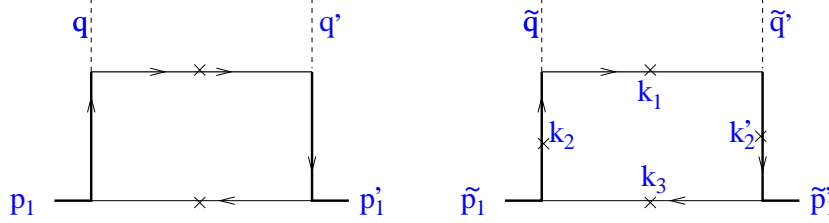


Fig. 34. a: The box diagram for $w_{\mu\nu}(p_1, p_2, q - q')$; b: its double discontinuity in the variables $s_1 = \tilde{p}_1^2$ and $s'_1 = \tilde{p}_1'^2$, $\tilde{w}_{\mu\nu}(\tilde{p}_1, \tilde{p}_2, \kappa = \tilde{q} - \tilde{q}')$. Crossed lines correspond to particles on the mass shell.

1. The spacelike region

The double discontinuity of the box diagram can be calculated in the region $q^2 \leq 0$ and $q'^2 \leq 0$ by placing all intermediate particles in the loop on their mass shell as shown in Fig. 34b. To obtain the corresponding expression for positive values $q^2 = q'^2 > 0$ corresponding to the real decay kinematics we shall perform the analytical continuation in q^2 .

At $q^2, q'^2 \leq 0$ the explicit expression for $\tilde{w}_{\mu\nu}^D$ reads

$$\begin{aligned}
\tilde{w}_{\mu\nu}^D(\tilde{p}_1, \tilde{p}_2, \kappa) &= \int dk_1 dk_2 dk'_2 dk_3 \delta(k_1^2 - m_1^2) \delta(k_2^2 - m_2^2) \delta(k_2'^2 - m_2^2) \delta(k_3^2 - m_3^2) \\
&\quad \times \delta(\tilde{p}_1 - k_2 - k_3) \delta(\tilde{p}_1' - k'_2 - k_3) \delta(\tilde{p}_2 - k_1 - k_3) \\
&\quad \times (-1) \text{Sp} \left(i\gamma_5 (m_3 - \hat{k}_3) i\gamma_5 (m_2 + \hat{k}_2') \gamma_\mu (1 - \gamma_5) (m_1 + \hat{k}_1) \gamma_\nu (1 - \gamma_5) (m_2 + \hat{k}_2) \right).
\end{aligned} \tag{7.31}$$

The function $\tilde{w}_{\mu\nu}(\tilde{p}_1, \tilde{p}_2, \kappa)$ contains several Lorentz structures multiplied by the invariant amplitudes. The latter depend on the six independent scalar variables

$$s_1, s'_1, s_2, q^2, q'^2, \kappa^2. \tag{7.32}$$

We are interested in the case $q^2 = q'^2$ and $\kappa^2 \rightarrow 0$.

Let us consider the trace in the integrand of $\tilde{w}_{\mu\nu}^D$. Hereafter we neglect terms proportional to κ . Since all particles are on the mass shell, we find

$$-(m_2 + \hat{k}_2) i\gamma_5 (m_3 - \hat{k}_3) i\gamma_5 (m_2 + \hat{k}_2) = (2k_2 k_3 + 2m_2 m_3)(m_2 + \hat{k}_2). \tag{7.33}$$

Therefore,

$$\begin{aligned}
&-\text{Sp} \left(i\gamma_5 (m_3 - \hat{k}_3) i\gamma_5 (m_2 + \hat{k}_2) \gamma_\mu (1 - \gamma_5) (m_1 + \hat{k}_1) \gamma_\nu (1 - \gamma_5) (m_2 + \hat{k}_2) \right) \\
&= 2(s_1 - (m_2 - m_3)^2) w_{\mu\nu}^0(k_1, k_2).
\end{aligned} \tag{7.34}$$

From the free quark decay we know that

$$w_{\mu\nu}^0(k_1, k_2) l_{\mu\nu}(q) = \frac{8\pi}{3} C_{SL}(m_2^2, m_1^2, q^2). \tag{7.35}$$

Clearly, the contribution of the traces in the spectral representation for $d\Gamma/dq^2$ turns out to be independent of the internal integration variables. Therefore, we only have to consider the scalar part of $\tilde{w}_{\mu\nu}^D$ defined according to the relation

$$\begin{aligned} \tilde{A}_D(s_1, s'_1, p_2^2, q^2, q'^2, \kappa^2) &= \int dk_1 dk_2 dk'_2 dk_3 \delta(k_1^2 - m_1^2) \delta(k_2^2 - m_2^2) \delta(k_2'^2 - m_2^2) \delta(k_3^2 - m_3^2) \\ &\times \delta(\tilde{p}_1 - k_2 - k_3) \delta(\tilde{p}'_1 - k'_2 - k_3) \delta(\tilde{p}_2 - k_1 - k_3). \end{aligned} \quad (7.36)$$

Explicit calculations give for \tilde{A}_D the following expression

$$\bar{A}_D(s_1, s_2, q^2) = \frac{\pi\theta(\dots)}{2\lambda^{1/2}(m_1^2, m_2^2, q^2)}. \quad (7.37)$$

Notice that the argument of the θ function in eq (7.37) is just the same as for the spectral density of the triangle graph for the form factor given by Eq. (2.79).

Eq. (7.36) provides the double discontinuity but, as usual, we need to define in addition a subtraction prescription. The form of this prescription cannot be determined within the dispersion approach and should be fixed from some other arguments. We shall determine the subtraction prescription by matching to the known QCD result and requiring the absence of the $1/m_Q$ corrections in the ratio of the bound and free quark decay rates. As we have discussed, in the quark model the absence of the $1/m_Q$ corrections is provided by the other diagrams shown in Fig. 31b,c which cancel the $1/m_Q$ term in the box diagram. Therefore requiring the absence of the $1/m_Q$ corrections corresponds to an effective account for these terms.

Our subtraction prescription explicitly reads

$$\tilde{A}(s_1, s_2, q^2) = \frac{M_1}{\sqrt{s_1}} \tilde{A}_D(s_1, s_2, q^2). \quad (7.38)$$

As we shall demonstrate in the next section, this prescription indeed provides the required absence of the $1/m_Q$ corrections in agreement with the OPE.

For the analysis of the limit $m_Q \rightarrow \infty$ it is convenient to have the 'external' integration over s_1 and the 'internal' integration over s_2 in the spectral representation for the decay rate. The solution of the θ function then takes the form

$$\begin{aligned} (m_2 + m_3)^2 &< s_1 < \infty \\ s_2^-(s_1, q^2) &< s_2 < s_2^+(s_1, q^2) \end{aligned}$$

where the limits s_2^\pm are obtained by setting $\eta = \pm 1$ in the relation

$$\begin{aligned} s_2(s_1, q^2) &= (m_1 + m_3)^2 + \frac{m_1}{m_2} (s_1 - (m_2 + m_3)^2) + \frac{m_1}{m_2} (\omega - 1)(s_1 - m_2^2 - m_3^2) \\ &+ \eta \frac{m_1}{m_2} \lambda^{1/2}(s_1, m_2^2, m_3^2) \sqrt{\omega^2 - 1}. \end{aligned} \quad (7.39)$$

The quark recoil ω is defined according to the relation

$$q^2 = (m_2 - m_1)^2 - 2m_1 m_2 (\omega - 1). \quad (7.40)$$

Isolating the free-quark decay amplitude we come to the following dispersion representation for the differential inclusive semileptonic decay rate at $q^2 \leq 0$

$$\frac{d\Gamma}{dq^2} = K_0(q^2) \int ds_1 \varphi^2(s) \frac{s_1 - (m_2 - m_3)^2}{8\pi^2 s_1} \frac{m_2^3}{\sqrt{s_1}} \int_{s_2^-(s_1, q^2)}^{s_2^+(s_1, q^2)} ds_2 \frac{\lambda^{1/2}(s_1, s_2, q^2)}{\lambda^{1/2}(m_1^2, m_2^2, q^2)}, \quad (7.41)$$

where

$$K_0(q^2) \equiv \frac{1}{\lambda^{1/2}(m_2^2, m_1^2, q^2)} \frac{d\Gamma_0}{dq^2}. \quad (7.42)$$

Note that in Eq. (7.41) the free-quark differential rate $d\Gamma_0/dq^2$ factorizes out, so that the differential rate for a bound quark is a product of the free-quark differential rate and a bound state factor, as already noted in [145]. As in the

previous chapters, we use the notation $\varphi(s) = G(s)/(s - M_1^2)$; the normalization condition for $\varphi(s)$ is given by Eq. (3.62).

It is convenient to rearrange Eq. (7.41) by isolating under the integral the structure similar to the structure of the normalization condition (3.62)

$$\begin{aligned} \frac{d\Gamma}{dq^2} &= \frac{d\Gamma_0}{dq^2} \int ds_1 \varphi^2(s_1) [s_1 - (m_2 - m_3)^2] \frac{\lambda^{1/2}(s_1, m_2^2, m_3^2)}{8\pi^2 s_1} r(s_1, q^2), \\ r(s_1, q^2) &= \int_{-1}^1 \frac{d\eta}{2} \frac{\lambda^{1/2}(s_1, s_2, q^2)}{\lambda^{1/2}(m_2^2, m_1^2, q^2)}, \end{aligned} \quad (7.43)$$

and s_2 is related to η by Eq. (7.39). As we shall see later,

$$r(s_1, q^2) \sim 1 \quad (7.44)$$

in the heavy-quark limit, such that thanks to the normalization condition of the soft wave function Eq. (3.62) one gets

$$\frac{d\Gamma}{dq^2} \rightarrow \frac{d\Gamma_0}{dq^2} \quad (7.45)$$

as $m_Q \rightarrow \infty$.

2. The timelike region and the anomalous contribution

To obtain the spectral representation at $q^2 > 0$ we perform the analytical continuation in q^2 . This procedure is done along the same lines as in the case of the transition form factor which has been discussed in detail in Chapter II. As a result of this procedure in addition to the normal part which is just the expression (7.43) taken at $q^2 > 0$, the anomalous part emerges due to the non-Landau type singularities of the Feynman graph. The location of the singularities in the complex s_1 and s_2 planes corresponding to the situation of the 'external' s_1 integration is shown in Fig. 35.

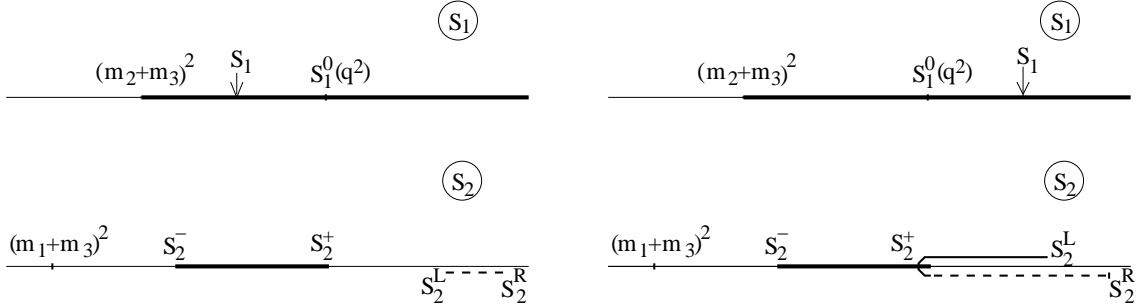


Fig. 35. The integration region for $m_2 > m_1$ and $q^2 > 0$ for the order of integration $\int ds_1 \int ds_2$: a. $s_1 < s_1^0$, b. $s_1 > s_1^0$. Solid lines - cuts on the physical sheet, dashed lines - cuts on the second sheet.

The definition of s_2^\pm is given by Eq. (7.39) and

$$\begin{aligned} s_2^R(s_1, q^2) &= (\sqrt{s_1} + \sqrt{q^2})^2, \\ s_2^L(s_1, q^2) &= (\sqrt{s_1} - \sqrt{q^2})^2, \\ \sqrt{s_1^0(q^2)} &= \frac{q^2 + m_2^2 - m_1^2}{2\sqrt{q^2}} + \sqrt{\left(\frac{q^2 + m_2^2 - m_1^2}{2\sqrt{q^2}}\right)^2 + m_3^2 - m_2^2}. \end{aligned} \quad (7.46)$$

As one can see, the anomalous cut appears on the physical s_2 sheet between $s_2^+(s_1, q^2)$ and $s_2^L(s_1, q^2)$ in the region $q^2 \leq (m_2 - m_1)^2$ for the values $s_1 > s_1^0(q^2)$.

Respectively, the spectral density $r(s_1, q^2)$ acquires the anomalous piece and takes at $q^2 > 0$ the following form

$$r(s_1, q^2) = \frac{m_2}{\sqrt{s_1}} \frac{m_2^2}{\lambda^{1/2}(s_1, m_2^2, m_3^2) \lambda(m_2^2, m_1^2, q^2)} \times \left[\int_{s_2^-(s_1, q^2)}^{s_2^+(s_1, q^2)} ds_2 \lambda^{1/2}(s_1, s_2, q^2) + 2\theta(q^2) \theta(s_1 > s_1^0) \int_{s_2^+(s_1, q^2)}^{s_2^L(s_1, q^2)} ds_2 \lambda^{1/2}(s_1, s_2, q^2) \right]. \quad (7.47)$$

The q^2 -behavior of the anomalous term is determined by the lower limit of the s_1 integration, $s_1^0(q^2)$. Namely, its contribution to the semileptonic rate reads

$$\frac{1}{\Gamma} \frac{d\Gamma^{anom}}{d\omega} \simeq \frac{\Lambda^3}{m_Q^3 \sqrt{\omega - 1}} R^{anom}(\omega), \quad (7.48)$$

where

$$R^{anom}(\omega) = \int_{m_Q \sqrt{\omega - 1}}^{\infty} dk k^2 w^2(k). \quad (7.49)$$

Here $k = \lambda^{1/2}(s_1, m_2^2, m_3^2)/2\sqrt{s_1}$ is the relative momentum of the quarks inside the B -meson. The wave function $w(k)$ is normalized according to the relation (2.94) leading to

$$R^{anom}(1) = 1. \quad (7.50)$$

Since the soft wave function is steeply falling beyond the confinement region where $\vec{k}^2 \lesssim \Lambda^2$, the anomalous contribution becomes inessential already at $\omega - 1 \simeq \Lambda/m_b$. Only in the endpoint region $\omega - 1 \lesssim \frac{\Lambda^2}{m_Q^2}$ the anomalous contribution to the differential distribution becomes strong and diverges like

$$\frac{1}{\Gamma} \frac{d\Gamma^{anom}}{d\omega} \simeq \frac{\Lambda^3}{m_Q^3} \frac{1}{\sqrt{\omega - 1}}. \quad (7.51)$$

The contribution of the anomalous term to the integrated semileptonic rate of the order

$$\Gamma^{anom}/\Gamma \simeq \Lambda^2/m_Q^2 \quad (7.52)$$

comes from the endpoint region, whereas the rest of the decay phase space provides only the relative Λ^3/m_Q^3 anomalous contribution to the semileptonic decay rate.

Therefore, the anomalous contribution is negligible at all ω except for the endpoint region $\omega - 1 \lesssim \frac{\Lambda^2}{m_Q^2}$, which is in fact a very narrow region near zero recoil. As we have discussed, the HQ expansion for the differential distributions is anyway ill-defined in this kinematical region. Contributions of the same order of magnitude come also from other terms in the expansion (7.12), and keeping this anomalous contribution is beyond the accuracy of our considerations. Thus we shall systematically omit the anomalous contribution in numerical calculations.

C. The $1/m_Q$ expansion of the semileptonic decay rate and $d\Gamma/dq^2$

In this section we perform the $1/m_Q$ expansion of the meson inclusive decay rate. We show that:

- a. in the leading $1/m_Q$ order the heavy meson inclusive decay rate is equal to the free quark decay rate;
- b. our subtraction prescription (7.38) leads to the differential distribution $d\Gamma/dq^2$ given by eq (7.43) which satisfies the relation

$$\frac{d\Gamma(B \rightarrow X_c \ell \bar{\nu}_\ell)/dq^2}{d\Gamma_0(b \rightarrow c \ell \bar{\nu}_\ell)/dq^2} = 1 + O(1/m_Q^2) \quad (7.53)$$

in most of the q^2 region except for a close vicinity of zero recoil point. This property guarantees the absence of the $1/m_Q$ corrections in the ratio of the integrated rates, i.e.

$$\frac{\Gamma(B \rightarrow X_c \ell \bar{\nu}_\ell)}{\Gamma_0(b \rightarrow c \ell \bar{\nu}_\ell)} = 1 + O(1/m_Q^2); \quad (7.54)$$

- c. the size of the $1/m_Q^2$ corrections can be tuned such that they become numerically close to the OPE prediction. This is done by introducing the cut in the spectral representation of the decay rate of the B meson. This cut affects only the differential distribution $d\Gamma(B \rightarrow X_c \ell \bar{\nu}_\ell)/dq^2$ at large q^2 near zero recoil, i.e. in the region $\omega \leq 1 + O(1/m_Q)$.

An important feature of the whole approach is that already the zero order expression provides a realistic M_X -distribution. As we shall see later, the modifications b) and c) while affecting the total rate and the q^2 -distributions at large q^2 , only moderately affect the M_X -distribution, so that the latter is completely determined by the soft B -meson wave function.

Let us consider the $1/m_Q$ expansion of the spectral density r_D . The normal part of $r_D(s_1, q^2)$ has a simple form

$$r_D(s_1, q^2) = \frac{m_2}{M_1} \int_{-1}^1 \frac{d\eta}{2} \frac{\lambda^{1/2}(s_1, s_2, q^2)}{\lambda^{1/2}(m_2^2, m_1^2, q^2)}. \quad (7.55)$$

This representation is a convenient starting point for performing the $1/m_Q$ expansion. Let us point out that although the integration in η can be easily performed, it is more convenient to work out the HQ expansion before the integration.

Assuming that m_2 is large and that the meson wave function is localized in the region $z_1 \simeq \Lambda$ we obtain the following expression for $\lambda(s_1, s_2, q^2)$ valid at all q^2

$$\begin{aligned} \lambda(s_1, s_2, q^2) &\rightarrow m_2^4 \left(1 + \frac{z_1 + m_3}{m_2}\right)^2 \\ &\times \left[\lambda(1, \hat{q}^2, \hat{r}^2) + \frac{2\eta}{m_2} \chi(z_1) \sqrt{z_1(z_1 + 2m_3)} (1 + \hat{q}^2 - \hat{r}^2) \lambda^{1/2}(1, \hat{q}^2, \hat{r}^2) \right. \\ &\left. + \frac{z_1(z_1 + 2m_3)}{m_2^2} (1 + \hat{q}^2 - \hat{r}^2)^2 + \frac{\eta^2}{m_2^2} z_1(z_1 + 2m_3) \lambda(1, \hat{q}^2, \hat{r}^2) \right] \end{aligned} \quad (7.56)$$

where $\hat{q}^2 = q^2/m_b^2$, $\hat{r} = m_1/m_2$ and $\chi(z_1) = 1 - (z_1 + m_3)/2m_2$. In the limit $m_2 \rightarrow \infty$ we can expand the $\lambda(s_1, s_2, q^2)$ in powers of $1/m_2$. Notice however that an actual expansion parameter is not $1/m_2$ but rather

$$\frac{\sqrt{z_1(z_1 + 2m_3)}}{m_2 \lambda^{1/2}(1, \hat{q}^2, \hat{r}^2)}, \quad (7.57)$$

and the averaging over the B meson state implies $\sqrt{z_1(z_1 + 2m_3)} \simeq \Lambda$. Hence the region where the expansion is fastly converging is

$$m_2 \lambda^{1/2}(1, \hat{q}^2, \hat{r}^2) \gg \Lambda. \quad (7.58)$$

This relation can be written as

$$|\vec{k}_1| = \lambda^{1/2}(m_2^2, m_1^2, q^2)/2m_2 \gg \Lambda, \quad (7.59)$$

which means that in the rest frame of the b quark the daughter quark has a 3-momentum much bigger than Λ .

The final expression reads

$$r_D(s_1, q^2) \rightarrow \frac{m_2}{M_1} \left(1 + \frac{z_1 + m_3}{m_2} \right) \left[1 + \frac{z_1(z_1 + 2m_3)}{2m_2^2} \left(1 + \frac{8\hat{q}^2}{3\lambda(1, \hat{q}^2, \hat{r}^2)} \right) \right]. \quad (7.60)$$

The $1/m_Q$ term in the ratio of the bound to free quark distributions is generated by the $(m_2 + z_1 + m_3)/M_1$ term in r_D .

As we have discussed this linear $1/m_Q$ term contained in the box diagram cancels against the $1/m_Q$ terms coming from other terms in the expansion (7.12). Thus the main contribution of these terms can be taken into account by performing the subtraction in the spectral representation for the box diagram which kills the $1/m_Q$ term. This is implemented by defining the subtraction prescription as follows:

$$r(s_1, q^2) = \frac{M_1}{\sqrt{s_1}} r_D(s_1, q^2). \quad (7.61)$$

After performing the subtraction and taking into account that in the heavy quark limit $z(z + 2m_3) = \vec{k}^2$ we come to the following relation

$$R(q^2) \equiv \frac{d\Gamma(B \rightarrow X_c \ell \bar{\nu}_\ell)/dq^2}{d\Gamma_0(b \rightarrow c \ell \bar{\nu}_\ell)/dq^2} \rightarrow 1 + \frac{\langle \vec{k}^2 \rangle}{2m_2^2} \left(1 + \frac{8\hat{q}^2}{3\lambda(1, \hat{q}^2, \hat{r}^2)} \right). \quad (7.62)$$

This expansion is valid in the region of q^2 such that $\lambda(1, \hat{q}^2, \hat{r}^2) = O(1)$, i.e. in most of the q^2 phase space except for the region near zero recoil where $\lambda(1, \hat{q}^2, \hat{r}^2) \simeq 0$.

The expression (7.62) has the following features:

1. In the leading $1/m_Q$ order the ratio $R(q^2)$ is equal to one. Thus the decay rate of the free and the bound quark coincide in the heavy quark limit for all q^2 . Beyond the leading order, the differential distribution coincide also within the $1/m_Q$ accuracy in most of the q^2 phase space, except for the region near zero recoil. This guarantees the absence of the $1/m_Q$ corrections in the ratio of the integrated rates as well. Thus, our description is in full agreement with the OPE results within the $1/m_Q$ order;
2. Since the box diagram represents only a part of the $1/m_Q^2$ corrections, we cannot expect the box diagram alone to reproduced correctly the $1/m_Q^2$ term in the ratio of the integrated rates Γ/Γ_0 . In fact, the sign of the $1/m_Q^2$ correction in eq. (7.62) turns out to be opposite to the OPE result (cf., e.g., with the results of refs. [138,137] at $q^2 = 0$). Moreover, the $1/m_Q^2$ term generated by the box diagram is expressed merely in terms of $\langle B|\vec{k}^2|B \rangle$, whereas the $1/m_Q^2$ corrections of the OPE series include also $\langle B|\hat{V}_1|B \rangle$, where \hat{V}_1 is the $1/m_Q$ term appearing in the expansion (7.9) of the effective potential (e.g., the chromomagnetic operator in QCD).

We argue however that it is possible to further modify the spectral representation of the box diagram to bring the size of the $1/m_Q^2$ term developed by this modified representation in agreement with the OPE result. This procedure corresponds to phenomenologically taking into account the contribution of other $1/m_Q^2$ terms of the expansion (7.12).

Omitting the anomalous contribution for the reasons explained above, the differential decay rate takes the form

$$\frac{d\Gamma}{dq^2} = K_0(q^2) \int_{(m_1+m_3)^2}^{\infty} ds_1 \varphi^2(s_1) \frac{s_1 - (m_2 - m_3)^2}{8\pi^2 s_1} \lambda^{1/2}(s_1, m_2^2, m_3^2) \frac{m_2}{\sqrt{s_1}} \int_{-1}^1 \frac{d\eta}{2} \lambda^{1/2}(s_1, s_2, q^2). \quad (7.63)$$

where s_2 depends on η through Eq. (7.39).

Now, our goal is to modify the differential distribution of Eq. (7.63) in such a way that the leading order result and the $1/m_Q$ correction in the integrated rate remain intact whereas the $1/m_Q^2$ term numerically reproduces the OPE-based estimate.

Obviously, we may allow a strong deformation of the differential q^2 -distribution at large q^2 near zero recoil, where the heavy-quark expansion is anyway ill-defined; we may also require $d\Gamma/dq^2(q^2 = 0)$ to exactly reproduce the OPE result within the $1/m_Q^2$ accuracy.

Most easily this program may be implemented through the following two steps:

First, by introducing the factor $F(s_1) = 1/(1 + \vec{k}^2/m_Q^2)$ which sets the $1/m_Q^2$ term in the *differential* rate at $q^2 = 0$;

Second, by cutting the s_2 -integration in (7.63) at some upper limit $s_2^{max}(q^2)$ which tunes the size of the $1/m_Q^2$ effects in the *integrated* rate.

The resulting differential q^2 differential distribution takes the form

$$\begin{aligned} \frac{d\Gamma}{dq^2} = & K_0(q^2) \int_{(m_1+m_3)^2}^{\infty} ds_1 \varphi^2(s_1) \frac{s_1 - (m_2 - m_3)^2}{8\pi^2 s_1} \lambda^{1/2}(s_1, m_2^2, m_3^2) \\ & \times \frac{m_2}{\sqrt{s_1}} F(s_1) \int_{-1}^1 \frac{d\eta}{2} \lambda^{1/2}(s_1, s_2, q^2) \theta(s_2 < s_2^{max}(q^2)). \end{aligned} \quad (7.64)$$

In order not to affect the integrated rate in the leading and the subleading $1/m_Q$ orders, the function $s_2^{max}(q^2)$ should satisfy certain properties. Let us look at them more closely.

Recall, that the soft wave function $\varphi(s_1)$ is localized in the region

$$s_1 \leq s_1^{max} \simeq (m_2 + m_3 + \gamma)^2$$

where γ is a constant of order Λ which does not scale with m_Q . Let us determine q_0^2 through the equation

$$s_2^+(s_1^{max}, q_0^2) = s_2^{max}(q_0^2) \quad (7.65)$$

where s_2^+ is the maximal value of s_2 corresponding to $\eta = 1$ in (7.39). Furthermore, assume that $s_2^{max}(q^2)$ decreases with q^2 , and take into account that $s_2^+(s_1, q^2)$ is a monotonous rising function of both s_1 and q^2 . Then, at $q^2 < q_0^2$ for all $s_1 < s_1^{max}$ one finds the relation $s_2^+(s_1, q^2) < s_2^{max}(q^2)$, and thus the q^2 -distribution does not feel the presence of the cut at all. For $q^2 > q_0^2$ the cut becomes really effective and strongly influences the q^2 -distribution. In order these changes in the cut q^2 -differential distribution not to change the integrated rate in the LO and $1/m_Q$ order, we need the q_0^2 to be not far from zero recoil such that the corresponding $\omega_0 = 1 + O(1/m_Q)$. Choosing the cut in the form

$$\sqrt{s_2^{max}(q^2)} = m_1 + m_3 + a \left(m_2 - m_1 - \epsilon - \sqrt{q^2} \right), \quad (7.66)$$

where $\epsilon \simeq \Lambda$ and a is a rising function of m_Q , satisfies these requirements.

The parameter ϵ accounts for a mismatch between the quark and the hadron threshold, and the form of $a(m_Q)$ can be found from fitting the size of the $1/m_Q^2$ corrections in the integrated rate to the OPE prediction. Notice also that the q^2 distributions obtained through the cut expression are even more realistic than those obtained from the uncut spectral representations.

We could of course choose a more sophisticated parameterization of $s_2^{max}(q^2)$ to reproduce a correct q^2 -behaviour of $d\Gamma/dq^2$ near zero recoil point. For instance, taking into account that the lightest final meson is pseudoscalar, we can write $\sqrt{s_2^{max}(q^2)} = m_1 + m_3 + a_P(m_Q)(M_{P_Q} - M_{P_{Q'}} - \sqrt{q^2})^{3/2}$ yielding the correct behavior near $\sqrt{q^2} = M_{P_Q} - M_{P_{Q'}}$, where only one P -wave decay channel $P_Q \rightarrow P_{Q'} \ell \bar{\nu}_\ell$ is opened. In addition, in the heavy quark limit the S -wave transition $P_Q \rightarrow V_{Q'} \ell \bar{\nu}_\ell$ requiring another functional dependence $\sqrt{s_2^{max}(q^2)} = m_1 + m_3 + a_V(m_Q)(M_{P_Q} - M_{P_{Q'}} - \sqrt{q^2})^{1/2}$ is opened at $\sqrt{q^2} = M_{P_Q} - M_{V_{Q'}}$ with only small delay in q^2 of order Λ^2 . So the effects of opening this channel are even more important and should be also taken into account. However in the region of large q^2 with few opened channels the inclusive consideration is anyway not working properly, and taking into account such subtle effects is beyond the accuracy of the method. So in numerical calculations we proceed with the phenomenological cut provided by eq (7.66).

The parameters of the model, such as the quark masses and the wave functions were already fixed in Chapter III and we now use them for inclusive decays.

We choose the parameters of the cut according to the criteria above in the following form

$$\begin{aligned} \epsilon &= (m_Q - m_{Q'}) - (M_Q - M_{Q'}) \\ a &= 1.82 + 0.029 m_Q, \end{aligned}$$

where $m_{Q'}$ is the mass of the parent heavy quark and $M_{Q'}$ is the final meson lowest mass. Effectively, this means that $q_{max}^2 = (M_Q - M_{Q'})^2$.

A remark is in order here: To compare the calculated integrated rate Γ as a function of m_Q with the OPE result within the $1/m_Q^2$ order, it is reasonable to adopt the expansions of the hadron masses M_Q and $M_{Q'}$ also up to the second order in $1/m_Q$. Then one finds $\epsilon = -\frac{1}{2}(\lambda_1 + 3\lambda_2) \cdot (1/m_{Q'} - 1/m_Q)$. Setting $\lambda_1 = -0.44 \text{ GeV}^2$ and $\lambda_2 = 0.12 \text{ GeV}^2$, yields $\epsilon = 0.10/m_Q$ at $m_{Q'}/m_Q = m_c/m_b \simeq 0.28$. We point out that in calculations for the real B decays we use experimental values of hadronic masses (involving all orders in $1/m_Q$).

The corresponding integrated semileptonic decay rate Γ is plotted in Fig. 36 as a function of $1/m_Q$ and compared with the OPE predictions (7.26).

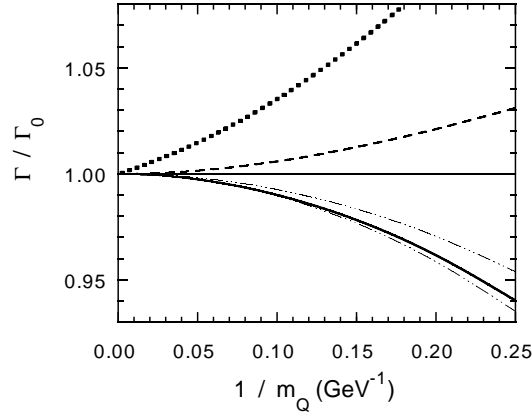


Fig. 36. The ratio of the integrated rates of the bound-to-free quark semileptonic decay $Q \rightarrow Q' \ell \bar{\nu}_\ell$ vs the inverse heavy-quark mass $1/m_Q$ at fixed value of $m_{Q'}/m_Q = m_c/m_b = 0.28$. Dotted line - the rate calculated from the initial spectral representation of the box diagram which contains $1/m_Q$ correction, dashed - with the proper subtraction killing the $1/m_Q$ term but without tuning the size of the $1/m_Q^2$ effects. Solid - final result which also includes the cut bringing the size of the $1/m_Q^2$ effects in agreement with the OPE prediction. Upper and lower dot-dashed lines are the OPE results (7.26) corresponding to $\lambda_1 = 0$ and $\lambda_1 = -0.6 \text{ GeV}^2$ (with $\lambda_2 = 0.12 \text{ GeV}^2$), respectively.

One can clearly see that the calculations based on both the spectral density r_D of Eq. (7.55) and the spectral density r of Eq. (7.61) which includes a subtraction predict a larger rate for a bound heavy quark compared to the free one, that contradicts OPE.

The introduction of the cut $s_2^{max}(q^2)$ (7.66) brings our dispersion approach results in perfect agreement with the standard OPE framework for the whole range of the considered values of m_Q .

Figure 37 shows the influence of the cut upon the q^2 -distribution for the $B \rightarrow X_c \ell \bar{\nu}_\ell$ decay.

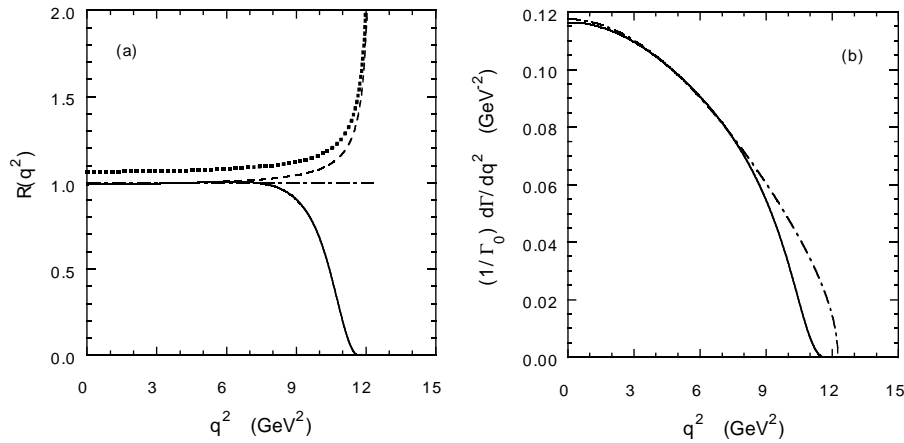


Fig. 37. Distribution $d\Gamma/dq^2$ in $B \rightarrow X_c \ell \bar{\nu}_\ell$ decays vs the squared four-momentum transfer q^2 : (a) ratio of the bound-to-free quark decay $R(q^2) \equiv (d\Gamma/dq^2)/(d\Gamma_0/dq^2)$, notation of lines same as in Fig. 36. (b) Differential distribution in the bound (solid) and free (dot-dashed) semileptonic quark decay. Parameters of the cut (7.66) are $a = 1.96$ and $\epsilon = 0.091 \text{ GeV}$.

As already discussed, the introduction of the q^2 -dependent cut in the spectral representation does not change the differential q^2 distributions at small q^2 but it strongly affects the region of large q^2 . In particular, the cut provides the vanishing of $d\Gamma/dq^2$ at the physical threshold $q^2 = (M_B - M_D)^2 = 11.6 \text{ GeV}^2$. Let us point out again that this

cutting procedure does not affect the *integrated* rate at the leading and subleading $1/m_Q$ orders. Note also that the differential distributions $d\Gamma/dq^2$ given by the dashed and solid lines in Fig 37(a), are equal to each other at $q^2 = 0$ and match the OPE result for $d\Gamma/dq^2(q^2 = 0)$.

As we shall see later, the improvements on the q^2 -differential distributions by approximate account of higher order graphs affect only moderately the M_X -distribution in $B \rightarrow X_c \ell \bar{\nu}_\ell$ (as well as the photon lineshape in the rare $B \rightarrow X_s \gamma$ decay). The latter are thus determined by the B -meson wave function.

This property allows us to obtain a realistic energy distribution and other observables through the soft wave function of the heavy meson. Thus we do not need to introduce any unknown 'smearing function' describing the motion of the b quark inside the B meson, but rather directly calculate the effects of the b quark motion with the soft meson wave function.

D. $d\Gamma/dM_X$

We now proceed to the calculation of the M_X -distribution.

Recall that in the free-quark decay, which is the leading-order process within the OPE framework, one finds the M_X distribution in the form $\delta(M_X - m_c)$ (neglecting the radiative corrections). Inclusion of the $1/m_Q$ corrections yields a singular series containing derivatives of the δ function. For the interpretation of these results one needs an introduction of a smearing function. In the quark model the M_X -spectrum is obtained already smeared because of the Fermi-motion of the b quark in the B meson. Therefore the shape of the M_X -spectrum is calculable through the B meson wave function determined in the Chapter II.

Let us calculate $d\Gamma/dM_X$ from our spectral representation for the decay rate. To this end it is necessary to change the order of integration in Eq. (7.43) as follows ($M_X^2 = s_2$ in our notations)

$$\frac{d\Gamma}{dq^2} = K_0(q^2) \int_{(m_1+m_3)^2}^{s_2^{max}(q^2)} ds_2 \int_{s_1^-(s_2, q^2)}^{s_1^+(s_2, q^2)} ds_1 \varphi^2(s_1) \frac{s_1 - (m_2 - m_3)^2}{8\pi^2} \left(\frac{m_2}{\sqrt{s_1}} \right)^3 \frac{\lambda^{1/2}(s_1, s_2, q^2)}{\lambda^{1/2}(m_2^2, m_1^2, q^2)}$$

This representation immediately gives $d^2\Gamma/dq^2 dM_X^2$. Integrating the latter over q^2 one obtains $d\Gamma/dM_X^2$. The calculated distribution is reported in Fig.38. Our result should be compared with the leading order OPE result $\delta(m_X - m_c)$. One can see that already the box diagram of the quark model provides a smooth and reasonable distribution (beyond the resonance region), which is only moderately affected by a proper account of the subleading $1/m_Q$ effects. Most important is that *at large M_X the calculated distribution does not require any additional smearing and can be directly compared with the experimental results.*

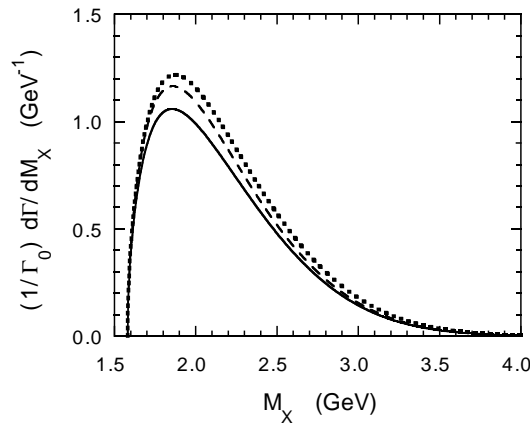


Fig. 38. Distribution $d\Gamma/dM_X$ in $B \rightarrow X_c \ell \bar{\nu}_\ell$ decays vs the invariant mass of the produced hadronic system M_X . Lines same as in Fig. 36.

E. The electron energy spectrum

In distinction to the Lorentz-invariant distributions $d\Gamma/dq^2$ and $d\Gamma/dM_X$ considered above, the lepton energy spectrum should be referred to a specific reference frame.

The starting point of the electron energy spectrum calculation is the double spectral representation (7.28) for the inclusive semileptonic decay rate. We define the variable E to be the energy of the lepton l_1 in the reference frame specified by the condition

$$\tilde{p}_1 = (\sqrt{s_1}, 0). \quad (7.67)$$

This is the rest frame of the $Q_2\bar{q}_3$ quark pair with the invariant mass $\sqrt{s_1}$.

As the first step, let us consider the hadronic tensor $\tilde{w}_{\mu\nu}^D$ given by Eq. (7.31). Using the expression (7.34) for the trace and performing the integration over $dk_1 dk_2$ leads to the following result

$$\tilde{w}_{\mu\nu}(\tilde{p}_1, \tilde{q}) = \frac{\pi\theta(\dots)(s_1 - (m_2 - m_3)^2)}{\lambda^{1/2}(m_2^2, m_1^2, q^2)} w_{\mu\nu}(\tilde{p}_1, \tilde{q}) \quad (7.68)$$

where $w_{\mu\nu}$ is represented in terms of the 'dispersion momenta' \tilde{p}_1 and $\tilde{q} = \tilde{p}_1 - \tilde{p}_2$ ($\tilde{p}_1^2 = s_1$, $\tilde{p}_2^2 = s_2$, $\tilde{q}^2 = q^2$) as follows

$$w_{\mu\nu}(\tilde{p}_1, \tilde{q}) = -g_{\mu\nu}w_1 + \frac{\tilde{p}_{1\mu}\tilde{p}_{1\nu}}{s_1}w_2 + i\epsilon_{\mu\nu\alpha\beta}\frac{\tilde{p}_{1\mu}}{\sqrt{s_1}}\tilde{q}_\beta w_3 + \frac{\tilde{p}_{1\mu}\tilde{q}_\nu + \tilde{p}_{1\nu}\tilde{q}_\mu}{\sqrt{s_1}}w_4 + \tilde{q}_\mu\tilde{q}_\nu w_5. \quad (7.69)$$

Lorentz structures containing the momentum κ are omitted in this expression.

The functions w_{1-3} necessary for the energy distribution have the form

$$\begin{aligned} w_1 &= 4(m_1^2 + m_2^2 - q^2) - 16\beta, \\ q^2 w_1 + \frac{\tilde{q}^2}{3}w_2 &= \frac{4}{3}C_{SL}(m_1^2, m_2^2, q^2), \\ w_3 &= 8\sqrt{s_1}(1 - \alpha_1 - \alpha_2), \end{aligned} \quad (7.70)$$

with α_1 , α_2 , and β given by Eqs. (3.52-3.54). We have introduced

$$|\vec{q}| = \frac{\lambda^{1/2}(s_1, s_2, q^2)}{2\sqrt{s_1}}, \quad q^0 = \frac{s_1 + q^2 - s_2}{2\sqrt{s_1}}, \quad (7.71)$$

the components of the momentum q in the reference frame (7.67)

It might be interesting to note that at $q^2 < 0$, and using the reference frame $q_+ = 0$, $p_{1\perp} = 0$ ($q^2 = -q_\perp^2$) one obtains

$$\beta = -\left(k_\perp^2 - \frac{(k_\perp q_\perp)^2}{q_\perp^2}\right), \quad 1 - \alpha_1 - \alpha_2 = 1 - x_3, \quad (7.72)$$

where x_3 and k_\perp are the (+) and (\perp) components of the spectator quark momentum, respectively. In the heavy meson one finds

$$\beta \simeq \Lambda^2, \quad x_3 \simeq \Lambda/m_Q. \quad (7.73)$$

Although at $q^2 > 0$ the interpretation of β and $\alpha_1 + \alpha_2$ in terms of k_\perp and x_3 is not straightforward, the estimates (7.73) remain valid also at $q^2 > 0$. This means that in $B \rightarrow X_c \ell \bar{\nu}_\ell$ decay our w_i 's differ only slightly from the corresponding free-quark expressions.

Now everything is prepared for the calculation of the lepton energy spectrum. The following steps are standard: We must take the convolution of the trace over the lepton loop with the hadronic tensor $\tilde{w}_{\mu\nu}$, and integrate the result over the part of the lepton pair phase space leaving out the integration over dE .

As a result, we obtain the following double differential distribution

$$\begin{aligned} \frac{d^2\Gamma}{dEdq^2} &= \frac{G_F^2 |V_{21}|^2}{128\pi^3} \int_{(m_2+m_3)^2}^{\infty} ds_1 \varphi^2(s_1) \frac{s_1 - (m_2 - m_3)^2}{8\pi^2 s_1} \lambda^{1/2}(s_1, m_2^2, m_3^2) \frac{F(s_1)}{m_2^2} \\ &\quad \int_{-1}^1 \frac{d\eta}{2} \theta\left(q_0 > E + \frac{q^2}{4E}\right) \theta(s_2 < s_2^{max}(q^2)) \\ &\quad \times \left\{ 2q^2 w_1(s_1, s_2, q^2) + [4E(q^0 - E) - q^2] w_2(s_1, s_2, q^2) + 2q^2(2E - q^0) w_3(s_1, s_2, q^2) \right\}. \end{aligned} \quad (7.74)$$

In this formula s_2 is connected with η through Eq. (7.39), and q_0 is given in terms of the integration variables by Eq. (7.71).

Eq. (7.74) includes modifications which tune the size of the $1/m_Q^2$ corrections as explained above.

Let us check that the integration of the double differential distribution (7.74) over E brings us to the expression (7.64) for $d\Gamma/dq^2$ obtained earlier.

By virtue of the relations

$$\int dE \theta(q^0 > E + q^2/4E) = |\vec{q}|, \quad (7.75)$$

$$\int E dE \theta(q^0 > E + q^2/4E) = q^0 |\vec{q}|/2, \quad (7.76)$$

$$\int E^2 dE \theta(q^0 > E + q^2/4E) = \frac{1}{12} |\vec{q}| (3q_0^2 + \vec{q}^2). \quad (7.77)$$

one finds

$$\int dE \{2q^2 w_1 + [4E(q^0 - E) - q^2] w_2 + 2q^2 (2E - q^0) w_3\} \theta(q^0 > E + q^2/4E) = 2|\vec{q}| (q^2 w_1 + \frac{1}{3} \vec{q}^2 w_2). \quad (7.78)$$

Thus, integrating the double differential distribution (7.74) over E and using (7.78) gives $d\Gamma/dq^2$ in the form (7.64). Clearly, for the calculation of $d\Gamma/dq^2$ we do not need to know all w_i , but only their linear combination (7.78). On the other hand, for calculating the electron energy spectrum $d\Gamma/dE$ all functions w_{1-3} are needed.

The electron spectrum $d\Gamma/dE$ is obtained by integrating (7.74) over q^2 . Fig. 39 plots the results of the calculations. Here the effects of the subleading $1/m_Q$ orders are more pronounced but nevertheless lead only to a moderate change of the quark model box-diagram result. We also compare the dispersion approach prediction with the electron spectrum in the free-quark decay process. At low values of the electron energy the spectrum in free quark decay and in the inclusive B decay are practically indistinguishable. As desired the spectrum is nonzero at large E above the free-quark threshold. At the intermediate E the spectrum in B decay is substantially than the spectrum in the free-quark decay, providing the known suppression of the integrated $\Gamma(B \rightarrow X_c \ell \bar{\nu}_\ell)$ compared to $\Gamma_0(b \rightarrow c \ell \bar{\nu})$.

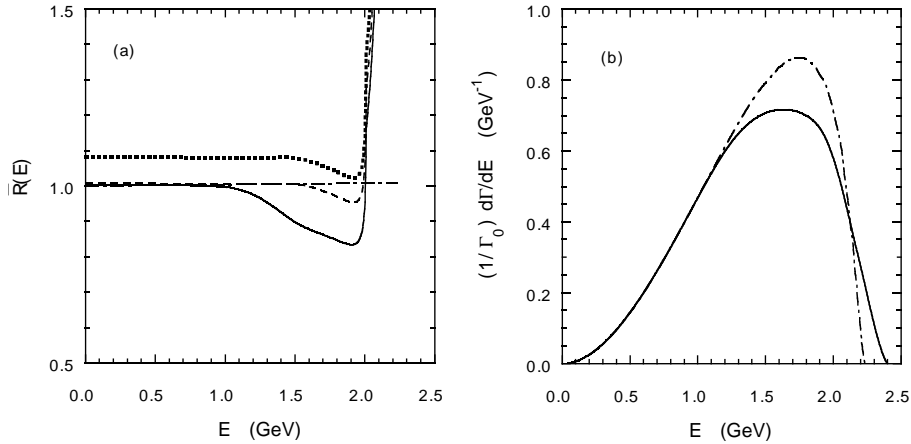


Fig. 39. Distribution $d\Gamma/dE$ in $B \rightarrow X_c \ell \bar{\nu}_\ell$ decays vs the lepton energy E : (a) ratio of the bound-to-free quark decay $\bar{R}(E) \equiv (d\Gamma/dE)/(d\Gamma_0/dE)$, lines same as in Fig. 36, (b) Our quark-model result (solid) vs free-quark result (dot-dashed).

F. Discussion

In this Chapter we discussed the dispersion approach to the description of quark-binding effects in the inclusive decays of heavy mesons. Our approach allows to express kinematical distributions in inclusive decays of heavy mesons in terms of the heavy meson soft wave function. This soft wave function describes long-distance effects both in exclusive and inclusive processes.

Summarising the main results of this Chapter:

1. We analysed the hadronic tensor in the quark model. We have shown that the diagrammatic representation of the hadronic tensor in the quark model yields an expansion in inverse powers of the heavy quark mass as well as the standard OPE. However in distinction to the standard OPE which is based on the free quark decay as the LO process, the LO process in the quark model is described by the box diagram with a free $Q\bar{q}$ in the final state. This yields some specific features of the hadronic tensor calculated within the quark model, both negative and positive.

On the one hand, a consideration based on the box diagram alone reproduces the correct LO result but contains also $1/m_Q$ corrections. These $1/m_Q$ terms are cancelled against contributions of other graphs thus leading to the agreement with the standard OPE result. Hence the effects of the subleading diagrams should be taken into account for obtaining a consistent approach.

On the other hand, the hadronic tensor calculated from the box diagram is a regular function in the kinematically allowed region of all variables, as well as all the subleading terms of order $1/m_Q$. This feature makes the quark model calculation of the hadronic tensor very suitable for describing the differential distributions;

2. We have constructed the double spectral representation of the hadronic tensor for the $B \rightarrow X_c \ell \bar{\nu}_\ell$ decay in terms of the B meson soft wave function and the double spectral density of the box diagram, and analysed its $1/m_Q$ expansion in the case of the heavy-to-heavy inclusive transition. The spectral representation is further modified in order to take into account essential effects of the other diagrams contributing in subleading orders. Namely, the subtraction term in this dispersion representation is determined such that the $1/m_Q$ correction in the integrated semileptonic rate is absent in agreement with OPE. Furthermore, a phenomenological cut function is introduced into the spectral representation to bring the size of the $1/m_Q^2$ terms in the differential q^2 -distribution at $q^2 = 0$ and in the integrated rate into full agreement with OPE. Thus our representation of the hadronic tensor obeys the OPE predictions in the regions where the latter are expected to be valid;
3. We have obtained numerical results on differential distributions in inclusive $B \rightarrow X_c \ell \bar{\nu}_\ell$ decays using the B -meson wave function and other quark model parameters previously determined from the description of exclusive meson transition form factors within the dispersion approach. So, basically our predictions are parameter-free. We notice that modifications of the spectral representations which take into account the subleading $1/m_Q$ effects within the box-diagram representation, introduce some uncertainties in our results. However, they do not affect our predictions strongly, and the main features of the inclusive distributions are determined by the soft meson wave function. Moreover, the size of the subleading corrections is in perfect agreement with the OPE result for the integrated rate, and we expect to describe also these subleading effects in differential distributions in a proper quantitative way.

The proposed approach can be applied to the inclusive $B \rightarrow X_{u,s}$ transitions. In particular it is especially suitable for the description of the photon line shape in $B \rightarrow X_s \gamma$ decays. However, certain subtleties in heavy-to-light transitions compared with the heavy-to-heavy decays emerge. They are mostly connected with the fact that in heavy-to-light transition the kinematically allowed q^2 -interval of the hadron semileptonic decay is larger than that of the quark decay, while in case of the heavy-to-heavy transitions the situation is just opposite and the q^2 -region of the quark decay is larger. This feature requires a detailed analysis of the q^2 -region near zero recoil in heavy-to-light inclusive decays.

It is also worth noting that our approach takes into account only non-perturbative effects in inclusive decays of heavy mesons. Perturbative corrections have been ignored. So, for comparing our results with the experimental differential distributions perturbative corrections should be also included into consideration.

VIII. CONCLUSION

We presented a review of the relativistic dispersion approach to meson transitions induced by the weak currents. This approach is based on the constituent quark picture and takes into account the leading two-particle singularities of the Feynman diagrams making use of spectral representations over the mass variables.

We reported the following main results:

1. Relativistic meson $Q\bar{q}$ wave function has been defined which describes in a universal way strong-QCD effects related to the meson structure in various meson interactions. Due to confinement, the wave function in terms of the relative quark momentum is localized in the region of the order of the confinement scale. The normalization condition for the wave function corresponds to the electric charge conservation and is thus related to the meson elastic electromagnetic form factor at zero momentum transfer.

2. We considered the elastic electromagnetic form factor of a pseudoscalar meson and form factors describing weak transition of a pseudoscalar meson to pseudoscalar and vector mesons at spacelike momentum transfers. Relativistic double spectral representations for these form factors have been constructed in terms of the double spectral densities of the corresponding triangle Feynman graphs and the wave functions of the participating mesons.

The subtraction prescription has been fixed by requiring the dispersion approach form factors to respect all properties of the transition form factors known from long-distance QCD in the limit of heavy quark mass.

3. The dispersion approach form factors were studied in the two limiting cases of the heavy-to-heavy and heavy-to-light weak transitions.

- *Heavy-to-heavy* transition

In this case the masses of the initial quark m_Q and the final quark $m_{Q'}$ participating in the weak transition $Q \rightarrow Q'$ are taken to be much larger than the confinement scale Λ

$$m_Q \simeq m_{Q'} \gg \Lambda.$$

The form factors from the dispersion approach have been shown to fully respect the structure of the $1/m_Q$ expansion known from QCD in the leading and subleading $1/m_Q$ orders. The Isgur-Wise function and the subleading-order universal form factors have been calculated in terms of the wave function of a meson containing an infinitely heavy quark.

- *Heavy-to-light* transition

In this case the quark masses satisfy the relation

$$m_Q \gg m_{Q'} \simeq \Lambda.$$

The dispersion approach form factors have been shown to obey the QCD-based relations between the form factors of the vector, axial vector and tensor currents valid within the $1/m_Q$ accuracy in the region of large q^2 .

4. We performed a detailed comparison of the dispersion approach with the light-front quark model for the description of weak transitions. Both approaches describe the dominance of the $q\bar{q}$ components of the meson wave function in meson interactions and therefore should lead to the same results.

Indeed, we have shown that for the transition between pseudoscalar mesons the results from both approaches in the region of spacelike momentum transfers $q^2 < 0$ are identical. On the other hand, for some of the form factors describing the pseudoscalar to vector meson transition the results are different. This is related to a different treatment of a vector meson, a composite system with spin-1, within both approaches. In the language of spectral representations, the difference between the two approaches can be traced back to different subtraction prescriptions. We have shown that the subtraction prescription implemented in the light-cone quark model does not fully respect the next-to-leading order constraints from QCD for the heavy-to-heavy transition.

Another advantage of the dispersion approach is the possibility for a consistent description of the region of timelike momentum transfers $q^2 > 0$ relevant for the decay kinematics. In the dispersion approach this is achieved by performing the analytical continuation in the variable q^2 . The light-front quark model in general cannot consistently treat the form factor at $q^2 > 0$: it describes only a reference-frame dependent part of the form factor, the partonic contribution, leaving out the nonpartonic contribution.

5. We obtained the form factors in the region $q^2 > 0$ by the analytical continuation. We observed the appearance of the anomalous cut in the complex s -plane, where s is the invariant mass of the $q\bar{q}$ pair. Accordingly, the spectral representation for the transition form factor acquires the anomalous contribution in the decay region. The anomalous contribution is small for small q^2 but becomes increasingly important in the region of large q^2 near zero recoil.

6. A model for pseudoscalar mesons was considered, which allowed us to study the transition regime to the heavy quark limit. Meson decay constants and transition form factors as functions of the quark masses have been analysed. It was found that the corrections to the leading order $1/m_Q$ relations can be as big as 10-20% for the quark masses in the region of the realistic c and b quarks.

7. We presented the results for the form factors for weak decays of $B_{(s)}$ and $D_{(s)}$ mesons to light pseudoscalar and vector mesons.

- The effective quark masses and meson wave functions were determined by fitting the quark model parameters to the available lattice QCD results for the $B \rightarrow \rho$ transition form factors at large momentum transfers and to the measured $D \rightarrow (K, K^*)l\nu$ decay rates. The knowledge of the quark model parameters allowed us to predict numerous form factors for many decay channels and for all kinematically accessible q^2 values.

In spite of the rather different masses and properties of mesons involved in weak transitions, all existing data on the form factors can be understood in the constituent quark picture, i.e. all form factors can be described by the few degrees of freedom of constituent quarks. Details of the soft wave functions are not crucial; only the spatial extension of these wave functions of order of the confinement scale is important. In other words, only the meson radii are essential.

- The calculated transition form factors are in good agreement with the results from lattice QCD and from sum rules in their regions of validity.
- Our predictions agree well with all available experimental data. An important example is the ratio of the semileptonic branching fractions of the B meson to light π and ρ mesons, $\mathcal{B}(B \rightarrow \rho l\nu)/\mathcal{B}(B \rightarrow \pi l\nu)$. A good agreement of the predicted ratio with the results of the experiment leads to close values of the matrix element V_{ub} extracted from the $B \rightarrow \rho$ and $B \rightarrow \pi$ channels.
- We estimated the products of the meson weak and strong coupling constants by extrapolating the form factors to the meson pole. The value of each coupling constant can be obtained independently from the residues of several form factors. In all cases the values extracted from the different form factors agree with each other within the 5-10% accuracy. They also agree with the results of the independent direct calculations of these decay constants within the dispersion approach. First direct measurement of the coupling constant $g_{D^*D\pi}$ which has become available recently is in perfect agreement with our estimate. This gives additional argument in support of the reliability of our results for the form factors.

8. Weak annihilation in a rare radiative decay was analysed. The relevant $B \rightarrow \gamma l\nu$ form factors were calculated in terms of the B meson wave function. Parameter-free estimates were obtained and found to agree well with estimated from perturbative QCD and QCD sum rules. The situation with contact terms was clarified.

A new contribution to the weak annihilation amplitude was reported, related to the photon emission from the light-quark loop. This contribution was believed to vanish in the limit of zero quark masses, and therefore neglected in previous analyses. A detailed study shows that this contribution stays finite and should be taken into account.

9. Non-factorizable effects in the $B^0 - \bar{B}^0$ mixing amplitude due to the soft gluon exchanges were studied assuming the local gluon condensate dominance. The corresponding correction to the factorizable amplitude was demonstrated to be negative. This correction contains specific B meson transition form factors which were calculated within the dispersion approach. Numerical estimate for the nonfactorizable effect was obtained.

10. The dispersion approach was applied to inclusive semileptonic decays. Spectral representations for the differential and integrated semileptonic decay rate $\Gamma(B \rightarrow X_c l\nu)$ were obtained. The decay rates calculated within the dispersion approach satisfy an important property known from the operator product expansion in QCD in the heavy quark limit: namely, the order $1/m_Q$ correction in the ratio of the bound to free quark decay rate $\Gamma(B \rightarrow X_c l\nu)/\Gamma_0(b \rightarrow cl\nu)$ is absent.

Different kinematical distributions such as the dilepton q^2 -spectrum $d\Gamma/dq^2$, $d\Gamma/dM_X$ and the electron energy spectrum $d\Gamma/dE_l$ were calculated in terms of the B meson wave function. This wave function determines the B meson form factors and has been tested in exclusive B decays.

ACKNOWLEDGMENTS

I take pleasure to express my gratitude to Vladimir Anisovich, Michael Beyer, Michail Kobrinsky, Alain Le Yaouanc, Bernard Metsch, Nikolai Nikitin, Victor Nikonov, Luis Oliver, Olivier Pène, Herbert Petry, Jean-Claude Raynal, Silvano Simula, and Berthold Stech for the most pleasant collaboration on many of the issues discussed in this paper.

I am grateful to Yasha Azimov, Damir Becirevic, Gregory Korchemsky, Otto Nachtmann, and Lidia Smirnova for useful and stimulating discussions.

I would like to thank the Alexander von Humboldt-Stiftung for financial support.

- [1] M. B. Voloshin and M. A. Shifman, ‘On annihilation of mesons built from heavy and light quark and $\bar{B}^0 \leftrightarrow B^0$ oscillations’, Sov. J. Nucl. Phys. **45**, 292 (1987), Yad. Fiz. **45**, 463-466 (1987);
‘On production of D and D^* mesons in B meson decays’, Sov. J. Nucl. Phys. **47** 511 (1988), Yad. Fiz. **47**, 801-806 (1988).
- [2] N. Isgur and M. B. Wise, ‘Weak decays of heavy mesons in the static quark approximation’, Phys. Lett. **B232**, 113 (1989); ‘Weak transition form-factors between heavy mesons’, Phys. Lett. **B237**, 527 (1990).
- [3] D. Politzer and M. Wise, ‘Effective field theory approach to processes involving both light and heavy fields’, Phys. Lett. **B208**, 504 (1988);
H. Georgi, ‘An effective field theory for heavy quarks at low-energies’, Phys. Lett. **B240**, 447 (1990).
- [4] J. Chay, H. Georgi, and B. Grinstein, ‘Lepton energy distributions in heavy meson decays from QCD’, Phys. Lett. **B247**, 399 (1990).
- [5] I. Bigi, M. Shifman, N. Uraltsev, and A. Vainshtein, ‘QCD predictions for lepton spectra in inclusive heavy flavor decays’, Phys. Rev. Lett. **71**, 496 (1993).
- [6] M. Luke, ‘Effects of subleading operators in the heavy quark effective theory’, Phys. Lett. **B252**, 447 (1990);
M. Neubert and V. Rieckert, ‘New approach to the universal form-factors in decays of heavy mesons’, Nucl. Phys. **B382**, 97 (1992).
- [7] M. Neubert, ‘Heavy quark symmetry’, Phys. Rep. **245**, 259 (1994) and references therein.
- [8] N. Isgur and M. B. Wise, ‘Relationship between form-factors in semileptonic B and D decays and exclusive rare B meson decays’, Phys. Rev. **D42**, 2388 (1990).
- [9] J. Charles *et al*, ‘Heavy to light form-factors in the heavy mass to large energy limit of QCD’, Phys. Rev. **D60**, 014001 (1999).
- [10] M. Wirbel, B. Stech, and M. Bauer, ‘Exclusive semileptonic decays of heavy mesons’, Z. Phys. **C29**, 637 (1985);
M. Bauer, B. Stech, and M. Wirbel, ‘Exclusive nonleptonic decays of D , $D(s)$, and B mesons’, Z. Phys. **C34**, 103 (1987);
M. Bauer and M. Wirbel, ‘Form-factor effects in exclusive D and B decays’, Z. Phys. **C42**, 671 (1989).
- [11] J. G. Körner and G. A. Schuler, ‘Exclusive semileptonic decays of bottom mesons in the spectator quark model’, Z. Phys. **C38**, 511 (1988).
- [12] N. Isgur, D. Scora, B. Grinstein, and M. Wise, ‘Semileptonic B and D decays in the quark model’, Phys. Rev. **D39**, 799 (1989).
- [13] D. Scora and N. Isgur, ‘Semileptonic meson decays in the quark model: an update’, Phys. Rev. **D52**, 2783 (1995).
- [14] W. Jaus, ‘Semileptonic decays of B and D mesons in the light front formalism’, Phys. Rev. **D41**, 3394 (1990);
‘Relativistic constituent quark model of electroweak properties of light mesons’, Phys. Rev. **D44**, 2319 (1991);
‘Semileptonic, radiative, and pionic decays of B , B^* , D , and D^* mesons’ Phys. Rev. **D53**, 1349 (1996).
- [15] W. Jaus and D. Wyler, ‘The rare decays of $B \rightarrow Kll$ and $B \rightarrow K^*ll$ ’, Phys. Rev. **D41**, 3405 (1990).
- [16] A. Dubin and A. Kaidalov, ‘Transition form factors for mesons containing heavy quarks’, Sov. J. Nucl. Phys. **56**, 164 (1993).
- [17] G. Zoller, S. Hainzl, C. Münz, and M. Beyer, ‘Weak decays of heavy mesons in the instantaneous Bethe-Salpeter approach’, Z. Phys. **C68**, 103 (1995).
- [18] R. N. Faustov and V. O. Galkin, ‘Heavy quark $1/m_Q$ expansion of meson weak decay form-factors in the relativistic quark model’, Z. Phys. **C66**, 119 (1995);
R. N. Faustov and V. O. Galkin, ‘Relativistic description of the exclusive rare radiative decays of B mesons’, Phys. Rev. **D52** 5131 (1995);
R. N. Faustov, V. O. Galkin, Yu. A. Mishurov, ‘Relativistic description of exclusive heavy to light semileptonic decays $B \rightarrow (\pi\rho)l\nu$ ’, Phys. Rev. **D53**, 6302 (1996).
D. Ebert, R. N. Faustov, and V. O. Galkin, ‘Exclusive semileptonic B decays to radially excited D mesons’, Phys. Rev. **D62**, 014032 (2000).
- [19] R. Aleksan, A. Le Yaouanc, L. Oliver, O. Pène, and J.-C. Raynal, ‘Critical analysis of theoretical estimates for B to light

- meson form-factors and the $B \rightarrow \psi K(K^*)$ data', Phys. Rev. **D51**, 6235 (1995);
A. Le Yaouanc, L. Oliver, O. Pene, and J.-C. Raynal, 'Covariant quark model of form-factors in the heavy mass limit', Phys. Lett. **B365**, 319 (1996);
V. Morenas, A. Le Yaouanc, L. Oliver, O. Pene, and J.C. Raynal, ' $B \rightarrow D^{**}$ semileptonic decay in covariant quark models a la Bakamjian-Thomas', Phys. Lett. **B386**, 315 (1996);
V. Morenas, A. Le Yaouanc, L. Oliver, O. Pene, J.C. Raynal, 'Slope of the Isgur-Wise function in the heavy mass limit of quark models a la Bakamjian-Thomas', Phys. Lett. **B408**, 357 (1997);
J. Charles, et. al, 'Heavy to light form-factors in the final hadron large energy limit: covariant quark model approach', Phys. Lett. **B451**, 187 (1999).
- [20] A. Le Yaouanc, et.al, ' B to light meson form-factors', Nucl. Instrum. Meth Phys. Res. Sect. **A351**, 15 (1994).
[21] F. Cardarelli, I. L. Grach, I. M. Narodetsky, E. Pace, G. Salme, and S. Simula, 'Hard constituent quarks and electroweak properties of pseudoscalar mesons', Phys. Lett. **B332**, 1 (1994);
'Electromagnetic form-factors of the ρ meson in a light front constituent quark model', Phys. Lett. **B349**, 393 (1995);
'Radiative $\pi\rho$ and $\pi\omega$ transition form-factors in a light front constituent quark model', Phys. Lett. **B359**, 1 (1995).
[22] S. Simula, 'Calculation of the Isgur-Wise function from a light front constituent quark model', Phys. Lett. **B373**, 193 (1996).
[23] I. L. Grach, I. M. Narodetskii and S. Simula, 'Weak decay form-factors of heavy pseudoscalar mesons within a light front constituent quark model', Phys. Lett. **B385**, 317 (1996);
N. B. Demchuk, I. L. Grach, I. M. Narodetskii and S. Simula, 'Heavy to heavy and heavy to light weak decay form-factors in the light front approach: the exclusive $0^- \rightarrow 0^-$ case', Phys. Atom. Nucl. **59**, 2152 (1996), Yad. Fiz. **59**, 2235-2246 (1996).
[24] D. Melikhov, 'Form-factors of meson decays in the relativistic constituent quark model', Phys. Rev. **D53**, 2460 (1996).
[25] D. Melikhov, 'Semileptonic decays $B \rightarrow (\pi, \rho) e \nu$ in relativistic quark model', Phys. Lett. **B380**, 363 (1996).
[26] D. Melikhov, 'Exclusive semileptonic decays of heavy mesons in quark model', Phys. Lett. **B394**, 385 (1997).
[27] D. Melikhov, 'Heavy quark expansion and universal form-factors in quark model', Phys. Rev. **D56**, 7089 (1997).
[28] P. Ball, V. Braun, H. Dosch, and M. Neubert, 'Sum rule analysis of the decay $D \rightarrow K^* l \nu$ ', Phys. Lett. **B259**, 481 (1989);
P. Ball, V. Braun, and H. Dosch, 'On vector dominance in the decay $B \rightarrow \pi l \nu$ ', Phys. Lett. **B273**, 316 (1991).
[29] P. Ball, V. Braun, and H. Dosch, 'Form-factors of semileptonic D decays from QCD sum rules', Phys. Rev. **D44**, 3567 (1991).
[30] V. M. Belyaev, A. Khodjamirian, R. Rückl, 'QCD calculation of the $B \rightarrow \pi, K$ form-factors', Z. Phys. **C60**, 349 (1993).
[31] P. Ball, 'The semileptonic decays $D \rightarrow (\pi, \rho) l \nu$ and $B \rightarrow (\pi, \rho) l \nu$ from QCD sum rules', Phys. Rev. **D48**, 3190 (1993).
[32] S. Narison, 'Precise determination of $f(p_s)/f(p)$ and measurement of the 'perturbative' pole mass from $f(p)$ ', Phys. Lett. **B322**, 247 (1994);
' $\Upsilon \bar{B} B$ couplings, slope of the Isgur-Wise function and improved estimate of $V(cb)$ ', Phys. Lett. **B325**, 197 (1994).
[33] M. Neubert, 'Theoretical update on the model independent determination of $|V(cb)|$ using heavy quark symmetry', Phys. Lett. **B338**, 84 (1994).
[34] P. Colangelo *et al.*, 'QCD sum rule analysis of the decays $B \rightarrow K l l$ and $B \rightarrow K^* l l$ ', Phys. Rev. **D53**, 3672 (1996);
'Rare $B \rightarrow K^* \nu \nu$ decays at B factories', Phys. Lett. **B395**, 339 (1997).
[35] P. Ball and V. M. Braun, 'Use and misuse of QCD sum rules in heavy to light transitions: the decay $B \rightarrow \rho l \nu$ reexamined', Phys. Rev. **D55**, 5561 (1997).
[36] P. Ball and V. M. Braun, 'Exclusive semileptonic and rare B meson decays in QCD', Phys. Rev. **D58**, 094016 (1998);
P. Ball, ' $B \rightarrow \pi$ and $B \rightarrow K$ transitions from QCD sum rules on the light cone', JHEP **09**, 005 (1998).
[37] V. M. Braun, 'QCD sum rules for heavy flavors', Invited talk at *8th International Symposium on Heavy Flavor Physics (Heavy Flavors 8)*, Southampton, England, 25-29 Jul 1999, e-print archive hep-ph/9911206 (1999) and references therein.
[38] T. M. Aliev *et al.*, 'Rare $B \rightarrow K^* l l$ decay in light cone QCD', Phys. Rev. **D56**, 4260 (1997);
'Light cone QCD sum rule analysis of $B \rightarrow K l l$ decay', Phys. Lett. **B400**, 194 (1997).
[39] V. V. Kiselev, A. K. Likhoded, A. I. Onishchenko, 'Semileptonic decays of the B_c meson', Phys. Atom. Nucl. **63**, 2123 (2000), Yad. Fiz. **63**, 2219 (2000);
V. V. Kiselev, A. E. Kovalsky, A. K. Likhoded ' B_c decays and lifetime in QCD sum rules', Nucl. Phys. **B585**, 353(2000);
V. V. Kiselev, A. K. Likhoded, A.I. Onishchenko, 'Semileptonic B_c meson decays in sum rules of QCD and NRQCD', Nucl. Phys. **B569**, 473 (2000).
[40] ELC Collaboration (A. Abada *et al*) 'Semileptonic decays of heavy flavors on a fine grained lattice', Nucl. Phys. **B416**, 675 (1994).
[41] APE Collaboration (C. R. Allton *et al*), 'Lattice calculation of D and B meson semileptonic decays using the clover action at beta = 6.0 on APE', Phys. Lett. **B345**, 513 (1995).
[42] UKQCD Collaboration (J. M. Flynn *et al*), 'Lattice study of the decay $B \rightarrow \rho l \nu$: model independent determination of $|V(ub)|$ ', Nucl. Phys. **B461**, 327 (1996).
[43] APE Collaboration (A. Abada *et al*), 'A lattice study of the exclusive $B \rightarrow K^* \gamma$ decay amplitude, using the clover action at beta = 6.0', Phys. Lett. **B365**, 275 (1996).
[44] UKQCD Collaboration (S. Booth *et al*), 'The Isgur-Wise function from the lattice', Phys. Rev. Lett. **72**, 462 (1994).

- [45] J. M. Flynn and C. T. Sachrajda, ‘Heavy quark physics from lattice QCD’, In Buras, A.J. (ed.), Lindner, M. (ed.): Heavy flavours II , 402-452, e-print archive hep-lat/9710057.
- [46] A. Abada *et al*, ‘Decays of heavy mesons’, Nucl. Phys. Proc. Suppl. **83**, 268 (2000), hep-lat/9910021.
- [47] UKQCD Collaboration (K. C. Bowler *et al*), ‘Improved $B \rightarrow \pi l \nu$ form-factors from the lattice’, Phys. Lett. **B486**, 111 (2000), hep-lat/9911011.
- [48] UKQCD (G. De Divitiis *et al*), ‘Towards a lattice determination of the $B^* B \pi$ coupling’, J. High Energy Phys. **10**, 010 (1998), hep-lat/9807032.
- [49] H. Leutwyler and M. Roos, ‘Determination of the elements $V(us)$ and $V(ud)$ of the Kobayashi-Maskawa matrix’, Z. Phys. **C25**, 91 (1984).
- [50] G. Burdman and J. Donoghue, ‘Reliable predictions in exclusive rare B decays’, Phys. Lett. **B270**, 55 (1991).
- [51] B. Stech, ‘Form-factor relations for heavy to light transitions’, Phys. Lett. **B354**, 447 (1995);
‘A form-factor model for exclusive B and D decays’, Z. Phys. **C75**, 245 (1997).
- [52] UKQCD Collaboration (L. Del Debbio *et al*), ‘Lattice constrained parametrizations of form-factors for semileptonic and rare radiative B decays’, Phys. Lett. **B416**, 392 (1998).
- [53] C. G. Boyd, B. Grinstein, and R. F. Lebed, ‘Model independent determinations of $B \rightarrow (D, D^*) l \nu$ form-factors’, Nucl. Phys. **B461**, 493 (1996).
- [54] D. Becirevic, ‘ $B \rightarrow \rho l \nu$ form factors’, Phys. Rev. **D54**, 6842 (1996).
- [55] L. Lellouch, ‘Lattice constrained unitarity bounds for $B \rightarrow \pi l \nu$ decays’, Nucl. Phys. **B479**, 353 (1996).
- [56] J. M. Soares, ‘Form-factor relations for heavy to light meson transitions: tests of the quark model predictions’, hep-ph/9810421.
- [57] M. V. Terent’ev, ‘On the structure of wave functions of mesons as bound states of relativistic quark’, Sov. J. Nucl. Phys. **24**, 106 (1976), Yad. Fiz. **24**, 207 (1976);
V. B. Berestetsky and M. V. Terent’ev, ‘Light front dynamics and nucleons from relativistic quark’, Sov. J. Nucl. Phys. **24**, 547 (1976), Yad. Fiz. **24**, 1044 (1976).
- [58] P. Chung, F. Coester, and W. Polyzou, ‘Hamiltonian light front dynamics of elastic electron deuteron scattering’, Phys. Rev. **C37**, 2000 (1988);
‘Charge form-factors of quark model pions’, Phys. Lett. **B205**, 545 (1988).
- [59] M. Beyer and D. Melikhov, ‘Form-factors of exclusive $b \rightarrow u$ transitions’, Phys. Lett. **B436**, 344 (1998).
- [60] D. Melikhov and M. Beyer, ‘Pionic coupling constants of heavy mesons in the quark model’, Phys. Lett. **B452**, 121 (1999).
- [61] D. Melikhov and B. Stech, ‘Weak form-factors for heavy meson decays: an update’, Phys. Rev. **D62**, 014006 (2000).
- [62] D. Melikhov, N. Nikitin, and S. Simula, ‘Rare decays $B \rightarrow (K, K^*)(l^+ l^-, \nu \bar{\nu})$ in the quark model’, Phys. Lett. **B410**, 290 (1997).
- [63] D. Melikhov, N. Nikitin, and S. Simula, ‘Rare exclusive semileptonic $b \rightarrow s$ transitions in the standard model’, Phys. Rev. **D57**, 6814 (1997).
- [64] M. Beyer, D. Melikhov, N. Nikitin, and B. Stech, ‘Weak annihilation in the rare radiative $B \rightarrow \rho \gamma$ decay’, Phys. Rev. **D64**, 094006 (2001).
- [65] D. Melikhov and B. Stech, ‘Nonlocal anomaly of the axial vector current for bound states’, hep-ph/0108165.
- [66] D. Melikhov and N. Nikitin, ‘Non-factorizable effects in the $B - \bar{B}$ mixing’, Phys. Lett. **B494**, 229 (2000).
- [67] D. Melikhov and S. Simula, ‘Quark-binding effects in inclusive decays of heavy mesons’, Phys. Rev. **D62**, 074012 (2000).
- [68] S. Godfrey and N. Isgur, ‘Mesons in a relativized quark model with chromodynamics’, Phys. Rev. **D32**, 189 (1985).
- [69] V. Anisovich, D. Melikhov, V. Nikonov, ‘Quark structure of the pion and pion form-factor’, Phys. Rev. **D52**, 5295 (1995).
- [70] V. Anisovich, D. Melikhov, V. Nikonov, ‘Photon-meson transition form-factors $\gamma \pi^0, \gamma \eta, \gamma \eta'$ at low and moderately high Q^2 ’, Phys. Rev. **D55**, 2918 (1997).
- [71] V. V. Anisovich, M. N. Kobrinsky, D. I. Melikhov, and A. V. Sarantsev, ‘Ward Identities and Sum Rules for Composite Systems in the Technique of Dispersion Integration over Mass’, Yad. Fiz. **55**, 1773 (1992).
- [72] V. V. Anisovich, M. N. Kobrinsky, D. I. Melikhov, and A. V. Sarantsev, ‘Ward identities and sum rules for composite systems described in the dispersion relation technique: the deuteron as a composite two nucleon system’, Nucl. Phys. **A544**, 747 (1992).
- [73] V. V. Anisovich, D. I. Melikhov, B. C. Metsch, and H. R. Petry, ‘The Bethe-Salpeter equation and the dispersion relation technique’, Nucl. Phys. **A563**, 549 (1993).
- [74] V. V. Anisovich, D. I. Melikhov, B. C. Metsch, and H. R. Petry, ‘On the description of a bound state within the light cone technique and the dispersion approach’, Yad. Fiz. **57**, 312 (1994).
- [75] D. I. Melikhov, ‘Soft and hard hadron form-factors’, Yad. Fiz. **57**, 2070 (1994).
- [76] G. F. Chew, S. Mandelstam, ‘Theory of low-energy pion-pion interactions’, Phys. Rev. **119**, 467 (1960).
- [77] S. Mandelstam, ‘Unitarity Condition Below Physical Thresholds in the Normal and Anomalous Cases,’ Phys. Rev. Lett. **4**, 84 (1960).
- [78] R. Blankenbecler, Y. Nambu, ‘Anomalous thresholds in dispersion theory’, Nuovo. Cim. **18**, 595 (1960).
- [79] R. Blankenbecler, L. F. Cook, ‘Bound states and dispersion relations’, Phys. Rev. **119**, 1745 (1960).
- [80] G. Burton, ‘Introduction to dispersion techniques in field theory’, W.A. Benjamin, NY-Amsterdam, 1965.

- [81] S. Weinberg, ‘Why do quarks behave like bare Dirac particles’, Phys. Rev. Lett. **65**, 1181 (1990).
- [82] R. Jaffe, ‘Ineffective field theory: when quarks are required in QCD’, Phys. Lett. **B245**, 221 (1990).
- [83] I. Bigi, M. Shifman, and N. Uraltsev, ‘Aspects of heavy quark theory’, Ann. Rev. Nucl. Part. Sci. **47**, 591 (1997) [hep-ph/9703290].
- [84] Particle Data Group, C. Caso et al, Eur.Phys.J. **C3**, 1 (1998); 1999 partial update for edition 2000, URL: <http://pdg.lbl.gov>.
- [85] A. Ryd, ‘Form-factors in B and D decays’, Presented at 7th International Symposium on Heavy Flavor Physics, Santa Barbara, CA, 7-11 Jul 1997, In *Santa Barbara 1997, Heavy flavor physics*, pp 19-28.
- [86] CLEO Collaboration (A. Bean et al.), ‘Measurement of exclusive semileptonic decays of D mesons’, Phys. Lett. **B317**, 647 (1993).
- [87] The rates for the $D \rightarrow \pi$ and $D \rightarrow \rho$ are obtained by combining the values for the $D \rightarrow K$ and $D \rightarrow K^*$ with the measurements of the ratios of the semileptonic branching fractions $D \rightarrow \pi/D \rightarrow K$ by CLEO [88] and $D \rightarrow \rho/D \rightarrow K^*$ by E653 [89].
- [88] CLEO Collaboration (F. Butler et al.), ‘Measurement of the ratio of branching fractions $B(D^0 \rightarrow \pi^- e^+ \nu)/B(D^0 \rightarrow K^- e^+ \nu)$ ’, Phys. Rev. **D52**, 2656 (1995).
- [89] E653 Collaboration (K. Kodama et al.), ‘Observation of $D^+ \rightarrow \rho^0 \mu^+ \nu$ ’, Phys. Lett. **B316**, 455 (1993).
- [90] CLEO Collaboration (T. E. Coan et al.), ‘First Measurement of $\Gamma(D^{*+})$ ’, hep-ex/0102007.
- [91] V. M. Belyaev, V. M. Braun, A. Khodjamirian, R. Rückl, ‘ $D^* D \pi$ and $B^* B \pi$ couplings in QCD’, Phys. Rev. **D51**, 6177-6195 (1995).
- [92] CLEO Collaboration (R. Duboscq et al.) ‘Measurement of the Form Factors for $\bar{B}^0 \rightarrow D^{*+} l^- \nu$ ’, Phys. Rev. Lett. **76**, 3898 (1996).
- [93] CLEO Collaboration (J. Bartelt et al.), ‘Measurement of the $B \rightarrow D l \nu$ Branching Fractions and Form Factor’, Phys. Rev. Lett. **82**, 3746 (1999).
- [94] CLEO Collaboration (B. Barish et al.), ‘Measurement of the $B \rightarrow D^* l \nu$ branching fractions and $|V(cb)|$ ’, Phys. Rev. **D51** 1014 (1995);
CLEO Collaboration (M. Athanas et al.), ‘Semileptonic branching fractions of charged and neutral B mesons’, Phys. Rev. Lett. **73**, 3503 (1994), Erratum- ibid. **74**, 3090 (1995).
- [95] CLEO Collaboration (S. Sanghera et al.), ‘Lepton asymmetry measurements in $B \rightarrow D^* l \nu$ and implications for $V - A$ and the form factors’, Phys. Rev. **D47**, 791 (1993).
- [96] CLEO Collaboration (J. P. Alexander et al.), ‘First measurement of the $B \rightarrow \pi l \nu$ and $B \rightarrow \rho(\omega) l \nu$ branching fractions’. Phys. Rev. Lett. **77**, 5000 (1996);
CLEO Collaboration (B. H. Behrens et al.), ‘Measurement of $B \rightarrow \rho l \nu$ decay and $|V_{ub}|$ ’, Phys. Rev. **D61**, 052001 (2000);
K. Ecklund, ‘Semileptonic B decays from CLEO’, Talk at *8th International Symposium on Heavy Flavor Physics (Heavy Flavours 8)*, Southampton, England, 25-29 Jul 1999, e-print archive hep-ex/9912034 (1999).
- [97] H. Kim, ‘ B semileptonic decays at Belle’, Talk given at the *9-th International Symposium on Heavy Flavour Physics*, September 10-13, 2001, Caltech, Pasadena, <http://3w.hep.caltech.edu/HF9/programdetail.html>
- [98] Th. Feldmann, P. Kroll, and B. Stech, ‘Mixing and decay constants of pseudoscalar mesons’, Phys. Rev. **D58**, 114006 (1998).
- [99] CLEO Collaboration (G. Brandenburg et al.), ‘Measurement of the $D_s^+ \rightarrow \eta l^+ \nu$ and $D_s^+ \rightarrow \eta' l^+ \nu$ branching ratios’, Phys. Rev. Lett. **75**, 3804 (1995).
- [100] J. L. Hewett and J. D. Wells, ‘Searching for supersymmetry in rare B decays’, Phys. Rev. **D55**, 5549 (1997).
- [101] T. G. Rizzo, ‘Breakdown of global fits to the Wilson coefficients in rare B decays: a left-right model example’ Phys. Rev. **D58**, 114014 (1998).
- [102] D. Melikhov, ‘Long distance contribution to exclusive rare decays of heavy mesons in quark model’, *Talk given at 32-nd Rencontres de Moriond: Electroweak Interactions and Unified Theories*, Les Arcs, France, 15-22, Mar 1997 [hep-ph/9704421].
- [103] G. Burdman, ‘Short distance coefficients and the vanishing of the lepton asymmetry in $B \rightarrow V l^+ l^-$ ’, Phys. Rev. **D57**, 4254 (1998).
- [104] D. Melikhov, N. Nikitin, and S. Simula, ‘Righthanded currents in rare exclusive $B \rightarrow (K, K^*) \nu \bar{\nu}$ decays’, Phys. Lett. **B428**, 171 (1998).
- [105] D. Melikhov, N. Nikitin, and S. Simula, ‘Lepton asymmetries in exclusive $b \rightarrow s l^+ l^-$ decays as a test of the standard model’, Phys. Lett. **B430**, 332 (1998).
- [106] D. Melikhov, N. Nikitin, and S. Simula, ‘Probing righthanded currents in $B \rightarrow K^* l^+ l^-$ transitions’, Phys. Lett. **B442**, 381 (1998).
- [107] A. Ali, P. Ball, L. T. Handoko, and G. Hiller, ‘A comparative study of the decays $B \rightarrow (K, K^*) l^+ l^-$ in standard model and supersymmetric theories’, Phys. Rev. **D61**, 074024 (2000).
- [108] CLEO Collaboration (R. Ammar et al.), ‘Evidence for penguin-diagram decays: First observation of $B \rightarrow K^*(892) \gamma$ ’, Phys. Rev. Lett. **71**, 674 (1993);
CLEO Collaboration (T. E. Coan et al.), ‘Study of exclusive radiative B meson decays’, Phys. Rev. Lett. **84**, 5283 (2000).
- [109] CLEO Collaboration (M. S. Alam et al.): ‘First Measurement of the Rate for the Inclusive Radiative Penguin Decay

- $b \rightarrow s\gamma$, Phys. Rev. Lett. **74**, 2885 (1995),
CLEO Collaboration (S. Ahmed *et al.*): ' $b \rightarrow s\gamma$ branching fractions and CP asymmetry', Preprint hep-ex/9908022.
- [110] B. Grinstein and D. Pirjol, 'Long-distance effects in $B \rightarrow V\gamma$ radiative weak decays', Phys. Rev. **D62**, 093002 (2000).
- [111] F. Krüger and L. M. Sehgal, 'Lepton polarization in the decays $B \rightarrow X_s \mu^+ \mu^-$ and $B \rightarrow X_s \tau^+ \tau^-$ ', Phys. Lett. **B380**, 199 (1996);
'CP violation in the exclusive decays $B \rightarrow \pi ll$ and $B \rightarrow \rho ll$ ', Phys. Rev. **D56**, 5452 (1997), Erratum-ibid. **D60**, 099905 (1999).
- [112] A. Khodjamirian, R. Rückl, G. Stoll, and D. Wyler, 'QCD estimate of the long distance effect in $B \rightarrow K^* \gamma$ ', Phys. Lett. **B402**, 167 (1997).
- [113] D. Melikhov, 'Factorizable $c\bar{c}$ contribution in the radiative $B \rightarrow K^* \gamma$ decay', Phys. Lett. **B516**, 61 (2001).
- [114] A. Khodjamirian, G. Stoll, D. Wyler, 'Calculation of long distance effects in exclusive weak radiative decays of B meson', Phys. Lett. **B358**, 129 (1995).
- [115] A. Ali and V. M. Braun, 'Estimates of the weak annihilation contributions to the decays $B \rightarrow \rho \gamma$ and $B \rightarrow \omega \gamma$ ', Phys. Lett. **B359**, 223 (1995).
- [116] G. Korchemsky, D. Pirjol, and T.-M. Yan, 'Radiative leptonic decays of B mesons in QCD', Phys. Rev. **D61**, 114510 (2000).
- [117] M. Neubert and B. Stech, 'Nonleptonic weak decays of B mesons', e-print archive hep-ph/9705292, published in Buras, A.J. (ed.), Lindner, M. (ed.): *Heavy flavours II*, pp. 294, World Scientific, Singapore.
- [118] T. Inami and C. S. Lim, 'Effects of superheavy quarks and leptons in low-energy weak processes $K_L \rightarrow \mu \bar{\mu}$, $K^+ \rightarrow \pi^+ \nu \bar{\nu}$ and $K^0 \leftrightarrow \bar{K}^0$ ', Prog. Theor. Phys. **65**, 297 (1981).
- [119] B. Grinstein, M. B. Wise and M. J. Savage, ' $B \rightarrow X_s ll$ in the six quark model', Nucl. Phys. **B319**, 271 (1989).
- [120] A. Buras and M. Münz, 'Effective hamiltonian for $B \rightarrow X_s ll$ beyond leading logarithms in the NDR and HV schemes', Phys. Rev. **D52**, 186 (1995).
- [121] A. Ali, ' B decays, flavor mixings and CP violation in the standard model', Lectures given at 20th International Nathiagali Summer College on Physics and Contemporary Needs (Dedicated to Abdus Salam on his 70th Birthday), Bhurban, Pakistan, 24 Jun - 11 Jul 1995, e-Print Archive: hep-ph/9606324.
- [122] A. Khodjamirian and D. Wyler, 'Counting contact terms in $B \rightarrow V\gamma$ decays', e-Print Archive: hep-ph/0111249 .
- [123] S. Adler, 'Axial vector vertex in spinor electrodynamics', Phys. Rev. **177**, 2426 (1969);
J. S. Bell and R. Jackiw, 'A PCAC puzzle: $\pi^0 \rightarrow \gamma\gamma$ in the Sigma model', Nuovo Cimento, **60A**, 47 (1969).
- [124] A. D. Dolgov and V. I. Zakharov, 'On conservation of axial current in massless electrodynamics', Yad. Fiz. **13**, 608 (1971), Nucl. Phys. **B27**, 525 (1971);
V. I. Zakharov, 'Two-loop chiral anomaly as an infrared phenomenon', Phys. Rev. **D42**, 1208 (1990).
- [125] A. Ali, A. Parkhomenko, 'Branching ratios for $B \rightarrow \rho \gamma$ decays in next-to-leading order in α_s including hard spectator corrections', hep-ph/0105302.
- [126] G. Buchalla, A. Buras and M. Lautenbacher, 'Weak Decays Beyond Leading Logarithms,' Rev. Mod. Phys. **68** (1996) 1125; A. J. Buras and R. Fleischer, 'Quark mixing, CP violation and rare decays after the top quark discovery', in *Heavy Flavours II*, World Scientific (1997), eds. A.J. Buras and M. Linder, p. 65, [hep-ph/9704376].
- [127] A. Pich, 'QCD Duality Analysis Of $B^0 - \bar{B}^0$ ', Phys. Lett. **B206**, 322 (1988).
- [128] A. A. Ovchinnikov and A. A. Pivovarov, 'Estimate Of The Hadronic Matrix Element Of $B^0 - \bar{B}^0$ Mixing Using The Method Of QCD Sum Rules,' Phys. Lett. **B207**, 333 (1988);
S. Narison and A. A. Pivovarov, 'QSSR estimate of the $B(B)$ parameter at next-to-leading order', Phys. Lett. **B327**, 341 (1994).
- [129] L. J. Reinders and S. Yazaki, 'A QCD Sum Rule Calculation Of The $B^0 - \bar{B}^0$ Matrix Element', Phys. Lett. **B212**, 245 (1988).
- [130] L. Lellouch and C.-J. Lin, ' $B^0 - \bar{B}^0$ mixing and decay constants from lattice QCD', Talk given at *Heavy Flavours 8*, Southampton, England, 25-29 July 1999, [hep-ph/9912322].
- [131] D. Becirevic et al, ' $B^0 - \bar{B}^0$ mixing and decay constants with the non-perturbatively improved action', preprint hep-lat/0002025.
- [132] M. A. Shifman, A. I. Vainshtein, and V. I. Zakharov, 'QCD And Resonance Physics. Sum Rules', Nucl. Phys. **B147**, 385 (1979).
- [133] A. J. Buras and P. H. Weisz, 'QCD Nonleading Corrections To Weak Decays In Dimensional Regularization And 'T Hooft-Veltman Schemes', Nucl. Phys. **B333**, 66 (1990);
A. J. Buras, M. Jamin and P. H. Weisz, 'Leading And Next-To-Leading QCD Corrections To Epsilon Parameter And $B^0 - \bar{B}^0$ Mixing In The Presence Of A Heavy Top Quark', Nucl. Phys. **B347**, 491 (1990).
- [134] A. V. Smilga, 'Calculation Of The Degree Corrections In Fixed Point Gauge', Yad. Fiz. **35**, 473 (1982);
B. L. Ioffe and A. V. Smilga, 'Meson Widths And Form-Factors At Intermediate Momentum Transfer In Nonperturbative QCD', Nucl. Phys. **B216**, 373 (1983).
- [135] F. D. R. Bonnet, P. O. Bowman, D. R. Leinweber, and A. G. Williams, 'Infrared behavior of the gluon propagator on a large volume lattice', Phys. Rev. **D62**, 051501(R) (2000).
- [136] M. N. Chernodub, M. I. Polikarpov, and V. I. Zakharov, 'Infrared behaviour of the gauge boson propagator in a confining

- theory', Phys. Lett. **B457**, 147 (1999).
- [137] A. Manohar and M. Wise, 'Inclusive semileptonic B and polarized Λ_b decays from QCD', Phys. Rev. **D49**, 1310 (1994).
 - [138] I. Bigi, M. Shifman, N. Uraltsev, and A. Vainshtein, 'Differential distributions in semileptonic decays of heavy flavors in QCD', Phys. Rev. **D49**, 3356 (1994).
 - [139] A. Falk, M. Luke, and M. Savage, 'Nonperturbative contributions to the inclusive rare decays $B \rightarrow X_s \gamma$ and $B \rightarrow X_s l^+ l^-$ ', Phys. Rev. **D49**, 3367 (1994).
 - [140] N. Isgur, 'Duality violating $1/m_Q$ effects in heavy quark decay', Phys. Lett. **B448**, 111 (1999).
 - [141] M. Neubert, 'QCD based interpretation of the lepton spectrum in inclusive $B \rightarrow X l \nu$ decays', Phys. Rev. **D49**, 3392 (1994);
 'Analysis of the photon spectrum in inclusive $B \rightarrow X_s \gamma$ decays', Phys. Rev. **D49**, 4623 (1994);
 T. Mannel and M. Neubert, 'Resummation of nonperturbative corrections to the lepton spectrum in inclusive $B \rightarrow X l \nu$ decays', Phys. Rev. **D50**, 2037 (1994).
 - [142] I. Bigi, M. Shifman, N. Uraltsev, and A. Vainshtein, 'On the motion of heavy quarks inside hadrons: universal distributions and inclusive decays', Int. J. Mod. Phys. **A9** 2467 (1994).
 - [143] G. Altarelli *et al.*, 'Leptonic decay of heavy flavors: a theoretical update', Nucl. Phys. **B208**, 365 (1982).
 - [144] A. Le Yaouanc *et al.*, 'Duality in semileptonic inclusive B decays in potential models: regular versus singular potentials', Phys. Lett. **B517**, 135, 2001;
 'Semileptonic inclusive heavy meson decay: duality in a nonrelativistic potential model', Phys. Rev. **D62**, 074007 (2000).
 - [145] S. Kotkovsky *et al.*, 'A connection between inclusive semileptonic decays of bound and free heavy quarks', Phys. Rev. **D60**, 114024 (1999);
 'The general relation between the weak inclusive decays of bound and free heavy quarks', Nucl. Phys. (Proc. Suppl.) **75B**, 100 (1999).